



Durham E-Theses

Highly Emissive Eu(III) Probes for Biological Assays

DELBIANCO, MARTINA

How to cite:

DELBIANCO, MARTINA (2014) *Highly Emissive Eu(III) Probes for Biological Assays*, Durham theses, Durham University. Available at Durham E-Theses Online: <http://etheses.dur.ac.uk/10904/>

Use policy

The full-text may be used and/or reproduced, and given to third parties in any format or medium, without prior permission or charge, for personal research or study, educational, or not-for-profit purposes provided that:

- a full bibliographic reference is made to the original source
- a [link](#) is made to the metadata record in Durham E-Theses
- the full-text is not changed in any way

The full-text must not be sold in any format or medium without the formal permission of the copyright holders.

Please consult the [full Durham E-Theses policy](#) for further details.



Department of Chemistry

**Highly Emissive Eu(III) Probes for
Biological Assays**

Martina Delbianco

A thesis submitted for the degree of Doctor of Philosophy

2014

Declaration

The work described herein was undertaken at the Department of Chemistry, Durham University between January 2012 and December 2014. All of the work is my own, except where specifically stated otherwise. No part has previously been submitted for a degree at this or any other university.

Statement of Copyright

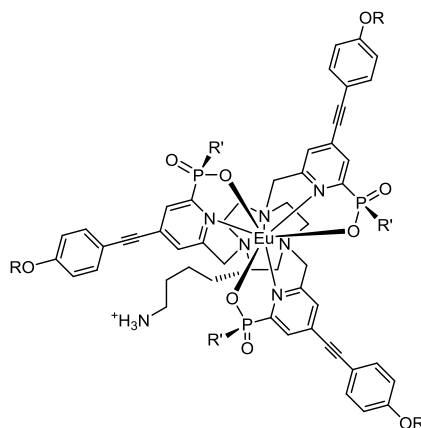
The copyright of this thesis rests with the author. No quotations should be published without prior consent and information derived from it must be acknowledged.

Abstract

Luminescent lanthanide complexes are important tools for molecular sensing and cellular staining due to their unique photophysical properties, including their long luminescence lifetimes that permit the use of time-gated measurements. However, a common drawback of such complexes is the non-specific binding associated with their low solubility in biological media.

A new class of bright, highly water soluble, and negatively charged sulfonate or carboxylate derivatives of substituted aryl-alkynyl triazacyclononane complexes has been synthesised and their photophysical properties analysed. In addition, new synthetic methodologies have been explored for the introduction of solubilising moieties into the ligand system and for the incorporation of a linkage point for conjugation with biomolecules.

Each complex exhibits extremely high quantum yields (up to 38 % in H₂O), large extinction coefficients (60,000 M⁻¹ cm⁻¹) and long luminescence lifetimes (1.1 ms). Introduction of the charged solubilising moieties suppresses cellular uptake or adsorption to living cells, making them applicable for labelling and performing assays on membrane receptors.



These Eu(III) complexes have been applied to monitor fluorescent ligand binding on cell-surface proteins (G-protein coupled receptors) with time-resolved fluorescence resonance energy transfer (TR-FRET) assays and TR-FRET microscopy.

In addition, the introduction of a linkage point for conjugation on the macrocyclic ring provided complete control of the stereochemistry of the final complex. Direct and selective formation of chiral complexes was observed with > 95 % optical purity resulting in an intense circularly polarised luminescence signal.

Acknowledgements

I would like to thank Prof. David Parker for the opportunity to work in his group, for the supervision and inspiration during the entire PhD.

Thanks to Dr Laurent Lamarque and the entire team of Cisbio Bioassay for financial support and guidance.

Thanks to Jurriaan, Victoria and Robek for the biology and microscopy studies.

Thanks to Dr Juan Aguilar, Catherine Heffernan and Dr Alan Kenwright for the help with NMR. Thanks to Pete Stokes and Dr Jackie Mosely for the help with MS, especially for the patience with all the buffered solutions.

Thanks to all the members of the DP group of these three years. In particular, thanks to Alex for his friendship, for the help with any technological device and for waiting for me almost every evening. Thanks to Brian for the support with any problem in the lab, for the great welcome at my arrival and for his translations English to English. Thanks to Nick for answering all my chemistry questions, for reading every report I had to write and for teaching me English. Thanks to Steve for the help with the synthesis, for the long HPLC sessions and for teaching me (bad) English. Thanks to Kanthi for being the “boss” of the lab and for taking care of every issue. Thanks to Rachel, Emily and Rob for the help with photochemistry and CPL. Thanks to Stuart for the synthesis (and sometimes subsequent disruption) of many useful intermediates.

In addition, thanks to Vale, Mickaele, Roberto, Vale, Ross, Helen, Santi, Sam, Jose, Salim, Francesco, Marie, Bansri, Soren, Mathias, Silvia, Anna, Kat, Colleen, Pete, Brad, Phil, Vig, Sergey, Matthieu, Asahi and all the great people that I had the chance to meet for a beer in the New Inn on Friday night.

List of abbreviations

°C	degrees Celsius
η	refractive index
9-N ₃	1,4,7-triazacyclononane
A	acceptor
B	brightness ($B = \Phi_0 \epsilon$)
BG	benzyl guanine
BSA	bovine serum albumin
CCK2	cholecystokinin-2
CD	circular dichroism
cm	centimetre
CP	circularly polarised
CPL	circularly polarised luminescence
d	doublet
D	donor
DCM	dichloromethane
dd	doublet of doublets
DFT	density functional theory
DMF	dimethylformamide
DMSO	dimethylsulfoxide
DO3A	1,4,7,10-tetraazacyclododecane-1,4,7-triacetic acid
ET	energy transfer
FP	fluorescent protein
FRET	fluorescence resonance energy transfer
g	gram
g_{em}	emission dissymmetry factor
GFP	green fluorescent protein
GPCR	G protein coupled receptor
h	hour
HEPES	4-(2-hydroxyethyl)piperazine-1-ethanesulfonic acid
HPLC	high pressure liquid chromatography
HRMS	high resolution mass spectroscopy
HSA	human serum albumin
HTRF	homogeneous time resolved fluorescence
Hz	Hertz

<i>J</i>	spectral overlap
K	Kelvin
ICT	internal charge transfer
IR	infra-red
ISC	intersystem crossing
LC-MS	liquid chromatography–mass spectrometry
Ln*	lanthanide excited state
LP	linearly polarised
m	multiplet
M	molar
mg	milligram
min	minute
mL	millilitre
mM	millimolar
mmol	millimole
mol	mole
ms	millisecond
MW	molecular weight
NHS	N-hydroxysuccinimide
nm	nanometre
nM	nanomolar
NMP	1-methyl-2-pyrrolidinone
NMR	nuclear magnetic resonance
NOTA	1,4,7-triazacyclononane-N,N',N'' triacetic acid
PG	protecting group
Pdot	polymer dot
PET	positron emission tomography
pM	picomolar
ppm	parts per million
QD	quantum dot
R_0	Förster radius
RT	room temperature
s	second / singlet
S_0	ground singlet state
S_1	singlet excited state

SPEC	Single Photon Emission Computed Tomography
t	triplet
T	Tesla
T ₁	triplet excited state
TFA	trifluoroacetic acid
TFE	trifluoroethyl
THF	tetrahydrofuran
TLC	thin layer chromatography
TR	time resolved
Trp	tryptophan
UV	ultra-violet

Table of content

1	Introduction.....	1
1.1	Luminescence spectroscopy and microscopy	1
1.1.1	Background.....	1
1.1.2	Luminescent probes in biological systems	2
1.1.2.1	Fluorescent dyes.....	3
1.1.2.2	Fluorescent proteins	4
1.1.2.3	Quantum dots	5
1.1.2.4	Emissive metal complexes	6
1.2	Emissive lanthanide complexes	7
1.2.1	Europium(III) emission spectrum.....	8
1.2.2	Lanthanide ion sensitisation.....	9
1.2.3	Chromophores for europium sensitisation.....	11
1.3	Fluorescence Resonance Energy Transfer (FRET).....	14
1.3.1	Principles of FRET	14
1.3.2	Application of FRET in biological systems.....	16
1.3.3	Lanthanide complexes used in FRET	17
1.4	Circularly polarised luminescence	20
1.4.1	Linearly and circularly polarised light.....	20
1.4.2	Circularly polarised luminescence spectroscopy	22
1.4.3	Lanthanide complexes in CPL spectroscopy	22
1.5	Aims of the project.....	24
2	A series of highly emissive europium complexes	26
2.1	Introduction	26
2.2	Photophysical investigation.....	27
2.3	Energy transfer analysis	29
2.3.1	Studies of energy transfer in methanol	30
2.3.2	Studies of energy transfer in water	32
2.3.3	Comparison with commercially available donors.....	35
2.4	Water solubility determination.....	37

2.5	Conclusions	38
3	A new series of C-substituted europium complexes	39
3.1	Introduction	39
3.2	A model C-substituted complex	39
3.2.1	Synthetic aspects	40
3.2.2	Photophysical analysis	43
3.3	A series of C-substituted complexes	44
3.3.1	Synthetic aspects	45
3.3.2	Incorporation of solubilising moieties	47
3.3.3	Photophysical and FRET studies	51
3.4	Applications in FRET bioassays	55
3.4.1	Conjugation with the biomolecule	57
3.4.2	Time resolved FRET assays.....	58
3.4.3	Microscopy studies	62
3.5	Conclusions	65
4	New hydrophilic sulfonated systems.....	66
4.1	Introduction	66
4.2	Improving the water solubility of the P-Ph system	67
4.2.1	The analogues of the P-Me phosphinate systems	68
4.2.2	Introduction of aromatic sulfonates	72
4.2.2.1	Synthetic investigations.....	72
4.2.2.2	Application of the new methodologies for the synthesis of new compounds	73
4.2.2.2.1	<i>First strategy</i>	73
4.2.2.2.2	<i>Second strategy</i>	77
4.2.3	Introduction of an aliphatic sulfonate substituent.....	83
4.2.3.1	Synthetic investigations.....	83
4.2.3.2	Application of the new methodology	86
4.3	Photophysical characterisation and FRET studies	87
4.4	Application in a new FRET based assay	93
4.5	Conclusions	97

5	Structural and chiroptical characterisation.....	99
5.1	Introduction	99
5.2	The C ₃ symmetric systems	99
5.3	The hybrid system	102
5.4	The C-substituted 9-N ₃ systems	105
5.4.1	The C-substituted systems bearing the alkynyl chromophore	110
5.5	Conclusions	113
6	Conclusions and future work	114
6.1	General conclusions	114
6.2	Future work	116
7	Experimental.....	121
7.1	General experimental	121
7.1.1	General procedures	121
7.1.2	HPLC analysis	122
7.1.3	Optical techniques.....	124
7.1.4	Cellular studies and microscopy	125
7.2	Synthetic procedures	129
8	Appendix.....	234
9	References.....	235

1 Introduction

1.1 Luminescence spectroscopy and microscopy

Biological imaging refers to many different methods that are used to gain information on morphology or structure and to follow biochemical processes in living systems. In the medical field, a large range of techniques is routinely used to diagnose and examine disease; the most common are magnetic resonance imaging (MRI), computed tomography (CT) and nuclear medicine imaging (*e.g.* PET and SPECT). These techniques can provide high quality images of large areas, but have a common limitation: their resolution is typically of the order of 0.5 to several millimetres. Fluorescence microscopy has become an essential tool in biology and biomedical sciences because of its greater inherent resolution (commonly down to 120 nm with a confocal microscope) that permits the visualisation of cells and organelles. This technique, combined with fluorescence spectroscopy, has been applied in quantitative assays for the determination of analytes in several samples and has also been extensively used to assess the spatial distribution of a given target molecule.¹ Drawbacks of this technique are auto-fluorescence and absorption of light by endogenous chromophores present in biological media.

1.1.1 Background

Luminescence is defined as the spontaneous emission of radiation from an electronically excited species.² There are various types of luminescence that are described by their mode of excitation: *i.e.* chemiluminescence is the emission of light as a result of a chemical reaction; photoluminescence is the emission of light as a result of absorption of photons and incorporates fluorescence and phosphorescence. The Jablonski diagram (*Figure 1*) qualitatively describes the energy levels involved in the excitation/emission process.

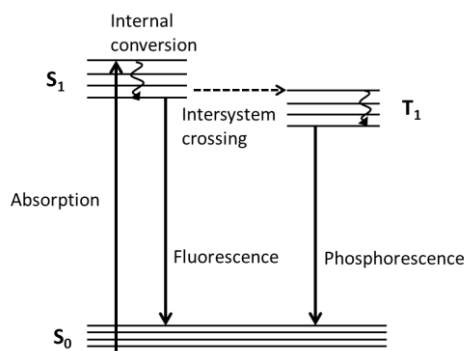


Figure 1: Jablonski diagram.

The initial absorption of light by a molecule (10^{-15} s) in its ground singlet state (S_0) takes the molecule to an excited electronic state (S_1). The upper vibrational states undergo radiationless decay (internal conversion) by releasing energy to the surroundings (10^{-13} to 10^{-11} s). At this stage three different pathways can happen: non-radiative decay, radiative transition (fluorescence, 10^{-9} to 10^{-7} s) or intersystem crossing to the triplet excited state (T_1). From the triplet state, non-radiative or radiative (phosphorescence, 10^{-4} to 10^{-1} s) decay can take place. The longer decay time for phosphorescence, compared to fluorescence, is associated with the forbidden nature of the triplet to singlet transition. Fluorescence and phosphorescence always occur at lower frequencies than the incident radiation due to dissipation of energy in the excited state (Stokes' shift).

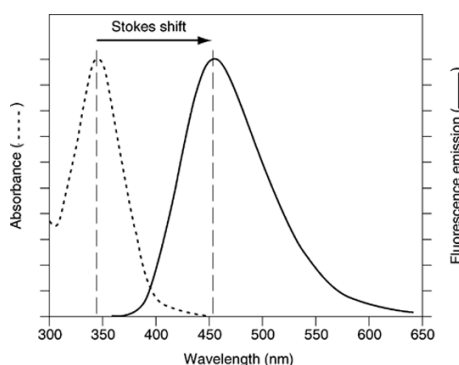


Figure 2: A representation of the Stokes' shift for a typical organic fluorophore.

1.1.2 Luminescent probes in biological systems

The majority of cellular processes remain invisible, even when using our brightest laser light sources. Further progress will depend on improvements in instrumentation and on the development of new bright fluorophores and sensors.³ Nowadays, extremely bright labelling reagents are available in many different colours. Fluorescent proteins can be incorporated in

genetically encoded proteins in living cells and ‘solid state’ quantum dot technology is used for multi-parameter labelling.⁴ In addition, emissive metal complexes are available as an alternative to purely organic labels. The challenge in this area is the synthesis of new very bright probes that are able to enter cells, selectively target specific organelles and respond to local changes in physical properties.

1.1.2.1 Fluorescent dyes

Fluorescent dyes are emissive organic molecules with large molar extinction coefficients ($50\text{--}250\text{ mM}^{-1}\text{ cm}^{-1}$) and high quantum yields (0.2 to 0.8). The most widely used fluorescent dyes are based on the xanthene or cyanine structures. Fluorescein (*Figure 1a*) was the first examples of such a label and it is still used despite certain disadvantages (photobleaching and pH sensitivity).⁵ Rhodamines (*Figure 1b*) are pH insensitive and more photostable, but are more difficult to use because of their relatively low water solubility.⁶ The introduction of solubilising moieties on the rhodamine structure permitted the development of a new class of dyes called Alexa Fluor.⁷ In the early 1990s, new cyanine dye labels (*Figure 1c*) became commercially available and provide significantly brighter fluorescence compared to any other fluorophores.⁸ Similar properties, such as high brightness and stability towards photobleaching, are reported for the more recently developed BODIPY series of fluorescent dyes and stains (*Figure 1d*).⁹

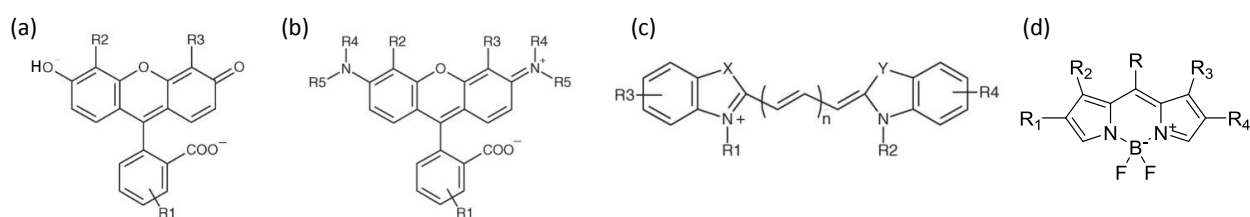


Figure 3: General structures of most common organic dyes: fluorescein (*a*), rhodamine (*b*), a cyanine (*c*), BODIPY (*d*).

All of these compounds are available in different reactive versions (*i.e.* active esters, isothiocyanates and sulfonyl chlorides) to allow easy conjugation with the biomolecules. The use of different substituents also permits the tuning of the absorption and emission wavelengths.

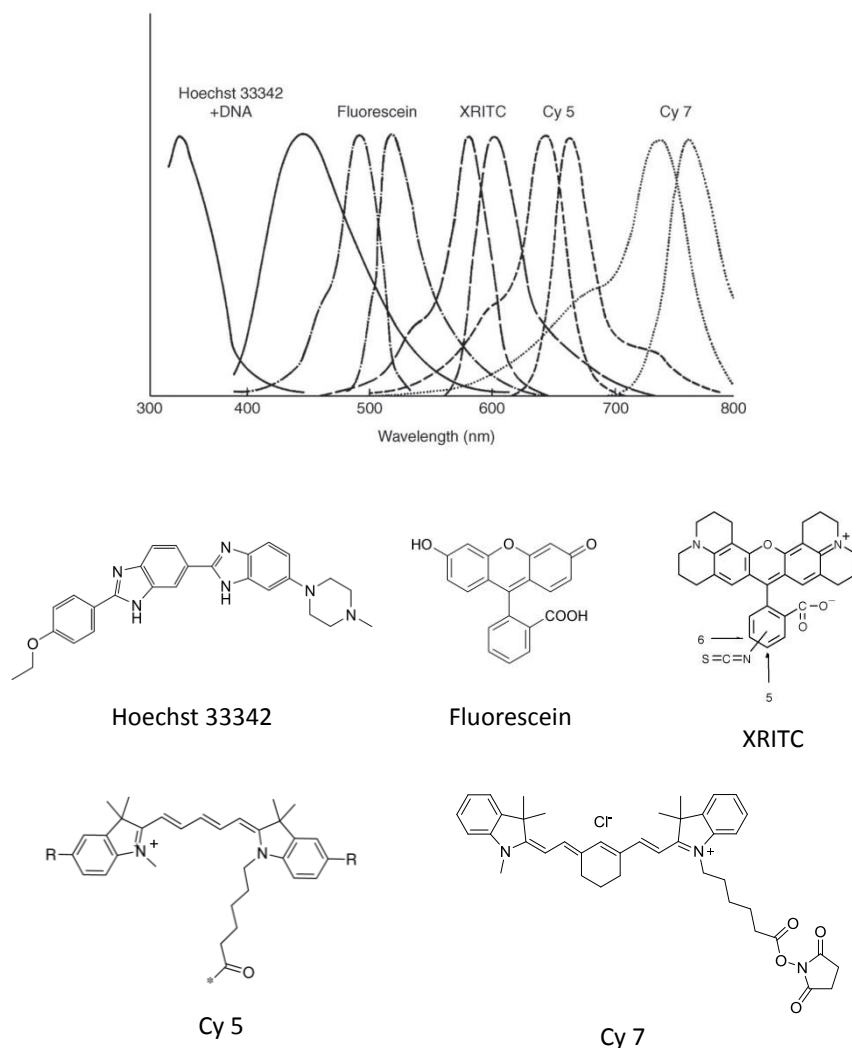


Figure 4: Absorption (left) and emission (right) spectra of five fluorescent dyes.⁴

Fluorescent dyes have found many applications in biological imaging as pH¹⁰ and ion¹¹ sensors. Problems with this class of probes are their short lived excited states, small Stokes' shifts and often broad emission spectra.

1.1.2.2 Fluorescent proteins

Green fluorescent proteins (GFPs) are spontaneously fluorescent biomolecules isolated from marine organisms. They convert the blue chemiluminescence of primary proteins, aequorin or luciferase, into green fluorescent light ($\lambda_{abs} = 395/475$ nm, $\lambda_{em} = 508$ nm).¹² GFPs consist of imidazolinone dyes within a β -barrel tertiary structure. Their high quantum yields (0.71 - 0.85), stability within cells and resistance to quenching mean that these GFPs have been used as reporters of gene expression and as fusion tags to monitor protein localization within living

cells.¹³ Most GFPs variants display pH-sensitive absorption; such behaviour has been exploited to monitor pH within cell compartments.¹⁴

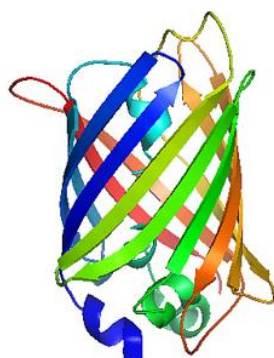


Figure 5: Tertiary protein structure of a GFP.¹⁵

Nowadays, a wide variety of FPs is available in different colours as new tools for biological imaging.¹⁶ Among all the examples, mCherry (red fluorescent monomer, $B = 15.8 \text{ mM}^{-1} \text{ cm}^{-1}$ at 580 nm in water) is one of the most used FPs, due to its colour and stability to photobleaching.¹⁷

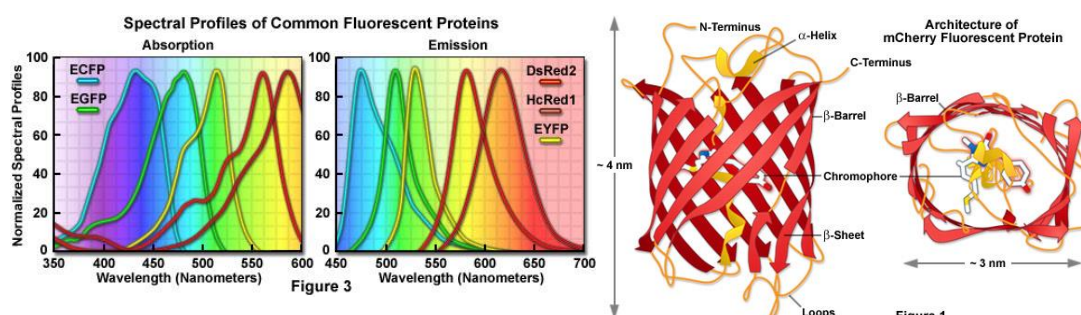


Figure 6: Spectral profiles of common FPs (*left*) and tertiary structure of mCherry (*right*).¹⁷

One limiting issue with the use of FPs as intracellular probes is their large size (27 kDa) and, therefore, they can be quite invasive.

1.1.2.3 Quantum dots

Quantum dots (QDs) are roughly spherical inorganic colloidal nanoparticles (diameters between 1 and 12 nm) with unique light emitting properties. Upon irradiation of QDs by UV light, they produce multicolour, extremely narrow and symmetric emission bands. Furthermore light emitted by a specific quantum dot is related directly to its size (the smaller the dot the lower the frequency of the light emitted).¹⁸



Figure 7: Solutions containing different sized CdSe quantum dots.¹⁸

The broadband excitation and narrow bandwidth emission make QDs excellent probes for use in multiplexed type analyses.¹⁹ The challenge in this area is to preserve their stability and improve their capability of labelling targets; in addition the slight toxicity of these nanoparticles can limit their application in living systems.

Recently, a purely organic alternative to QDs has been reported (Pdots). This new class is based on π -conjugated semiconducting polymers; Pdots possess similar emission properties as Qdots, and in addition excellent photostability and low cytotoxicity.²⁰

1.1.2.4 Emissive metal complexes

Emissive metal complexes can be divided into two main classes: the first is based on *d*-block metals (*e.g.* Re(I), Ru(II), Os(II), Rh(I), Ir(III), and Pt(II))²¹ and the second is based on luminescent lanthanide(III) ions.²²

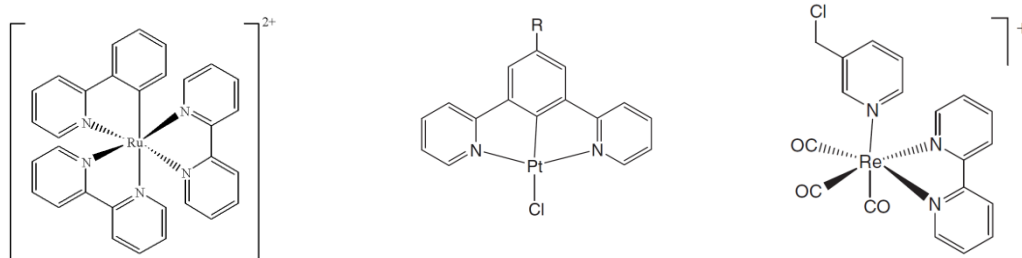


Figure 8: Examples of emissive transition metal complexes.

These complexes show large Stokes' shifts (hundreds of nm) and long luminescent lifetimes (microseconds to milliseconds range). This allows for their use as probes in time-gated measurements,²³ offering the possibility of eliminating the short-lived background fluorescence of the endogenous chromophores (order of nanoseconds), (*Figure 9*).²⁴

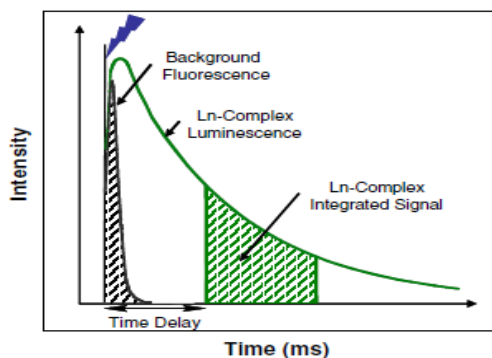


Figure 9: Use of metal complexes in time-resolved luminescence microscopy.

These complexes have been used mainly for cellular staining and oxygen sensing.²⁵ In general, they exhibit a lack of responsiveness to their surroundings; however, in the last few years, many publications have emerged showing the utility of metal complexes as responsive probes, able to penetrate the cell membrane and report on changes in the local ionic composition.²⁶ In particular, the emission spectrum of lanthanide complexes, which presents many emission bands, makes these complexes suitable for ratiometric analysis, avoiding the problem of monitoring the probe concentration *in vivo*.

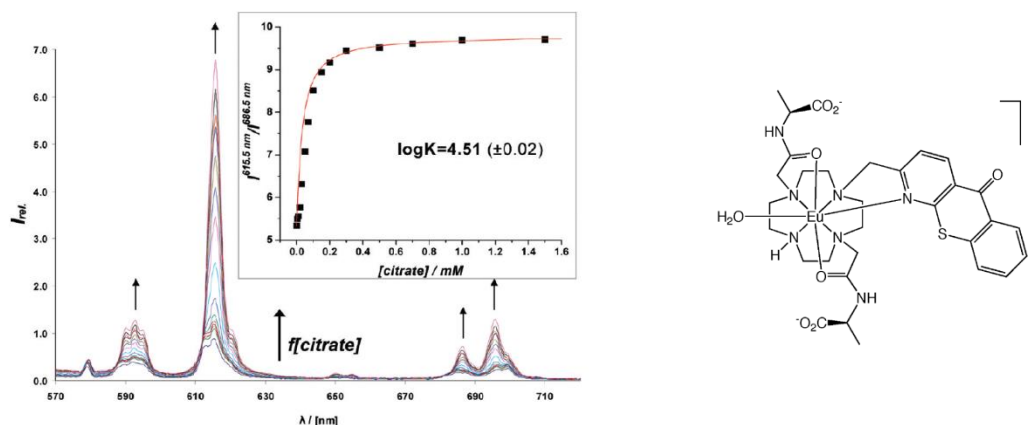


Figure 10: Europium emission spectrum as a function of added citrate concentration ($\lambda_{ex} = 380$ nm).²⁶

1.2 Emissive lanthanide complexes

Lanthanide ions in aqueous media form trivalent cations with partially filled 4f orbitals, due to the balance between ionisation energy and hydration enthalpy.²⁷ Most lanthanides have electronic excited states which radiatively decay to the ground state: Sm^{3+} , Eu^{3+} , Tb^{3+} and Dy^{3+} emit in the visible region, while Nd^{3+} , Ho^{3+} , Er^{3+} and Yb^{3+} emit in the near-IR region. The two longest lived and most commonly used emissive lanthanide ions are Eu^{3+} and Tb^{3+} ,

with 5D_0 and 5D_4 electronic excited states, with an energy of 17200 and 20500 cm^{-1} respectively.²⁸

1.2.1 Europium(III) emission spectrum

The lowest energy excited state for Eu(III) is the 5D_0 level with an energy of 17200 cm^{-1} . Due to spin-orbit coupling, the ground state manifold (7F) is split, causing several bands in the emission spectrum (Figure 11). Every band is denoted by its ΔJ value. The Eu(III) emission spectrum consists of five intense emission bands, arising from transitions from the 5D_0 excited state to the 7F_J ($J = 0, 1, 2, 3, 4$) ground state levels. Due to the different nature of the f orbitals compared to the d orbitals, the emission spectrum of lanthanides complexes is not as strongly affected by the nature of the ligand. However, additional fine splitting can be observed depending on the coordination environment. This is due to the loss of degeneracy of the J levels associated with crystal field splitting. The form and fine splitting of the Eu^{3+} spectrum is known to be dependent upon the symmetry at the metal centre. In general, the spectrum shows less fine structure when the symmetry of the complex is high.²⁹

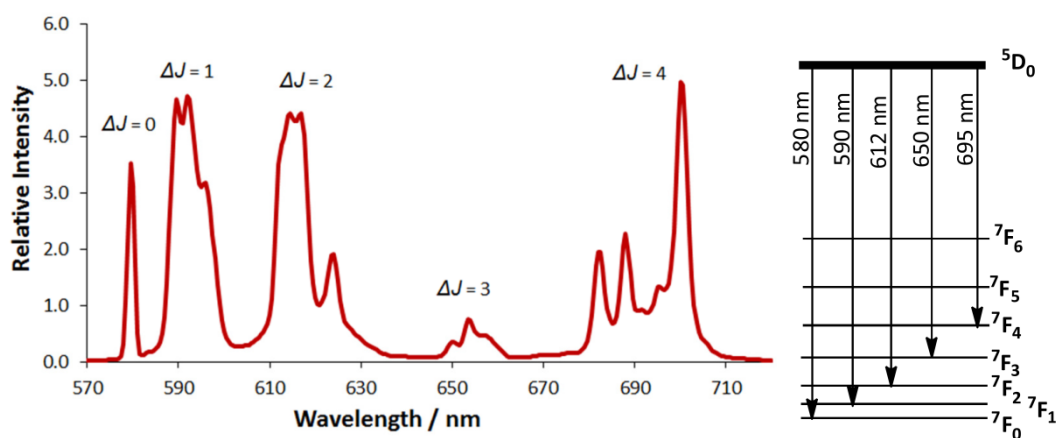


Figure 11: A typical Europium(III) emission spectrum in a low symmetry complex.

The form of the Eu^{3+} emission spectrum can be predicted with the following rules: the $\Delta J = 0$ transition is formally forbidden and sensitive to the symmetry of the complex; the magnetic-dipole allowed $\Delta J = 1$ transition (around 590 nm) is insensitive to the coordination environment and typically consists of two (axially symmetric complexes) or three (low symmetry complexes) bands; the electric-dipole allowed $\Delta J = 2$ (around 615 nm) and $\Delta J = 4$ (around 700 nm) manifolds change their intensity considerably as a function of the ligand field.³⁰

1.2.2 Lanthanide ion sensitisation

Lanthanide $f-f$ transitions are Laporte-forbidden and therefore very weak. This renders direct excitation of the lanthanide ion very inefficient and only practicable with high power lasers. This problem is usually solved by grafting an antenna or chromophore (aromatic moiety) into the ligand complexing the metal ion. This antenna absorbs light and sensitises the lanthanide ion that can emit (*Figure 12*).³¹

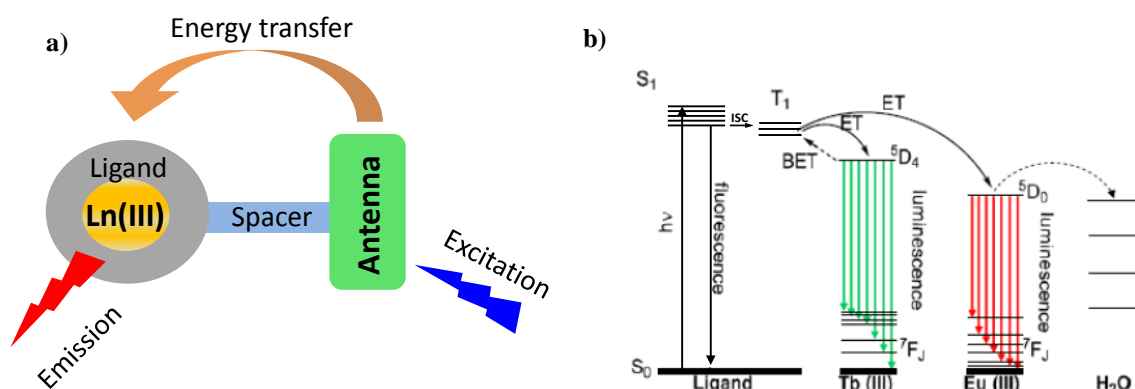


Figure 12: Indirect excitation of a lanthanide *via* an antenna (a). Jablonski diagram showing the main energy transfer pathways during sensitization of lanthanide luminescence *via* the antenna (b).

The classical interpretation of the process of indirect excitation (*Figure 12b*) of a lanthanide ion involves initial excitation of the antenna from its ground state to its singlet excited state (S₁). This is followed by intersystem crossing (ISC) to the antenna's triplet state (T₁). Due to the presence of the Ln(III) ion, a heavy atom, significant amounts of spin-orbit coupling occur which facilitate this spin forbidden process. After this, an internal energy transfer step (ET) from the antenna to the excited state of the lanthanide occurs, followed by relaxation to the lanthanide ground state with emission of lanthanide luminescence.

Recently, a different mechanism that takes place *via* the solvent-relaxed internal charge transfer (ICT) excited state has been suggested for ligands that possess an intense ICT transition (*Figure 13*). Significant solvatochromism and a notable temperature dependence confirmed this hypothesis, although sensitization *via* a triplet state can still participate to the process, for certain substituted systems.³²

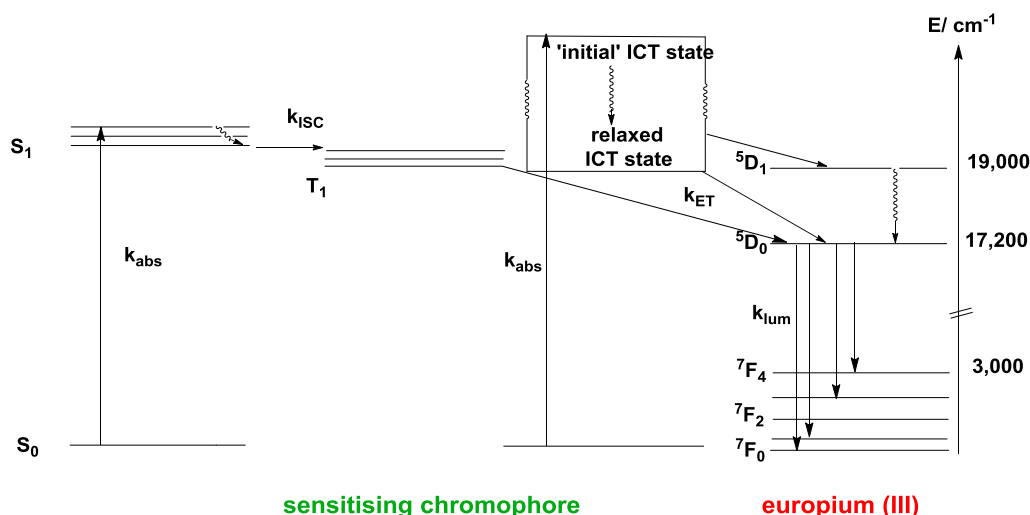


Figure 13: Jablonski diagram showing the energy transfer pathways during sensitization of lanthanide luminescence via the solvent-relaxed internal charge transfer excited state.³³

In rare cases, a process of sensitisation from the antenna singlet excited state (S_1) to the lanthanide excited state (Ln^*) is also thought to occur.³⁴

The overall emission quantum yield (Φ_{em}) is representative of the efficiency of each of the main steps involved in the sensitisation process (Figure 14).

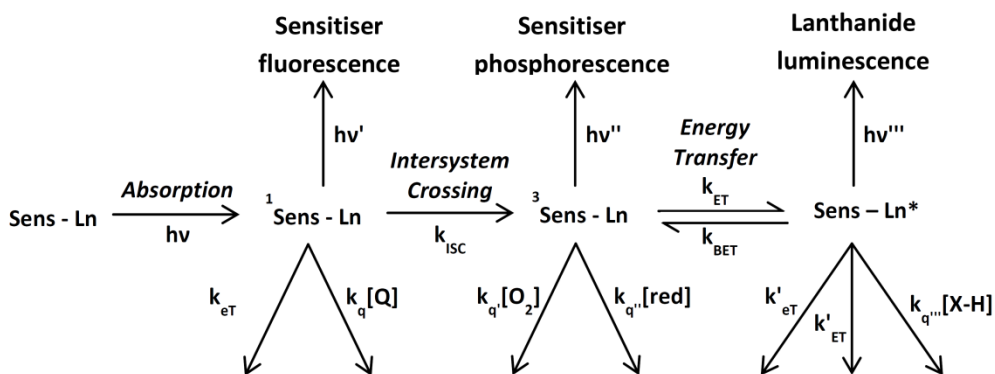


Figure 14: Photophysical processes that occur during sensitised lanthanide luminescence.³⁵

Three main processes are involved in the classical mechanism of sensitisation. The formation of the intermediate triplet state is determined by the feasibility of the inter-system crossing process (η_{ISC}). The next step, which involves the energy transfer from the antenna's triplet state to the lanthanide, is maximised when there is a short distance between the chromophore and the lanthanide ion (ET follows an r^{-6} dependence, η_{ET}). For intramolecular energy transfer to occur, the triplet excited state of the antenna must be higher in energy than the

excited state of the lanthanide by at least 1700 cm^{-1} to avoid back energy transfer. Finally, the intrinsic emissive quantum yield of the lanthanide ion needs to be considered (Φ_{Ln}).

$$\Phi_{tot} = \Phi_{Ln}\eta_{ISC}\eta_{ET} \quad [1]$$

Different types of quenching can occur for each of these steps: radiative decay (fluorescence) or quenching by electron transfer can deactivate the sensitiser's singlet excited state. Phosphorescence or quenching by molecular oxygen competes with energy transfer to the Ln^{3+} ion in deactivating the chromophore's triplet state. Finally, the main quenching process that deactivates the lanthanide excited state, involves vibrational energy transfer to solvent molecules or ligand oscillators. The excited lanthanide energy level approximately corresponds in energy to higher energy vibrations of an OH or NH oscillator.³⁶ Therefore, the highest emission quantum yields are found for complexes that do not possess any coordinated water molecules and are not bound to NH donors.

1.2.3 Chromophores for europium sensitisation

The antenna for europium sensitisation should have the following properties: a high molar extinction coefficient, an excitation wavelength above 320 nm to avoid the excitation of common biomolecules (protein and nucleic acids), a relatively low singlet excited state energy with a small S_1 - T_1 energy gap to maximize the intersystem crossing efficiency and a triplet state energy of around 20000 cm^{-1} . This is higher than the 5D_0 lanthanide excited state at 17200 cm^{-1} to avoid back energy transfer, but is not too high in order to maximise the rate of energy transfer. In addition, the distance between the lanthanide ion and the chromophore should be small.

A large variety of ligands bearing various highly conjugated moieties has been used as lanthanide sensitisers. A list of some of the more important sensitisers with their spectroscopic characteristics is presented (*Table 1*). These chromophores can be part of the actual chelating ligand (*Figure 15*) or be covalently attached to a chelate such as DO3A or 9-N₃ (*Figure 16*).

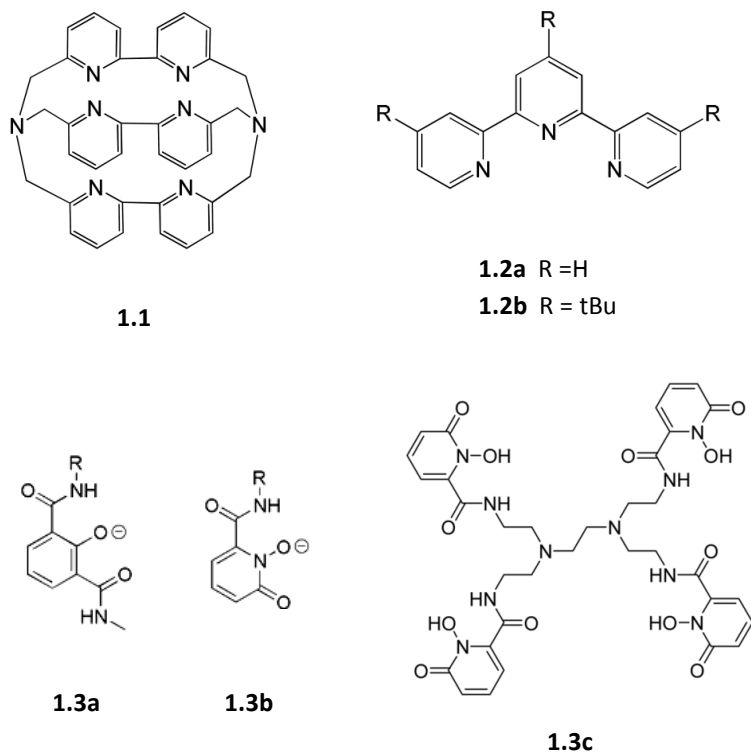
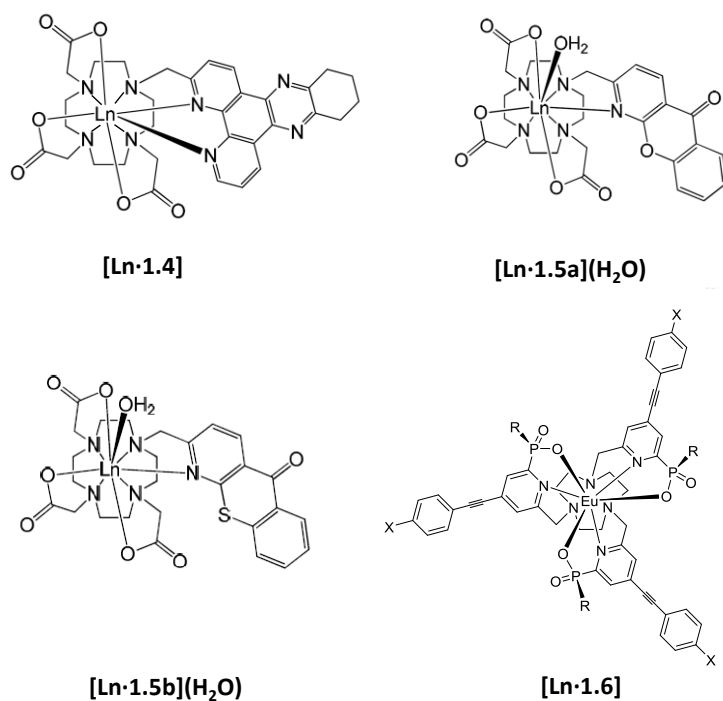
Figure 15: Examples of chelating antenna ligands.³⁷⁻³⁸⁻³⁹⁻⁴⁰Figure 16: Examples of lanthanide complexes bearing a pendant antenna.⁴¹⁻⁴²⁻⁴⁴

Table 1: Summary of the photophysical properties of selected chromophores.^a All values were measured at 295 K in H₂O except [Eu·(1.2a)₃]³⁺ and [Eu·(1.2b)₃]³⁺ which were measured in CH₃CN and [Eu·1.6] which was measured in MeOH.

Complex	λ_{\max} / nm	ϵ / mM ⁻¹ cm ⁻¹	Φ_{em} / %
[Eu·1.1] ³⁺	303	18	2
[Eu·(1.2a) ₃] ³⁺	305	9	3
[Eu·(1.2b) ₃] ³⁺	305	8	10
[Eu·1.3c] ⁻	345	18	21
[Eu·1.4]	340	4	18
[Eu·1.5a]	330	7	7
[Eu·1.5b]	375	5	2
[Eu·1.6] (X=OMe, R=Ph)	340	58	52

^a Errors on λ_{\max} , ϵ and Φ_{em} are $\pm 10\%$.

The tris(bipyridine) cryptate [Eu·1.1]³⁺ was reported by Lehn and Mathis in 1987.³⁷ It has an excitation wavelength at 303 nm with a molar extinction coefficient of 18000 M⁻¹ cm⁻¹. Because of its broad absorption spectrum, excitation at 337 nm is possible. The quantum yield in water is very low (2 %) due to the presence of two water molecules in the inner coordination sphere, which are involved in the quenching of the Eu(III) excited state. This problem can be avoided by using this complex in the presence of a large molar excess (0.4 M) of F⁻ ions, which replace the two coordinated water molecules ($\Phi_{em} = 10\%$).

Another ligand that coordinates the metal directly with the chromophore is the terpyridine ligand **1.2a** which forms complexes of the type [Ln·(1.2a)₃]³⁺. This avoids the presence of water in the inner coordination sphere leading to better quantum yields. Introducing alkyl substituents in the *para* position of the rings ([Ln·(1.2b)₃]³⁺) further improves the emission quantum yield (up to 10 %).³⁸ Although these systems displayed higher quantum yields, their low water solubility limits their utility.

In 2003, the group of K.N. Raymond introduced the 2-hydroxyisophthalamide 'IAM' **1.3a** and 1-hydroxypyridin-2-one '1,2-HOPO' **1.3b** based ligands.³⁹ They act as strongly chelating ligands and also function as antennae. The *R* group can be modified to control both the denticity of the ligand and the geometry at the metal centre. One example is the 1-hydroxypyridin-2-one '1,2-HOPO' based ligand **1.3c** which is very effective in chelating Eu(III) ions and gives rise to quantum yields of around 21 %.⁴⁰

Complexes based on DO3A, bearing a sensitizer arm, have found many applications in fluorescence microscopy. One example is the tetraazatriphenylene-based DO3A complex **[Ln·1.4]**.⁴¹ The chromophore binds directly to the metal centre leading to a quantum yield of 18 %, with excitation at 355 nm.

Other chromophores, which are exploited to bind directly to the metal centre in DO3A-based complexes, include tricyclic heterocyclic aromatics, such as an azaxanthone **[Ln·1.5a]** and an azathioxanthone **[Ln·1.5b]**.⁴² Excitation of the heterocyclic chromophore in the range 330 to 382 nm leads to low background fluorescence; moreover, a triplet state energy of around 25400 cm⁻¹ makes azaxanthenes very good candidates for europium sensitization. One problem with this class of chromophores is that their molar extinction coefficients are not very high (around 5000 M⁻¹ cm⁻¹).

In 2011, the use of three *p*-substituted pyridyl-alkynyl-aryl moieties ($\epsilon = 20000 \text{ M}^{-1} \text{ cm}^{-1}$ each)⁴³ combined with the shielding of the Eu(III) ion using nonadentate ligands based on triazacyclononane was reported (**[Eu·1.6]**).⁴⁴ Overall extinction coefficients of about 60000 M⁻¹ cm⁻¹ and high quantum yields (up to 50 %) make these complexes the brightest luminescent europium(III) complexes available.

1.3 Fluorescence Resonance Energy Transfer (FRET)

1.3.1 Principles of FRET

Fluorescence Resonance Energy Transfer (FRET) is a process in which the excited-state energy is transferred from an excited donor (D) to an acceptor (A).⁴⁵ This process does not involve photon emission, but requires an interaction between the transition dipoles of the donor and the acceptor. The donor absorbs and emits light; when the acceptor comes in proximity to the donor, the energy is transferred to the acceptor that emits and the emission of the donor is quenched.

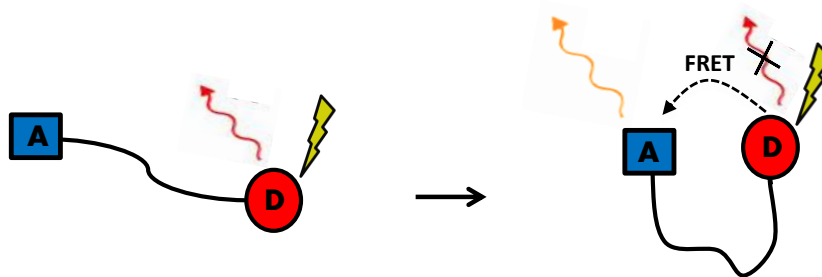


Figure 17: Cartoon explaining the principle of FRET.

A necessary condition required for this process to occur is an overlap between the emission spectrum of the donor and the absorption spectrum of the acceptor; the bigger the spectral overlap, the more efficient will be the energy transfer process. It is also important that the donor's emission spectrum does not show any overlapping regions with the acceptor's emission spectrum, in order to be able to measure each partner's fluorescence individually.

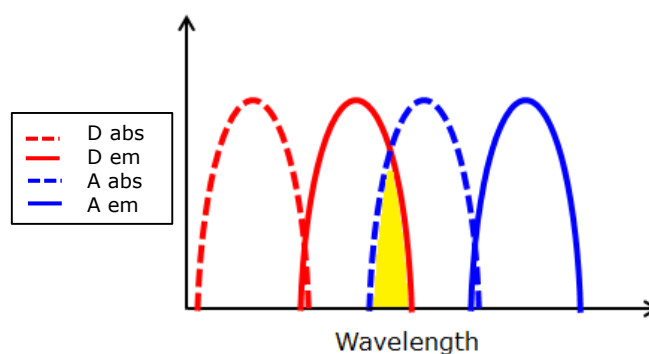


Figure 18: Condition required for FRET, spectrum overlap is in yellow.

The rate of energy transfer k_T from D to A is strongly dependent on the distance between the two partners (r^{-6}) and it is described by the following equation:

$$k_T = \frac{1}{\tau_0} \left(\frac{R_0}{r} \right)^6 \quad [2]$$

where τ_0 is the lifetime of the donor in absence of acceptor and R_0 is the Förster distance (distance at which FRET is 50 % efficient). The distance R_0 is constant for a specific D-A pair and is given by:

$$R_0 = (Jk^2\Phi_0\eta^{-4})^{\frac{1}{6}} \cdot (9.79 \cdot 10^2) \quad [3]$$

in which J is the spectral overlap integral (in $\text{cm}^3 \text{M}^{-1}$), k^2 is the orientation factor ($2/3$), Φ_0 is the quantum yield of the donor in the absence of transfer, and η is the refractive index of the

medium. The spectral overlap integral, J , can be calculated from the donor's emission spectrum and the acceptor's absorption spectrum:

$$J(\lambda) = \frac{\int F(\lambda)\epsilon(\lambda)\lambda^4 d\lambda}{\int F(\lambda)d\lambda} \quad [4]$$

$F(\lambda)$ is the fraction of donor emission at wavelength λ , and $\epsilon(\lambda)$ is the extinction coefficient of the acceptor at wavelength λ , in units of $M^{-1} \text{ cm}^{-1}$.

1.3.2 Application of FRET in biological systems

Fluorescence Resonance Energy Transfer occurs at distances comparable with biomolecular dimensions (R_0 is typically 10 - 100 Å)⁴⁶ and has a strong distance dependence; these are the reasons why FRET is used in biological systems to measure distances between two points in macromolecules or to study macromolecular interaction. A summary of the most common bio-applications of FRET is given below.

In the past, FRET has been used as a biological ruler; in fact, by labelling two different sites of a protein with a donor and an acceptor, it is possible to calculate the A-D distance by measuring the FRET efficiency (*Figure 19*).⁴⁷ Because of the flexibility of the probe linkers and the FRET dependence on the dipole-dipole orientation, the distances can only be measured with a significant degree of uncertainty. In addition, this technique cannot give reliable results for very short distances (< 10 nm).

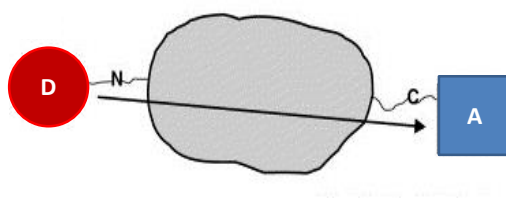


Figure 19: Use of fluorescent labels to measure distances between two points on a protein with FRET.

FRET has also been used to study protein folding; by monitoring the changes in fluorescence of the acceptor, it is possible to follow the time-dependence of the folding of a protein (*Figure 20*).⁴⁸

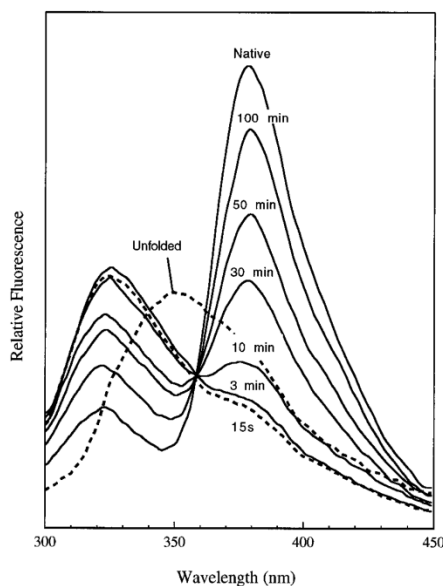


Figure 20: Fluorescence emission spectrum of Trp183 PyP-eSHMT as a function of time after initiation of refolding at 4 °C. Trp is used as the acceptor in the energy transfer.⁴⁸

Energy transfer occurs independently of the constitution of the linker joining the donor and the acceptor; it depends only on the D-A distance. This is the reason why FRET has found many applications in the study of biomolecular associations. In the following example (Figure 21) one strand of DNA was labeled with fluorescein (F_1) and the other strand with rhodamine (F_2). When association occurs, the emission of fluorescein is quenched and the rhodamine emission is enhanced.⁴⁹

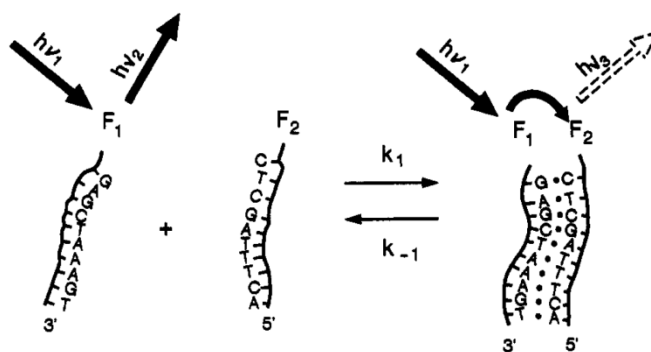


Figure 21: DNA association observed with labeled oligonucleotides.⁴⁹

1.3.3 Lanthanide complexes used in FRET

The extremely long luminescence lifetime and the sharp emission bands of lanthanide complexes make them suitable candidates as donors in FRET applications. In fact, the long emission lifetime of these donors leads to a slow deactivation of the acceptor's excited state,

resulting in an increased acceptor lifetime; the acceptor can therefore emit light for up to hundreds of microseconds. To exploit this property, the Homogeneous Time Resolved Fluorescence technology (HTRF) was introduced; HTRF combines standard FRET technology with time-resolved measurement of fluorescence (*Figure 22*).⁵⁰ Introducing a time delay (50 to 150 μs) between the system excitation and fluorescence measurement, allows the signal to be clear of short-lived background fluorescence.

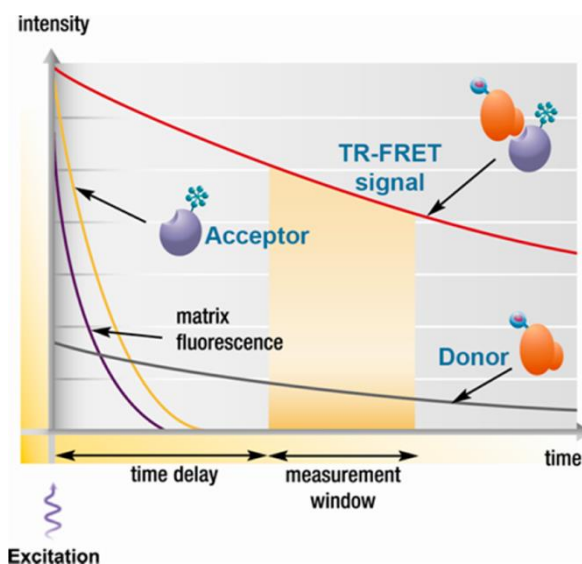


Figure 22: Schematic representation of HTRF.⁵⁰

One of the most studied lanthanide donors is the **Eu(TBP)** cryptate, developed by G. Mathis and J.M. Lehn. The Eu^{3+} cryptates are mainly compatible with red acceptors that show an emission peak at 665 nm (*Figure 23*). The first acceptor used in HTRF experiments was allophycocyanin XL665, a large heterohexameric protein of 105 kDa.⁵¹ The second generation of acceptors is characterised by cyanine dyes (*d2*) that are 100 times smaller, which avoids steric problems.⁵² As mentioned in *Section 1.2.3*, **Eu(TBP)** has to be used in the presence of 0.4 M KF to prevent the quenching from two bound water molecules, but even with this addition, its quantum yield is not higher than 10 % ($B = 0.4 \text{ mM}^{-1} \text{ cm}^{-1}$ at 304 nm in water).

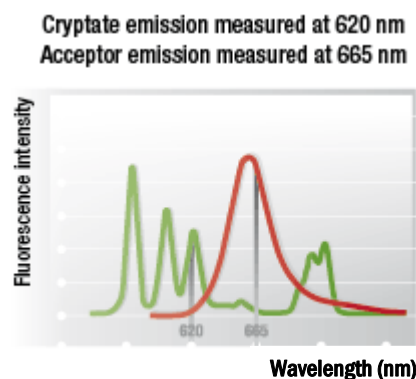
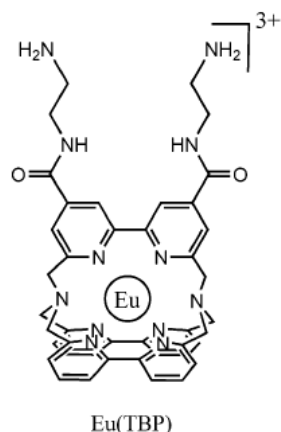


Figure 23: **Eu(TBP)** cryptate (left). Donor emission (green) and acceptor emission (red), (right).

Lumi4-Tb cryptate is a more recent and bright ($B = 13.5 \text{ mM}^{-1} \text{ cm}^{-1}$ at 340 nm in water) donor developed by S. Petoud and K. Raymond.⁵³ **Lumi4-Tb** is compatible with green acceptors like fluorescein or GFP (emission around 520 nm) and it can also be coupled with red acceptors (emission at 665nm).⁵⁴

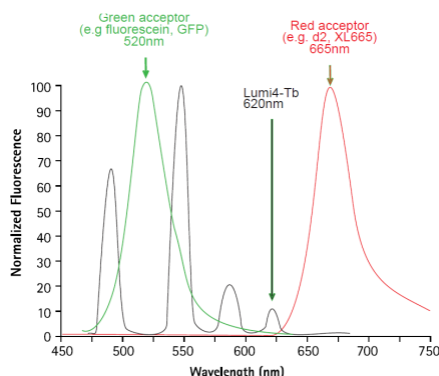
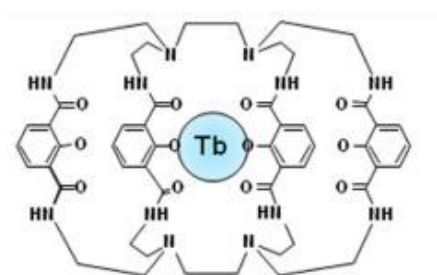


Figure 24: **Lumi4-Tb** cryptate (left). Donor emission (black), acceptors emission (green and red), (left).

These two complexes, both available from Cisbio, have been used in a variety of *in vitro* and *in vivo* assays to probe molecular interaction,⁵⁵ to monitor the concentration changes of second messengers after stimulation of membrane receptors⁵² and to determine the membrane receptor structure, conformation, and ligand binding.⁵⁶ By monitoring two single wavelengths (620 nm for the donor and 665 nm for the acceptor), all these assays give quantitative information. It is easy to notice that the band at 620 nm for the two donors presented above (band used for energy transfer and detection) is not the biggest in the total emission of the complexes. This factor can lower the inherent efficiency of the energy transfer process and raise the detection limit for the assay.

An alternative to these systems is offered by the LANCE technology provided by Perkin Elmer, in which the europium chelating agent (general structure based on the complex in *Figure 25*) is optimised for labelling proteins and peptides. These Eu(III) donors can be used with small molecules or large protein acceptors.⁵⁷ These complexes are based on the EDTA structure with seven coordination sites; for this reason their stability in media is lower than for the highly stable nine coordinated donors. These complexes are also susceptible to Mn²⁺ quenching.⁵⁸ The presence of only one chromophore makes these donors not the brightest donor on the market ($\epsilon = 27000 \text{ M}^{-1} \text{ cm}^{-1}$).

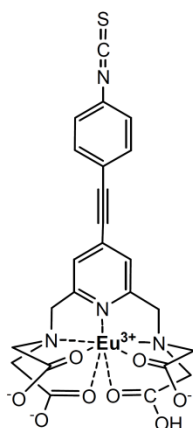


Figure 25: General structure of LANCE Eu(III) chelating reagent (**Eu-W1024**).

Recently, much interest has grown in the use of lanthanide complexes as donors with quantum dots as acceptors.⁵⁹ The QDs can offer various perspectives such as the possibility of very large Förster radii (about twice the value estimated for organic dyes) and multiplex analysis.⁶⁰ This technology is best applied for *in vitro* assays, due to QDs' slight toxicity.

1.4 Circularly polarised luminescence

1.4.1 Linearly and circularly polarised light

Light can be described with a transverse waves and its polarisation is determined by the direction of its electric field.⁶¹ When the electric field oscillations are confined to a single plane we have linearly polarised light (LP).

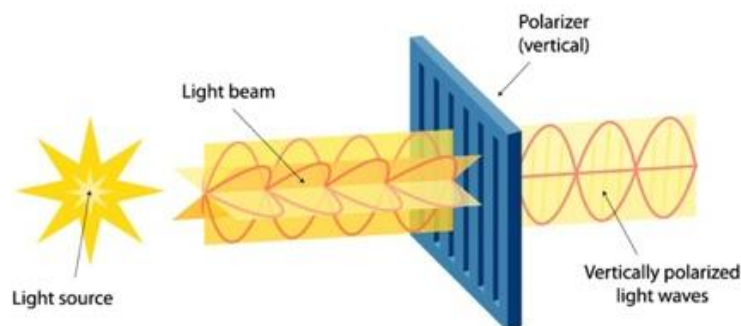


Figure 26: Unpolarised and linearly polarised light.

When the electric field vector maintains the same magnitude, but changes its orientation describing a helix in the direction of propagation, we have circularly polarised light (CP); this type of polarisation can be described as the vector sum of vertical and horizontal polarised lights that are 90° out of phase. The helix described can be right (R-CP light) or left (L-CP light) handed.

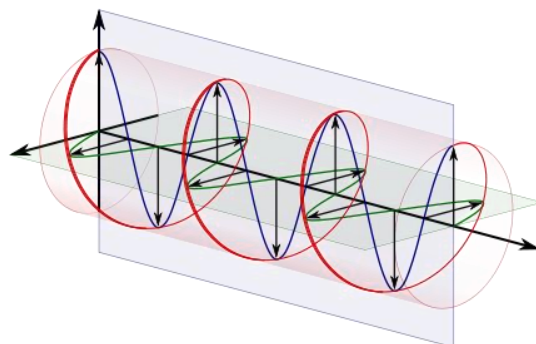


Figure 27: Right circularly polarised light (*red*) as a sum of vertical (*blue*) and horizontal (*green*) polarised light.

Linear polarised light can be seen as the sum of right and left CP light. A chiral molecule interacts differently with these two components of LP light. The different absorbance of right and left CP is the base of circular dichroism (CD). CD spectroscopy has found many applications in the studies of chiral macromolecules or complex biological structures, such as proteins, due to their high degree of chirality.⁶²

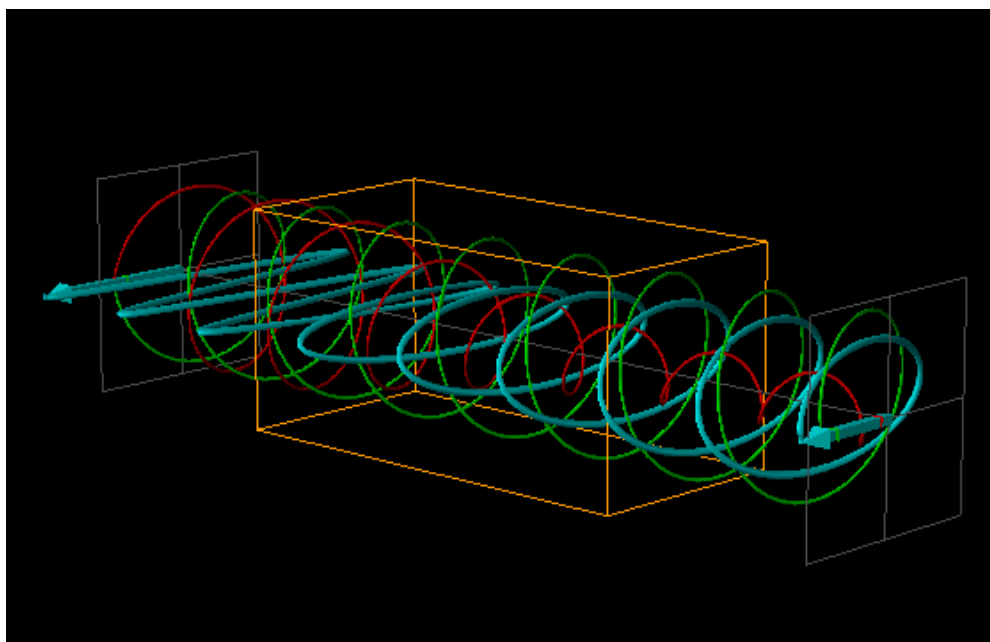


Figure 28: Cartoon explaining CD. LP light (blue) becomes elliptically polarised light after interaction with the sample (orange box) because of the predominant absorption of R-CP light (red) compared to L-CP light (green).

1.4.2 Circularly polarised luminescence spectroscopy

The equivalent in emission of circular dichroism is circularly polarised luminescence (CPL).⁶³ In CPL spectroscopy the difference in intensity of left (I_L) and right (I_R) circularly polarised components is monitored as a function of wavelength. The degree of CPL is quantified by the emission dissymmetry factor g_{em} .

$$g_{em} = \frac{2(I_L - I_R)}{I_L + I_R} \quad [5]$$

Although CPL can be measured for organic molecules⁶⁴⁻⁶⁵ and transition metal complexes,⁶⁶⁻⁶⁷ the properties of lanthanide complexes make them most commonly used with this technique. In fact, lanthanide ions are considered pure spherical emitters avoiding problems of anisotropy. In addition, the magnetic-dipole nature of the f - f transitions of lanthanides gives rise to large values of $|g_{em}|$ (usually between 0.1 and 0.5 compared to < 0.01 for organic molecules).

1.4.3 Lanthanide complexes in CPL spectroscopy

The advantageous CPL properties of lanthanide cations have been exploited for the design of emissive optical probes in order to get information on the chiral environment.⁶⁸ Two classes

of CPL lanthanides probes can be considered depending on the chirality of the functional ligand.

The use of an achiral ligand generally gives rise to a 50 : 50 mixture of interconverting Δ and Λ enantiomers (*Figure 29*). The perturbation of the dynamic equilibrium between the two interconverting enantiomers in the presence of an added chiral species leads to the activation of an observable CPL signal. This can happen with a non-covalent association between the complex and the chiral species studied⁶⁹ or with an actual change in the coordination environment of the lanthanide ion.⁷⁰

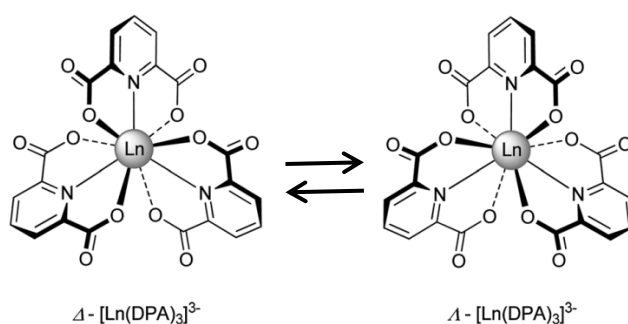


Figure 29: Examples of the use of an achiral ligand, pyridine-2,6-dicarboxylate (DPA), for the formation of a 50 : 50 mixture of Δ and Λ enantiomers.⁷¹

On the contrary, the use of an enantiopure ligand typically provides the presence of a dominant stereoisomer in solution. In this case, the interaction between the complex and the species of interest results in an altered CPL signal.

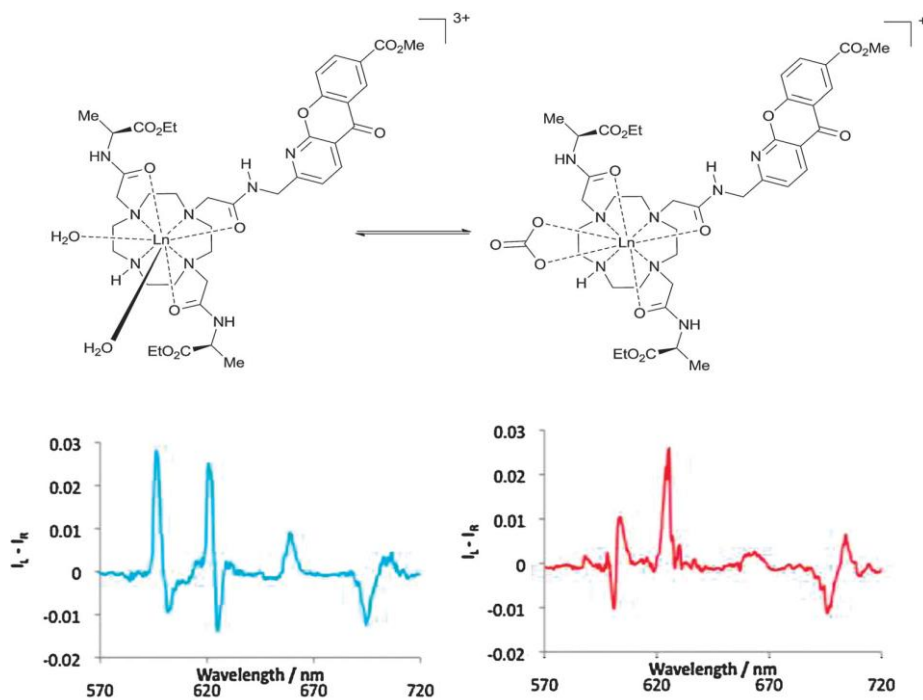


Figure 30: Changes in the Eu(III) CPL fingerprints upon addition of bicarbonate.⁷²

The synthesis of an enantiopure system is very challenging, often requiring long and tedious chiral chromatography purifications. A logical way to proceed is the transmission of the chiral information from the ligand to the metal centre. The incorporation of a single C-substitution into the ligand system to control the final geometry at the metal centre offers a promising method for the production of enantiomerically pure systems.⁷³

1.5 Aims of the project

Although the commercially available complexes described in *Section 1.3.3* are excellent for fluorescence microscopy and spectroscopy, an improvement regarding their energy transfer properties can be achieved by increasing the spectral overlap and the efficiency of energy transfer. This will permit the design of novel bioassays that use smaller quantities of material and reduced costs.

A new series of very bright emissive europium complexes was required to be synthesised and characterised, in order to provide better and more efficient donors for time resolved FRET applications.

The characteristics required for the design of the Eu(III) complex as a good donor are:

- **High brightness:** the combination of large molar extinction coefficients and high quantum yields is essential for the visualisation of low concentrations of the complex in cellular bioassays;
- **Excitation wavelength:** the antenna requires an excitation wavelength above 330 nm, in order to avoid the excitation of endogenous chromophores and to match well with available excitation sources at 337, 355 and 365 nm;
- **Long luminescence lifetime:** a luminescence lifetime of at least 1 ms is necessary for the use of time gated measurements;
- **Chemical stability:** the complex has to be kinetically and thermodynamically stable towards dissociation in biological media;
- **Appropriate spectral properties:** as the acceptor will be a cyanine dye (red acceptor), the emission spectrum should present high emission intensity in the spectral region around 600 - 630 nm and low emission in the other parts of the spectrum, notably around 650 - 710 nm (emission of the donor);
- **Water solubility:** the complex should be soluble in buffered aqueous solution at pH = 7;
- **Point of conjugation:** the complex should present a reactive functional group, such as a primary amine or a carboxylic acid that permits easy conjugation with the biomolecule chosen for the assay.

The first five points have, to a considerable extent, been realised by prior work in the period 2008-11 using complexes with the general structure of **[Eu·1.6]** (*Section 1.2.3*). These complexes will be analysed first in order to understand their behaviour as donors in FRET experiments. The synthetic work in this thesis focuses on the introduction of a linkage point for conjugation with biomolecules and on the improvement of the water solubility of these systems, involving the development of new methodology.

2 A series of highly emissive europium complexes

2.1 Introduction

The Eu(III) complex [Eu•1.6] presented in Section 1.2.3 is the brightest example of a europium complex reported in the literature ($B = 32 \text{ mM}^{-1} \text{ cm}^{-1}$ at 332 nm in MeOH).⁴⁴ The combination of three pyridyl-alkynyl-aryl moieties and the effective shielding of the Eu(III) ion using a triazacyclononane ligand provides a big overall extinction coefficient of $60,000 \text{ M}^{-1} \text{ cm}^{-1}$ and extremely high quantum yields (up to 50 % in MeOH). Many examples have been synthesised incorporating different donor groups to complex the metal ion (*e.g.* carboxylate and phosphinate). In addition, a large variety of substituted aryl groups has been tested, in order to tune the photophysical properties, in particular λ_{max} and ϵ .⁷⁴

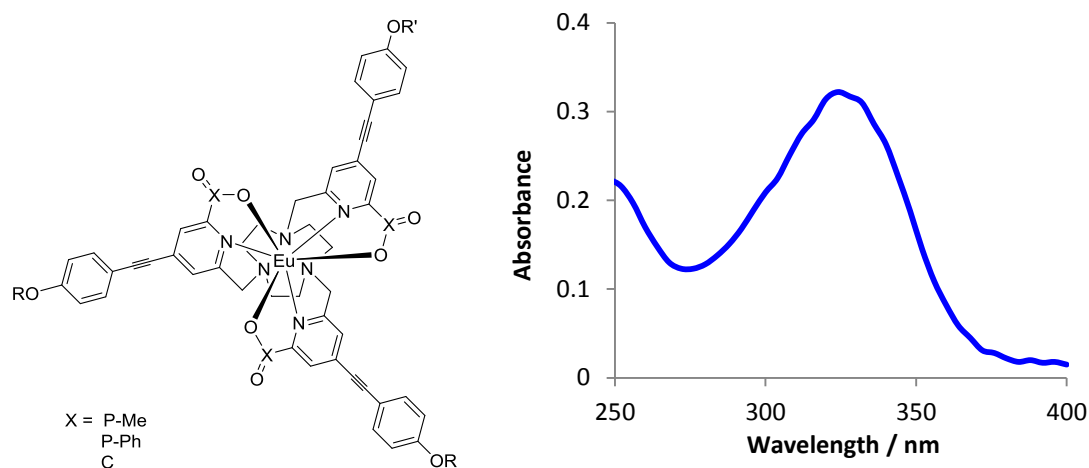


Figure 31: General structure of the series of highly emissive europium complexes (*left*), typical absorption spectrum for these complexes (*right*).

The maximum of absorption for these complexes is typically around 330 nm, into the broad absorption band. The absorption band extends to 355 nm and even 365 nm (*Figure 31*) permitting the use of various excitation sources.

Especially for the phosphinate systems, the very effective shielding of the Eu(III) ion provides long luminescence lifetimes (typically $\geq 1 \text{ ms}$) and enhanced stability towards intramolecular quenching (*e.g.* by Mn^{2+} , urate or citrate).

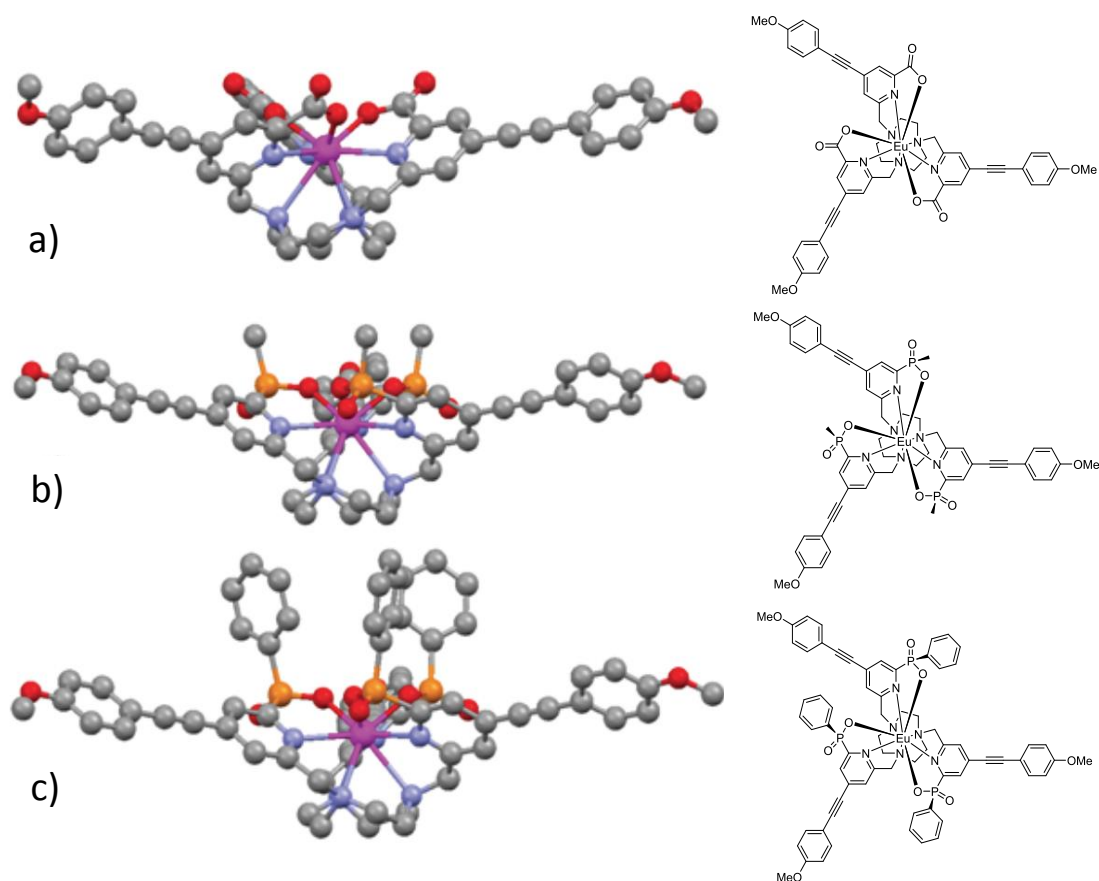


Figure 32: DFT calculated structures for carboxylate (a), P-Me (b) and P-Ph (c) phosphinate systems, showing the steric shielding for the phosphinate series (in particular for the P-Ph system).^{75 a}

2.2 Photophysical investigation

The photophysical analysis of three different Eu(III) complexes (Figure 33) was carried out in order to understand if these complexes were suitable as donors in standard FRET experiments. These complexes differ from each other in the nature of the substituent on the pyridine ring; two of them possess phosphinate donors (P-Me and P-Ph) and the third is the carboxylate analogue. Each complex presents a slightly distorted C_3 symmetry that leads to minimal splitting of the $\Delta J = 1$ and $\Delta J = 2$ manifolds in their Eu(III) emission spectra.

^a The phosphinate complexes exist as a pair of enantiomers (*RRR-Δ* and *SSS-Δ*), from now on only one isomer will be drawn. A detailed discussion of the stereochemistry of these complexes can be found in Chapter 5.

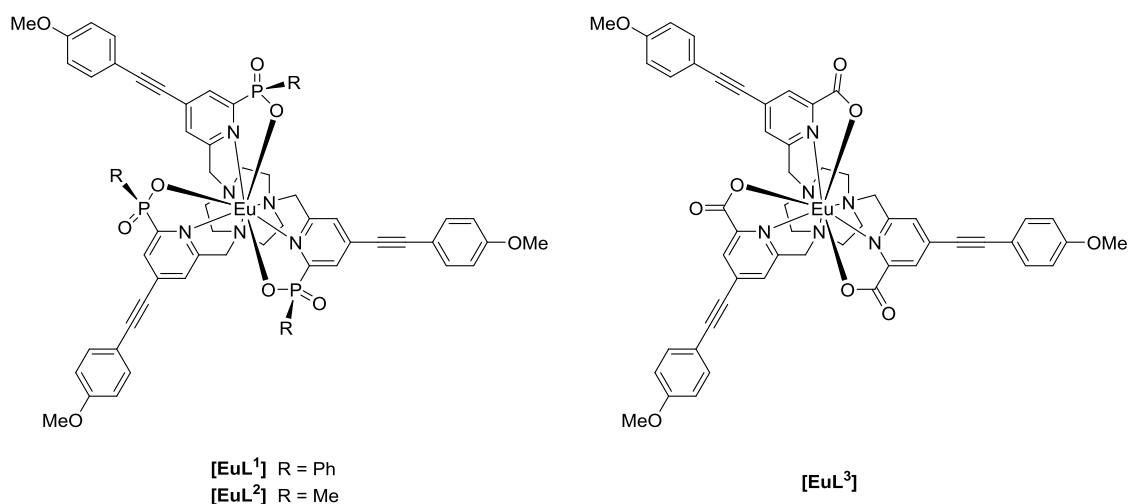


Figure 33: Structure of three Eu(III) complexes bearing different donor substituents.

The emission spectra were recorded at the same concentration (5 μM) in methanol to allow for direct comparison. A very intense set of $\Delta J = 2$ transitions was observed around 610 - 620 nm for each of the three complexes. The spectra revealed that the carboxylate system has the largest $\Delta J = 2/\Delta J = 1$ intensity ratio by about 10 %. Minor changes in the form of the hypersensitive $\Delta J = 2$ manifold were observed, most probably associated with variation of oxygen donor polarisability. The spectra for the two phosphinate derivatives did not display any significant differences.

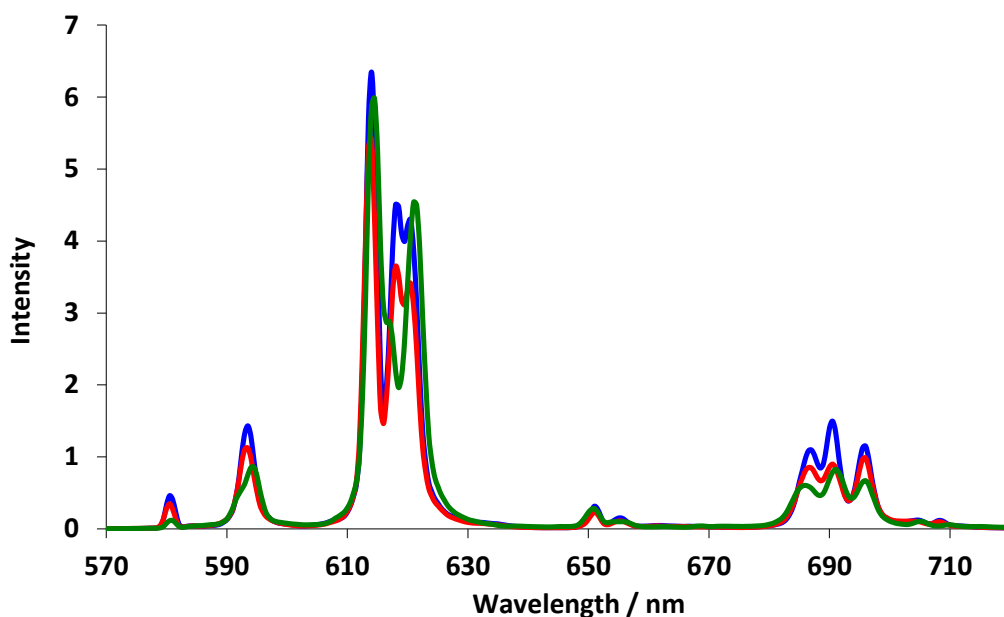


Figure 34: Emission spectra of **[EuL¹]** (blue), **[EuL²]** (red) and **[EuL³]** (green), (MeOH, 295 K).

Overall quantum yields and lifetimes were calculated and showed similar values for each complex (Table 2). The crystal structure of $[\text{EuL}^1]$ (Figure 35) revealed that the Eu(III) ion is encapsulated by the ligand in a tricapped trigonal prismatic array where the nearest water molecules are over 6 Å from the metal ion. The long distance to the nearest quenching OH oscillator partly explains the high quantum yields.

Table 2: Photophysical properties of three Eu(III) complexes. (MeOH, 295 K).^a

	$\lambda_{\text{max}} / \text{nm}$	$\epsilon / \text{mM}^{-1} \text{cm}^{-1}$	τ_0 / ms	$\Phi_{\text{em}} / \%$
$[\text{EuL}^1]$	332	58.0	1.26	52
$[\text{EuL}^2]$	332	58.1	1.18	43
$[\text{EuL}^3]$	340	58.0	0.95	48

^a Errors on λ_{max} , ϵ , τ_0 and Φ_{em} are $\pm 10\%$.

The Eu(III) emission lifetimes follow the trend P-Ph > P-Me > carboxylate, in accord with the tendency of the phosphorus substituents to block the “upper face” of the complex.

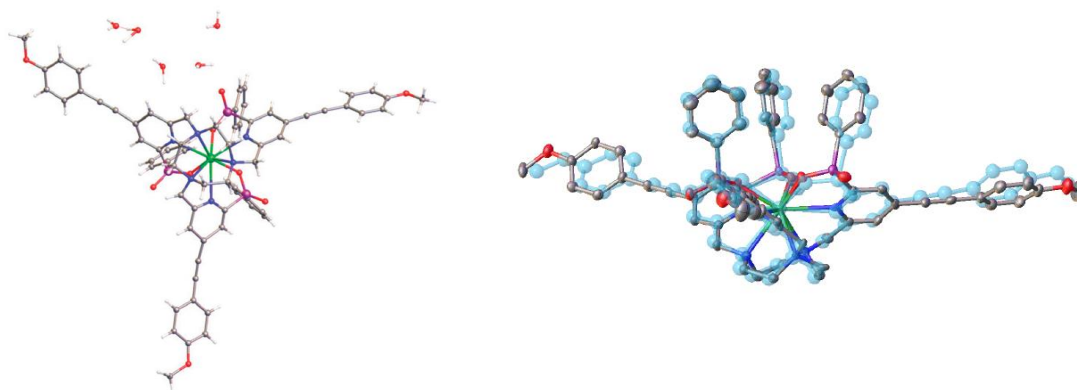


Figure 35: Molecular structure of $[\text{EuL}^1]$ showing part of the hydration sphere (120 K) (left), comparison between X-ray and DFT calculated structures (right).⁴⁴

2.3 Energy transfer analysis

The acceptor chosen for the energy transfer studies is the commercially available cyanine dye **Dy647-NH₂** (Figure 36). This dye was selected because it is the acceptor used for the commercial bioassays marketed by Cisbio Bioassays.

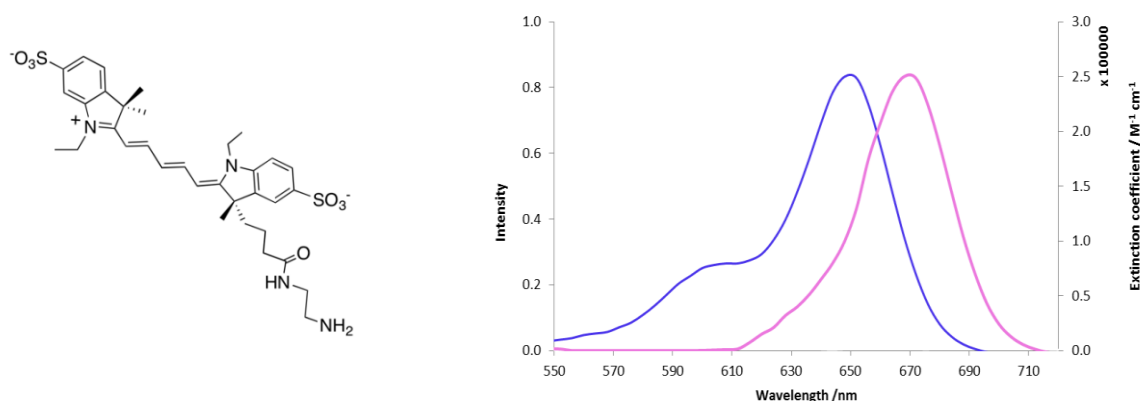


Figure 36: Structure of the cyanine dye **Dy647-NH₂** and its absorption (blue) and emission (purple) spectra, (H₂O, 295 K).

The emission form of the three Eu(III) complexes described above presents the optimal profile required for efficient energy transfer. Indeed, the intense emission at 610-620 nm provides good spectral overlap with the acceptor absorption band and the absence of emission at 670 nm permits the monitoring of the two species without significant spectral overlap.

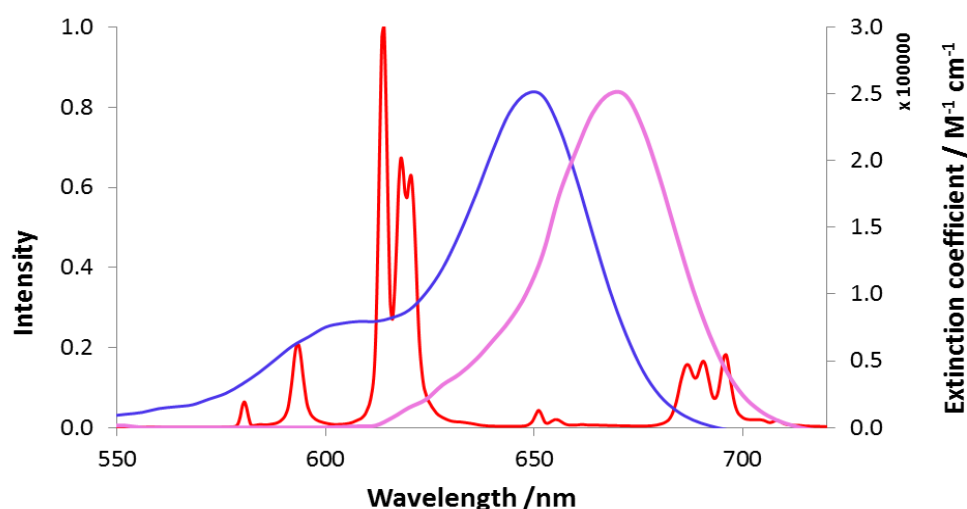


Figure 37: Cyanine dye absorbance (blue) and emission (purple) spectra and **[EuL¹]** emission spectrum (red), (MeOH, 295 K).

2.3.1 Studies of energy transfer in methanol

The quenching of these three complexes by the cyanine dye **Dy647-NH₂** was examined by observing changes in Eu(III) lifetime as a function of added acceptor concentration over the range 0.3 to 5 μ M, using 5 μ M solutions of the Eu(III) complex.

In the rapid diffusion limit, energy transfer from a donor to the quenching acceptor obeys pseudo-first order kinetics.⁷⁶

$$\frac{1}{\tau_0} = k_0 \quad [6] \quad \frac{1}{\tau} = k_{obs} \quad [7] \quad k_{obs} = k_0 + k_2[Q] \quad [8]$$

$$\frac{\tau_0}{\tau} = \frac{k_{obs}}{k_0} = 1 + \frac{k_2}{k_0}[Q] \quad [9]$$

Hence, the slope of a plot of τ_0/τ vs $[Q]$ represents k_2/k_0 , allowing the second order rate constant for energy transfer, k_2 , to be estimated.

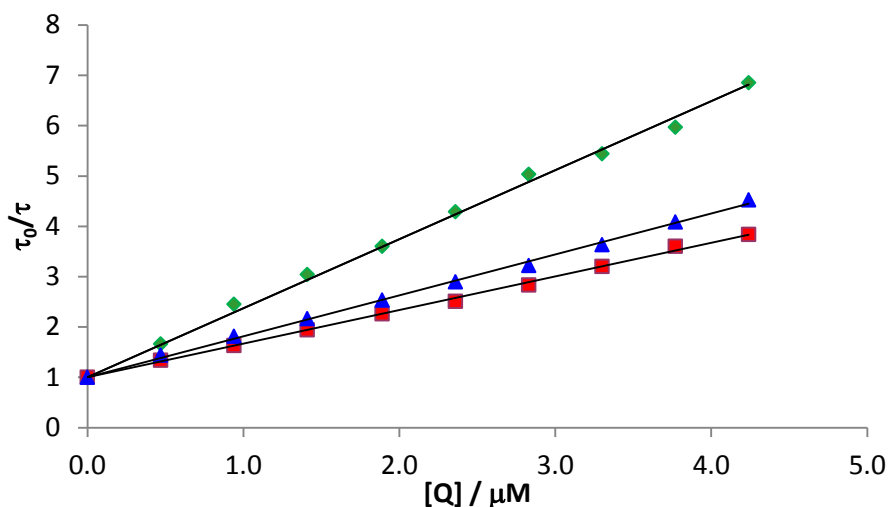


Table 3: Quenching studies for $[\text{EuL}^1]$ (blue), $[\text{EuL}^2]$ (red) and $[\text{EuL}^3]$ (green), (Values recorded ($\pm 5\%$) in MeOH, 295 K).

	<i>gradient</i>	τ_0 / ms	$k_2 / \text{mM}^{-1}\text{s}^{-1}$ (± 0.05)
$[\text{EuL}^1]$	0.81	1.26	0.64
$[\text{EuL}^2]$	0.67	1.18	0.57
$[\text{EuL}^3]$	1.33	0.95	1.40

The order of the rate constants shows that an enhanced rate of energy transfer from the carboxylate derivative occurs compared to the pair of phosphinates, which are more or less the same within experimental error. This can be tentatively ascribed, in part, to a slightly better spectral overlap integral for the carboxylate system, examining the $\Delta J = 2$ band intensity vs acceptor dye absorption band. Another possible difference is the electric dipole transition moments for each system: here, the extended conjugation of the carboxylate system (C=O is conjugated into the pyridyl chromophore) and associated greater polarisability may favour this system over the phosphinates, where the P=O is not in conjugation. Finally, it

may simply be a steric effect, where the P-substituents inhibit the approach of the acceptor, although this seems less likely, given the long distances over which such energy transfer process are believed to occur.

Following the quenching studies, some calculations were undertaken in order to estimate the Förster radius (R_0) and the spectral overlap (J) for the three Eu(III) complexes with this acceptor (Table 4).

$$R_0 = (Jk^2\Phi_0\eta^{-4})^{\frac{1}{6}} \cdot (9.79 \cdot 10^2) \quad [3]$$

$$J(\lambda) = \frac{\int F(\lambda)\epsilon(\lambda)\lambda^4 d\lambda}{\int F(\lambda)d\lambda} \quad [4]$$

Table 4: Förster radii calculated for three Eu(III) complexes, (MeOH, 295 K).^a

	[EuL ¹]	[EuL ²]	[EuL ³]
$J / \text{M}^{-1}\text{cm}^3$	1.016×10^{-12}	1.184×10^{-12}	1.109×10^{-12}
Φ	0.52	0.43	0.48
τ_0 / ms	1.26	1.18	0.95
R_0 / nm	6.81	6.77	6.86
$k_2 / \text{mM}^{-1}\text{s}^{-1}$	0.64	0.57	1.40

^a The spectral overlap was calculated for $550 < \lambda < 720$ nm. The refractive index for MeOH is 1.328, compared to 1.333 for H₂O. Errors on τ_0 , and Φ_{em} are $\pm 10\%$.

2.3.2 Studies of energy transfer in water

Due to the extremely low water solubility of [EuL¹] and the carboxylate analogue [EuL³] it was possible to carry out the quenching studies in water (50 mM HEPES buffer, 50 mM NaCl, pH = 7.4) only for the P-Me derivative [EuL²].

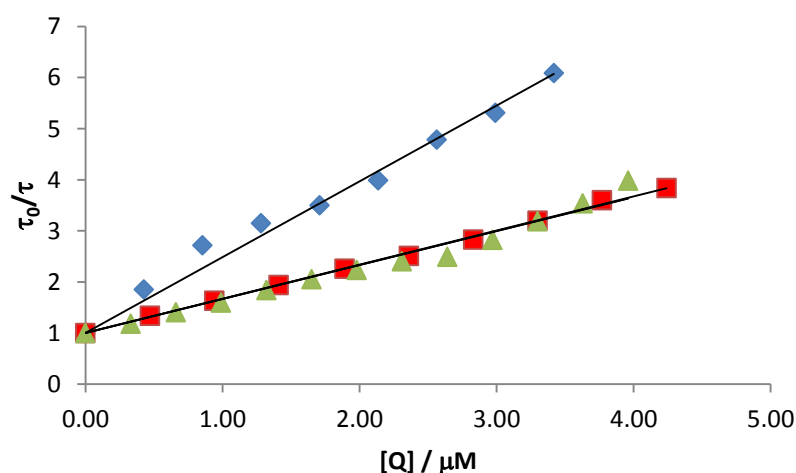
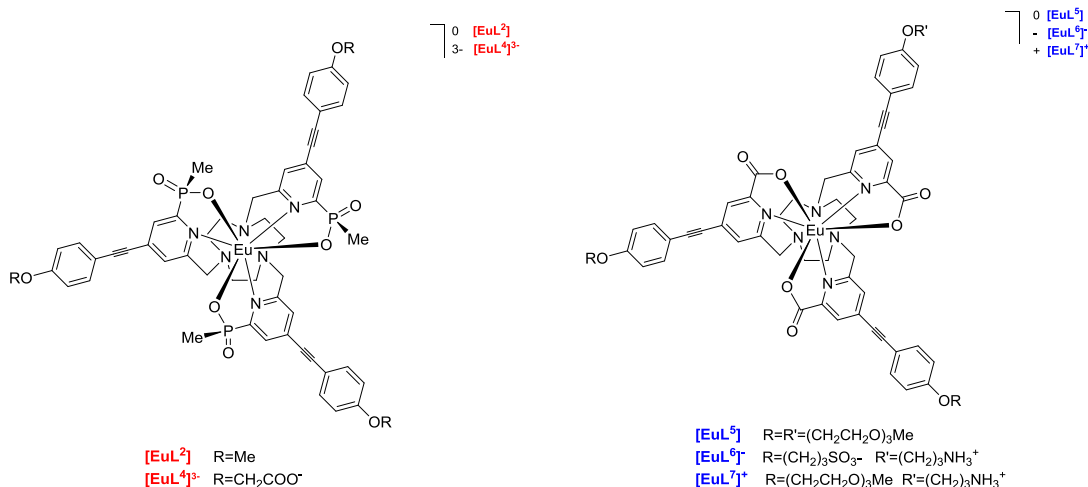


Table 5: Quenching studies for $[\text{EuL}^2]$ in different solvents. (Values recorded ($\pm 5\%$) at 295 K in: 100 % 50 mM HEPES buffer, 50 mM NaCl, pH = 7.4 (*blue*); 50% 50 mM HEPES buffer, 50 mM NaCl and 50 % MeOH (*green*); 100 % MeOH (*red*). $\lambda_{\text{ex}} = 332$ nm).

Solvent	gradient	τ_0 / ms	$k_2/\text{mM}^{-1}\text{s}^{-1}$ (± 0.05)
MeOH	0.62	1.18	0.57
MeOH : H ₂ O (50:50)	0.67	1.11	0.56
H ₂ O	1.64	1.03	1.59

The results showed a small increase in the value of k_2 calculated in water compared to that measured in MeOH. This result can be ascribed to the increased polarity of water. No differences in k_2 were observed between 100 % MeOH and MeOH/H₂O 50:50. This is probably due to specific solvation of the complex by methanol. Indeed, Soper has shown that in binary mixtures of water and alcohols, clusters of alcohol molecules occur (or vice versa), so that the more hydrophobic solute is undergoing specific solvation by such a cluster.⁷⁷

In order to understand the FRET mechanism better, and in particular consider the differences in behaviour of the carboxylate and phosphinate complexes, additional different complexes were analysed in water (50 mM HEPES buffer, 50 mM NaCl, pH = 7.4). Complexes $[\text{EuL}^2]$ and $[\text{EuL}^4]^{3-}$ were provided by Dr. Brian McMahon and Dr. Stephen Butler, complexes $[\text{EuL}^5]$, $[\text{EuL}^6]$, $[\text{EuL}^7]^+$ and $[\text{EuL}^9]^+$ were supplied by Cisbio and $[\text{EuL}^8]$ was synthesised (details of the synthesis are given in *Chapter 5*).⁷⁸ The quenching of these complexes was examined using 4 μM solutions of the Eu(III) complex in the presence of quencher concentrations over the range 0.3 to 2.5 μM .



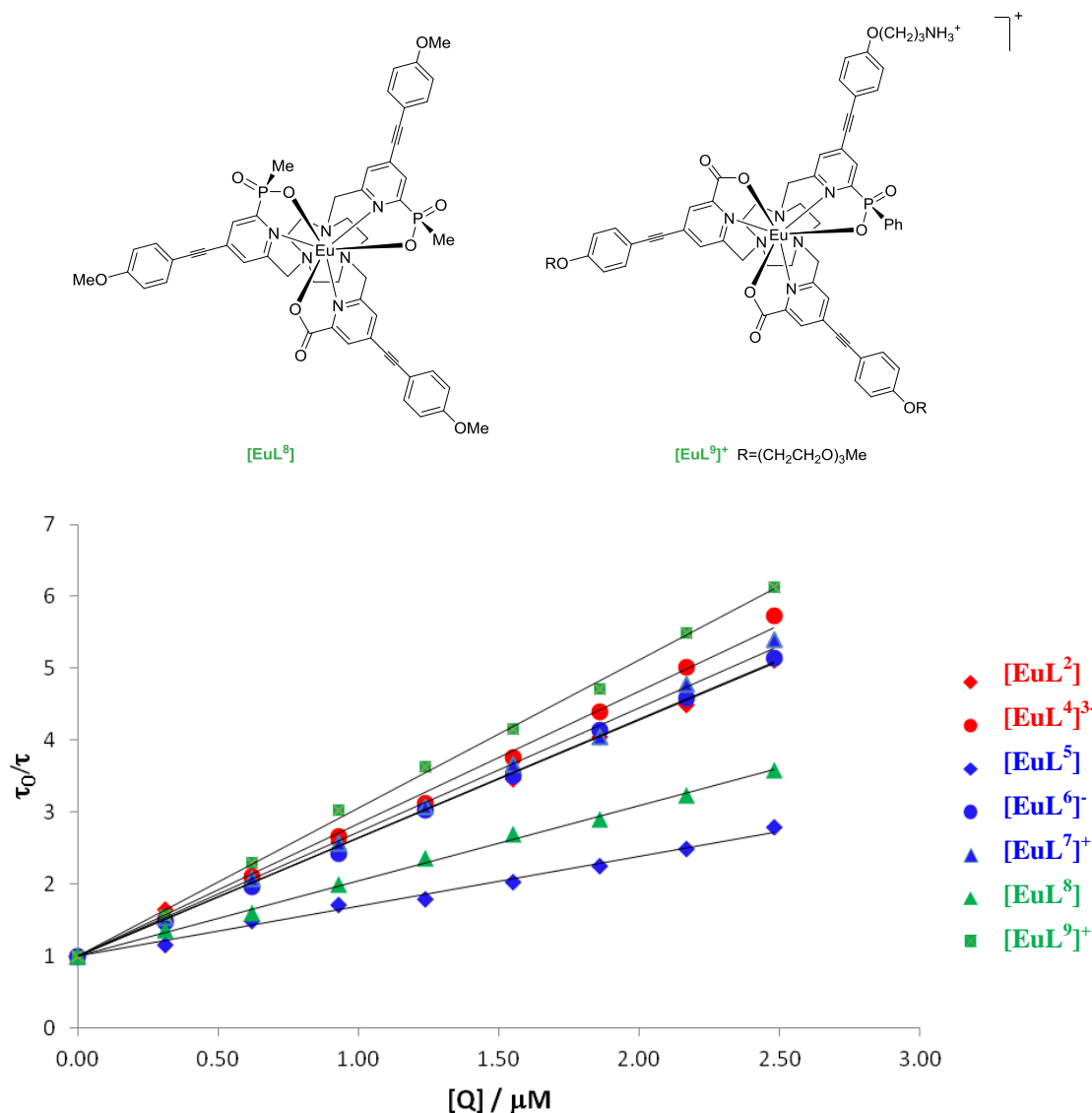


Table 6: Quenching studies. (Values recorded (\pm 5%) in 50 mM HEPES buffer, 50 mM NaCl, pH = 7.4, 295 K).

		gradient	τ_0 / ms	k_2 / $\text{mM}^{-1}\text{s}^{-1}$
[EuL ²]	3P-Me (3OMe)	1.64	1.03	1.59
[EuL ⁴] ³⁻	3P-Me (3OCH ₂ COO ⁻)	1.84	1.04	1.77
[EuL ⁵]	3COO ⁻ (3PEG)	0.68	0.82	0.84
[EuL ⁶] ⁻	3COO ⁻ (2SO ₃ ⁻ , 1NH ₃ ⁺)	1.65	0.80	2.06
[EuL ⁷] ⁺	3COO ⁻ (2PEG, 1NH ₃ ⁺)	1.72	0.76	2.26
[EuL ⁸]	2P-Me 1COO ⁻ (3OMe)	0.95	0.89	1.07
[EuL ⁹] ⁺	1P-Ph 2COO ⁻ (2PEG, 1NH ₃ ⁺)	2.06	0.84	2.45

The analysis of the rate constants calculated for these complexes showed that in water there is very little difference between the phosphinate and the carboxylate systems. In addition, the

hybrid system (carboxylate and phosphinate) did not offer any obvious advantages with regard to rate constants. The negative charges on the chromophore helped water solubility; moreover, they did not seem to affect energy transfer kinetics. On the contrary, the PEG groups on the chromophore helped water solubility to some degree, but also seemed to protect the complex from quenching by the acceptor, and hence $[\text{EuL}^5]$ gave rise to the slowest rate of energy transfer observed in the series.

2.3.3 Comparison with commercially available donors

In order to have a comparison with the commercially available donors, the same quenching studies were performed for the donors $\text{Eu}(\text{TBP})$ and Lumi4-Tb (Section 1.3.3) in the presence of a range of concentrations of the cyanine dye acceptor Dy647-NH_2 . The structures and emission spectra for these two complexes are reported in Figure 38.

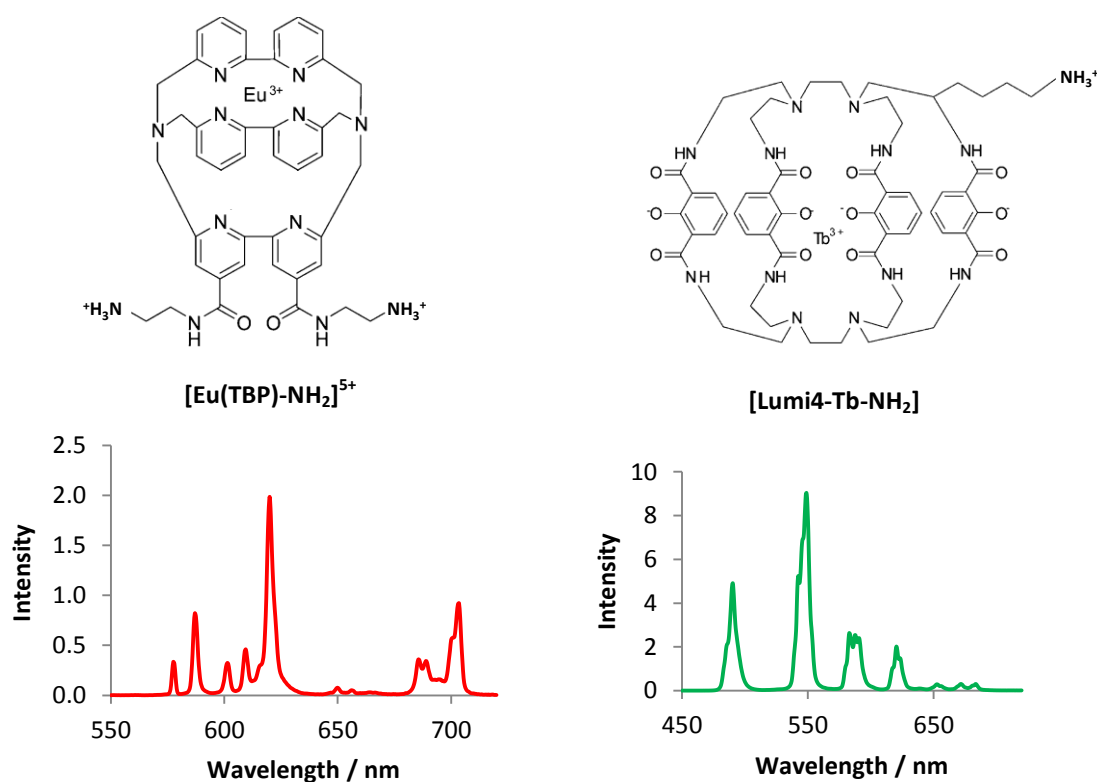


Figure 38: Structures and emission spectra of $\text{Eu}(\text{TBP})\text{-NH}_2$ (red) and Lumi4-Tb-NH_2 (green), (H_2O , 295K).

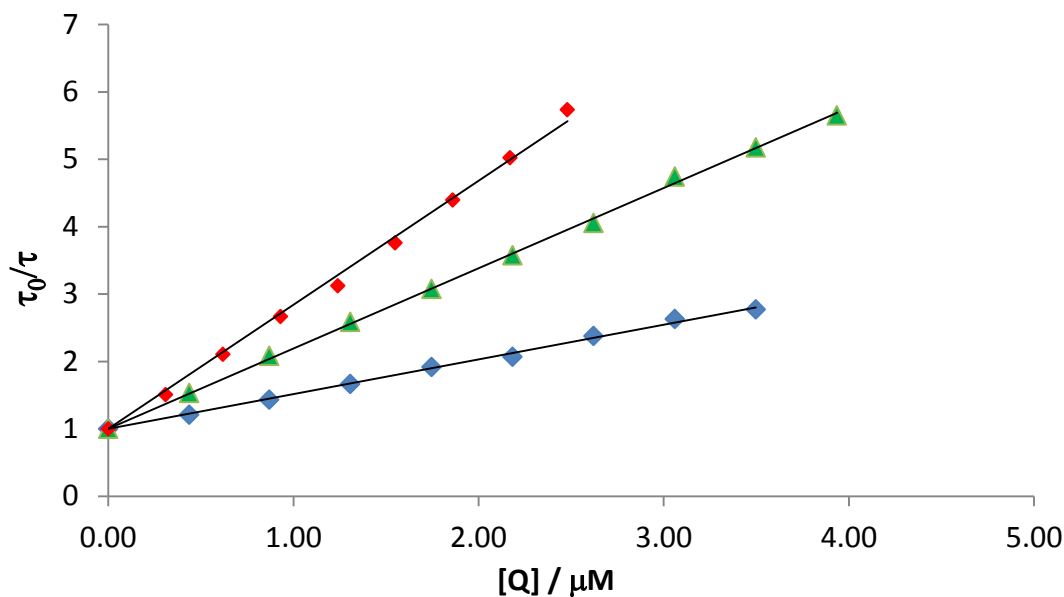


Table 7: Quenching studies for $[\text{EuL}^4]$ (red), Lumi4-Tb-NH_2 (green) and Eu(TBP)-NH_2 (blue). (Values recorded ($\pm 5\%$) in 50 mM HEPES buffer, 50 mM NaCl, pH = 7.4, 295 K).

	$\lambda_{\text{max}} / \text{nm}$	$\varepsilon / \text{M}^{-1}\text{cm}^{-1}$	$\Phi_{\text{em}} / \%$	τ_0 / ms	$k_2 / \text{mM}^{-1}\text{s}^{-1}$	$J / \text{M}^{-1}\text{cm}^3$	R_0 / nm
$[\text{EuTBP-NH}_2]^{5+}$	304	3600	2	0.56	0.92	8.5×10^{-13}	3.8
$[\text{Lumi4-Tb-NH}_2]$	340	26000	52	2.46	0.48	3.3×10^{-13}	5.6
$[\text{EuL}^4]^{3-}$	330	60000	22	1.04	1.77	10.0×10^{-13}	5.9

The spectral overlap was calculated for $550 < \lambda < 720$ nm. The refractive index for H_2O is 1.333. To allow for comparison, the results for $[\text{EuL}^4]^{3-}$ are reported as an average for all the complexes reported in Table 6.

The comparison showed a good improvement in terms of energy transfer properties for the new series of compounds. Indeed, a faster rate of energy transfer and a larger spectral overlap were calculated.

Although these results describe a diffusional energy transfer process, an estimation of the FRET efficiency for the couple donor-acceptor can be made measuring the differences in lifetime in the absence (τ_0) and in the presence of one equivalent of acceptor (τ_{DA}).

$$E = 1 - \frac{\tau_{DA}}{\tau_0} \quad [10]$$

For each of these complexes, extremely high values (higher than 90 %) can be estimated, making this process very efficient.

2.4 Water solubility determination

To complete this study, an experiment to quantify the relative hydrophilicity of these complexes ($\log P$ in water/octanol) was carried out in order to assess the correlation between the rate of energy transfer with the lipophilicity of each complex.

Three equimolar solutions of complex were prepared in MeOH. The solvent was removed under reduced pressure and the resulting solid was dissolved and stirred for 24 h in 0.9 mL of a mixture of water/octanol (2:1, 1:1, 1:2) giving a total concentration of approximately $2 \mu\text{M}$ for each mixture. After equilibration, an emission spectrum for each layer was recorded in MeOH (50 μL of solution in 1 mL of MeOH). For each mixture, the $\log P$ value was calculated, according to the following equation:

$$\text{Log}P = \text{Log} \left(\frac{\int_{605\text{nm}}^{635\text{nm}} I(\text{oct})}{\int_{605\text{nm}}^{635\text{nm}} I(\text{H}_2\text{O})} \right) \quad [11]$$

Final $\log P$ values were calculated as the average of three solvent mixtures.

In addition to the previously reported complexes, new examples were examined in order to have a better understanding of the functionalities that play a key role in the hydrophilicity of these systems.

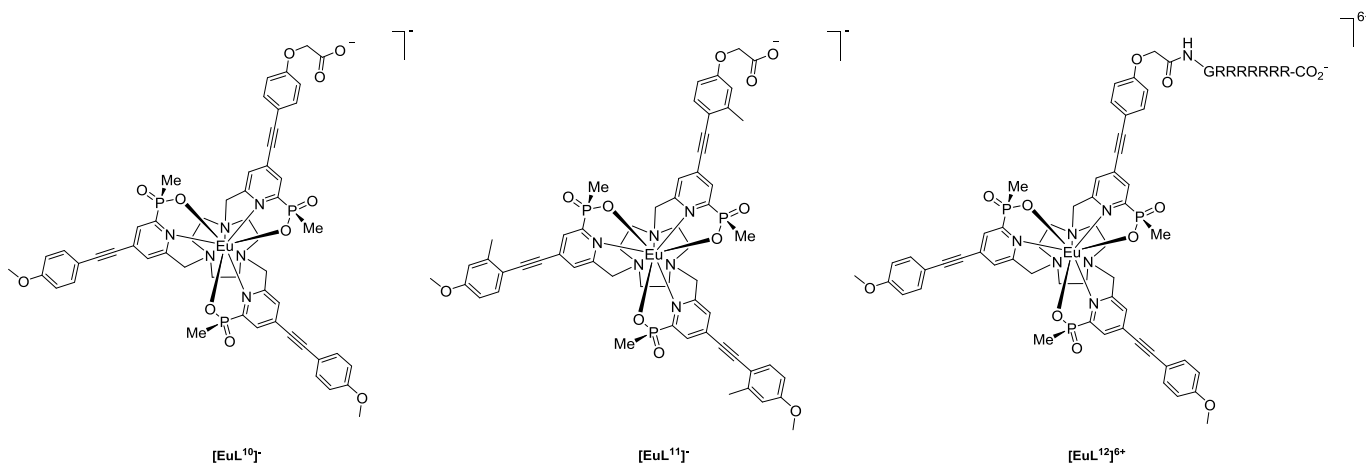


Figure 39: New Eu(III) complexes examined.

Table 8: $\log P$ values for a series of Eu(III) complexes.

	$\log P$
$[\text{EuL}^2]$	1.4 ± 0.3
$[\text{EuL}^9]^+$	1.2 ± 0.2

[EuL ⁵]	1.1 ± 0.2
[EuL ⁸]	1.1 ± 0.2
[EuL ¹¹] ⁻	0.8 ± 0.2
[EuL ⁷] ⁺	0.7 ± 0.2
[EuL ¹⁰] ⁻	0.3 ± 0.1
[EuL ¹²] ⁶⁺	0.3 ± 0.1
[EuL ⁶] ⁻	- 1.1 ± 0.2
[EuL ⁴] ³⁻	- 2.2 ± 0.4

Complex [EuL¹] and [EuL³] have a logP > 2

From these data, it is clear that the introduction of charged moieties close to the chromophore (*e.g.* [EuL⁴]³⁻) increased the water solubility of the system. On the contrary, the PEG groups only showed a small effect (*i.e.* [EuL⁵]). Unfortunately, these results did not show any particular correlation with the rate of energy transfer.

2.5 Conclusions

The photophysical analysis of a series of very bright Eu(III) complexes, based on the 9-N₃ ring substituted with three pyridyl-alkynyl-aryl chromophores, showed very promising properties. For example, the complexes possess a very intense set of $\Delta J = 2$ transitions (610 - 620 nm), high quantum yields (> 20 % in water) and long lifetimes (1.0 ms). These features are of fundamental importance for the use of these complexes as donors in FRET based experiments.

The quenching of these complexes by the cyanine dye acceptor, **Dy647-NH₂**, revealed an improvement in terms of FRET properties; faster rates of energy transfer and bigger spectral overlaps were measured, compared to the commercially available donors **Eu(TBP)** and **Lumi4-Tb**.

These results provide the starting point for the design of a new series of compounds as very efficient donors for FRET experiments.

3 A new series of C-substituted europium complexes

3.1 Introduction

As discussed in *Section 1.5*, a linkage point for conjugation with the biomolecule is of fundamental importance for the use of these complexes in bioassays. Maintaining the general structure of the complexes described in *Chapter 2*, the introduction of an aliphatic chain on the azamacrocycle, terminally substituted with a primary amine, was studied. This approach avoids the introduction of different antennae substituents on the macrocyclic ring, as asymmetry in the aryl–alkynyl antennae complicates the synthesis.

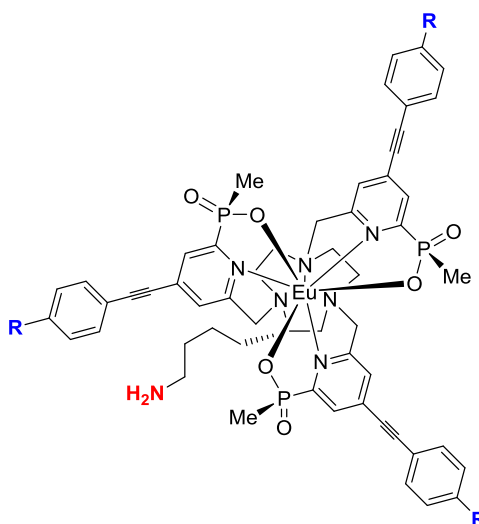


Figure 40: General structure of the new C-substituted series of complexes.

Due to the better water solubility and good stability towards quenching, the P-Me phosphinate donor was chosen for the general structure. In addition, the introduction of solubilising moieties at the end of the aryl–alkynyl antennae was considered, to increase water solubility even further.

3.2 A model C-substituted complex

The synthesis of a model C-substituted 9-N₃ derivative, which allows for linkage *via* the C-substituent, was examined initially, in order to assess the effect of substitution on the europium emission spectral form (specifically the $\Delta J = 2/\Delta J = 1$ intensity ratio).

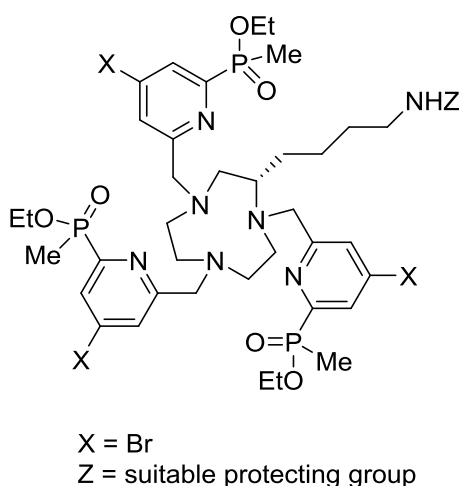


Figure 41: Structure of the model C-substituted 9-N₃ derivative.

The *p*-Br substituent on the pyridyl ring allows for the synthesis of an extended chromophore by Sonogashira coupling.⁷⁹

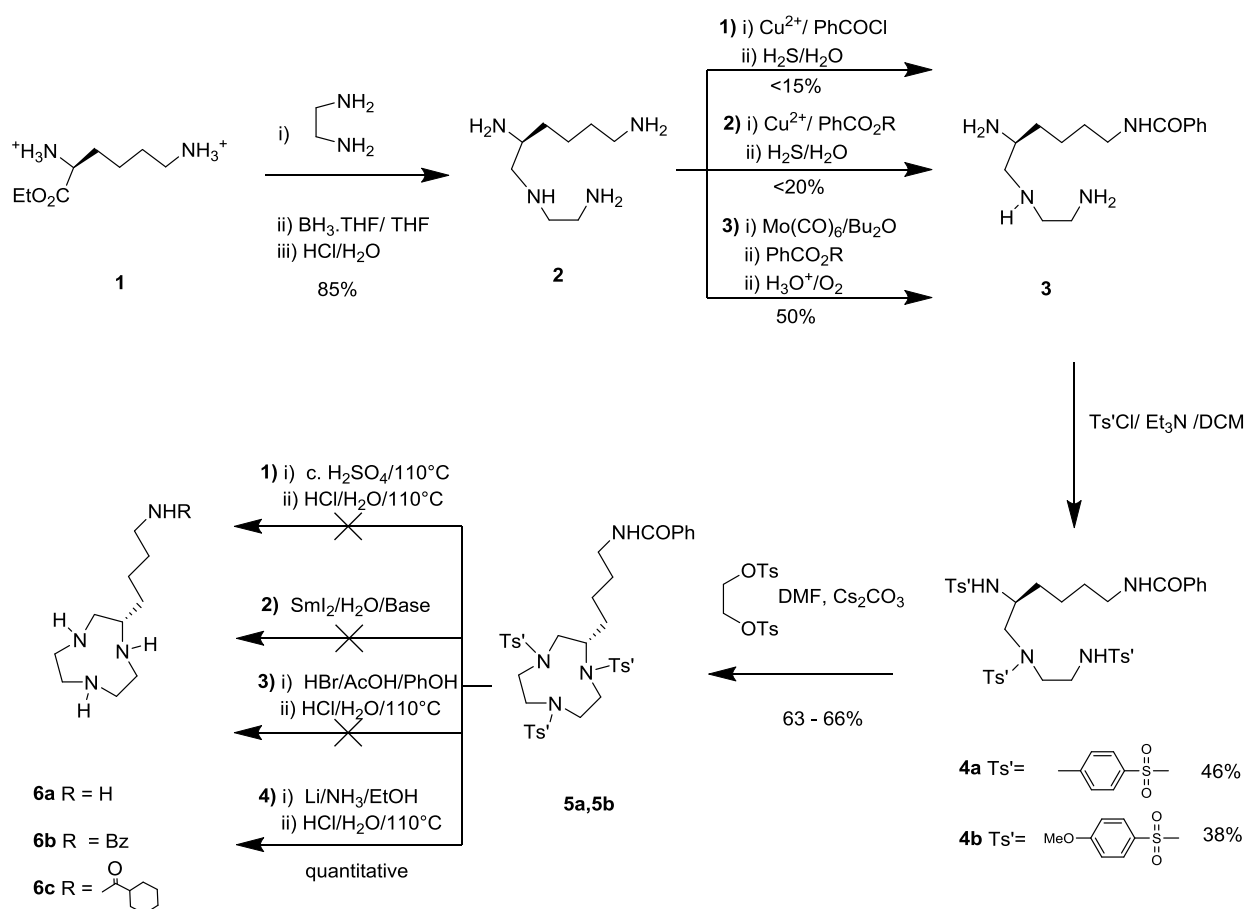
3.2.1 Synthetic aspects

The following methodology for the synthesis of the C-substituted azamacrocycle is based on a procedure reported by Parker et al.,⁸⁰ that has subsequently been scaled-up to 2 g for GMP (Celltech). Some modifications to improve yield and chemoselectivity of certain steps will be discussed in detail.

The synthesis started with the reaction of the ethyl ester of lysine **1** with neat ethylenediamine to form the monoamide, which was reduced using the BH₃-THF complex to give the tetraamine **2**, isolated as the hydrochloride salt in quantitative yield.

Protection of three nitrogens with Cu²⁺_(aq) permitted the selective acylation of the remote amino group with benzoyl chloride (in the presence of KOH). Treatment of the copper complex with H₂S permitted isolation of the free benzamide **3** in a 15 % yield. In order to improve the yield of the second step, which had disappointingly low yields on multi-gram scales, two alternative reactions were investigated. The replacement of benzoyl chloride with the corresponding NHS active ester permitted the avoidance of pH variation during the reaction. Unfortunately, this method did not show a great yield improvement (isolated yield of **3** < 20 % vs < 15 %). The treatment of **2** (as the free amine) with Mo(CO)₆ was found to be a better strategy for this selective reaction. Mo(CO)₆ formed an octahedral complex with the three amines close to each other, leaving the remote NH₂ free to react with the active ester

of benzoic acid.⁸¹ This route gave a better yield of **3** (50 %) and it was successfully scaled up to 1 g.



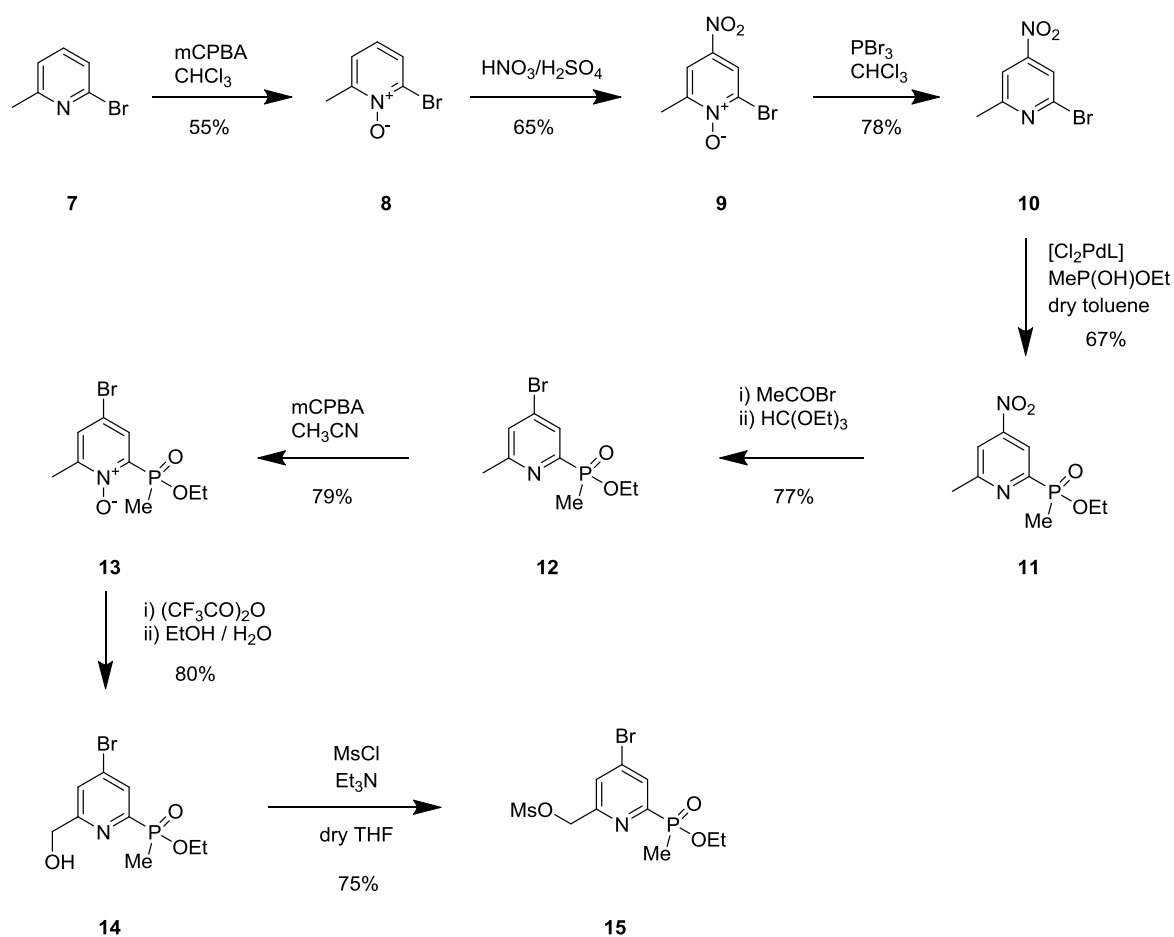
Scheme 1: Synthesis and yield optimisation of the C-substituted azamacrocycle, **6**.

Tosylation with TsCl in DCM in the presence of Et_3N gave the intermediate **4a**, which was used for condensation with ethylene glycol ditosylate in DMF using Cs_2CO_3 as base, to afford the 9-membered macrocycle **5a** in a reasonable yield (66 %).

Deprotection of compound **5a** was attempted with concentrated H_2SO_4 but the product **6b** was isolated only in a very poor yield (< 10 %). Another strategy that could lead directly to compound **6a** was the treatment with SmI_2 in presence of H_2O and pyrrolidine.⁸² Mass spectral analysis of the product mixture showed complete deprotection of the 9- N_3 ring, but the product could not be easily separated from the pyrrolidine that is required in large excess (18 eq). The use of *p*-methoxybenzenesulfonyl chloride is described as an alternative to tosyl chloride; in principle it should be removed under milder acidic conditions, *e.g.* with HBr in AcOH in the presence of PhOH (80 °C).⁸¹ Mass spectral and ^1H -NMR analysis showed

partial desotylation, but the addition of further HBr did not push the reaction to completion. The best way to cleave the tosyl group involved reduction with lithium in liquid ammonia that gave compound **6c** as the major product (MS showed the presence of compound **6a** in trace amounts). Treatment with 6 N HCl hydrolysed the amide bond and gave the desired compound **6a** as the tetrachloride salt. For the model complex, compound **6c**, containing traces of **6a**, was taken on without further purification and used for the subsequent alkylation step.

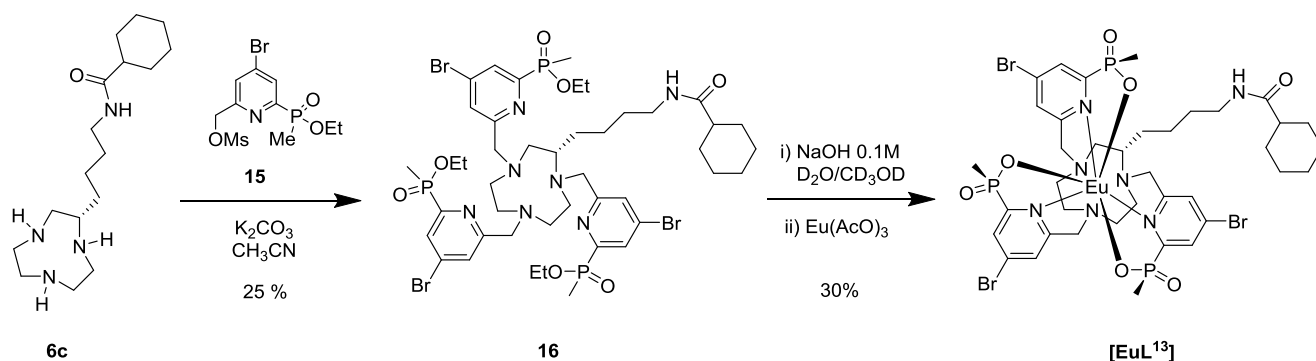
The synthesis of the pyridine platform **15** is a well-established procedure in the Durham group, involving 9 steps.⁴⁴



Scheme 2: Synthesis of the P-Me phosphinate pyridine platform.⁴⁴

2-Bromo-6-methyl pyridine **7** was treated with *m*CPBA in CHCl₃ to give the N-oxide **8**. Nitration with HNO₃/H₂SO₄, followed by deoxygenation with PBr₃, gave the 2-bromo-4-nitro-6-methyl pyridine **10** in high yield. Coupling between intermediate **10** and ethyl

methylphosphinate in degassed toluene with Et_3N using $\text{Cl}_2\text{Pd}[\text{bis}(\text{diphenylphosphino})\text{ferrocene}]$ as a catalyst was successful (67 % yield). Bromination with acetyl bromide followed by re-esterification of the phosphinic acid with $\text{HC}(\text{OEt})_3$ allowed for the isolation of intermediate **12** in 77 % yield. Compound **12** was treated with *m*CPBA in CH_3CN to give *N*-oxide **13** in 79 % yield. Boekelheide rearrangement with $(\text{CF}_3\text{CO})_2\text{O}$ and subsequent hydrolysis in $\text{EtOH} / \text{H}_2\text{O}$ gave the intermediate **14** in 80 % yield. Mesylation under standard conditions gave compound **15** that was used directly for alkylation of the 9- N_3 derivative **6c**.



Scheme 3: Synthesis of the complex $[\text{EuL}^{13}]$.

The crude reaction material, from the alkylation of **6c**, was purified by HPLC to give compound **16**, which was hydrolysed with 0.1 M NaOH in $\text{CD}_3\text{OD}/\text{D}_2\text{O}$ (3 : 1). Completion of hydrolysis was confirmed by ^{31}P -NMR. After pH adjustment, the material was reacted with $\text{Eu}(\text{AcO})_3$ to prepare the $\text{Eu}(\text{III})$ complex $[\text{EuL}^{13}]$.

3.2.2 Photophysical analysis

An emission spectrum of $[\text{EuL}^{13}]$ was recorded and compared to that recorded for the unsubstituted analogue $[\text{EuL}^{13a}]$.⁸³ The two spectra did not show any significant differences, confirming that the C-substitution on the ring did not affect the emission spectral form. The lifetime of $[\text{EuL}^{13}]$ was also measured ($\tau_0 = 1.50$ ms in MeOH); this value is comparable with that of $[\text{EuL}^{13a}]$ ($\tau_0 = 1.56$ ms in H_2O).

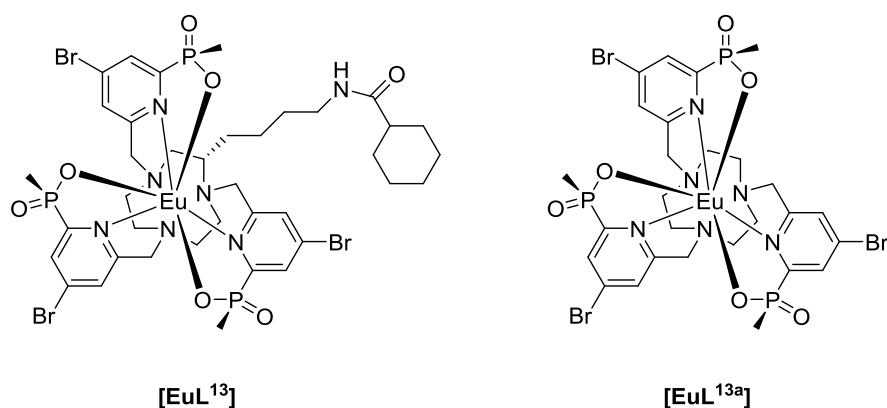


Figure 42: Structure of **[EuL¹³]** and its unsubstituted analogue **[EuL^{13a}]**.

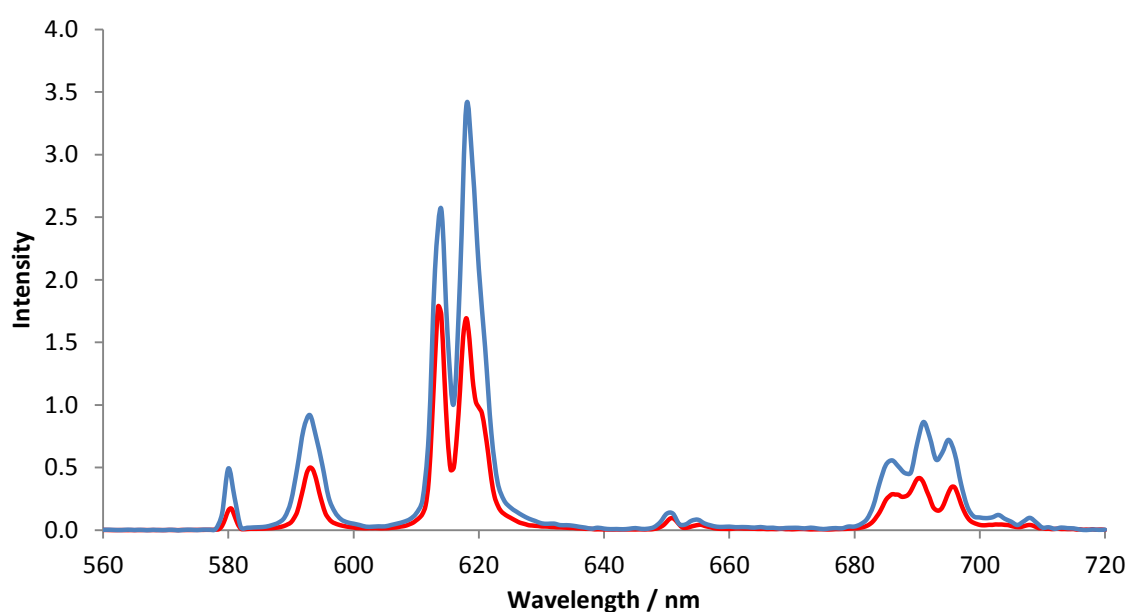


Figure 43: Emission spectra of **[EuL¹³]** (red) and the unsubstituted analogue **[EuL^{13a}]** (blue), (MeOH, 295 K, $\lambda_{ex} = 272$ nm).

A detailed investigation of the chiroptical features of this compound will be discussed in Chapter 5.

3.3 A series of C-substituted complexes

Following the promising results obtained for complex **[EuL¹³]**, the design of a series of C-substituted europium complexes was undertaken (Figure 44). These complexes bear the pyridylalkynyl chromophore, which permits excitation in the range 330 - 365 nm. In addition, substitution of the *p*-methoxy functionality on the chromophore with a negatively

charged moiety (e.g. carboxylate and sulfonate) was also expected to increase the water solubility of the complex.

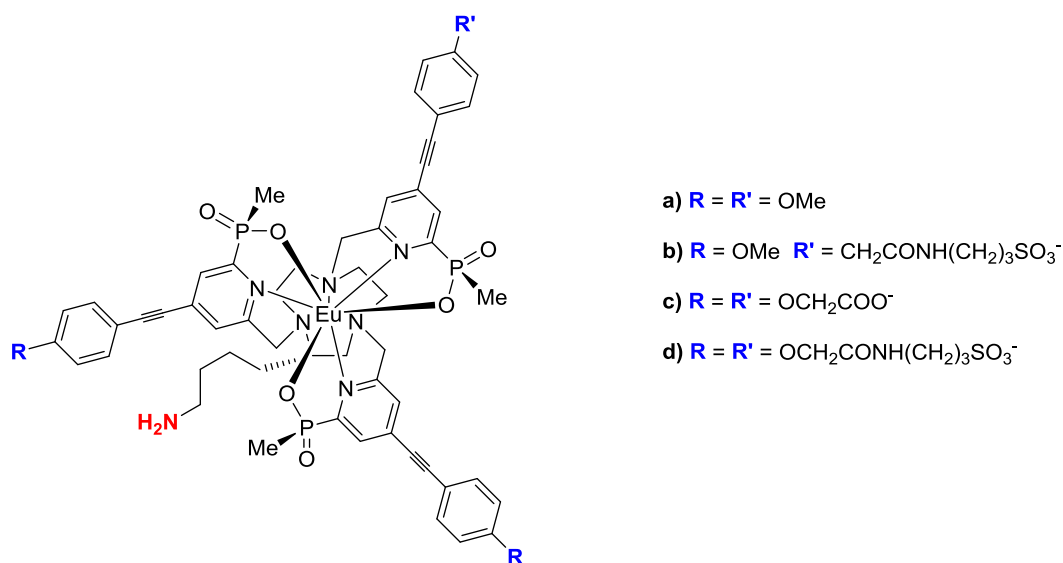
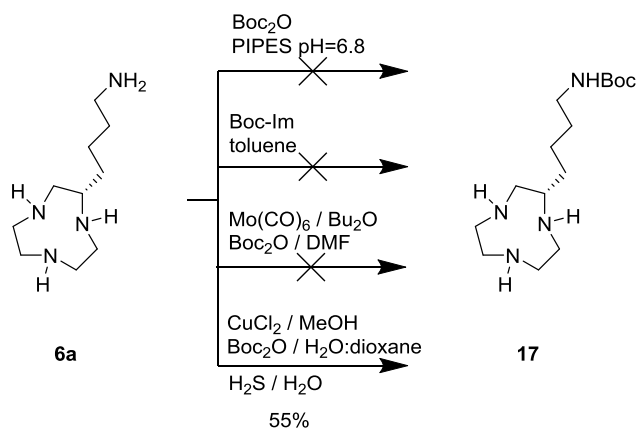


Figure 44: New series of C-substituted europium complexes.

3.3.1 Synthetic aspects

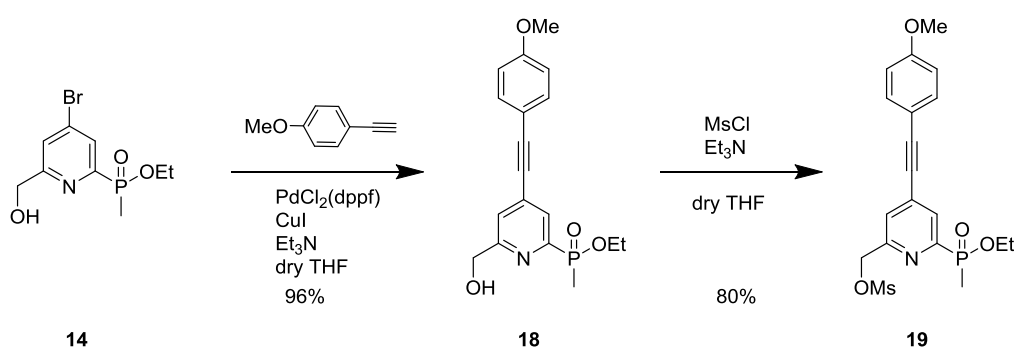
For the new series of compounds an easy cleavable protecting group (*i.e.* Boc) had to be introduced, instead of the cyclohexyl amide present in compound **[EuL¹³]**. This will permit the unmasking of the amine at the end of the synthesis without affecting the integrity of the chromophores. After complete hydrolysis of the amide **6c** with 6 N HCl, various strategies for the selective protection of the tetraamine **6a** were considered.



Scheme 4: Selective Boc protection of the remote NH_2 .

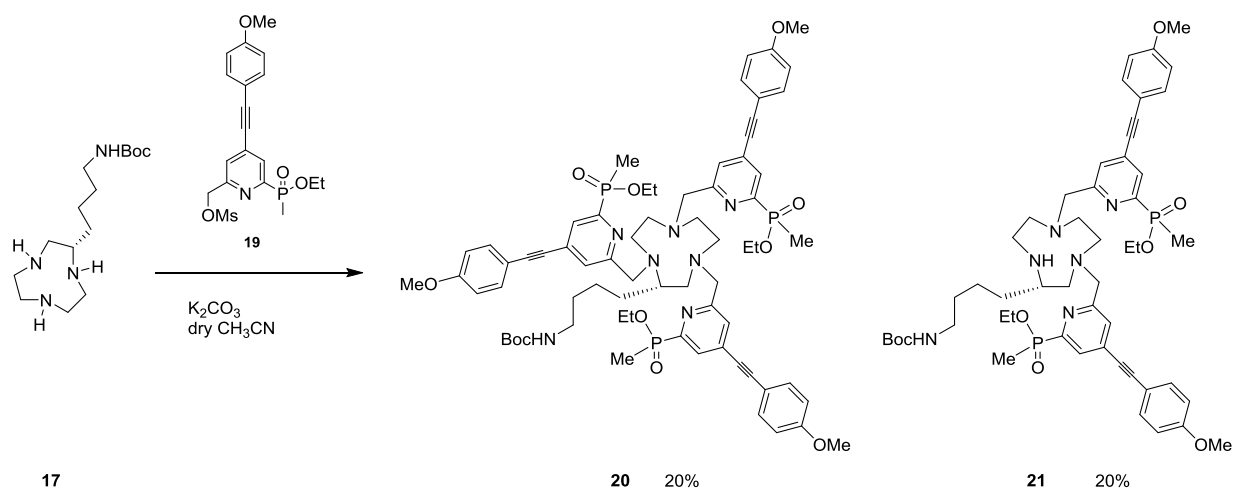
The treatment of **6a** with one equivalent of di-*tert*-butyl dicarbonate in the presence of PIPES buffer (pH = 6.8)⁸⁴ was unsuccessful, leading to a mixture of mono, di, and tri-protected compounds. The use of Boc-imidazole, a reagent that is supposedly less reactive than di-*tert*-butyl dicarbonate and selective for primary amines,⁸⁵ unfortunately gave the same mixture of products. The attempted treatment of the free amine **6a** with Mo(CO)₆ was unsuccessful because of the very low solubility of the starting material in dibutyl ether. The treatment of 9-N₃ with copper (II) chloride forms a very stable complex.⁸⁶ This property was exploited. The copper complex of compound **6a** was formed and the subsequent selective reaction of the remote free NH₂ with di-*tert*-butyl dicarbonate was successful. Bubbling H₂S into an aqueous solution of this complex removed the Cu(II) as its insoluble sulphide, and permitted isolation of compound **17**.

The pyridylalkynylaryl chromophore **18** was synthesised by Sonogashira coupling between the *p*-Br pyridyl derivative **14** and ethynyl anisole, using a catalytic amount of Pd(dppf)Cl₂. Mesylation under standard conditions gave compound **19**, which was used for direct alkylation of the macrocycle **17**.



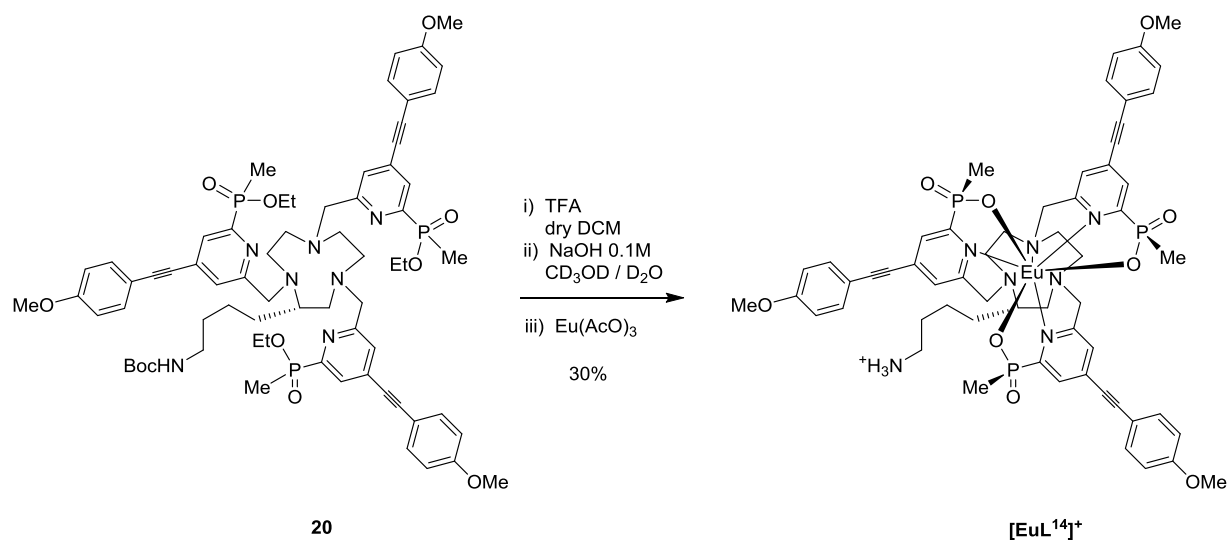
Scheme 5: Synthesis of the extended pyridylalkynylaryl chromophore **19**.

The alkylation of the 9-membered ring derivative **17** with compound **19** was carried out in acetonitrile. A mixture of tri-substituted ligand **20** and the di-substituted analogue **21** was obtained, that was separated by column chromatography (Scheme 6). The third alkylation reaction, next to the C-substituent, occurred more slowly than in the parent unsubstituted system.



Scheme 6: Synthesis of the tri-substituted ligand **20** and di-substituted ligand **21**.

Deprotection of the primary amine was achieved with TFA (10 % in DCM) at RT. Hydrolysis of the phosphinate esters with aqueous NaOH (0.1 M), followed by reaction with $Eu(AcO)_3$, gave the complex $[EuL^{14}]^+$.



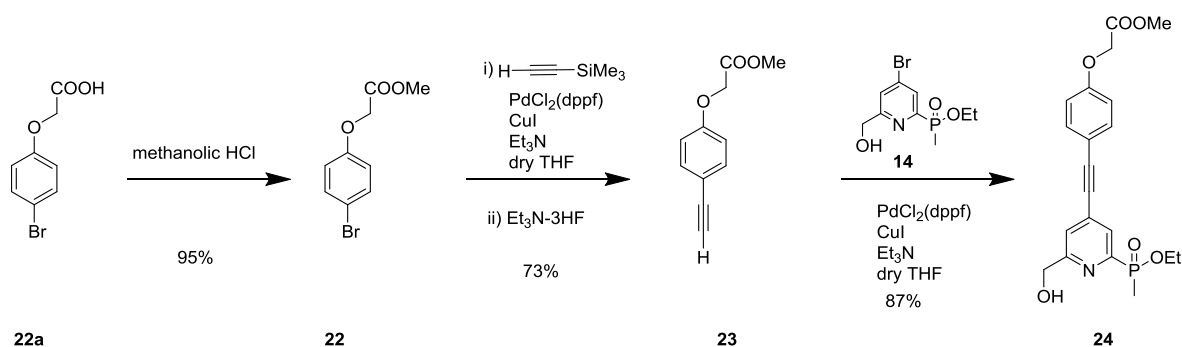
Scheme 7: Synthesis of $[EuL^{14}]^+$.

3.3.2 Incorporation of solubilising moieties

The introduction of negatively charged moieties on the chromophores was expected to increase the water solubility of the Eu(III) complex. Both carboxylate and sulfonate functionalities were considered. Carboxylic acids enhance the hydrophilicity of a molecule (when deprotonated) and are easy to handle, but are also rather reactive functionalities that

might interfere during the labelling of the biomolecule. On the other hand, sulfonates give similar degree of water solubility, but they are not reactive groups and should not affect the labelling. They are usually introduced at the end of the synthesis, because of their poor solubility in organic solvents that makes them difficult to manipulate. Both strategies were pursued.

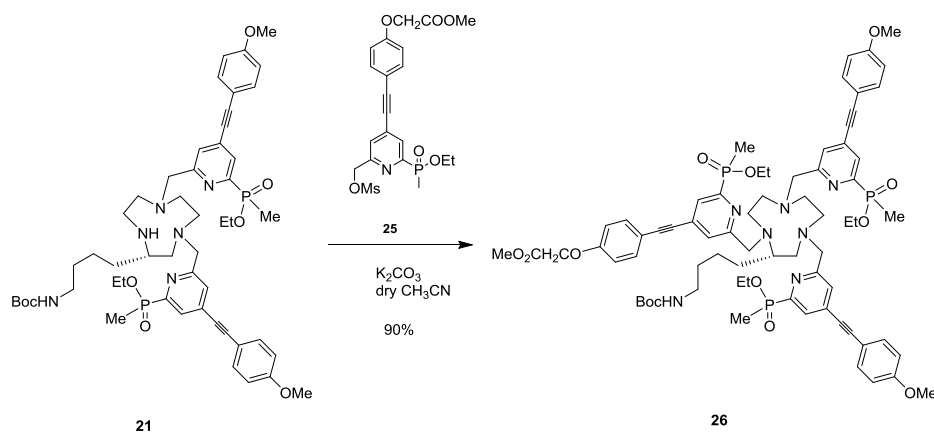
A modified version of the extended chromophore was prepared in order to introduce the carboxylate moieties.⁸⁷



Scheme 8: Synthesis of the pyridylalkynylaryl chromophore, **24**.

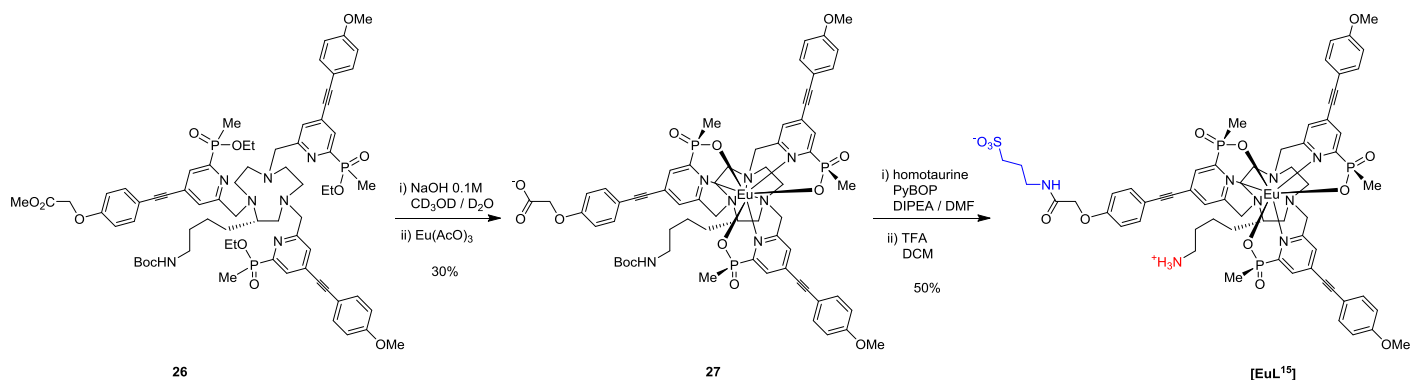
Compound **22a** was reacted with methanolic HCl to give the Me-ester **22** in almost quantitative yield. Sonogashira coupling with ethynyl-trimethylsilane followed by deprotection of the triple bond with $\text{Et}_3\text{N}\cdot\text{3HF}$ gave compound **23** in 73% yield. A second palladium-catalysed coupling between *p*-Br pyridyl derivatives **14** and compound **23** gave the target chromophore **24**.

The di-substituted ligand **21**, obtained from the previously described alkylation (Scheme 6), was reacted with the mesyl derivative of compound **24**, *i.e.* **25**, to give ligand **26**.



Scheme 9: Synthesis of ligand **26**.

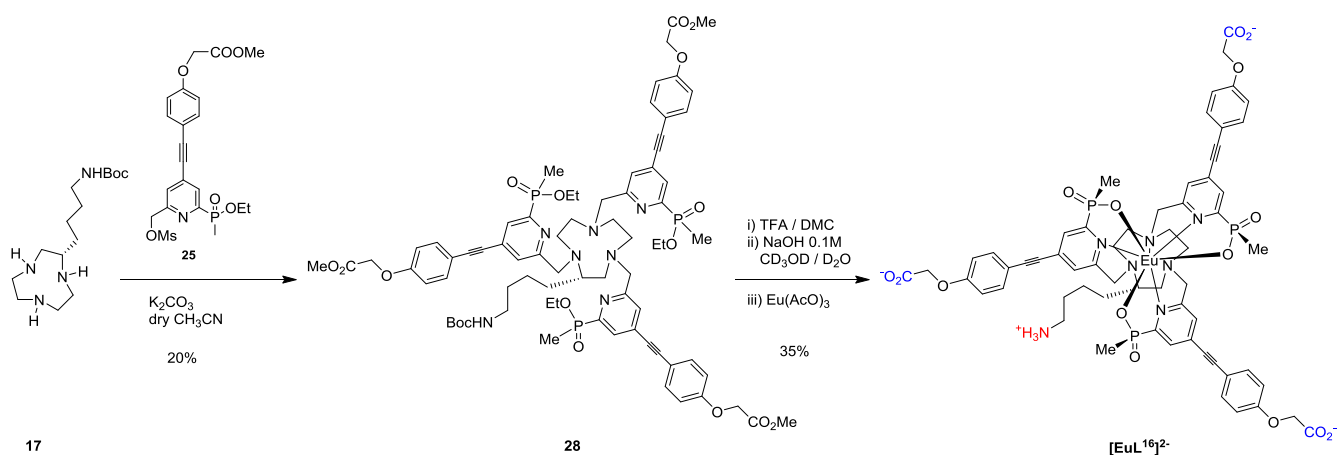
Ligand **26** was treated with aqueous NaOH, followed by reaction with $\text{Eu}(\text{AcO})_3$, to give complex **27**. Coupling with homotaurine in presence of PyBOP and DIPEA, followed by BOC deprotection with TFA, allowed for formation of complex $[\text{EuL}^{15}]$, which was purified by reverse phase HPLC.



Scheme 10: Synthesis of $[\text{EuL}^{15}]$.

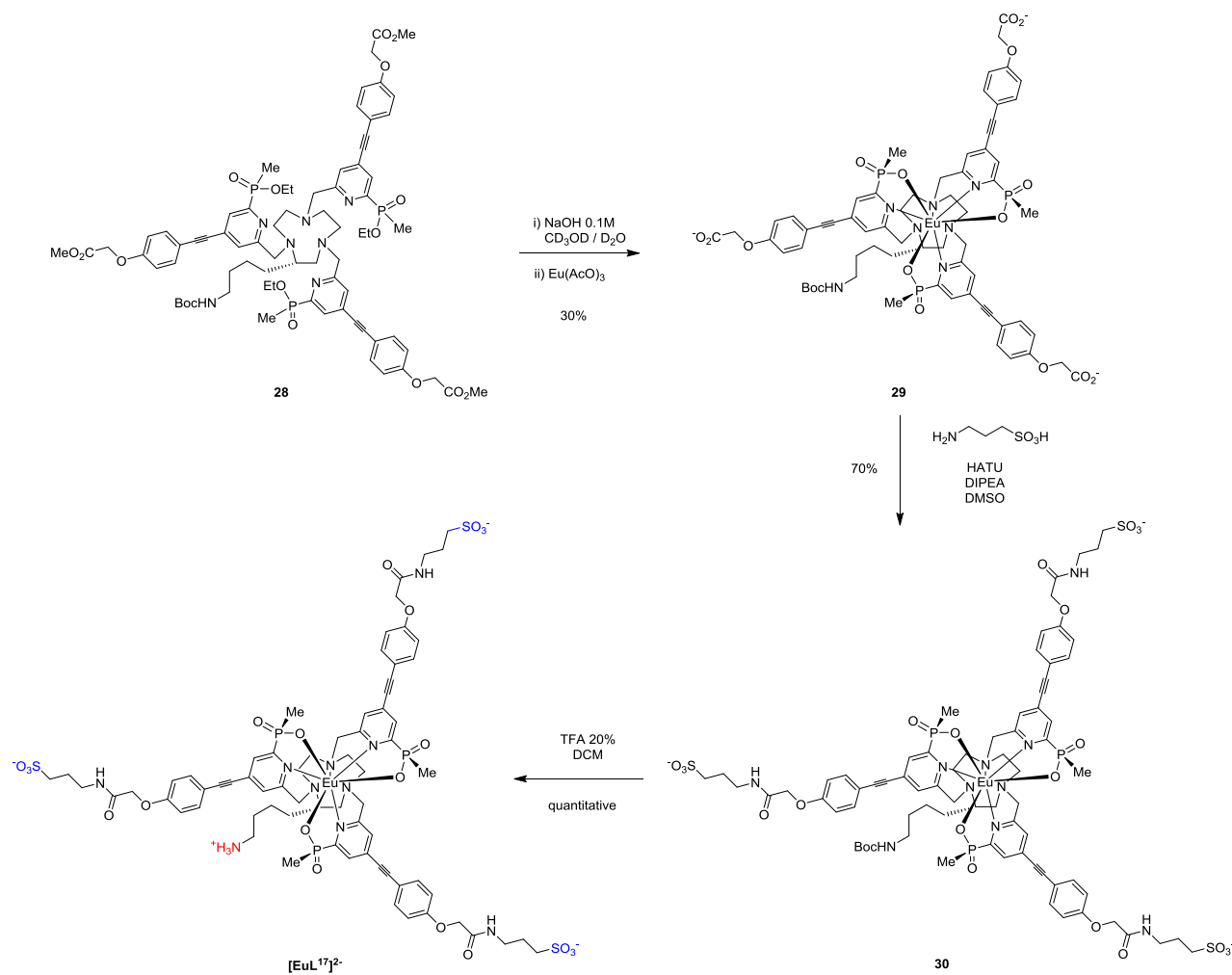
Although the presence of one negative charge improved slightly the water solubility of the complex, it was decided to introduce three negative charges to improve it even further.

Tri-carboxylate ($[\text{EuL}^{16}]^{2-}$) and tri-sulfonate ($[\text{EuL}^{17}]^{2-}$) analogues have been prepared from common intermediates. The alkylation of the 9-membered ring derivative **17** with the mesylate **25** was carried out in order to obtain ligand **28**. In the first case, deprotection of the primary amine with TFA in DCM, simultaneous base hydrolysis of the phosphinate and carboxylate groups followed by reaction with $\text{Eu}(\text{OAc})_3$ yielded the complex $[\text{EuL}^{16}]^{2-}$.



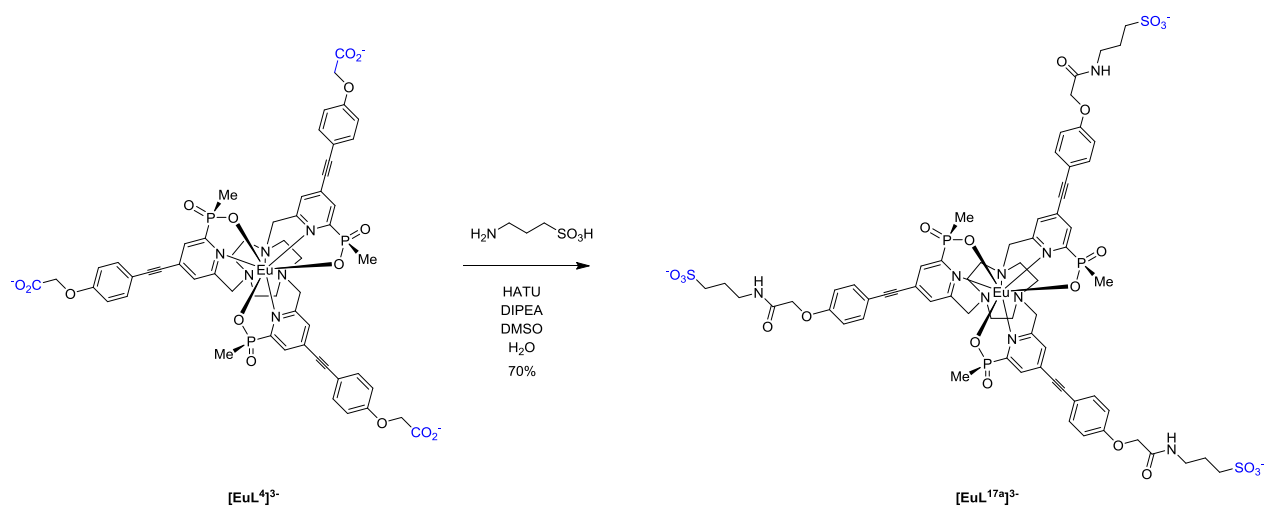
Scheme 11: Synthesis of $[\text{EuL}^{16}]^{2-}$.

For the synthesis of $[\text{EuL}^{17}]^{2-}$, ligand **28** was complexed after basic hydrolysis. The coupling with homotaurine in the presence of HATU and DIPEA in DMSO was successful and the subsequent deprotection of the BOC group with TFA gave the desired compound which was purified by reverse phase HPLC in the presence of triethylammonium acetate and isolated as its triethylammonium salt.



Scheme 12: Synthesis of $[\text{EuL}^{17}]^{2-}$.

In a similar manner, the unsubstituted analogue $[\text{EuL}^{17a}]^{3-}$ was synthesised from $[\text{EuL}^4]^{3-}$ to allow for a comparative analysis of the behaviour in bioassays.



Scheme 13: Synthesis of the unsubstituted tri-sulfonated system $[\text{EuL}^{17a}]^{3-}$.

3.3.3 Photophysical and FRET studies

The photophysical properties of the new series of C-substituted complexes were measured and compared to those of the unsubstituted analogues. Even in the presence of the extended chromophore, no significant differences between the two systems were observed.

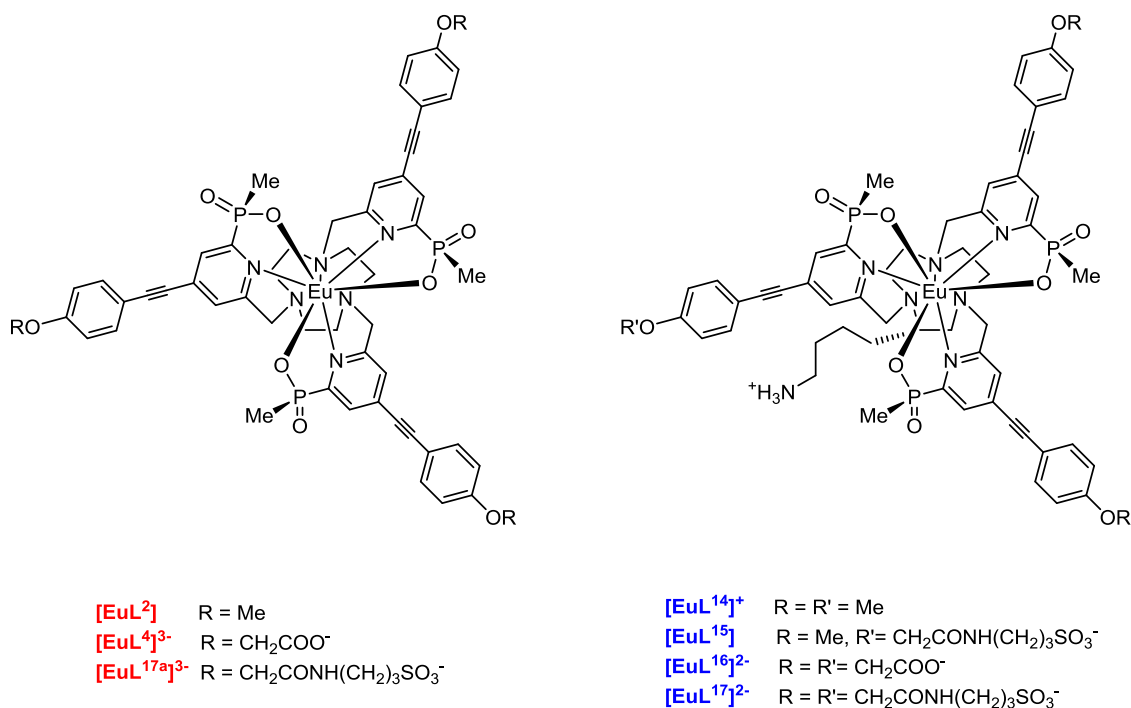


Figure 45: Series of C-substituted complexes and unsubstituted analogues.

The absorption and emission profiles are very similar for each of these complexes; an example for $[\text{EuL}^{17}]^{2-}$ is shown in *Figure 46*. A summary of the photophysical properties is presented in *Table 9*.

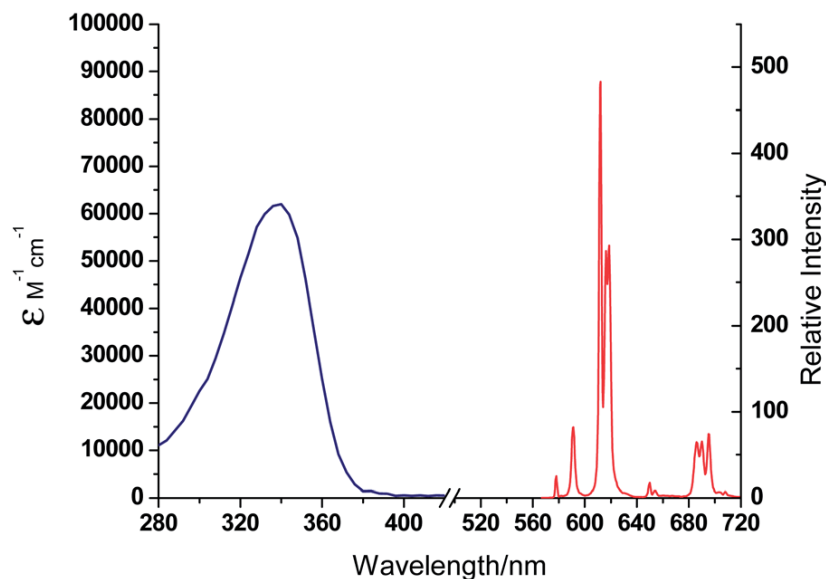


Figure 46: Absorption (blue) and total emission (red) spectra for $[\text{EuL}^{17}]^{2-}$, (H_2O , 295 K, $\lambda_{\text{ex}} = 328$ nm).

Table 9: Summary of the photophysical properties for the new series of C-substituted complexes and unsubstituted analogues, (H_2O , 295 K).

	$\lambda_{\text{max}} / \text{nm}$	τ_0 / ms	$\Phi_{\text{em}} / \%$	$\varepsilon / \text{mM}^{-1}\text{cm}^{-1}$	$\log P$
$[\text{EuL}^2]$	328	1.03	24	58	+ 1.4
$[\text{EuL}^4]^{3-}$	330	1.04	28	57	- 2.2
$[\text{EuL}^{17a}]^{3-}$	328	1.01	26	57	- 2.2
$[\text{EuL}^{14}]^+$	328	1.00	22	58	<i>n.d.</i>
$[\text{EuL}^{15}]$	328	1.08	25	58	<i>n.d.</i>
$[\text{EuL}^{16}]^{2-}$	330	1.05	26	57	<i>n.d.</i>
$[\text{EuL}^{17}]^{2-}$	328	1.00	26	57	<i>n.d.</i>

^a Errors on λ_{max} , τ_0 , Φ_{em} and ε are $\pm 10\%$, errors on $\log P$ are $\pm 20\%$.

From the results, it was clear that the introduction of the negative charges into the ligand system did not affect the photophysical properties of the complexes. In addition, the negative values of $\log P$ (- 2.2) proved that the carboxylate and the sulfonate moieties gave high water solubility to the complex.

Some relative stability tests were carried out for the unsubstituted complexes in order to predict the behaviour of these systems in the media used commonly for bioassays, or *in cellulo*.

Ascorbate and urate are two intracellular antioxidants that are able to quench the sensitiser's triplet excited state.⁸⁸ Luminescence spectra and excited state lifetimes were measured in the presence of excess of quencher (10 mM for ascorbate, 5 mM for urate); no quenching was observed from either antioxidant.

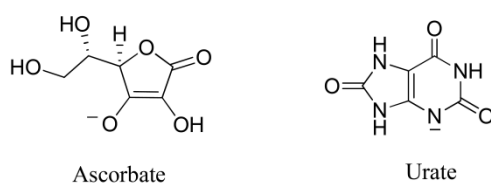
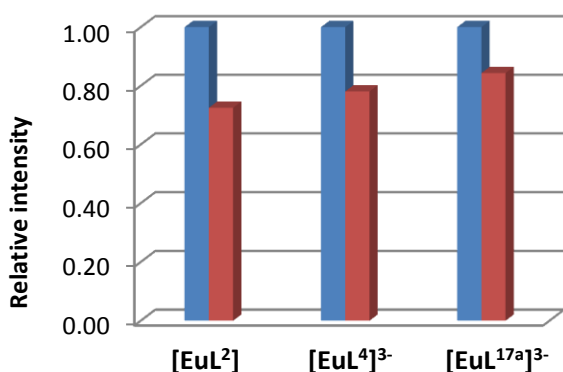


Figure 47: Ascorbate and urate structures.

To analyse the possible interactions of these compounds with proteins in the media, emission spectra were recorded for the three complexes (4 μM in water, $\text{pH} = 7.4$) in the absence and in the presence of 0.4 mM HSA (human serum albumin). Albumin was chosen as it is present in a cell growth medium, and is the most abundant protein in serum.

Table 10: Photophysical properties of different Eu(III) complex in the absence (*blue*) and in the presence of 0.4 mM HSA (*red*), (with added HSA, excitation spectroscopy was used to assess λ_{max}).



	[EuL ²]	[EuL ⁴] ³⁻	[EuL ^{17a}] ³⁻
$\lambda_{\text{max}} / \text{nm}$	328	330	328
$\lambda_{\text{max}} \text{ HSA} / \text{nm}$	333	337	329
τ_0 / ns	1.03	1.04	1.01
$\tau_0 \text{ HSA} / \text{ns}$	1.10	1.01	1.12

^a Errors on λ_{max} and τ_0 are $\pm 10\%$.

The addition of HSA to the complex caused a decrease in the total emission intensity (up to 30 %) without affecting the emission spectral form. The most affected complex was [EuL²], probably due to its higher lipophilicity promoting a hydrophobic interaction with HSA. Also, emission lifetimes were generally increased in the presence of HSA (exception [EuL⁴]³⁻).

Importantly, the absorption wavelength shifted to the red slightly in every case. This change was observed by recording the excitation spectra (rather than the absorption spectrum) in the presence of protein. Controls in the absence of added protein showed that the excitation and absorption spectra corresponded. The excitation spectral change implied that there was either an interaction between the protein's aromatic chromophores and the arylalkynylpyridyl moiety, or that there was a change in the effective dielectric constant of the 'local medium', following the non-specific protein-complex interaction that perturbs the energy of the ICT transition and modifies the intramolecular energy transfer step. Indeed, the ICT band is known to be strongly solvatochromic. A spectral titration, adding different concentrations of HSA to the Eu(III) complex, did not show any sign of binding, suggesting that these results can be tentatively ascribed to a change of local polarity and viscosity of the medium.

To substantiate this hypothesis, the same photophysical properties were measured in solvents with different polarities (*Table 11*). A general increase in the emission lifetime was measured in different solvents; also the overall quantum yield was affected by the polarity of the medium. These results proved that changing the medium polarity had a similar effect to that observed following addition of HSA.

Table 11: Photophysical properties for $[\text{EuL}^{17\text{a}}]^{3-}$ measured in solvents with different polarities.^b

$[\text{EuL}^{17\text{a}}]^{3-}$	E_{T}^{N} ^a	λ_{max} / nm	Φ_{em} / %	τ_0 / ms
H₂O	1.00	328	26	1.01
TFE-OH	0.90	328	24	1.26
MeOH	0.76	330	37	1.21
EtOH	0.65	330	36	1.23
DMF	0.40	328	53	1.22
NMP	0.36	336	38	1.16

^a E_{T}^{N} is Reichardt's normalised solvent polarity parameter.⁸⁹ ^b Errors on λ_{max} , Φ_{em} and τ_0 are $\pm 10\%$.

The FRET properties of the new sulfonate compound $[\text{EuL}^{17\text{a}}]^{3-}$ were assessed in the presence of different concentration of acceptor **Dy647-NH₂** and compared to the results presented in *Section 2.3.2*.

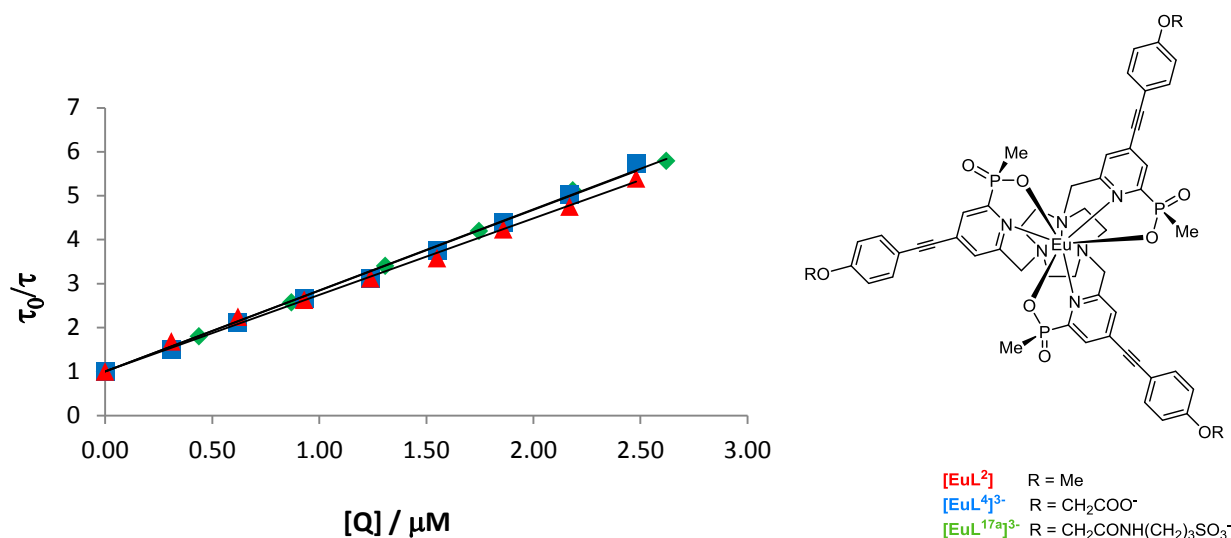


Table 12: Quenching studies for [EuL²] (red), [EuL⁴]³⁻ (blue) and [EuL^{17a}]³⁻ (green). (Values recorded (\pm 5%) in 50 mM HEPES buffer, 50 mM NaCl, pH = 7.4, 295 K).

	gradient	λ_{max} / nm	Φ_{em} / %	τ_0 / ms	k_2 / mM ⁻¹ s ⁻¹
[EuL²]	1.64	328	24	1.03	1.59
[EuL⁴]³⁻	1.84	330	28	1.04	1.77
[EuL^{17a}]³⁻	1.86	328	26	1.01	1.84

The three complexes did not show any significant differences in their photophysical properties nor in the rates of energy transfer, proving that the peripheral anionic groups are not interfering with the energy transfer process.

3.4 Applications in FRET bioassays

After solving the problem of water solubility, the behaviour of these complexes in FRET bioassays was evaluated using SNAP-tag technology.⁹⁰ This is a general strategy that permits the irreversible covalent labelling of a fusion protein *in vivo* with a suitable ligand (*e.g.* optical probe). SNAP-tag is a 20 kDa engineered protein that can be inserted in the protein of interest. Its behaviour is based on a human DNA-repair protein *O*₆-alkylguanine-DNA alkyltransferase (hAGT); hAGT transfers irreversibly the alkyl group from its substrate, *O*₆-alkylguanine-DNA, to one of its cysteine residue (*Figure 48a*). In the same way, SNAP-tag reacts with benzylguanine (BG) derivatives permitting the transfer of the optical probe to the fusion protein of interest (*Figure 48b*).

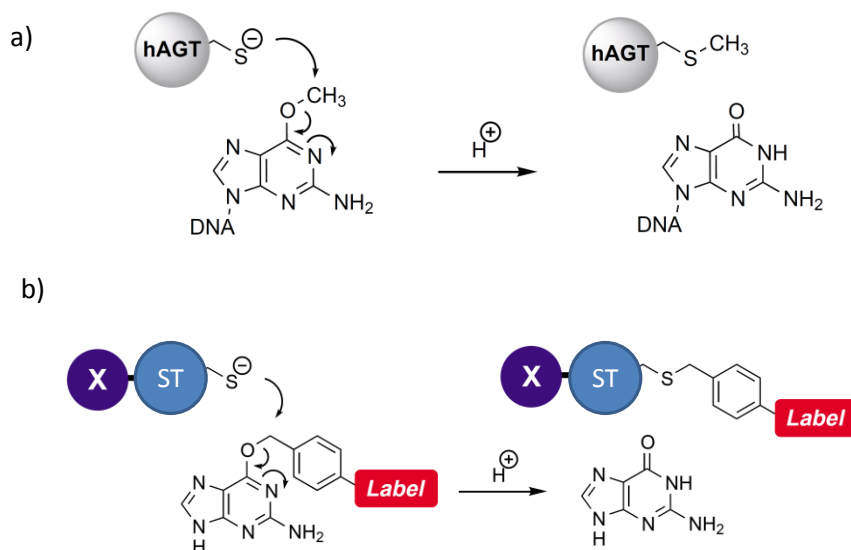


Figure 48: Schematic mechanism of hAGT (a) and SNAP-tag (b) technology.⁹⁰

For our purposes, the SNAP-tag method was used for the labelling of G protein-coupled receptors (GPCRs), which have elevated expression levels when transiently transfected in HEK293 cells. The results are presented for the cholecystokinin-2 (CCK2) and dopamine-d2 receptors (membrane receptors). CCK2 receptors are located primarily in the brain, spinal cord and stomach and are involved in neurotransmission and regulation of anxiety, feeding and locomotion.⁹¹ Dopamine-d2 receptors are located in the central nervous system and control the neural signalling of behaviour, such as spatial working memory, by modulating the production of neurotransmitters.⁹²

The assay provides the labelling of the receptor with the Eu(III) complex (Figure 49). To permit this labelling using the SNAP-tag technology, a BG derivative of the Eu(III) complex had to be synthesised (Section 3.4.1). This labelling does not interfere with the interaction of the substrate with the receptor, and permits the visualisation of the receptor on the cell surface. When a substrate, labelled with the cyanine dye FRET acceptor, interacts with the receptor, the emission of the Eu(III) is quenched and the FRET signal is activated.

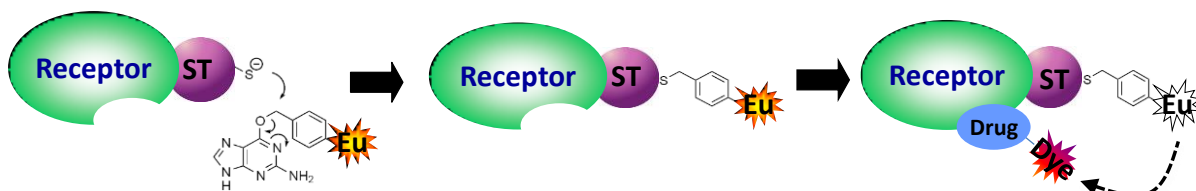
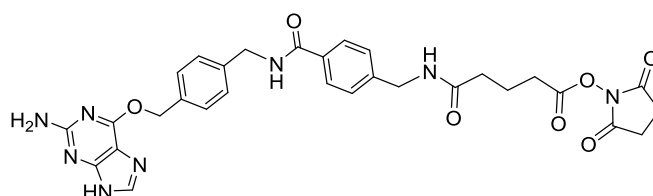


Figure 49: Cartoon explaining the processes involved in the bioassay. The reaction of SNAP-tag with the BG-labelled Eu(III) complex permits the labelling of the receptor. Upon addition of a substrate for the receptor labelled with the organic dye (acceptor), the emission of the Eu(III) complex is quenched and the FRET signal is activated.

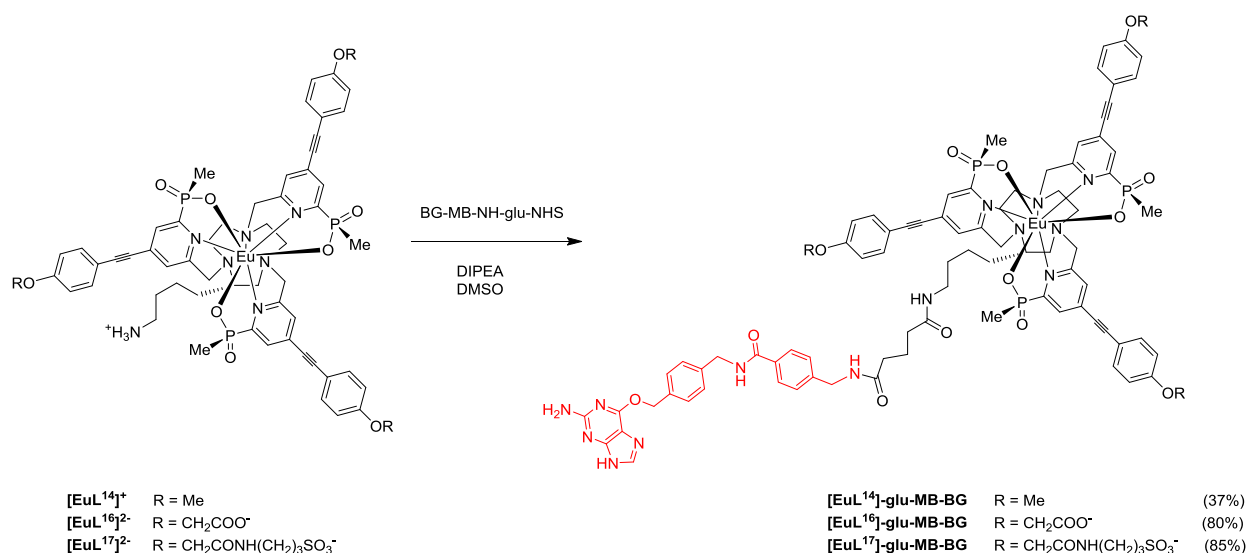
3.4.1 Conjugation with the biomolecule

For the G protein-coupled receptors assay, three BG-labelled complexes were prepared. The complexes were directly reacted with the active ester of BG-MB-NH-glu-COOH, giving the desired compounds in good yields.



BG-MB-NH-glu-NHS

Figure 50: Structure of BG-MB-NH-glu-NHS.



Scheme 14: Synthesis of three BG-labelled Eu(III) complexes.

3.4.2 Time resolved FRET assays

These results were obtained in collaboration with Dr Victoria Sadovnikova and Dr Jurriaan Zwier at Cisbio Bioassays.

The complexes presented in *Section 2* were originally developed as stains for various intracellular compartments, such as mitochondria, following non-specific cell uptake by micropinocytosis.⁸⁷ This behaviour is disadvantageous for GPCRs assays. In fact, in order to selectively label the desired GPCRs (membrane receptors), it is important that the BG-complexes do not show any non-specific interactions with the cells, such as internalisation or adsorption to the membrane.

As the cell membrane consists of phospholipids and is thus considered to be negatively charged, the carboxylate and sulfonate moieties on complexes $[\text{EuL}^{16}]^{2-}$ and $[\text{EuL}^{17}]^{2-}$ should decrease the interaction with the cell membrane, as a result of repulsive Coulombic interactions. In addition, the hydrophilic nature of these substituents on the aryl-alkynyl structure should prevent non-specific protein binding that can occur *via* hydrophobic interactions of the chromophore.

The specific binding for the three BG-Eu(III) complexes was measured using a saturation binding assay. The time-gated luminescence intensity at 620 nm was monitored on HEK293 cells expressing the SNAP-tagged receptors and on non-transfected HEK293 cells (control), after 1 h incubation with different concentrations of the BG-Eu(III) complex (*Figure 52* and *Figure 53*). Unfortunately, significant labelling of non-transfected cells occurred with the more lipophilic compound $[\text{EuL}^{14}]$ -glu-MB-BG, probably due to cellular uptake. As predicted, better behaviour was observed for the negatively charged complexes $[\text{EuL}^{16}]$ -glu-MB-BG and $[\text{EuL}^{17}]$ -glu-MB-BG; negligible values for non-specific interaction were found, permitting the selective labelling of the GPCRs on the cell membrane (*Figure 52* and *Figure 53*).

Following these excellent results, some ligand-binding assays were performed using an agonist for the receptor, which was labelled with a cyanine dye acceptor. Addition of increasing concentrations of the fluorescently labelled agonist to the Eu(III) labelled living cells activated the FRET signal at 665 nm (emission of the acceptor). By measuring the time resolved (TR) emission intensity at 620 nm (donor) and at 665 nm (acceptor), it was possible

to calculate a saturation curve for the binding of the agonist. By non-linear least squares iterative fitting of the data to a one-site binding model, the affinity of the red-agonist for the receptor, was calculated.

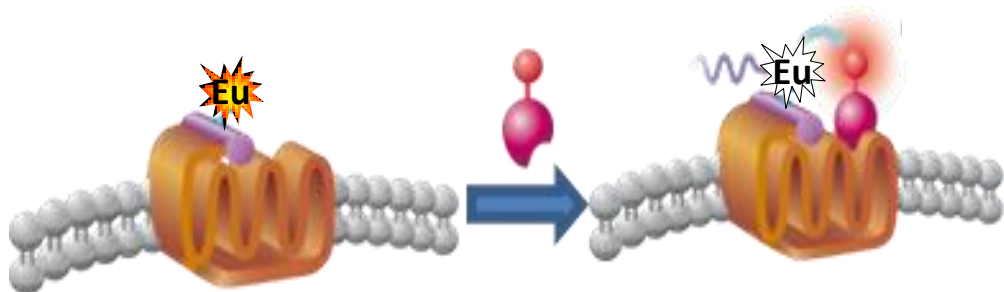


Figure 51: Cartoon explaining the ligand-binding assay. The receptor is labelled with the Eu(III) complex, upon addition of fluorescent agonist, the Eu(III) emission is quenched and the FRET signal is activated.

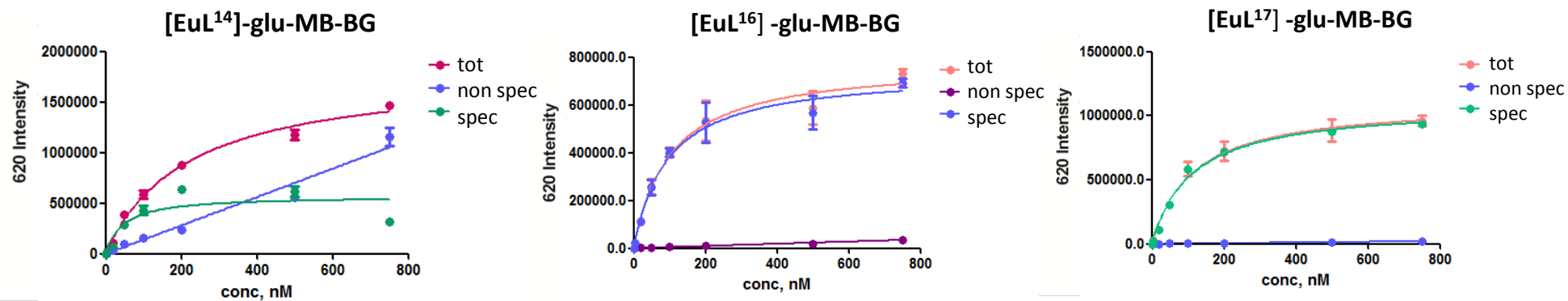


Figure 52: Saturation curves for labelling of HEK293 cells expressing SNAP-CCK2 and non-transfected HEK293 cells monitoring time-gated luminescence intensity ($\lambda = 620 \pm 5$ nm, 60 - 460 μ s) after 1h incubation.

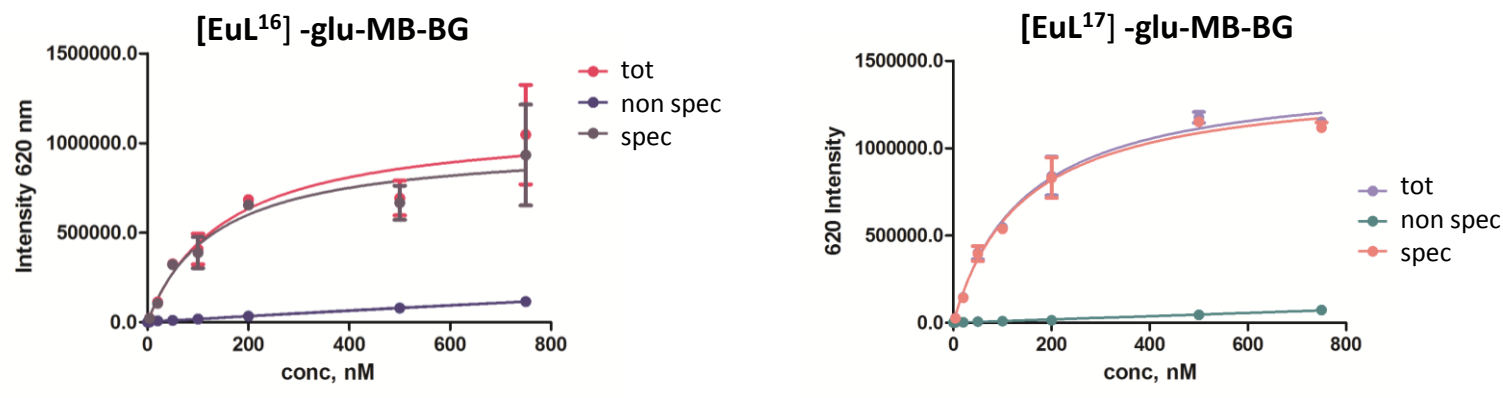


Figure 53: Saturation curves for labelling of HEK293 cells expressing SNAP-d2 and non-transfected HEK293 cells monitoring time-gated luminescence intensity ($\lambda = 620 \pm 5$ nm, 60 - 460 μ s) after 1h incubation.

The binding of the agonist was shown to be completely reversible, in a dose-dependent way, by the addition of excess quantities of an antagonist of the receptor (not labelled with the acceptor).

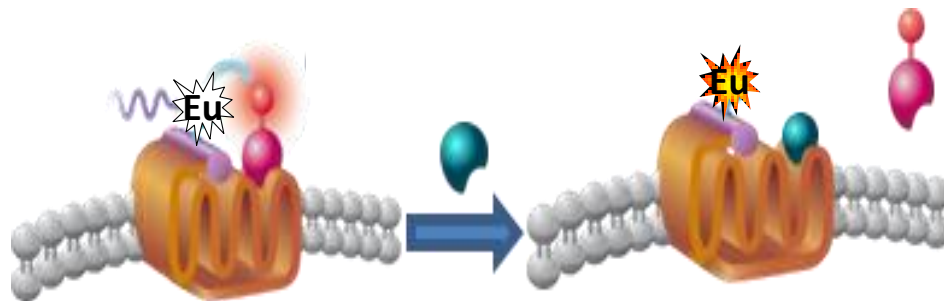


Figure 54: Cartoon explaining the competition-binding assay. The receptor labelled with the Eu(III) complex is saturated with the fluorescent agonist (*red*), upon addition of excess of not labelled antagonist (*blue*), FRET signal disruption occurs and the Eu(III) emission is reactivated.

In this TR competition binding assay, the disruption of the FRET signal can be monitored as a function of the antagonist concentration. At the same time, the full Eu(III) emission intensity was re-established. By fitting the dose-response data, the affinity of the antagonist for the receptor, can be calculated. This provides a general strategy for high-throughput screenings of new drugs, avoiding the problem of labelling the compound to be tested.

An example of the TR-FRET ligand-binding assay and the TR-FRET competition binding assay is presented for the Eu(III) labelled SNAP-CCK2 receptors on living HEK293 cells.⁹³ Compound **[EuL¹⁷]-glu-MB-BG** (200 nM) was used for the labelling of the receptors in this example (**[EuL¹⁶]-glu-MB-BG** gave similar results). Addition of increasing concentration of the agonist **CCK(26-33)-red** (polypeptide labelled with the red acceptor) resulted in activation of FRET signal. The fitting of the data permitted the calculation of the dissociation constant of the red agonist ($K_d = 8$ nM), this value is in agreement with previously reported results.⁹⁴ Addition of excess quantities of **PD135158** (unlabelled antagonist, *Figure 55c*) resulted in FRET disruption; with these results, the inhibition constant for the antagonist was calculated ($K_i = 6$ nM), also in good agreement with previously reported results.⁹⁴

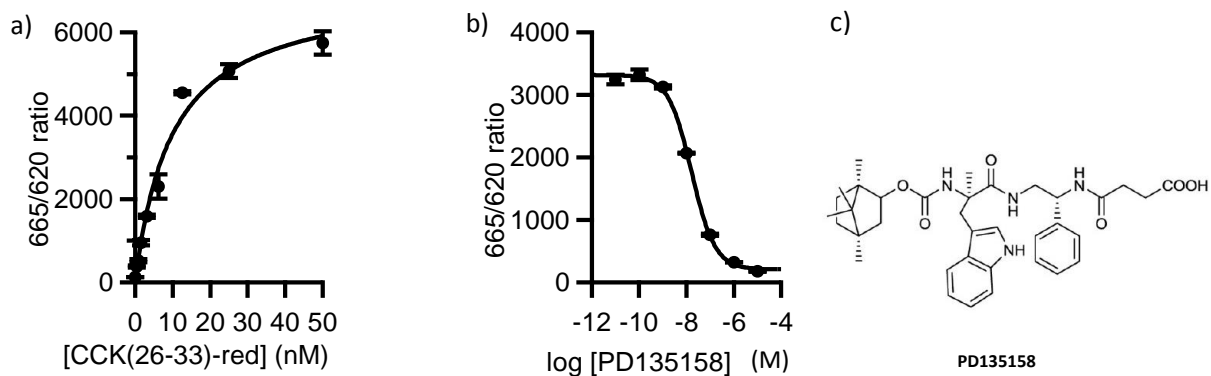


Figure 55: Binding of **red-CCK(26-33)** to HEK293 cells expressing SNAP-CCK2, labelled with **[EuL¹⁷]-glu-MB-BG** (200 nM), monitored by following the ratio of the emission intensity at $\lambda = 665$ and 620 nm $\times 10000$, $K_d = 8$ nM (a). TR-FRET competition binding assay, monitoring the dose–response curve for the displacement of **red-CCK(26-33)** by CCK2 antagonist **PD135158**. The ratio of the emission intensity at wavelengths $\lambda = 665$ and 620 nm $\times 10000$ was measured, $K_i = 6$ nM (b). Structure of the antagonist **PD135158** (c).

3.4.3 Microscopy studies

Due to the high brightness of these complexes, it was also possible to visualise these cell-surface interactions using confocal microscopy; very small quantities of material were required (nM concentration). The Eu(III) labelled SNAP-d2 dopamine receptors on living HEK293 cells were visualised on the cell surface (A1), compound **[EuL¹⁷]-glu-MB-BG** (200 nM) was used for the labelling. The FRET channel did not show any signal (A2). When the red-acceptor (**NAPS-red**, a well-known substrate for the d2-dopamine receptor labelled with a cyanine dye, *Figure 56*)⁹⁵ was introduced to the system, the Eu(III) emission was quenched (B1) and the FRET signal was activated (B2). Three dimensional z-stacks (pixel 0.120 \times 0.120 \times 700 nm) revealed cell surface localisation for both the complex and the acceptor.

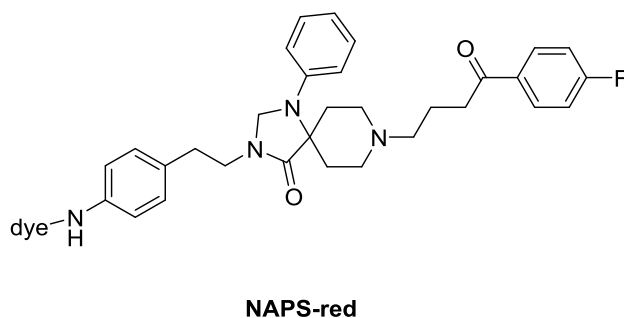


Figure 56: Structure of the red-acceptor, **NAPS-red**.

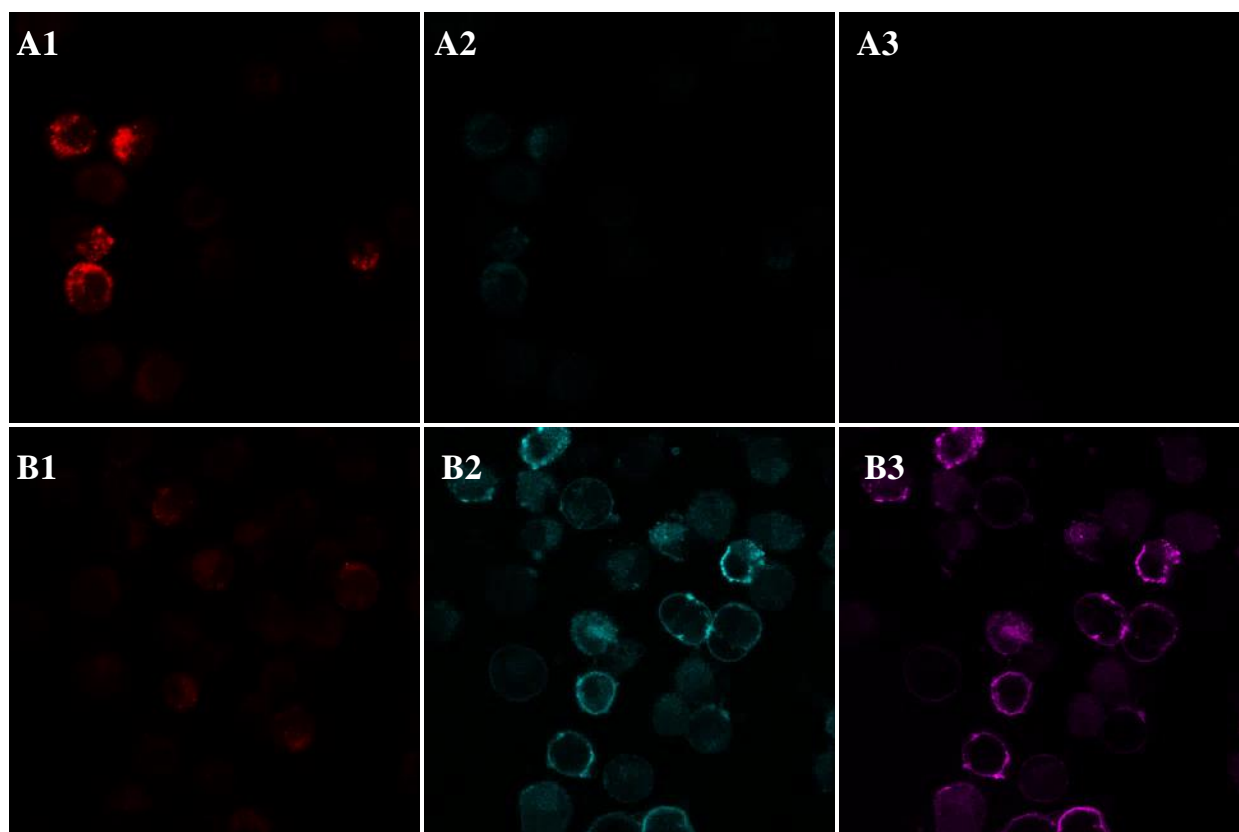


Figure 57: 293 HEK cells expressing SNAP-d2 dopamine surface receptor labelled with Eu(III) complex, standard (A), in the presence of FRET acceptor (B). Eu(III) Channel (A1 and B1) $\lambda_{exc} = 355$ nm at 4 mW, detector 590-650 nm. FRET Channel (A2 and B2) $\lambda_{exc} = 355$ nm at 4 mW, detector 650-690 nm. Acceptor Channel (A3 and B3) $\lambda_{exc} = 633$ nm at 2 mW, detector 650-690 nm.

Following these promising results, the visualisation of these interactions with time-resolved FRET microscopy was also pursued. This technique has been reported only recently for lanthanide based systems,⁸⁷⁻⁹⁶ primarily using long lived Tb(III) donor complexes.⁹⁷

Using a delay of 100 μ s and a gate time of 2 ms, time resolved (TR) images were recorded, showing the Eu(III) labelled receptors on the cell surface (d2-dopamine receptors in *Figure 58A1*, CCK2 receptors in *Figure 59A1*). Upon addition of the red agonist, TR-FRET images were recorded at $\lambda = 670 \pm 20$ nm showing a high signal in the FRET channel (B2). A decrease in the intensity of the Eu(III) channel was also observed (B1).

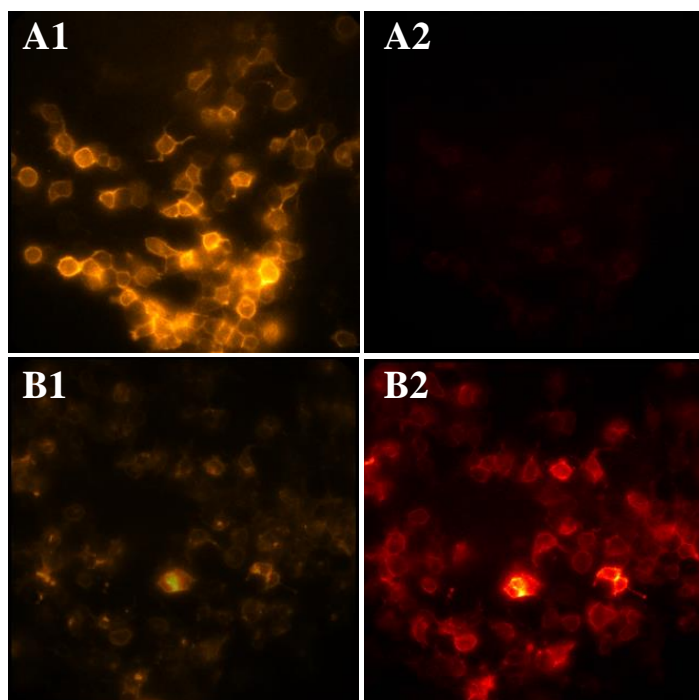


Figure 58: 293 HEK cells expressing SNAP-d2 dopamine surface receptor labelled with the Eu(III) complex, standard (A), in the presence of FRET acceptor (B). TR-Eu(III) Channel (A1 and B1) $\lambda = 615 \pm 10$ nm ($\lambda_{exc} = 337$ nm, 30 Hz, $\tau_{delay} = 100$ μ s, $\tau_{gate} = 2000$ μ s). TR-FRET Channel (A2 and B2) $\lambda = 670 \pm 20$ nm ($\lambda_{exc} = 337$ nm, 30 Hz, $\tau_{delay} = 100$ μ s, $\tau_{gate} = 2000$ μ s).

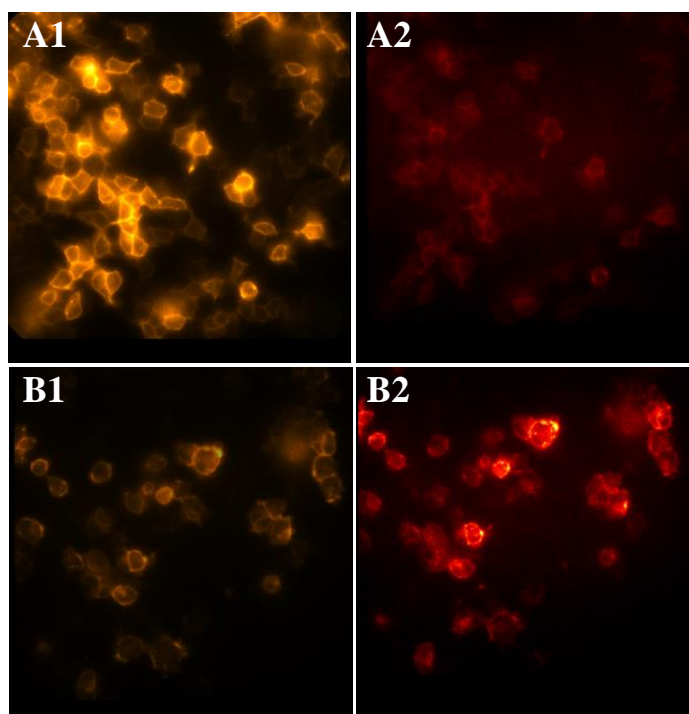


Figure 59: 293 HEK cells expressing SNAP-CCK2 surface receptor labelled with Eu(III) complex, standard (A), in the presence of FRET acceptor (B). TR-Eu(III) Channel (A1 and B1) $\lambda = 615 \pm 10$ nm ($\lambda_{exc} = 337$ nm, 30 Hz, $\tau_{delay} = 100$ μ s, $\tau_{gate} = 2000$ μ s). TR-FRET Channel (A2 and B2) $\lambda = 670 \pm 20$ nm ($\lambda_{exc} = 337$ nm, 30 Hz, $\tau_{delay} = 100$ μ s, $\tau_{gate} = 2000$ μ s).

3.5 Conclusions

A new series of bright, kinetically stable and highly water soluble Eu(III) complexes was developed. For this purpose, the synthesis of a C-substituted macrocycle core was optimised, permitting the production of complexes with a linkage point for conjugation. The C-substitution on the ring did not affect the emissive properties and created a useful intermediate that can be easily functionalised for a variety of applications.

These complexes were designed to permit excitation with lasers at 337, 355 or 365 nm for *in vivo* FRET experiments. The introduction of carboxylate or sulfonate functionalities onto the antenna avoided the non-specific labelling of living HEK cells, permitting the selective targeting of membrane receptors.

TR-FRET binding assays were performed on two GPCRs (d2-dopamine and CCK2) in living cells with promising results for the use of this technology in high-throughput screening assays. Due to the high brightness of these Eu(III) complexes, the visualisation of these systems was possible with confocal and TR-FRET microscopy, using only small quantities of material (nM concentrations).

4 New hydrophilic sulfonated systems

4.1 Introduction

The P-Me phosphinate C-substituted systems described in the previous chapter exhibited very good behaviour in the *in vivo* bioassay. The introduction of negatively charged functionalities provided high water solubility to the molecule and suppressed the non-specific labelling of living cells.

Notwithstanding the high brightness of the P-Me system ($B = 14 \text{ mM}^{-1} \text{ cm}^{-1}$ at 332 nm in water), some modifications to improve the quantum yield are possible. The P-Ph phosphinate analogue, described in Section 2.2, presented a higher quantum yield (by about 10 % in MeOH) and longer lifetime (by about 10 %). The main issue with this complex was the lack of water solubility.

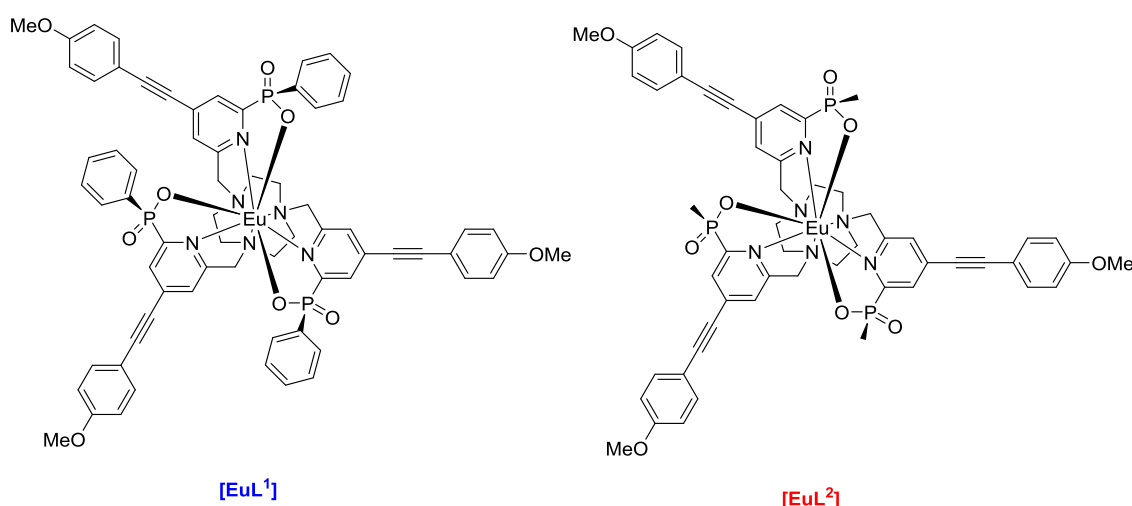


Table 13: Photophysical properties of two phosphinate Eu(III) complexes, (MeOH, 295 K). The values in parenthesis for [EuL²] are measured in H₂O.^a

	$\lambda_{\text{max}} / \text{nm}$	$\epsilon / \text{mM}^{-1} \text{ cm}^{-1}$	τ_0 / ms	$\Phi_{\text{em}} / \%$
[EuL ¹]	332	58.0	1.26	52
[EuL ²]	332 (328)	58.1 (58.0)	1.18 (1.00)	43 (22)

^a Errors on λ_{max} , ϵ , τ_0 , and Φ_{em} are $\pm 10\%$.

In this chapter, the introduction of solubilising moieties into the P-Ph system is discussed.

4.2 Improving the water solubility of the P-Ph system

Different approaches were considered in order to improve the water solubility of the P-Ph phosphinate system. The study of the behaviour of the P-Ph analogues of compounds $[\text{EuL}^{16}]^{2-}$ and $[\text{EuL}^{17}]^{2-}$ seemed to be the more straightforward option (Figure 60).

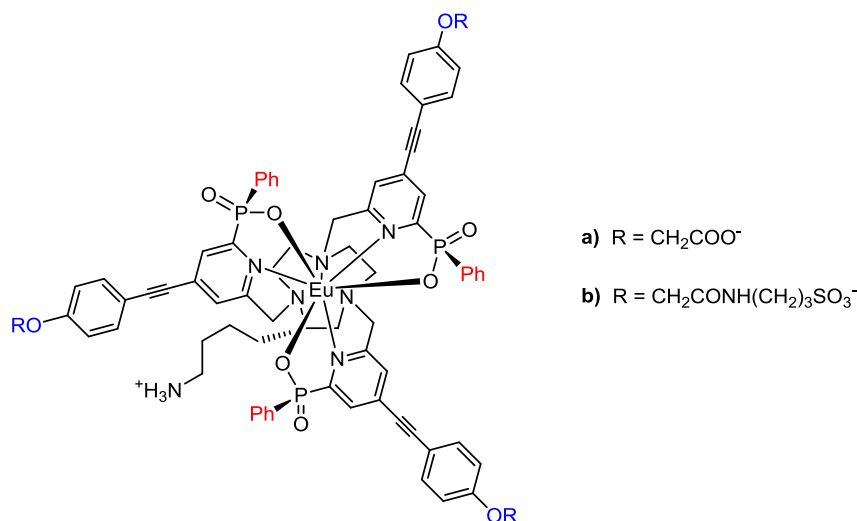


Figure 60: Structures of the P-Ph phosphinate analogues.

The introduction of sulfonate moieties at different position on the ligand was also investigated. The sulfonation of the P-Ph aromatic ring was pursued (Figure 61); in addition to an enhanced water solubility, this system possesses negative charges close to the Eu(III) centre, that could affect the energy transfer properties in a FRET process.

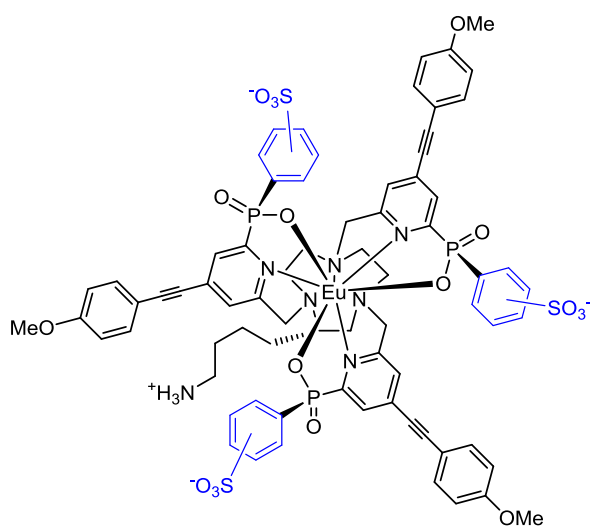


Figure 61: General structures of the P-Ph sulfonate complexes.

The last modification considered was the introduction of an aliphatic chain, with a terminal sulfonate group, at the 3 position of the aryl group (Figure 62). In fact, the introduction of an electron donating group in this position has been established to shift the excitation wavelength by about 10 nm to the red.⁸⁷ This makes the excitation more efficient with less energetic (higher wavelength) excitation sources (e.g. 355 and 365 nm).

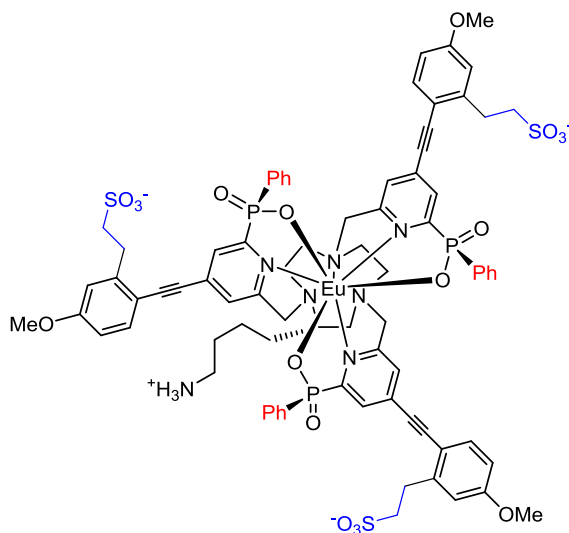
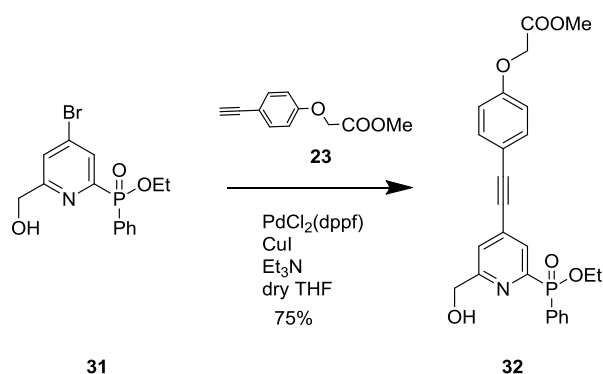


Figure 62: Structure of the P-Ph complex substituted with an aliphatic chain.

4.2.1 The analogues of the P-Me phosphinate systems

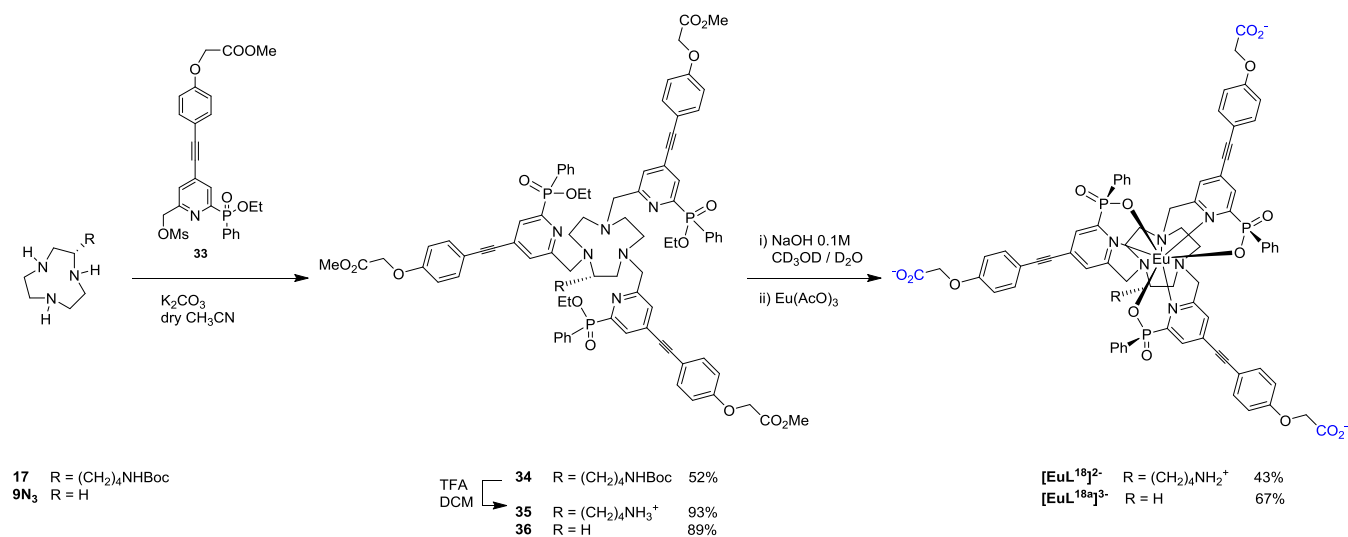
The P-Ph analogue chromophore **32** was synthesised by Sonogashira coupling between the *p*-Br pyridyl derivative **31** and compound **23**, using Pd(dppf)Cl₂ as the catalyst.



Scheme 15: Synthesis of the P-Ph phosphinate chromophore.

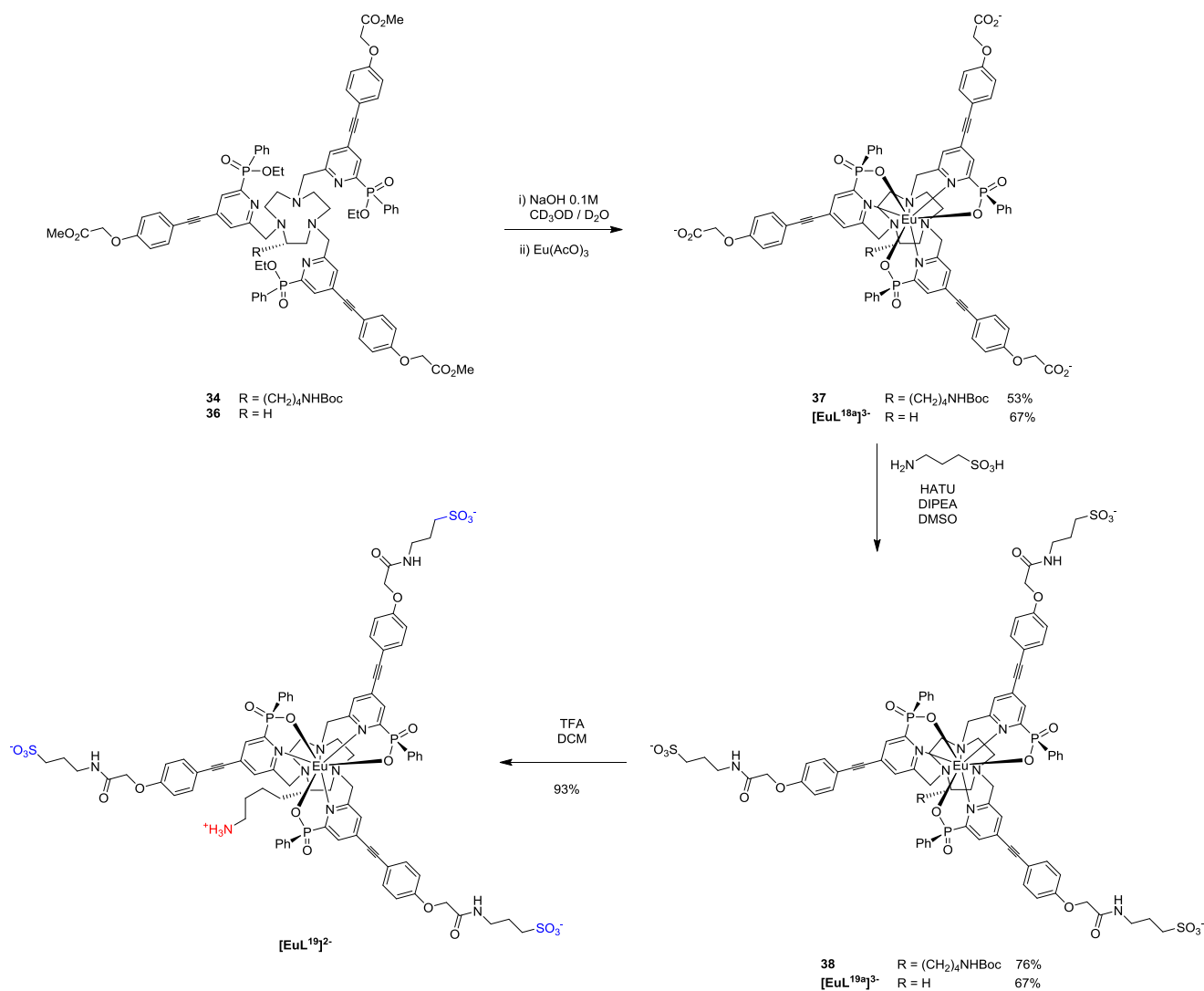
The synthesis of the two P-Ph analogues followed the same procedure described for the P-Me systems (Section 3.3.2). The unsubstituted analogues were also synthesised to allow for comparison.

The alkylation of the 9-membered rings with the mesylate derivative **33** was carried out, using standard condition, to obtain the trisubstituted ligands **34** and **35**. Deprotection of the primary amine with TFA in DCM (only for ligand **34**), basic hydrolysis of the phosphinate and carboxylate groups followed by complexation yielded $[\text{EuL}^{18}]^{2-}$ and the unsubstituted analogue $[\text{EuL}^{18a}]^{3-}$.



Scheme 16: Synthesis of $[\text{EuL}^{18}]^{2-}$ and its unsubstituted analogue $[\text{EuL}^{18a}]^{3-}$.

For the synthesis of complex $[\text{EuL}^{19}]^{2-}$, ligand **34** was reacted with $\text{Eu}(\text{OAc})_3$ after basic hydrolysis. The coupling with homotaurine in the presence of HATU and DIPEA in DMSO was successful and the subsequent deprotection of the BOC group with TFA gave the desired compound in near quantitative yield. The unsubstituted analogue $[\text{EuL}^{19a}]^{3-}$ was synthesised from the coupling reaction between homotaurine and $[\text{EuL}^{18a}]^{3-}$.



Scheme 17: Synthesis of [EuL¹⁹]²⁻ and its substituted analogue [EuL^{19a}]³⁻.

The photophysical properties of the new series of P-Ph phosphinate complexes were investigated and compared to the P-Me systems (Table 14).

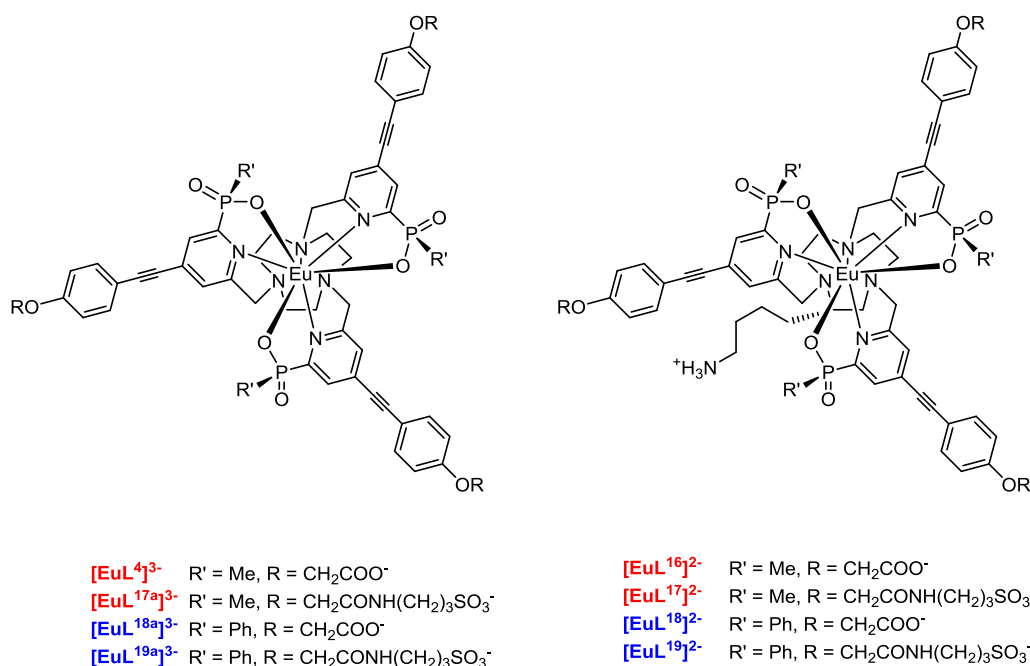


Table 14: Summary of the photophysical properties for the new series of P-Ph C-substituted complexes (blue) and unsubstituted analogues compared to the P-Me analogues (red), (H₂O, 295 K).^a

	λ_{max} / nm	τ_0 / ms	Φ_{em} / %	ε / mM ⁻¹ cm ⁻¹	logP
[EuL⁴]³⁻	330	1.04	28	57	- 2.2
[EuL^{17a}]³⁻	328	1.01	26	57	- 2.2
[EuL^{18a}]³⁻	330	1.11	38	58	- 1.9
[EuL^{19a}]³⁻	328	1.12	32	57	- 2.1
[EuL¹⁶]²⁻	330	1.05	26	57	<i>n.d.</i>
[EuL¹⁷]²⁻	328	1.00	26	57	<i>n.d.</i>
[EuL¹⁸]²⁻	330	1.10	37	58	<i>n.d.</i>
[EuL¹⁹]²⁻	328	1.11	31	57	<i>n.d.</i>

^a Errors on λ_{max} , τ_0 , Φ_{em} and ε are $\pm 10\%$, errors on logP are $\pm 20\%$.

As expected, this new series of complexes possess both a higher quantum yield (up to 38 % for **[EuL^{18a}]**) and a longer emission lifetime (around 1.1 ms). The logP measurements confirmed the good water solubility of the new P-Ph series of complexes (blue), comparable with the values measured for the P-Me complexes (red).

4.2.2 Introduction of aromatic sulfonates

The second strategy considered for the enhancement of water solubility of the P-Ph complex was aromatic sulfonation. This is a well-known method that has been applied to create water soluble dyes and polymers.⁹⁸⁻⁹⁹ This series of compounds was designed in order to maintain the good properties observed for the P-Ph system (*i.e.* high quantum yields and long emission lifetimes). The sulfonation of this position was not expected to perturb the chromophore characteristics significantly, as the phosphorus oxygen bond and the aryl group to which it is attached are not strongly conjugated. X-ray structural studies (*Figure 35*) had earlier confirmed that the phosphorus–oxygen double bond lies out of the plane of the aryl rings (torsion angle = 20°). In addition, the effect of three negative charges close to the europium centre may affect the energy transfer properties.

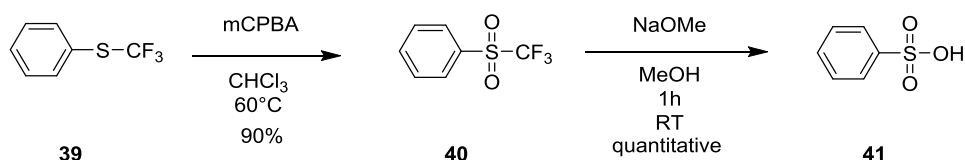
4.2.2.1 Synthetic investigations

Classically, the introduction of sulfonate functionalities into aryl rings is undertaken at the end of the synthesis. In fact, the poor solubility of these anionic compounds in organic solvents makes them difficult to separate and purify. However, aryl sulfonation occurs under forcing electrophilic conditions and is generally not suitable for multifunctional compounds.

For our purpose, the sulfonate moiety had to be introduced at an early stage in the synthesis, so the use of different protecting groups was considered. These PGs are typically electron poor or sterically hindered sulfonate esters (*e.g.* neopentyl or halogenated-ethyl esters)¹⁰⁰⁻¹⁰¹ that prevent a nucleophilic substitution reaction on the C-O bond. Deprotection can be achieved either using base,¹⁰² acid¹⁰³ or enzymatic-catalysis,¹⁰⁴ releasing the sulfonate group in a final reaction step. The protecting group also permits the use of conventional purification methods (*i.e.* column chromatography) avoiding the handling of intermediate anionic systems.

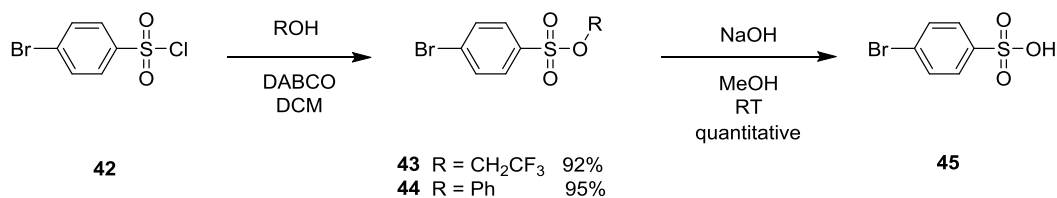
Three PGs, that provide stability to strong acids, nucleophilic substitution and palladium catalysed cross coupling, were considered at the outset.

In the first case, the sulfonate group was masked as a trifluoromethylthio functionality. Oxidation with *m*CPBA converted the thioether into the sulfone analogue that is reported to be hydrolysed in the presence of NaOMe.¹⁰⁵ Test reactions showed high yields for this process, so this strategy was examined first for the synthesis of the target ligand (*Scheme 18*).



Scheme 18: Protecting group for sulfonate, first strategy.

Two other protecting groups, brought to prominence by the work of Miller,¹⁰¹ were also considered. Trifluoroethyl (TFE) and phenyl (Ph) sulfonate esters as protecting groups for the sulfonic acid moiety have been reported to be stable to strong acids and nucleophilic substitution; they are cleaved under basic conditions. Positive results for the test reactions confirmed the utility of these PGs for the synthesis of the target compound (Scheme 19).

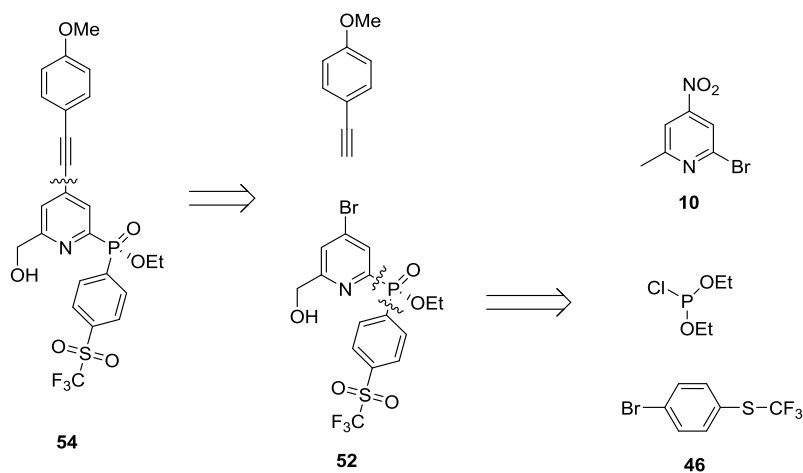


Scheme 19: Protecting groups for sulfonate, second and third strategies.

4.2.2.2 Application of the new methodologies for the synthesis of new compounds

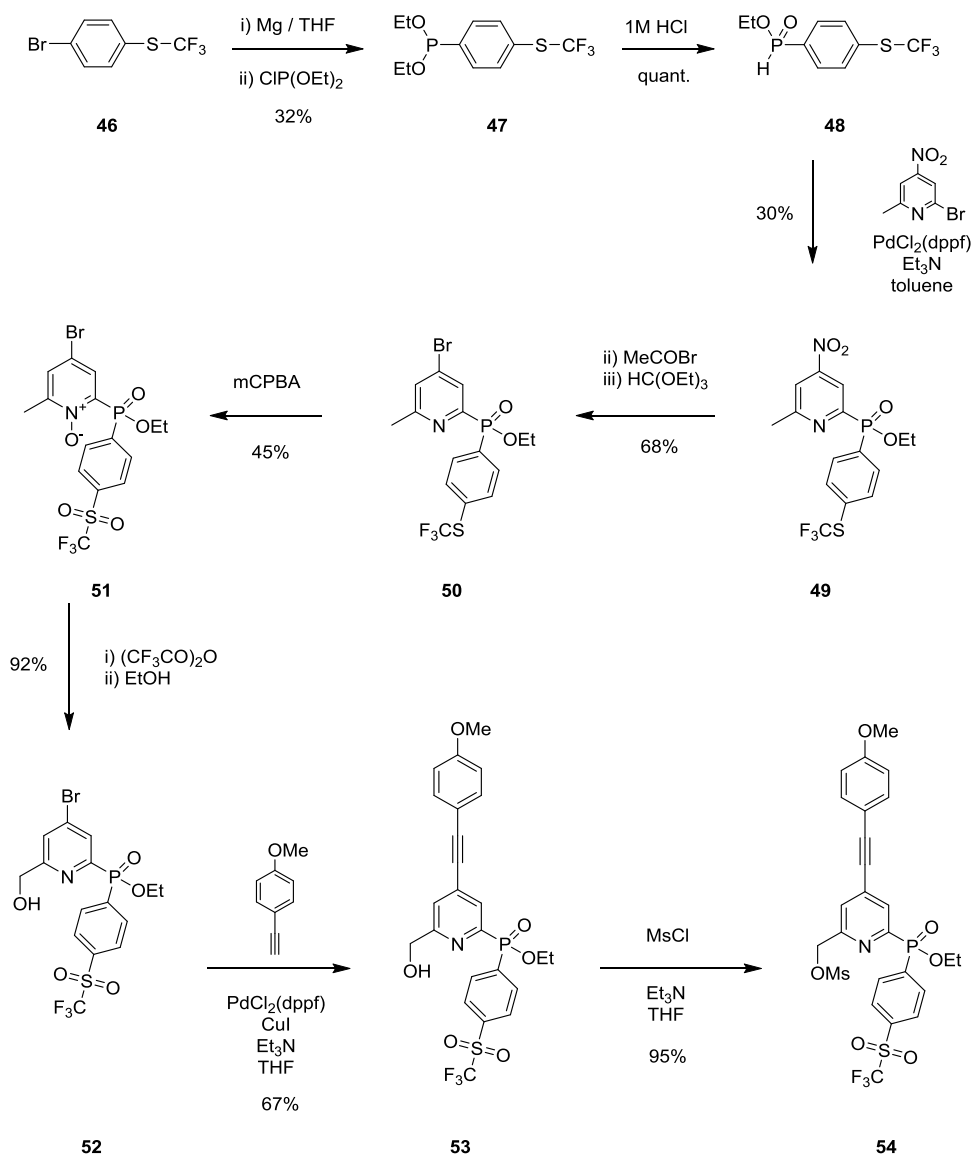
4.2.2.2.1 First strategy

A retrosynthetic analysis (Scheme 21) identified the 2,4,6-trisubstituted pyridine **52**, with a 4-Br group, as the main building block for the production of the extended chromophore **54**. The pyridine derivative **52** can be further disconnected, foreseeing two subsequent C-P bond-forming reactions. This led to the identification of 2-bromo-6-methyl pyridine **10** and 1-bromo-4-(trifluoromethylthio)benzene **46** as starting materials.

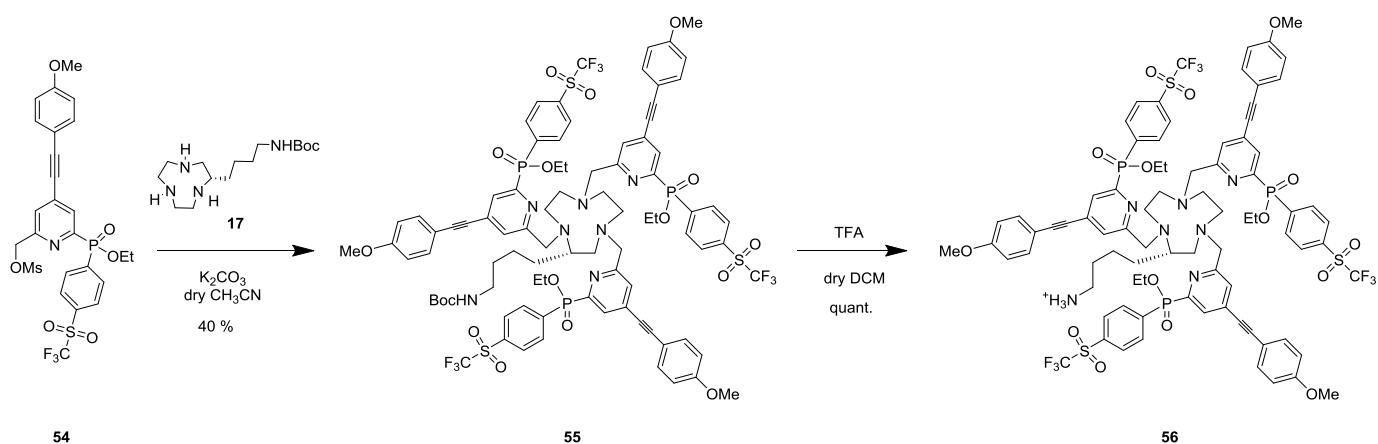


Scheme 20: Retrosynthetic approach for pyridine intermediates, first strategy.

The bromo derivative, **46**, was converted to the Grignard reagent and reacted with diethylchlorophosphite. Hydrolysis to the corresponding phosphinate **48** was achieved with one equivalent of 1 M HCl.¹⁰⁶ Coupling between intermediate **48** and 2-bromo-4-nitro-6-methyl pyridine in degassed toluene with Et₃N using Cl₂Pd[bis(diphenylphosphino)ferrocene] as a catalyst was successful. Bromination with acetyl bromide followed by re-esterification of the phosphinic acid with HC(OEt)₃ allowed the isolation of intermediate **50** in 68 % yield. Compound **50** was treated with *m*CPBA in CHCl₃ to give the N-oxide **51**, with simultaneous oxidation of the thioether to the corresponding sulfone (45 % yield). Treatment with (CF₃CO)₂O and subsequent hydrolysis in EtOH / H₂O gave the building block **52** in 92 % yield. The introduction of the aryl alkynyl moiety by Sonogashira coupling was successful (yield = 67 %). Mesylation under standard conditions gave compound **54**, which was used for the alkylation of the azamacrocyle, **17** to give ligand **55** (Scheme 22). Deprotection of the primary amine with TFA in dry DCM allowed for the formation of ligand **56**, in a quantitative yield.

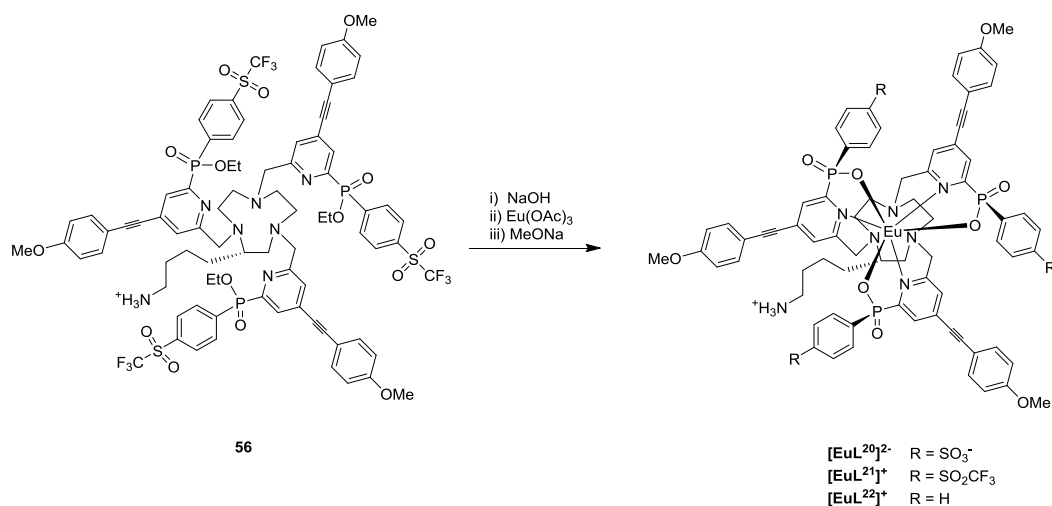


Scheme 21: Synthesis of the new phosphinate donor, first strategy.



Scheme 22: Synthesis of the new phosphinate ligand, first strategy.

The unmasking of the sulfonate groups was attempted on ligand **56** and on the complex $[\text{EuL}^{21}]^+$. Unfortunately, the isolated product was $[\text{EuL}^{22}]^+$ and not the expected product, $[\text{EuL}^{20}]^{2-}$. Cooling down the reaction to $-20\text{ }^\circ\text{C}$ only resulted in hydrolysis of the phosphinate esters leaving the trifluoromethylsulfone unreacted. Evidently, cleavage of the C-S bond generates a better aryl leaving group under these reaction conditions, than the CF_3^- , despite being cleaved as desired in the model system.



Scheme 23: Synthesis of the new phosphinate complex.

Despite the unsuccessful synthesis of $[\text{EuL}^{20}]^{2-}$, the complex $[\text{EuL}^{21}]^+$ was isolated and analysed by UV-Vis spectroscopy (Figure 63). The absorption spectrum showed a red shift of 10 nm to 342 nm, compared to the parent system, which is interesting from a spectroscopic point of view, moving the excitation wavelength further away from the excitation of endogenous chromophores. The emission lifetime was recorded in MeOH: $\tau_0 = 1.1\text{ ms}$. The quantum yield was measured in MeOH ($\Phi_{em} = 48\%$).

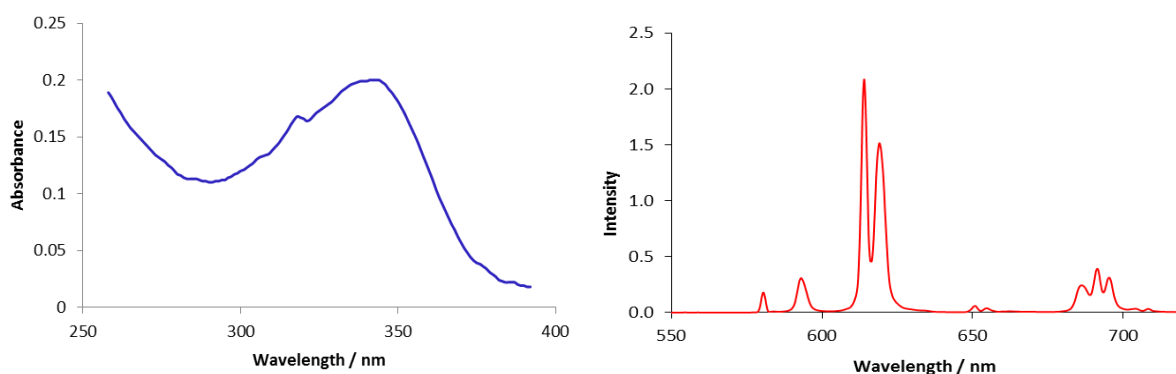
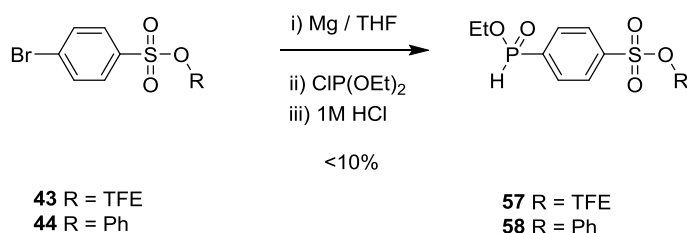


Figure 63: Absorption (left) and emission (right) spectra of $[\text{EuL}^{21}]^+$, (MeOH, 295 K, $\lambda_{ex} = 342\text{ nm}$).

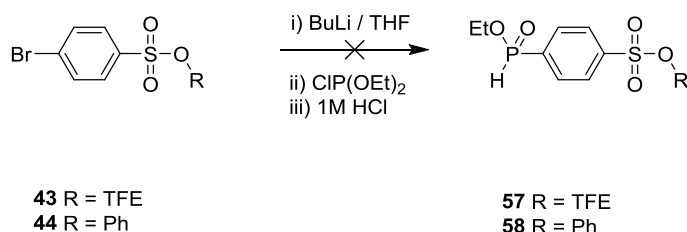
4.2.2.2.2 Second strategy

The use of TFE and Ph sulfonate esters as PGs, that require milder cleavage conditions, was undertaken in order to achieve the target compound. The same Grignard strategy described for compound **46** (Scheme 24) was attempted in order to synthesise compound **57** and **58**; unfortunately, for both esters, the desired compound was isolated in poor yield (< 10 %), with a considerable amount of unreacted starting material being recovered.



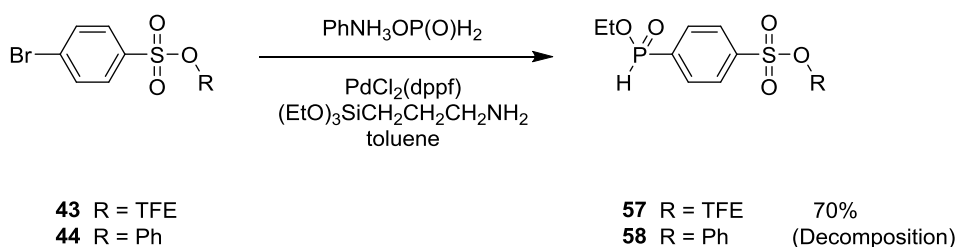
Scheme 24: Synthesis of the new phosphinate donor, Grignard strategy.

Lithiation was also tried (Scheme 25), but the bromo compounds **43** and **44** were found to be very stable towards BuLi and, once lithiated, completely unreactive towards the chlorophosphine.



Scheme 25: Synthesis of the new phosphinate donor, lithiation strategy.

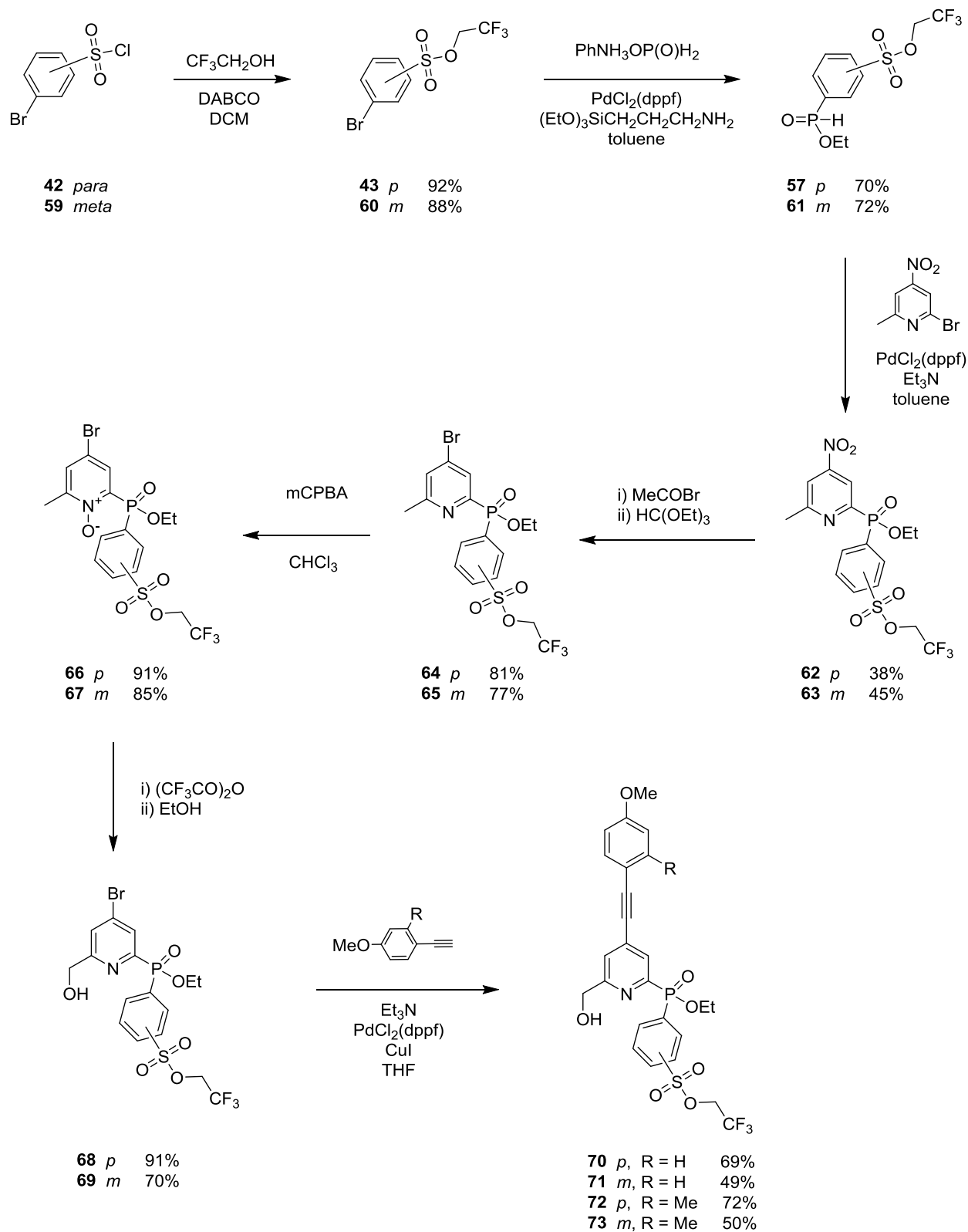
In order to form the P-C bond, a palladium cross-coupling reaction using anilinium hypophosphite as a source of phosphorous was investigated (Scheme 26).¹⁰⁷⁻¹⁰⁸ The use of a bidentate ligand for Pd(II) (*i.e.* dppf) is important to inhibit the competing reaction to give the di-aryl substituted phosphinate ester. Aminopropyltriethoxysilane (1 eq) serves as a base for the Pd(II) coupling and enables the *in situ* esterification of the phosphinic acid.¹⁰⁹



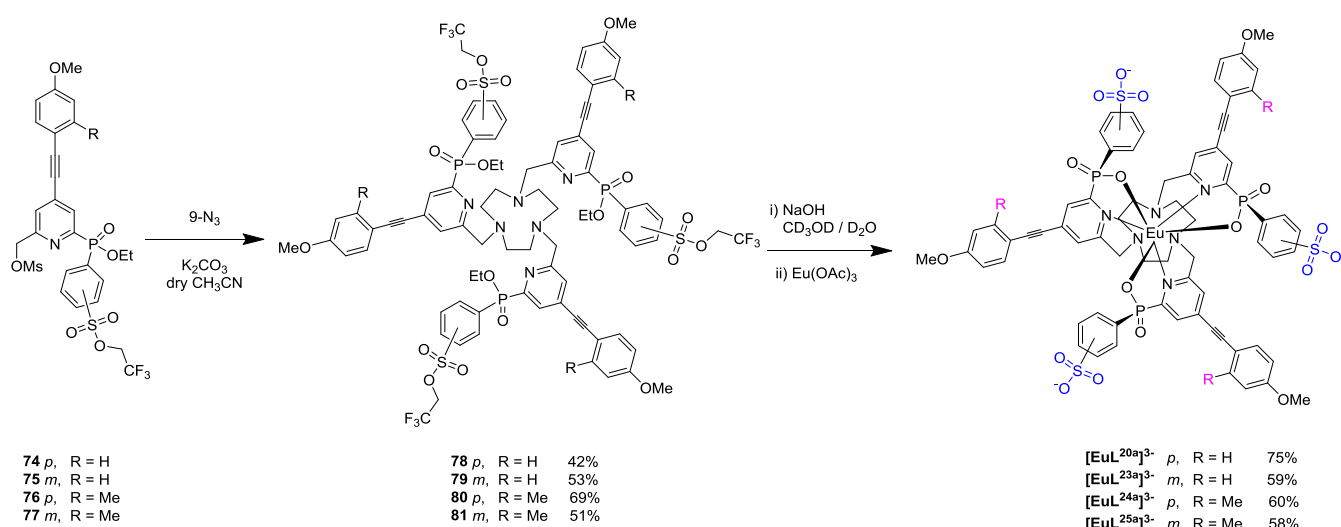
Scheme 26: Synthesis of the new phosphinate donor, palladium catalysed strategy.

The cross-coupling reaction proceeded in 70 % yield for the TFE ester, but failed with the Ph ester, probably due to competitive insertion into the O–Ph bond.

Following the positive result for the TFE protected compound, the synthesis of the extended chromophore was pursued (Scheme 27);¹¹⁰ both *meta* and *para* sulfonated aryl derivative were considered. The di-esters **57** and **61** were used in a second coupling reactions with 2-bromo-4-nitro-6-methyl pyridine in degassed toluene using $\text{Cl}_2\text{Pd}[\text{bis}(\text{diphenylphosphino})\text{ferrocene}]$ as the catalyst to give the phosphinate esters **62** and **63**. Bromination with neat acetyl bromide followed by re-esterification of the phosphinic acid group with $\text{HC}(\text{OEt})_3$ allowed the isolation of intermediates **64** and **65** in 81 and 77 % yield respectively. Treatment of the 4-bromo-pyridyl esters with *m*CPBA in CHCl_3 gave the corresponding *N*-oxides **66** and **67**. Activation of the proximate methyl group occurred following treatment with $(\text{CF}_3\text{CO})_2\text{O}$, in a Boekelheide rearrangement; subsequent hydrolysis of the trifluoroacetate esters *in situ*, using wet ethanol gave the intermediates **68** and **69**. The aryl-alkynyl moiety was introduced by a Sonogashira coupling; four chromophores were prepared, two of them with a simple 4-OMe aryl group (**70** and **71**) and two bearing a methyl group in the *meta* position of the aryl group (**72** and **73**). This substitution has been reported to shift the absorption wavelength of the conjugated chromophore by 7–10 nm to the red.⁸⁷

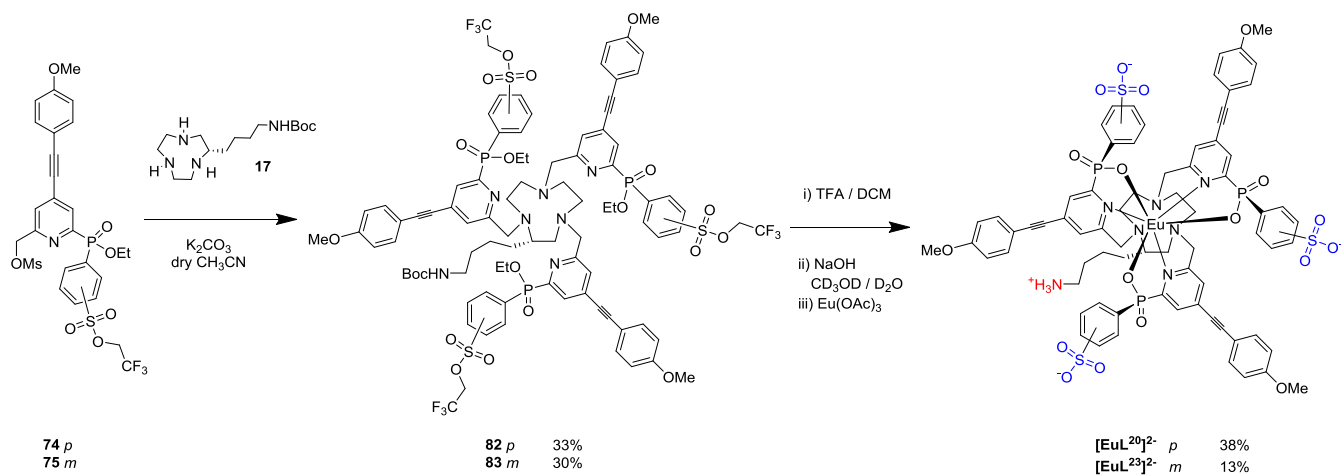
Scheme 27: Synthesis of the new P-Ph-SO₃⁻ chromophores.

Trialkylation of 1,4,7-triazacyclononane (9-N₃) with the appropriate mesylate afforded the fully protected neutral ligands. Treatment with aqueous base (NaOH in water/methanol, pH = 12) hydrolysed the phosphinate and the sulfonate esters. In the latter case, hydrolysis of the sulfonate occurred at a similar rate to the phosphinate cleavage reaction and was conveniently monitored by observing formation of trifluoroethanol by ¹⁹F-NMR spectroscopy. Complexation of the ligand in aqueous methanol at pH 6 gave the Eu(III) complexes which were purified by reverse phase HPLC in the presence of triethylammonium acetate and isolated as their triethylammonium salts. Ion-pair adducts of the ammonium salts were identified by ES-MS to confirm the constitution of the isolated salt.



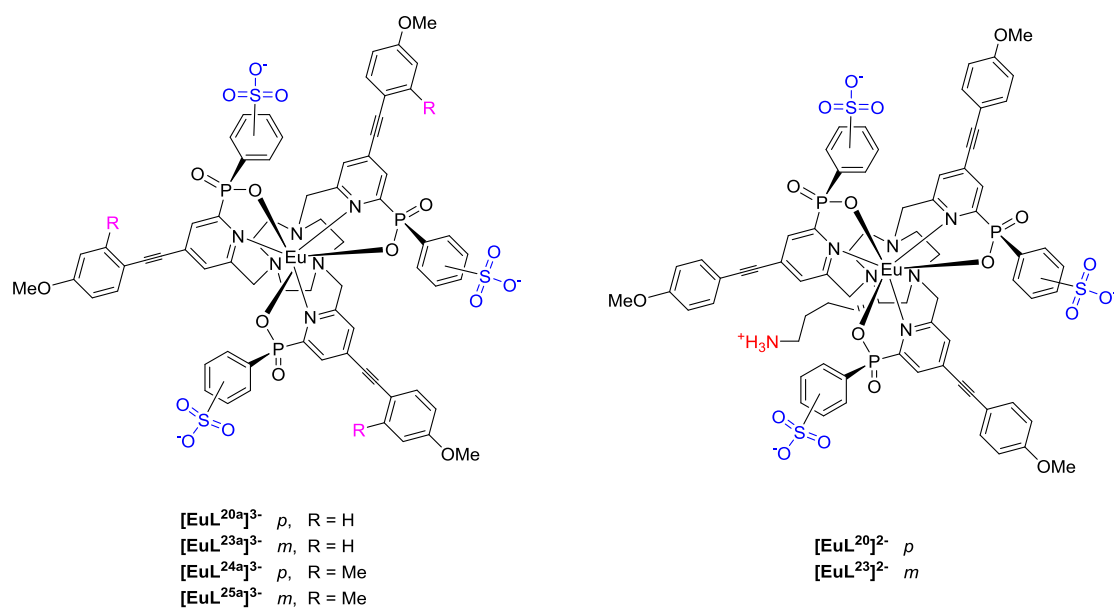
Scheme 28: Synthesis of the P-Ph-SO₃⁻ complexes.

Two C-substituted analogues were also prepared *via* alkylation of the Boc-protected amine **17** (Scheme 29). The Boc group was removed with TFA at room temperature, prior to base hydrolysis and europium complexation.

Scheme 29: Synthesis of the C-substituted P-Ph-SO₃⁻ complexes.

The low yields for the last step are due to hydration of the triple bond in the presence of acid (TFA); lowering the temperature of the reaction (4 °C) and dry solvents did not change the yield. This problem was not observed (or to a lesser extent) with the previously described series of complexes and was found to be prominent in the presence of more electron rich chromophores (*e.g.* chromophores **72** and **73**).

Comparison of the photophysical properties of the new P-Ph-SO₃⁻ complexes (Table 15) showed that they possess similar optical properties (λ , ϵ , τ , ϕ) to each other and to the parent phenylphosphinate complex ([EuL¹], Chapter 2). This is consistent with the absence of perturbation of the sensitizer excited state energies or the coordination environment around the Eu(III) centre by the sulfonate negative charge.

Table 15: Summary of the photophysical properties for the new series of P-Ph-SO₃⁻, (H₂O, 295 K).^a

	λ_{max} / nm	τ_0 / ms	Φ_{em} / %	ε / mM ⁻¹ cm ⁻¹	logP
$[\text{EuL}^{20\text{a}}]^{3-}$	332	1.11	31	58	- 0.7
$[\text{EuL}^{23\text{a}}]^{3-}$	332	1.10	29	58	- 2.2
$[\text{EuL}^{24\text{a}}]^{3-}$	340	1.09	32	58	- 0.1
$[\text{EuL}^{25\text{a}}]^{3-}$	340	1.12	33	58	- 1.4
$[\text{EuL}^{20}]^{2-}$	332	1.10	30	58	<i>n.d.</i>
$[\text{EuL}^{23}]^{2-}$	332	1.09	28	58	<i>n.d.</i>

^a Errors on λ_{max} , τ_0 , Φ_{em} and ε are $\pm 10\%$, errors on logP are $\pm 20\%$.

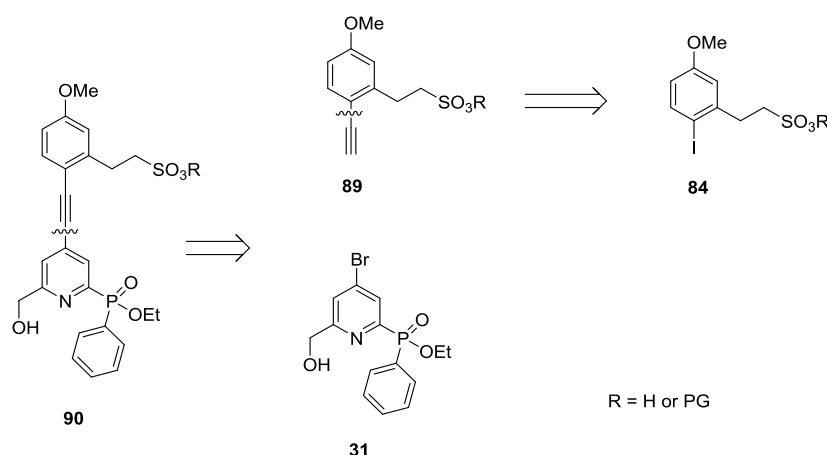
In each case, the Eu(III) complexes presented good water solubility. The logP measurements showed that the introduction of the methyl group in the three phenyl rings led to an increased lipophilicity, and that the *meta*-sulfonated complex $[\text{EuL}^{23\text{a}}]$, rather surprisingly, had a higher negative logP value than the *para*-substituted isomer. High quantum yields (up to 33 %) and long emission lifetimes were registered (around 1.1 ms) for the entire series and a red shift of 8 nm in the maximum of absorption was observed for the methyl substituted complexes, ($[\text{EuL}^{24\text{a}}]^{3-}$ and $[\text{EuL}^{25\text{a}}]^{3-}$).

4.2.3 Introduction of an aliphatic sulfonate substituent

The introduction of an aliphatic chain in the *meta* position of the aryl group was considered in order to get a red shift for the maximum absorption wavelength.⁸⁷ To give water solubility to the system, the chain was designed to terminate with a sulfonate group. The length of the aliphatic chain (two carbons) was chosen in order to generate an overall electron releasing substituent onto the aryl group, notwithstanding the presence of the electron withdrawing sulfonate moiety on the chain.

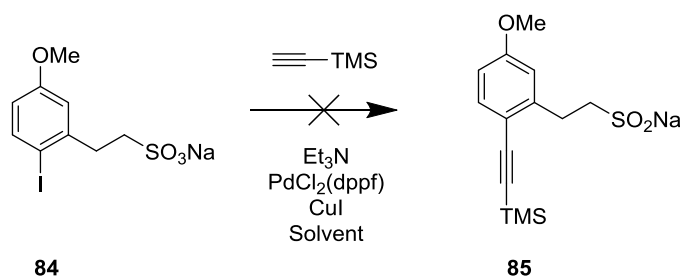
4.2.3.1 Synthetic investigations

A retrosynthetic analysis (*Scheme 30*) identified the 2,4,6-trisubstituted pyridine, **31**, and the trifunctionalised aryl-alkyne derivative, **89**, as the main building blocks for the synthesis of the extended chromophore, **90**. Compound **89** can be accessed through a second cross-coupling reaction between compound **84** and ethynyl-trimethylsilane.



Scheme 30: Retrosynthetic analysis of compound **90**.

The sodium salt of compound **84**, provided by Cisbio, was chosen as starting material for the Sonogashira cross coupling with ethynyl-trimethyl silane to form compound **85** (*Scheme 31*). The functionalisation of the iodo-sulfonated compound proved to be difficult, due to the lack of solubility of the sodium salt in the organic medium required for the Pd(II) catalysed reaction.



Solvent : 100% THF, 100% DMF, 50:50 THF / DMF

Scheme 31: First attempt at functionalisation of compound **85**.

Different strategies to convert the sodium sulfonate moiety into the protected TFE ester were attempted, in order to gain sufficient solubility in organic solvents. Direct esterification and conversion into the sulfonyl chloride analogues were considered, but failed due to the lack of solubility of compound **84**.

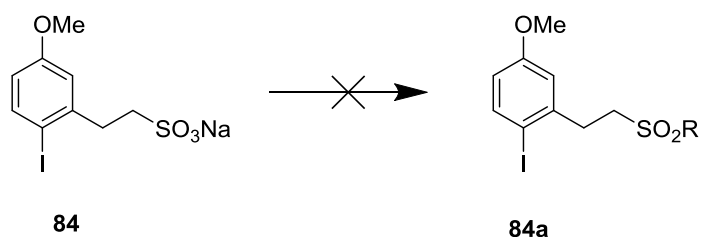
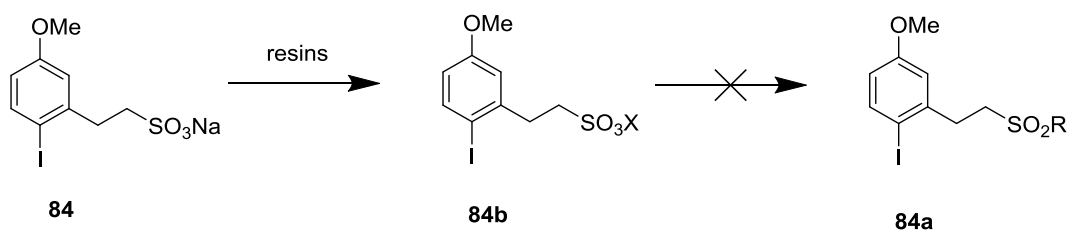


Table 16: Attempts to functionalise compound **84**.

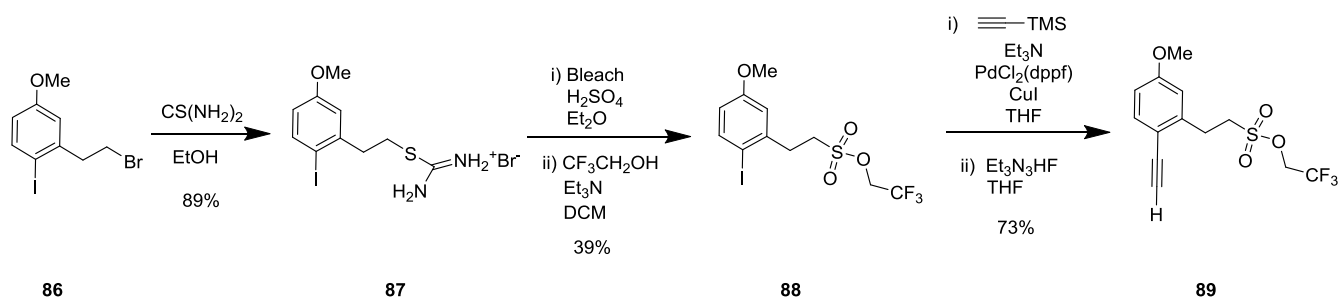
	Reagents	Solvent	T (°C)	R
1	POCl ₃	neat	120	Cl
2 ¹¹¹	Cyanuric-Cl / Et ₃ N	acetone	60	Cl
3 ¹¹²	HC(OCH ₂ CF ₃)	neat	140	OCH ₂ CF ₃
4 ¹¹³	HC(OCH ₂ CF ₃) / TBAI	neat	140	OCH ₂ CF ₃

Strong cation exchange resin (DOWEX 50W x 4-100) was used in order to convert the sodium salt **84** into the free sulfonic acid (*Table 17, entries 1-3*) or into the more lipophilic pyridinium salt (*Table 17, entries 4-6*). Although these compounds presented enhanced solubility in the organic solvent, the esterification of the sulfonate remained problematic, due to the low electrophilicity of this functionality. The use of sulfonates as nucleophiles in a Mitsunobu-like reaction has been described for the formation of tosylates (*Table 17, entry 3 and 6*), but failed for this substrate.

Table 17: Conversion of sulfonate **84** into more soluble derivatives and further attempted functionalisations.

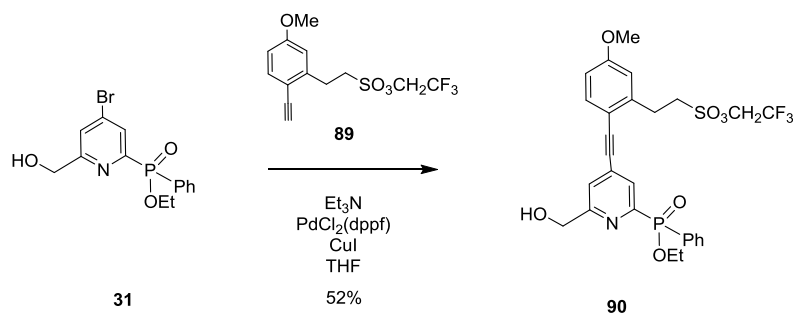
	X	Reagents	Solvent	T (°C)	R
1	H	POCl ₃	neat	80	Cl
2 ¹¹¹	H	Cyanuric-Cl / Et ₃ N	acetone	60	Cl
3 ¹¹⁴	H	Ph ₃ P / DIAD / Et ₃ N / CF ₃ CH ₂ OH	toluene	70	OCH ₂ CF ₃
4 ¹¹²	PyH	HC(OCH ₂ CF ₃)	DCM	60	OCH ₂ CF ₃
5 ¹¹⁵	PyH	Ph ₃ PO / (CF ₃ SO ₂) ₂ O / Et ₃ N / CF ₃ CH ₂ OH	DCM	40	OCH ₂ CF ₃
6 ¹¹⁴	PyH	Ph ₃ P / DIAD / CF ₃ CH ₂ OH	toluene	70	OCH ₂ CF ₃

A different strategy was attempted in order to introduce the sulfonate ester directly from the corresponding bromo-derivative (*Scheme 32*).¹¹⁶ The treatment of the bromo-derivative **86** with thiourea gave compound **87** in good yield. The subsequent treatment of the crude bromide salt, **87**, with bleach in the presence of acid, followed by trifluoroethanol, gave compound **88** in a “one-pot”, two step reaction sequence. This new synthetic approach established a quick method to synthesise a compound soluble in most organic solvents that was easy to handle. Compound **88** was reacted with TMS-acetylene under standard Sonogashira conditions. The alkyne derivative **89** was isolated in good yield, after cleavage of the TMS group with triethylammonium hydrofluoride.

Scheme 32: Synthesis of the sulfonate protected alkynyl derivative **89**.

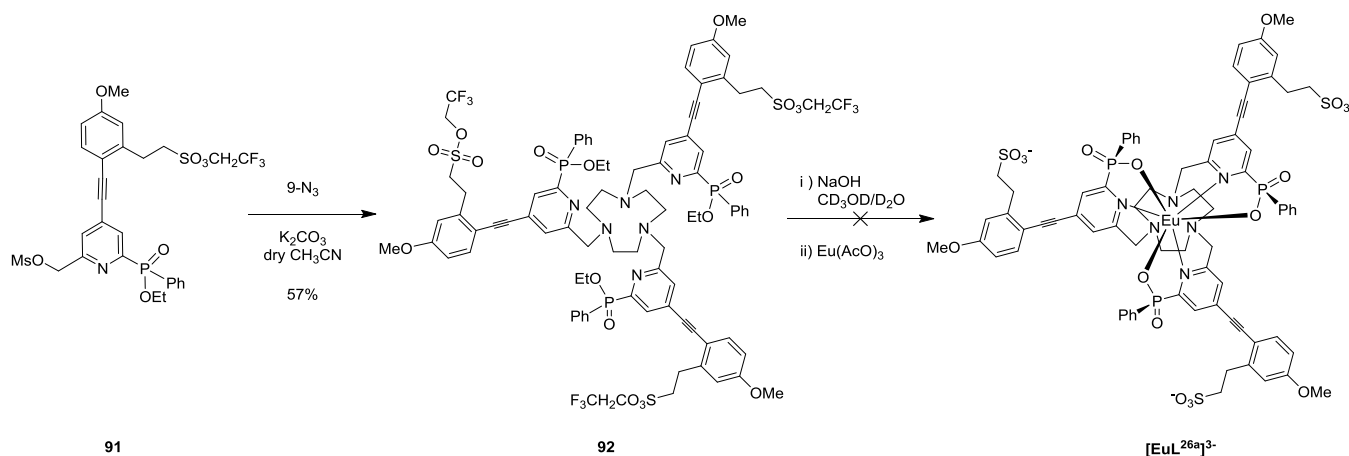
4.2.3.2 Application of the new methodology

The synthesis of the extended chromophore, **90**, was achieved with a Sonogashira cross-coupling reaction between the bromo-substituted pyridine platform, **31**, and the TFE-protected alkyne derivative, **89**.



Scheme 33: Successful synthesis of the extended chromophore, **90**.

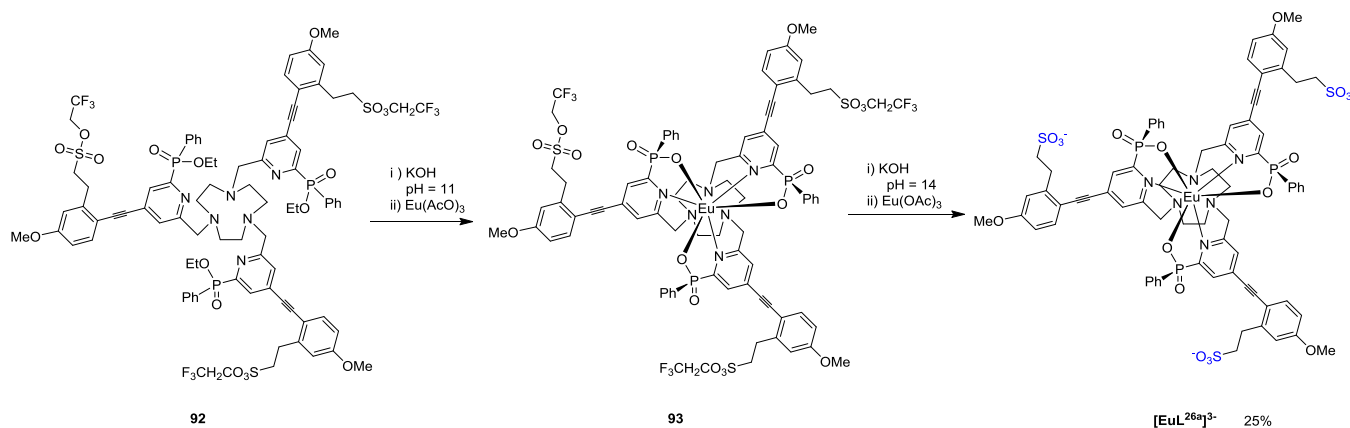
Alkylation of the 9- N_3 with the mesylate derivative, **91**, afforded the fully protected ligand **92**. Hydrolysis of the six esters with aqueous NaOH was slow and required forcing conditions ($\text{pH} = 13$, 60°C , 48 h); reaction completion was confirmed by ^{31}P and ^{19}F NMR. Surprisingly, the addition of $\text{Eu}(\text{AcO})_3$ at $\text{pH} 7$ did not show any sign of complexation. This behaviour can be tentatively linked to the presence of the negative charges of the sulfonate somehow preventing the complexation.



Scheme 34: Attempted complexation of ligand **92**.

In order to avoid the problems with complexation, the hydrolysis of the phosphinate esters was performed with milder conditions, in the presence of KOH ($\text{pH} = 11$, 60°C , 3 h) leaving the sulfonate protecting group intact. Complexation with $\text{Eu}(\text{OAc})_3$ gave compound **93**, that

was further deprotected with KOH (pH = 14, 60 °C, 48 h). Possibly, the strong deprotecting conditions caused partial decomplexation, therefore the pH was adjusted to 7 and further $\text{Eu}(\text{OAc})_3$ was added to the reaction that was heated up for another 16 h giving the complex $[\text{EuL}^{26a}]^{3-}$.

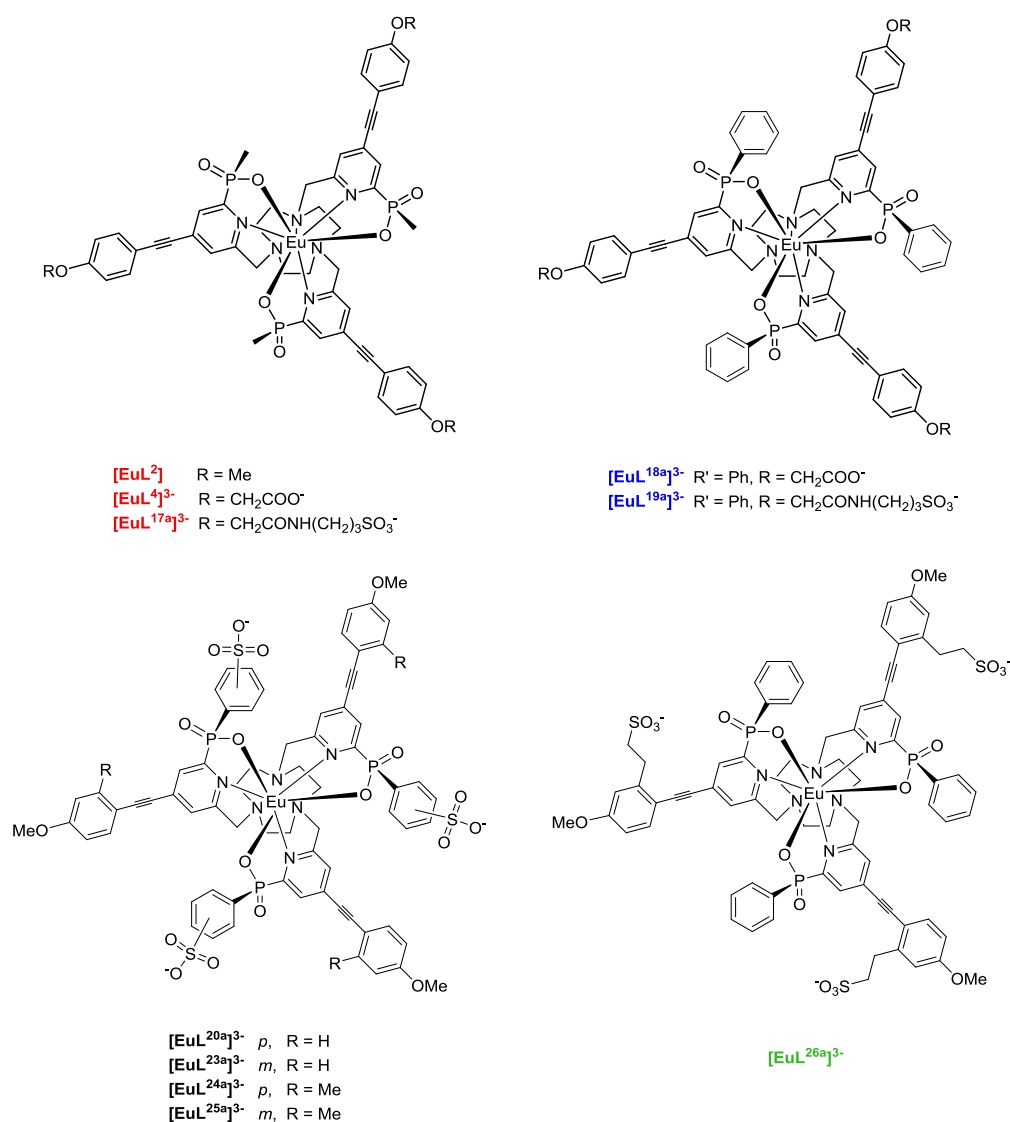


Scheme 35: Synthesis of complex $[\text{EuL}^{26a}]^{3-}$.

The complex $[\text{EuL}^{26a}]$ possessed a quantum yield of 27 % and a lifetime of 1.15 ms in water. The absorption maximum shifted to the red ($\lambda_{max} = 336$ nm), but not by as much as had been expected. The logP measurements (logP = + 0.5) indicate that this complex is much more lipophilic than the other sulfonate examples. Due to these results the C-substituted analogue was not synthesised.

4.3 Photophysical characterisation and FRET studies

The photophysical properties for this new series of hydrophilic complexes have been reported previously in the chapter (Section 4.2.1, 4.2.2.2 and 4.2.3.2). Here, some data are analysed to allow for comparison.

Table 18: Summary of the photophysical properties for the four series of Eu(III) complexes, (H₂O, 295 K).^a

	λ_{\max} / nm	Φ_{em} / %	τ_0 / ms	logP
[EuL²]	328	24	1.03	+ 1.4
[EuL⁴]³⁻	330	28	1.04	- 2.2
[EuL^{17a}]³⁻	328	26	1.01	- 2.2
[EuL^{18a}]³⁻	330	38	1.11	- 1.9
[EuL^{19a}]³⁻	328	32	1.12	- 2.1
[EuL^{20a}]³⁻	332	31	1.11	- 0.7
[EuL^{23a}]³⁻	332	29	1.10	- 2.2
[EuL^{24a}]³⁻	340	32	1.09	- 0.1
[EuL^{25a}]³⁻	340	33	1.12	- 1.4
[EuL^{26a}]³⁻	336	27	1.15	+ 0.5

^a Errors on λ_{\max} , τ_0 and Φ_{em} and are $\pm 10\%$, errors on logP are $\pm 20\%$.

The presence of the phenyl ring led to higher quantum yields (above 30 %) and longer luminescence lifetime (1.1 ms) compared to the P-Me analogues (*red*). The introduction of sulfonate groups in different positions of the ligand provides good water solubility with negative values of logP for all the complexes, except for $[\text{EuL}^{26a}]^{3-}$.

The high quantum yields observed resulted in enhanced brightness for these compounds ($B = 20 \text{ mM}^{-1} \text{ cm}^{-1}$ at 332 nm in water). An experiment to calculate the limit of detection on a PHERAstar FS plate reader was set up. The emission intensity from eight solutions of $[\text{EuL}^{20a}]^{3-}$ at different dilutions (50 mM HEPES buffer, pH = 7, 0.1 % BSA) was plotted as a function of the complex concentration. The emission from the buffer (I_0) was measured for six solutions and the standard deviation (σ) calculated. A value of $(I_0 + 3\sigma)$ is considered to lie above the instrument noise. The detection limit was calculated to be 0.1 pM, ten times lower than for the commercial probe **Lumi4-Tb**, under the same conditions.

$$(I_0 + 3\sigma) = a[\text{EuL}^{20a}] + I_0 \quad [12]$$

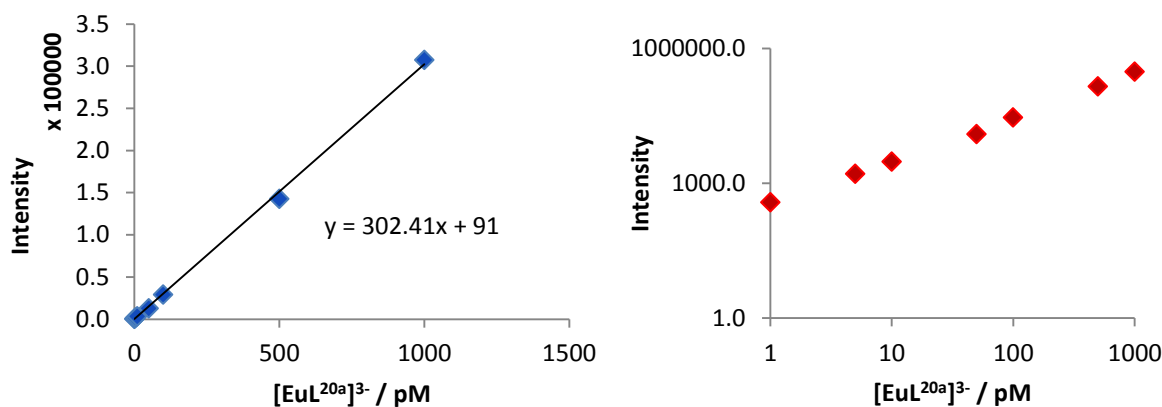


Figure 64: Calculation of the detection limit for compound $[\text{EuL}^{20a}]^{3-}$ using a PHERAstar FS plate reader, $\lambda_{\text{ex}} = 337 \text{ nm}$, $\lambda_{\text{em}} = 620 \text{ nm}$ (left). Values on a logarithmic scale (right).

The stability of these complexes in the presence of endogenous quenchers was studied and compared to the results obtained for the P-Me series (Section 3.3.3) Luminescence spectra and excited state lifetimes were measured in the presence of excess ascorbate or urate (10 mM for ascorbate, 5 mM for urate); similarly to the P-Me series; no quenching was observed by either antioxidant.

Emission spectra were recorded for the complexes (4 μM in water, pH = 7.4) in the absence and in the presence of 0.4 mM HSA, to analyse any possible interactions with protein in the medium caused by the addition of the phenyl rings.

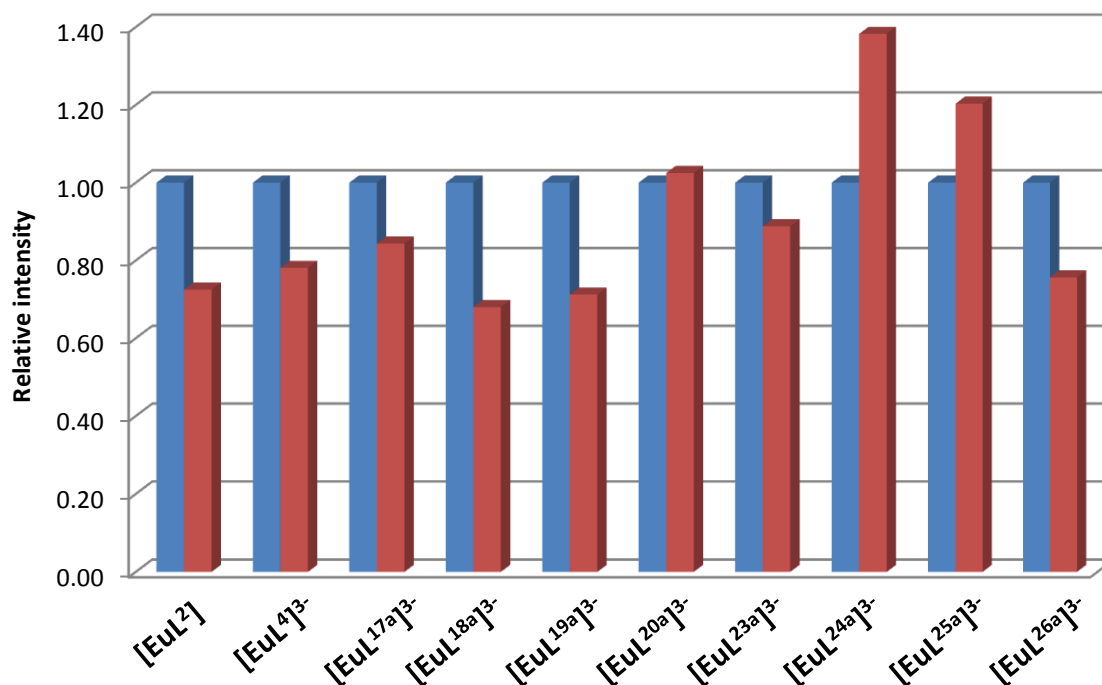


Table 19: Photophysical properties of different Eu(III) complexes in the absence (*blue*) and in the presence of 0.4 mM HSA (*red*), (with added HSA, excitation spectroscopy used to assess λ_{max}).^a

	$\lambda_{\text{max}} / \text{nm}$	$\lambda_{\text{max}} \text{HSA} / \text{nm}$	τ_0 / ms	$\tau_0 \text{HSA} / \text{ms}$	logP
[EuL ²]	328	333	1.03	1.10	+ 1.4
[EuL ⁴] ³⁻	330	337	1.04	1.01	- 2.2
[EuL ^{17a}] ³⁻	328	329	1.01	1.12	- 2.2
[EuL ^{18a}] ³⁻	330	338	1.11	1.20	- 1.9
[EuL ^{19a}] ³⁻	328	331	1.12	1.23	- 2.1
[EuL ^{20a}] ³⁻	332	341	1.11	1.16	- 0.7
[EuL ^{23a}] ³⁻	332	339	1.10	1.17	- 2.2
[EuL ^{24a}] ³⁻	340	345	1.09	1.16	- 0.1
[EuL ^{25a}] ³⁻	340	346	1.12	1.15	- 1.4
[EuL ^{26a}] ³⁻	336	340	1.15	1.18	+ 0.5

^a Errors on λ_{max} and τ_0 are $\pm 10\%$, errors on logP are $\pm 20\%$.

Unlike the P-Me series that reported a decreased emission intensity (*Section 3.3.3*), the addition of HSA to the P-Ph complexes caused a variation (enhanced or decreased intensity

depending on the chromophore) of the total emission intensity; in every case the emission spectral form remained unchanged. Increased emission lifetimes and an absorption wavelength that had shifted slightly to the red were also noticed (*e.g.* τ_0 increased from 1.12 to 1.23 ms for $[\text{EuL}^{19\text{a}}]^{3-}$ and λ_{max} shifted from 332 to 341 nm for $[\text{EuL}^{20\text{a}}]^{3-}$).

A spectral titration adding different concentrations of HSA to the europium complex did not show any sign of binding, in agreement with the results for the P-Me systems; such behaviour supported the hypothesis that there is a change in the effective dielectric constant of the ‘local medium’, following the non-specific protein-complex interaction. This interaction is perturbing the energy of the ICT transition. The measurement of the photophysical properties for two representative complexes in solvents with different polarities (*Table 20*) supported this idea. For example, $[\text{EuL}^{19\text{a}}]^{3-}$ reported a shift of 6 nm in the λ_{max} going from water to the less polar NMP. Similarly, a red-shift of 4 nm was observed for $[\text{EuL}^{20\text{a}}]^{3-}$ going from water to alcohols. Although it is difficult to identify a trend for the changes, also the quantum yields and the emission lifetimes for the two complexes are strongly affected by the nature of the solvent system.

Table 20: Photophysical properties for $[\text{EuL}^{19\text{a}}]^{3-}$ and $[\text{EuL}^{20\text{a}}]^{3-}$ measured in solvents with different polarities.^a

$[\text{EuL}^{19\text{a}}]^{3-}$	E_{T}^{N}	$\lambda_{\text{max}} / \text{nm}$	$\Phi_{\text{em}} / \%$	τ_0 / ms
H₂O	1.00	328	32	1.12
TFE-OH	0.90	330	36	1.34
MeOH	0.76	332	43	1.27
EtOH	0.65	332	39	1.25
DMF	0.40	328	57	1.28
NMP	0.36	334	39	1.18
$[\text{EuL}^{20\text{a}}]^{3-}$	E_{T}^{N}	$\lambda_{\text{max}} / \text{nm}$	$\Phi_{\text{em}} / \%$	τ_0 / ms
H₂O	1.00	332	31	1.11
TFE-OH	0.90	336	37	1.31
MeOH	0.76	336	56	1.23
EtOH	0.65	336	49	1.26
DMF	0.40	328	46	1.26
NMP	0.36	336	41	1.18

^a E_{T}^{N} is Reichardt’s normalised solvent polarity parameter.⁸⁹ ^b Errors on λ_{max} , Φ_{em} and τ_0 are $\pm 10\%$.

The quenching of the P-Ph complexes with the cyanine dye **Dy647-NH₂** was analysed and compared with the previously synthesised complexes, as described in *Chapter 2* and in *Section 3.3.3*.

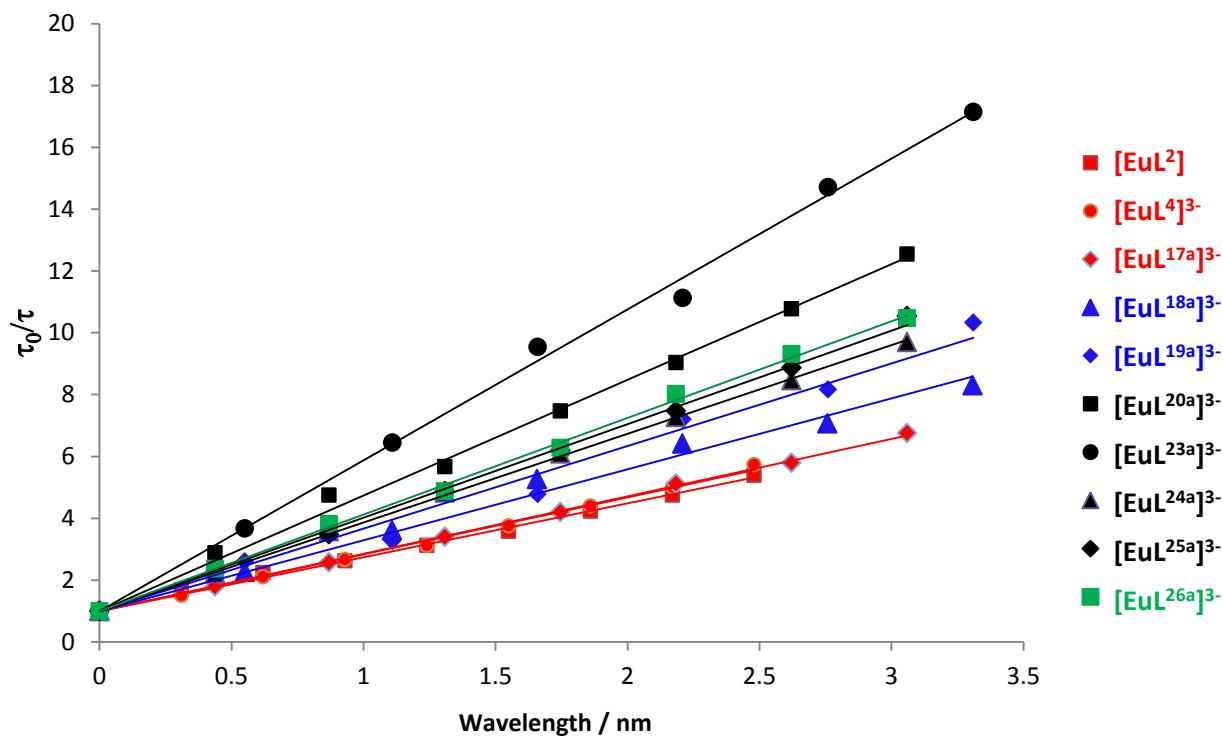


Table 21: Quenching studies. (Values recorded ($\pm 5\%$) in 50 mM HEPES buffer, 50 mM NaCl, pH = 7.4, 295 K).

	gradient	τ_0 / ms	$k_2 / \text{mM}^{-1}\text{s}^{-1}$
[EuL ²]	1.74	1.03	1.71
[EuL ⁴] ³⁻	1.84	1.04	1.77
[EuL ^{17a}] ³⁻	1.86	1.01	1.84
[EuL ^{18a}] ³⁻	2.28	1.11	2.06
[EuL ^{19a}] ³⁻	2.70	1.12	2.40
[EuL ^{20a}] ³⁻	3.74	1.11	3.37
[EuL ^{23a}] ³⁻	4.78	1.10	4.35
[EuL ^{24a}] ³⁻	2.87	1.09	2.63
[EuL ^{25a}] ³⁻	3.02	1.12	2.70
[EuL ^{26a}] ³⁻	3.12	1.15	2.71

The P-Ph series and, in particular, the P-Ph-SO₃⁻ series (*black*) showed an enhanced rate constant for energy transfer compared to the previously analysed P-Me complexes (*red*), highlighting the importance of the phenyl ring in the energy transfer process. It is difficult to understand why this should occur, as the presence of aryl π orbitals should not promote the overlap of the donor and acceptor wavefunctions in the energy transfer process.

The development of the C-substituted analogues of these complexes for use in FRET assays is under investigation at Cisbio. Preliminary microscopy studies and ICP analysis showed the lack of internalisation of these compounds in non-transfected 293 HEK cells after a 3 h incubation, predicting low values for non-specific binding.

4.4 Application in a new FRET based assay

The lack of cellular internalisation of these compounds suggested the use of these Eu(III) complexes in a new FRET based assay. The compound in *Figure 65*, synthesised by Dr Neil Sim, is being investigated as a near-IR emitting acousto-optical probe for NMDA-2B receptors on astrocytes.¹¹⁷ These receptors, found on the surface of neurons (*e.g.* astrocytes), represent a family of ionotropic glutamate receptor and play a key role in neurotransmission, memory and learning.¹¹⁸ Mis-regulation of NMDA receptors can be the cause of different central nervous system disorders, such as epilepsy, Parkinson's and Alzheimer's diseases.¹¹⁹

The dye conjugated **NS155** binds to the glutamate receptors on the cell surface *via* the diamine moiety, which is an established antagonist for these receptors (ifendopril).¹²⁰ However, it proved challenging to visualise the dye on the cell-surface. Direct excitation of **NS155** has to be performed with a 785 nm laser that requires a long pass filter (> 800 nm) for detection of the weak fluorescence. A common linear CCD detector loses sensitivity at such wavelengths (> 800 nm), resulting in a very weak signal.

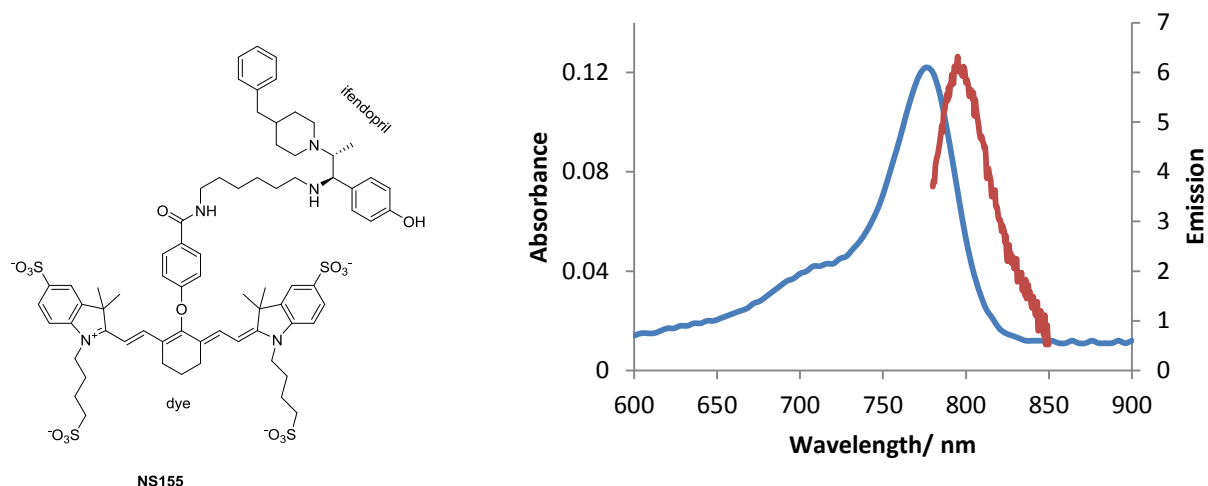


Figure 65: Structure of the IR emitting acousto-optical probe **NS155** (left), Absorption (blue) and emission (red) spectra of **NS155** (right), (H₂O, 295 K).

The Eu(III) complexes described before, although designed to maximise the energy transfer properties with a different cyanine dye acceptor (**Dy-647-NH₂**, Section 4.3), presented a reasonable degree of spectral overlap with this IR emitting dye (notably in the $\Delta J = 4$ transition, Figure 66). They can hence be used as donors for the excitation of **NS155**, via the FRET mechanism.

A study of the energy transfer process was therefore performed *in vitro* to confirm this possibility. The changes in the [EuL^{20a}]³⁻ emission lifetime were monitored as a function of added dye concentration. An efficiency of 65 % was found for this donor-acceptor couple. This is, as expected, lower than the efficiency calculated for the **Dy-647-NH₂** acceptor (93 %), due to the smaller spectral overlap (Table 22). The spectral overlap, J , is only twice as small as for **Dy-647-NH₂**, and the second order rate constant is ten times less. Nevertheless, these data suggested the possibility of using [EuL^{20a}]³⁻ as donor for the excitation of **NS155**.

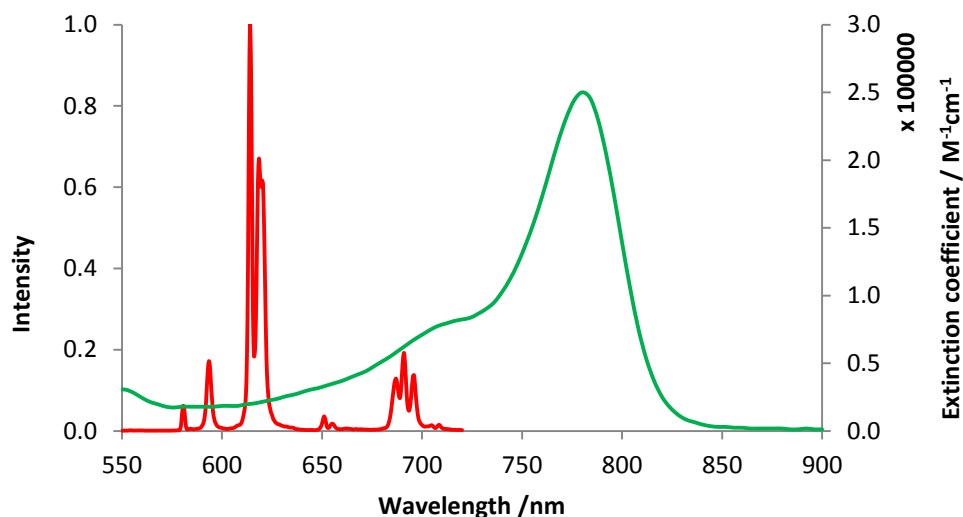


Figure 66: NS155 dye absorption (green) and $[\text{EuL}^{20a}]^{3-}$ emission (red) spectra, (H_2O , 295 K).

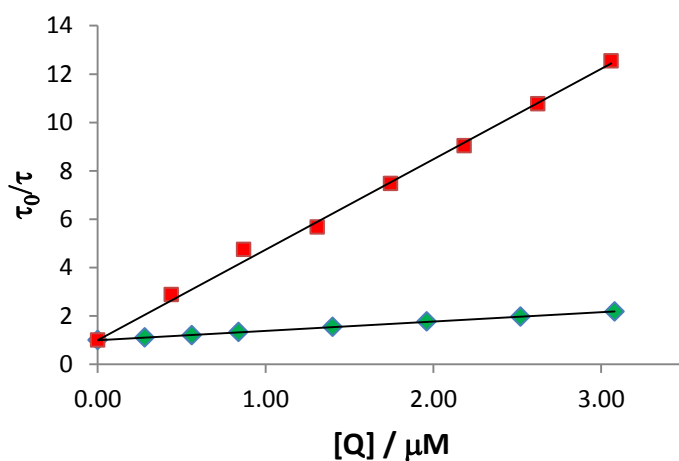


Table 22: Quenching studies for $[\text{EuL}^{20a}]^{3-}$ with NS155 dye (green) and with Dy-647-NH₂ (red) as acceptor. (Values recorded ($\pm 5\%$) at 295 K in 50 mM HEPES buffer, 50 mM NaCl, pH = 7.4; $\lambda_{\text{ex}} = 332$ nm).

	gradient	τ_0 / ms	$k_2 / \text{mM}^{-1}\text{s}^{-1}$	$J / \text{M}^{-1}\text{cm}^3$	R_0 / nm	E / %
NS155	0.39	1.11	0.35	5.3×10^{-13}	5.6	65
Dy-647-NH ₂	3.74	1.11	3.37	10.2×10^{-13}	6.3	93

The differentiated NSC-34 astrocytes cells, labelled with compound NS155 (10 μM solution), were incubated with $[\text{EuL}^{20a}]^{3-}$ (20 μM solution) for 10 min. The Eu(III) complex itself was found not to internalise in the cell; as revealed by examination with confocal microscopy, it remained in the incubation media. By exciting $[\text{EuL}^{20a}]^{3-}$ in the medium using a UV LED at 365 nm, following the energy transfer process, it was possible to visualise the emission from

NS155 on the cell surface. The excitation with a 365 nm UV LED allowed the use of a 780 nm long pass filter; the visualisation of **NS155**, selectively at the cell surface, was hence possible due to the higher sensitivity of the linear CCD detector at such wavelengths ($780 < \lambda < 800$ nm), (*Figure 67*).

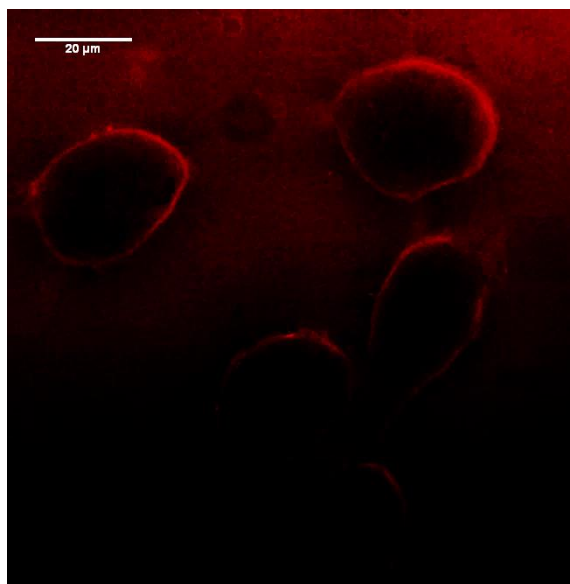


Figure 67: Confocal microscopy image of differentiated NSC-34 astrocytes cells expressing NMDA-2B surface receptors labelled with **NS155** and $[\text{EuL}^{20\text{a}}]^{3-}$ in the incubation medium. FRET Channel: $\lambda_{\text{ex}} = 365$ nm, detector > 780 nm.

The binding of **NS155** on the receptor was shown to be reversible, by following emission changes by microscopy after the addition of five successive aliquots ($V_{\text{tot}} = 500 \mu\text{L}$) of a glutamate-rich (1 mM) culture medium. A ten-fold drop in fluorescence intensity, compared to the original cell staining experiment, was observed after treatment of the cells with fresh buffer containing $20 \mu\text{M}$ of the $[\text{EuL}^{20\text{a}}]^{3-}$ (*Figure 68B*). Furthermore, prior incubation of differentiated NSC-34 cells with glutamate-rich (1 mM) solution to block the NMDA receptors, the subsequent treatment with both components, **NS155** and $[\text{EuL}^{20\text{a}}]^{3-}$, led to a re-establishment of the original fluorescent intensity (*Figure 68C*).

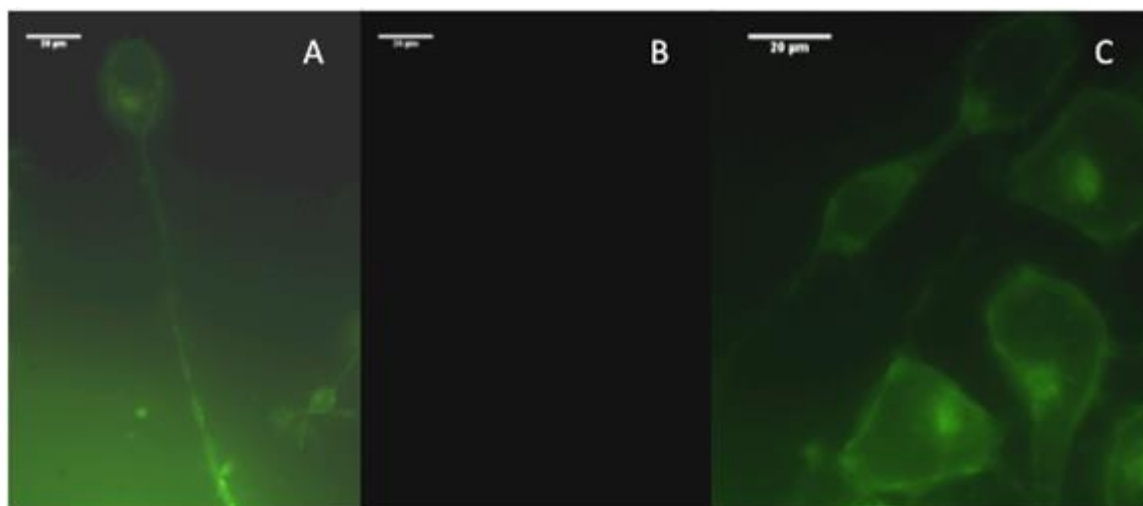


Figure 68: Live cell fluorescence microscopy images ($\lambda_{ex}/\lambda_{em} = 365/780$ nm) of differentiated NSC-34 cells labelled with NS155 (10 μ M, 30 minutes) and [EuL^{20a}]³⁻ in the incubation media (A); As image (A) but with a post glutamate (1 mM) wash (B); Cells first treated with a glutamate (1 mM) rich culture media to block the receptors, washed and then re-incubated with both NS155 (10 μ M, 30 minutes) and [EuL^{20a}]³⁻ (20 μ M) (C).

4.5 Conclusions

New series of highly water soluble sulfonated Eu(III) complexes were developed. The introduction of a P-Ph phosphinate made these complexes amongst the brightest Eu(III) complexes in aqueous solution ($B = 20 \text{ mM}^{-1} \text{ cm}^{-1}$ at 332 nm in water). The presence of the phenyl ring also improved the Eu(III) emission lifetime by about 10 % compared to the methyl analogue. In terms of FRET properties, the P-Ph systems gave rise to faster rates of energy transfer to the cyanine dye donor; this enhancement was most well-defined for the P-Ph-SO₃⁻ series.

To achieve these multifunctional sulfonated ligands, the application of some new synthetic methodology was developed. The utility of TFE sulfonate as a protecting group was emphasised in more complex examples than those previously reported in the literature. The stability of this PG towards some vigorous reaction conditions was proven, including treatment with an acyl bromide, mCPBA oxidation, acid-catalysed trans-esterification and palladium catalysed coupling reactions. The production of aliphatic sulfonates was achieved in a “one-pot” reaction, resulting in the introduction of a TFE protected sulfonic acid from a bromoalkane precursor. Moreover, the release of the trifluoroethyl ester under basic conditions, in the final deprotection step, permitted standard normal phase chromatography separations and purifications of the intermediate up to that point.

The introduction of sulfonate functionalities suppressed the non-specific binding of the Eu(III) complexes to hydrophobic pockets in proteins, interactions with the cell membranes and inhibited complex internalisation within the cell. These features make these anionic complexes ideal for surface receptor visualisation and related bioassays. The development of new TR-FRET binding assays on GPCRs using these systems is in progress at Cisbio.

5 Structural and chiroptical characterisation

5.1 Introduction

The relatively large values of $|g_{em}|$ (between 0.1 and 0.5) for lanthanide ions make them suitable for the design of emissive CPL probes, in order to get information on the chiral environment. Two classes of CPL lanthanides probes exist, depending on the chirality of the functional ligand (*Section 1.4.3*). An achiral ligand usually gives rise to a 50 : 50 mixture of interconverting Δ and Λ enantiomers, whereas an enantiopure ligand typically give rise to a dominant stereoisomer in solution.

In this chapter, the stereochemical aspects of chiral triazacyclononane (9- N_3) based complexes are examined.

5.2 The C_3 symmetric systems

Complexes based on triazacyclononane (*Figure 69*) have been studied for NMR applications¹²¹ and have also been used in binding studies of radioisotopes.¹²² These complexes present C_3 symmetry with a distorted octahedral coordination at the metal centre.

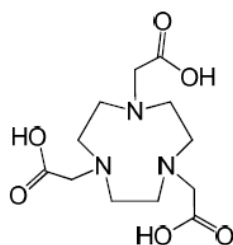


Figure 69: 1,4,7-triazacyclononane- N,N',N'' triacetic acid (NOTA).

Four possible stereoisomers can be considered that arise from carboxylate arm rotation and ring inversion of the azamacrocyclic. The first chiral element to consider is the N-C-C-O torsional angle of the carboxylate arm, which can be positive or negative. It is described with the symbols Δ (+ sign, clockwise) and Λ (- sign, anticlockwise) (*Figure 70a*). The second element is the N-C-C-N torsional angle of the ethylene group on the macrocyclic ring. It is depicted with the symbols δ (+ sign, clockwise) and λ (- sign, anticlockwise) (*Figure 70b*). The combination of these two elements of chirality gives rise to two pairs of enantiomers ($\Delta(\lambda\lambda\lambda)/\Lambda(\delta\delta\delta)$ and $\Delta(\delta\delta\delta)/\Lambda(\lambda\lambda\lambda)$). The exchange between Δ and Λ isomers is possible *via*

cooperative arm rotation, whereas the synchronous ring inversion permits the exchange between ($\delta\delta\delta$) and ($\lambda\lambda\lambda$) isomers.

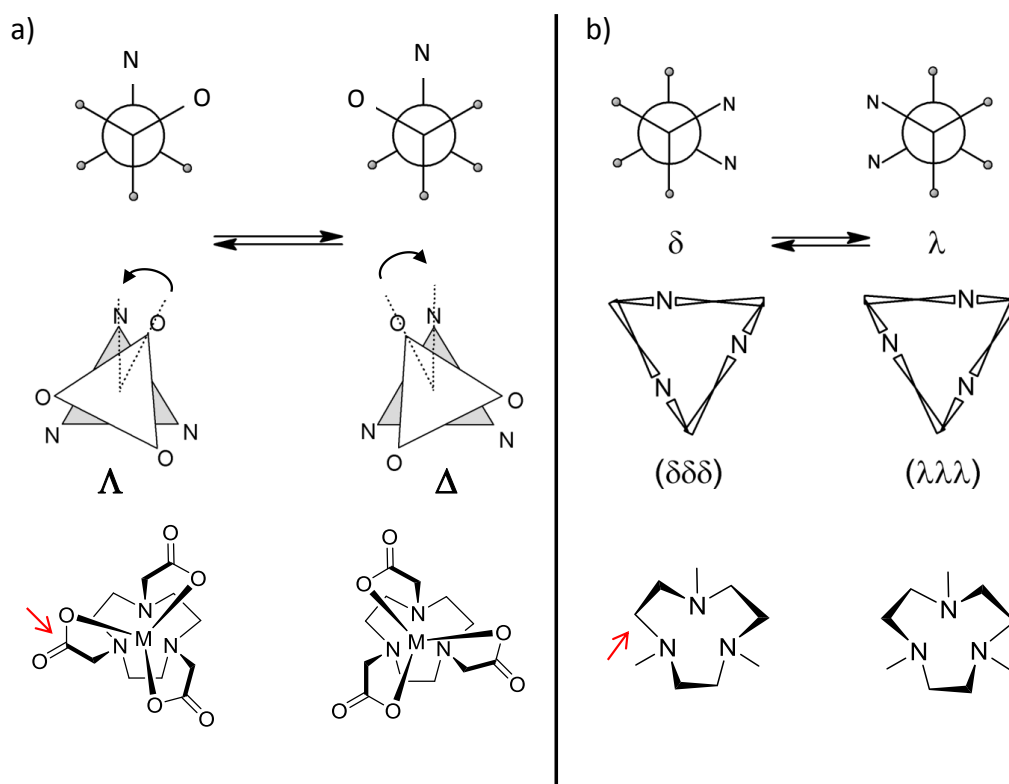


Figure 70: Stereochemistry resulting from the carboxylate arm rotation (a) and from ring inversion (b) of a NOTA complex. Newman projections of the C-C bond of the acetate arm (*top-a*) and of the C-C bond of the macrocyclic ring (*top-b*).

Two examples of substituted pyridyl derivatives of the 9- N_3 system (Figure 71) have been reported that provide 9 coordination sites to accommodate Ln^{3+} ions¹²³⁻⁸³. These complexes possess a tricapped trigonal prismatic coordination geometry. In theory, four stereoisomers are possible for these complexes. Crystal structure analysis revealed the presence of only the $\Delta(\lambda\lambda\lambda)$ and $\Lambda(\delta\delta\delta)$ enantiomeric pair. It was found that in solution the ring inversion does not occur at a measurable rate at room temperature for these systems. In addition, the Δ/Λ interconversion process has a high activation energy and is likely to be increased further with the introduction of more sterically demanding substituents, instead of the carboxylate arms (e.g. a phosphinate).⁶⁸ Due to the high energy barrier to racemisation, the two enantiomers can be separated by chiral HPLC.

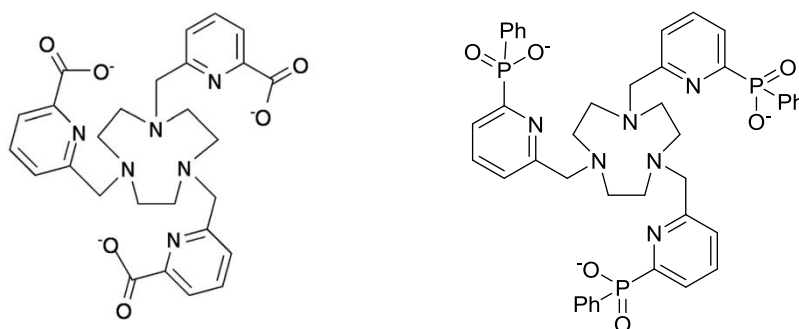


Figure 71: Two examples of 1,4,7-triazacyclononane substituted ligands.⁸³⁻¹²³

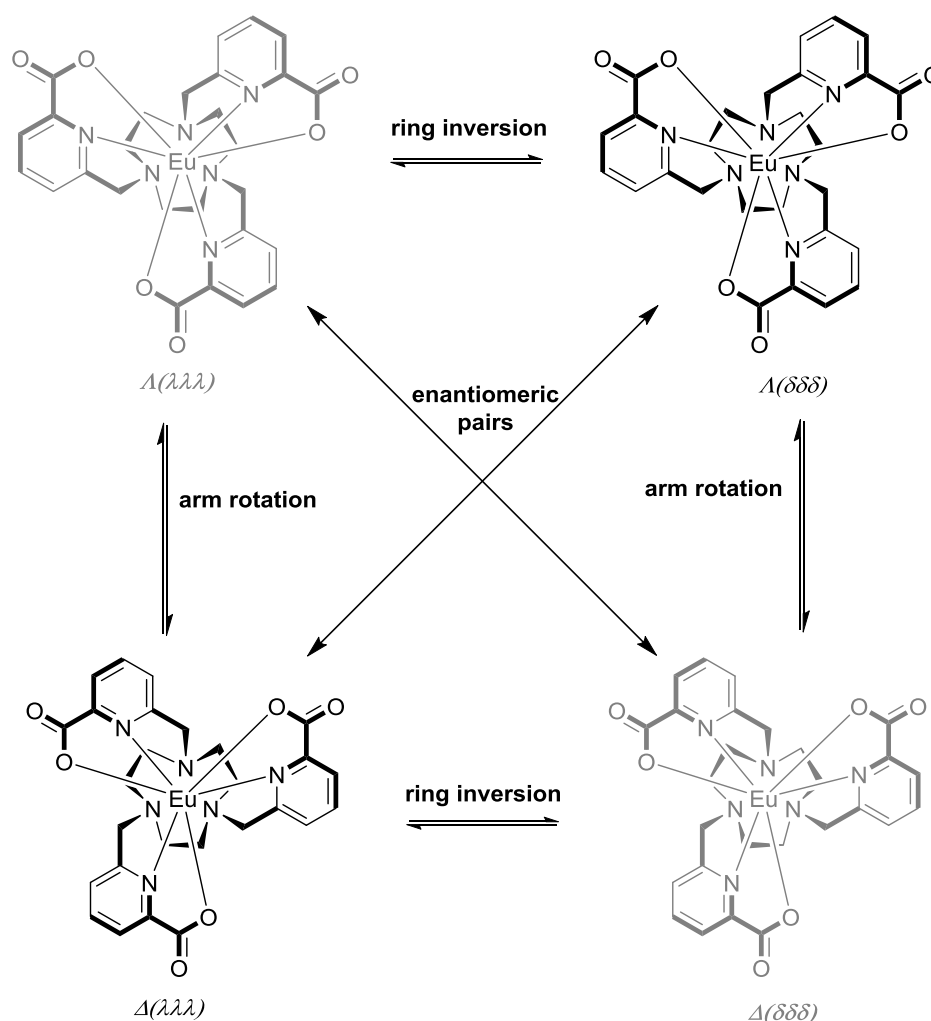


Figure 72: The four possible stereoisomers of the Eu(III) pyridyl 9-N₃ derivative. Only the $\Delta(\lambda\lambda\lambda)$ and $\Delta(\delta\delta\delta)$ enantiomers are observed.

In the phosphinate series (Figure 71), metal coordination allows the P centre to become stereogenic; once the first phosphinate oxygen has bound to the metal centre, assuming an *R* or *S* configuration, the other two also tend to adopt the same configuration.¹²⁴ In addition, for an *R* configuration at P, the ring NCCN and substituent NCCN_{py} torsion angles are consistent

with a $\delta\delta\delta$ ring conformation and Λ configuration. Hence, the complex exists as a racemic mixture of two enantiomers (RRR)- $\Lambda(\delta\delta\delta)$ and (SSS)- $\Lambda(\lambda\lambda\lambda)$.

Upon chiral resolution, the CPL spectra of the two enantiomers can be recorded (*Figure 73*).

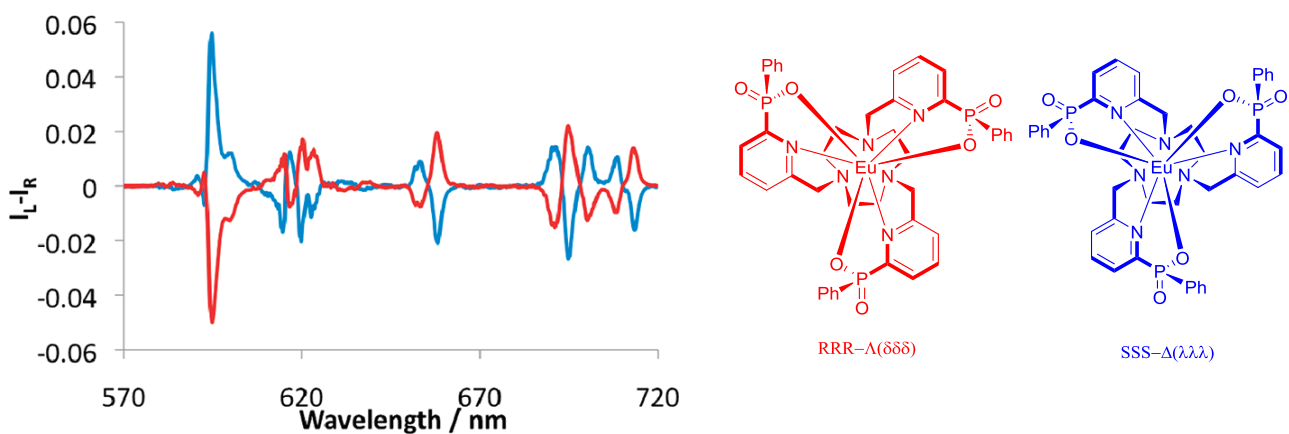
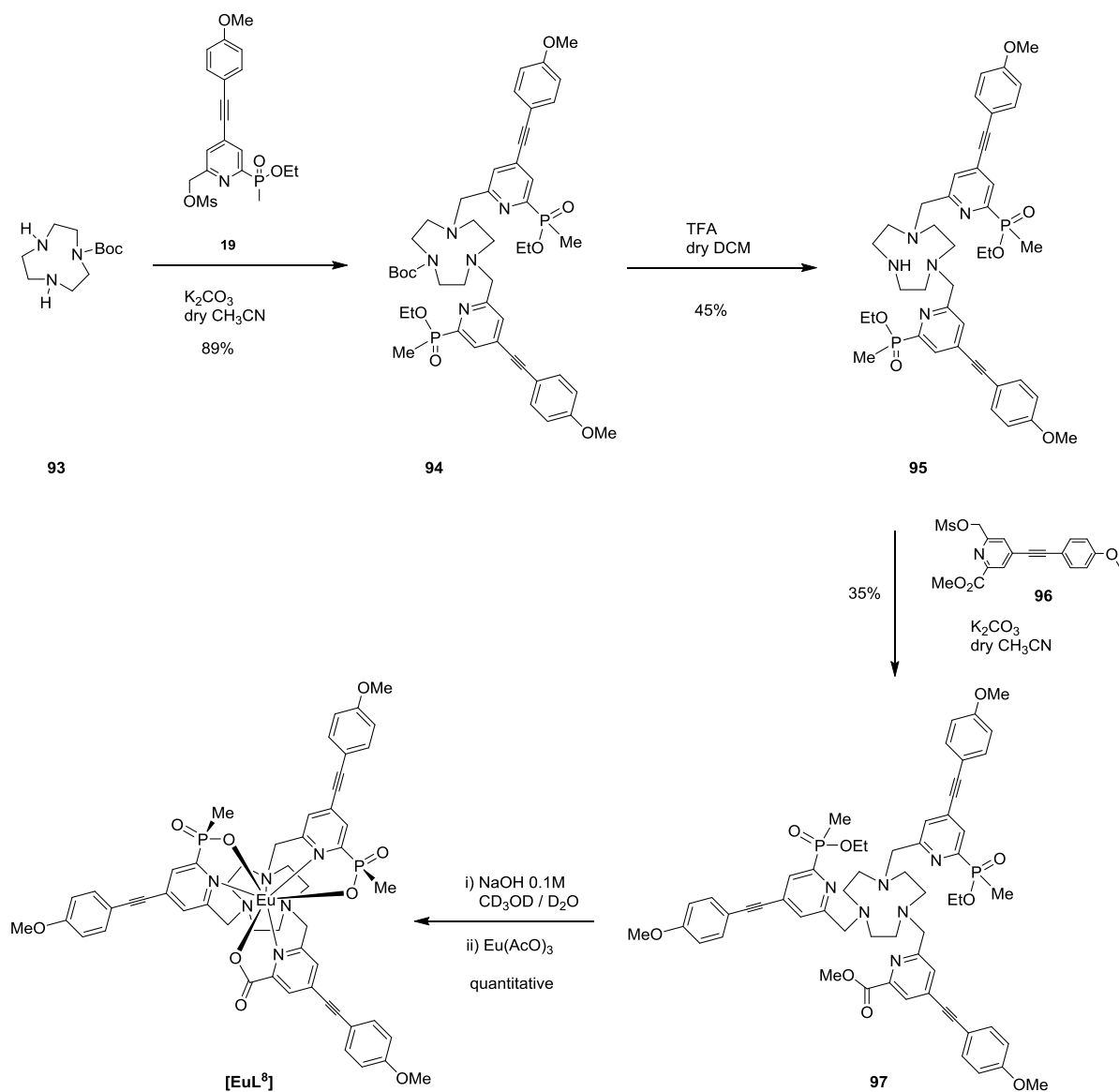


Figure 73: CPL spectra for the Eu(III) complexes of the (RRR)- Λ - $\delta\delta\delta$ (red) and (SSS)- Λ - $\lambda\lambda\lambda$ (blue) enantiomers, (H_2O , 295 K).⁸³

5.3 The hybrid system

The hybrid system, $[\text{EuL}^8]$, described in *Chapter 2*, bearing two phosphinate and one carboxylate donors, has been prepared and its stereochemical features were analysed.

The 9- N_3 mono Boc **93**, was alkylated with the mesylate derivative of the P-Me phosphinate chromophore, **19**. After Boc deprotection with TFA, compound **95** was reacted with the carboxylate derivative **96**. Hydrolysis followed by complexation yielded the hybrid complex, $[\text{EuL}^8]$.

Scheme 36: Synthesis of the hybrid complex [EuL⁸].

An emission spectrum was recorded (*Figure 74*) and emission lifetimes were measured ($\tau_0 = 1.12$ ms in MeOH and $\tau_0 = 0.89$ ms in H₂O). The splitting of the $\Delta J = 2$ band and the lifetime values fall in between those for the tris-carboxylate [EuL³] and the tris-phosphinate analogues [EuL²], as expected (*Section 2.3.1*).

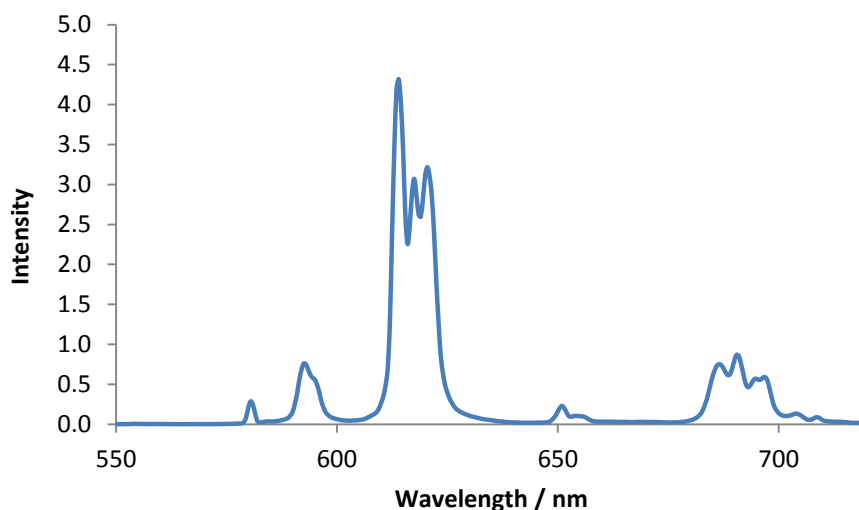


Figure 74: Emission spectrum for $[\text{EuL}^8]$, (MeOH, 295 K, $\lambda_{ex} = 332$ nm).

The complex was characterised by ^{31}P -NMR spectroscopy and HPLC (Figure 75 and Figure 76). Due to the asymmetric nature of the complex, the ^{31}P -NMR spectrum revealed two signals, one for each phosphorus in the molecule.

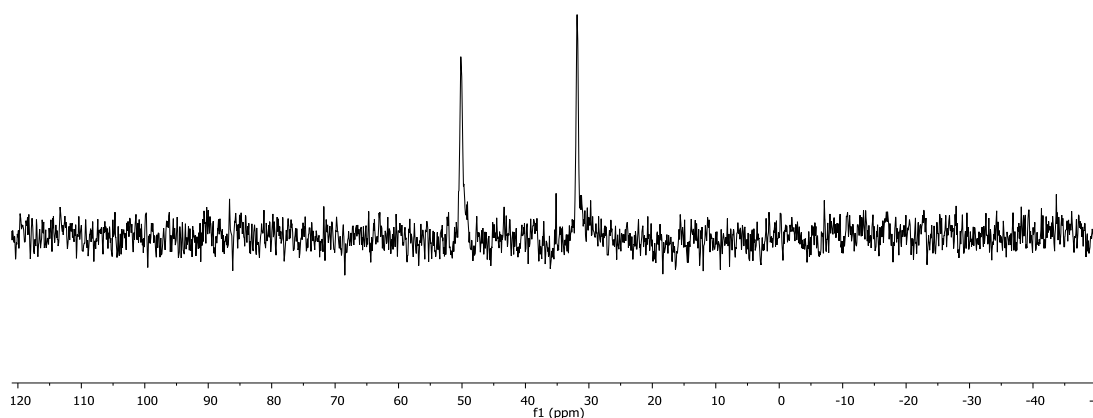


Figure 75: ^{31}P NMR spectrum of complex $[\text{EuL}^8]$, (CD_3OD , 14.1 T, 295 K).

Chiral HPLC analysis confirmed that the complex is present as a 50:50 mixture of two enantiomers (RR and SS at P). Presumably, the two isomers are RR - $\Lambda(\delta\delta\delta)$ and SS - $\Lambda(\lambda\lambda\lambda)$.

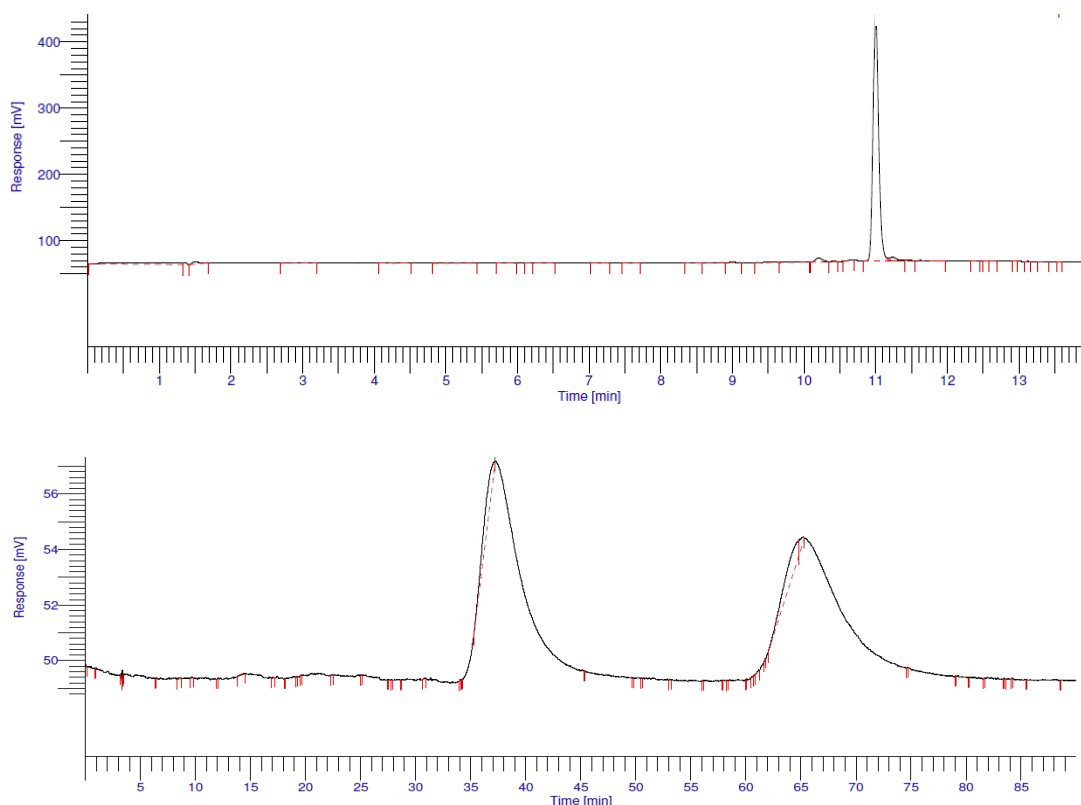


Figure 76: HPLC analysis of $[\text{EuL}^8]$. Method C, $t_R = 11.0$ (top). CHIRALPAK-IC 250 x 4.6 mm 5 μM column, 100 % MeOH (bottom).

5.4 The C-substituted 9-N₃ systems

The synthesis of an enantiopure system is very challenging, often requiring long and tedious chiral chromatography purifications. The incorporation of a single C-substituent into the ligand system has been recently described as a possibility to control the final geometry at the metal centre.⁷³ The introduction of a stereocentre on the macrocyclic ring has been reported to induce the preferential formation of one stereoisomer (upon Cu(II) complexation) in a 9 to 1 ratio.

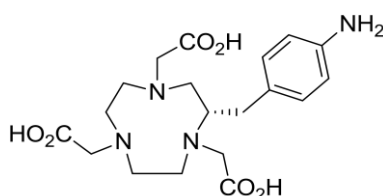


Figure 77: Structure of the C-substituted 9-N₃ ligand which induced the preferential formation of one stereoisomer upon Cu(II) complexation.⁷³

In the same way, the C-substitution on the 9-N₃ in complex **[EuL¹³]** (Section 3.2) was expected to induce the formation of one isomeric species preferentially.

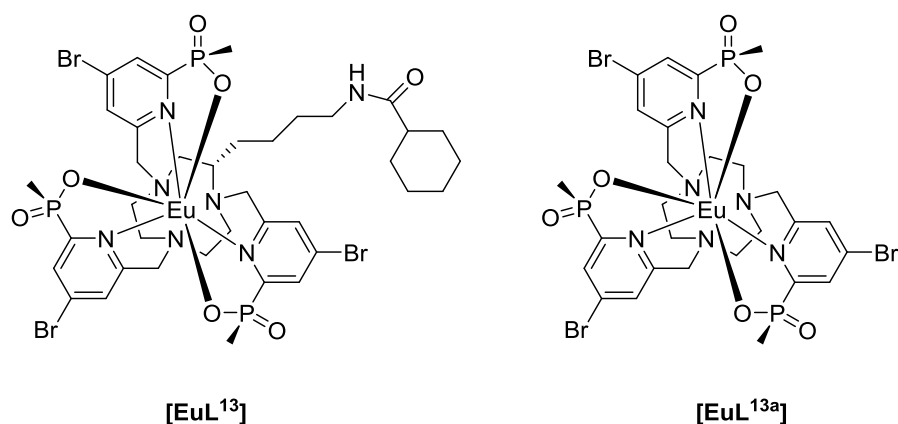


Figure 78: Structure of **[EuL¹³]** and the unsubstituted analogue **[EuL^{13a}]**.

The NMR profile for the C-substituted complex **[EuL¹³]** was compared to that for the unsubstituted analogue **[EuL^{13a}]**. The relatively simple pattern of the ¹H-NMR and ³¹P-NMR spectra suggested the presence of one major stereoisomer in each case (Figure 79c and d). The non-equivalence of the P atoms in the substituted phosphinate complex **[EuL¹³]** is revealed by the presence of three resonances in the ³¹P NMR spectrum (Figure 79d).

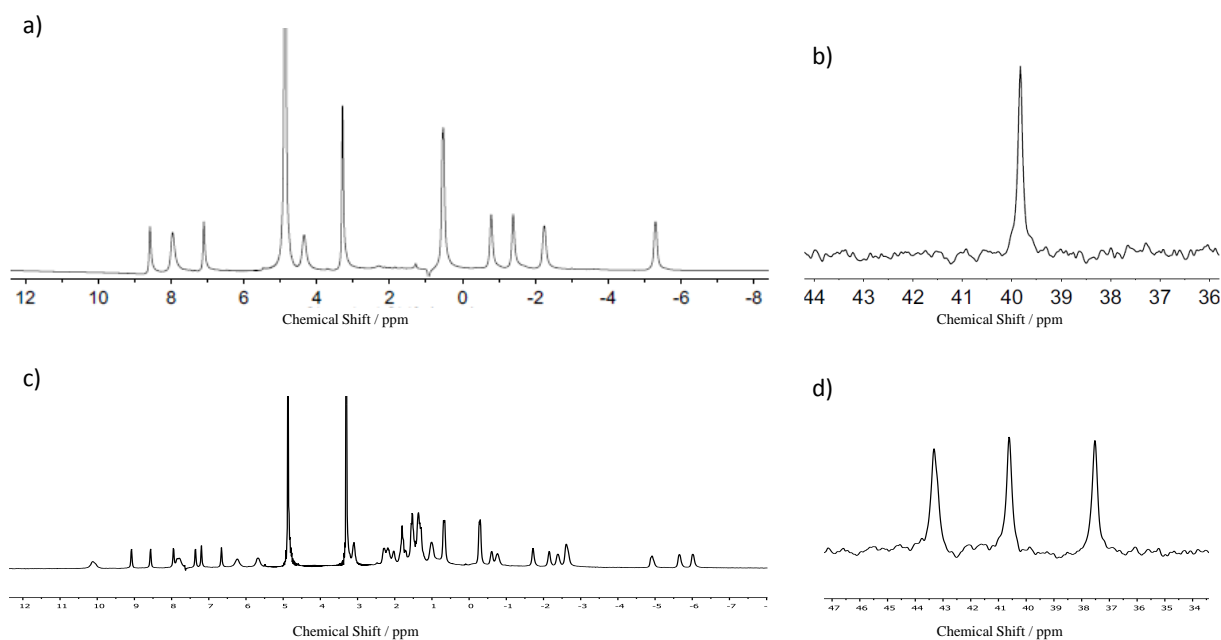


Figure 79: NMR characterization of **[EuL^{13a}]** (top) and **[EuL¹³]** (bottom), (CD₃OD, 295 K, 9.4 T).

The presence of a major stereoisomer was further investigated using HPLC. The complex $[\text{EuL}^{13\text{a}}]$ exists as 50 : 50 mixture of enantiomers that can be separated by chiral HPLC (Figure 80). For the C-substituted complex, chiral HPLC under the same conditions verified the preferential formation of one stereoisomer in 80 % diastereomeric excess (Figure 81).¹²⁵

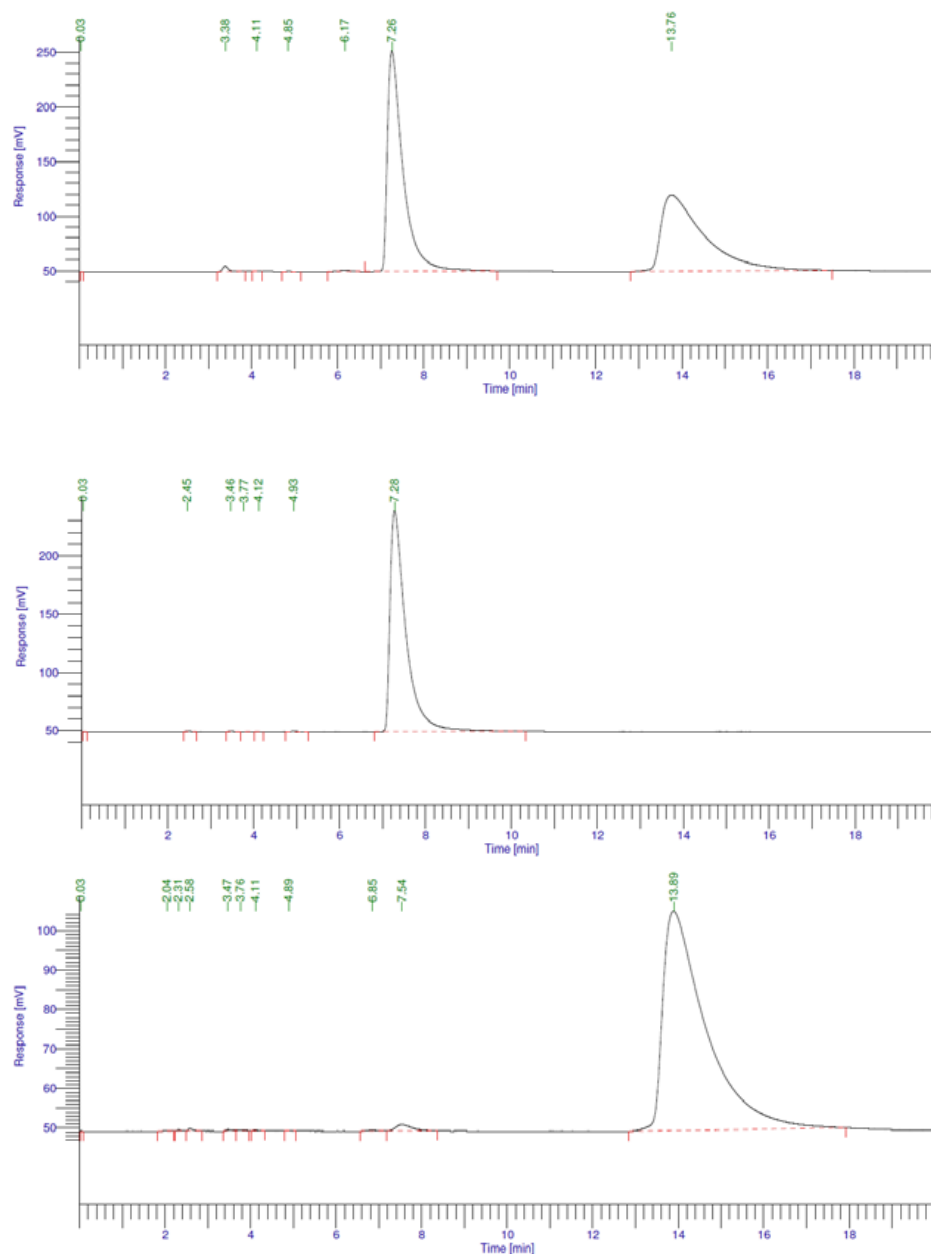


Figure 80: Chiral HPLC trace for $[\text{EuL}^{13\text{a}}]$: racemate (top), Δ enantiomer (middle), Λ enantiomer (bottom). (CHIRALPAK-ID 4.0 mm \times 250 mm, MeOH, 1 mL/min, λ = 268 nm, 290 K).

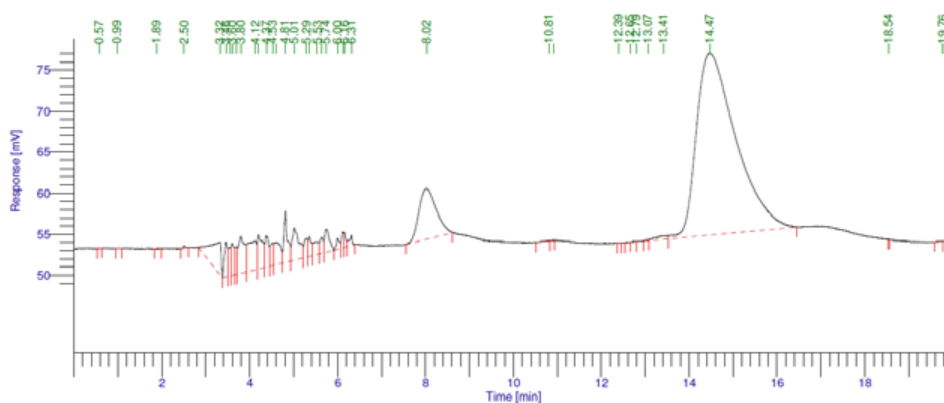
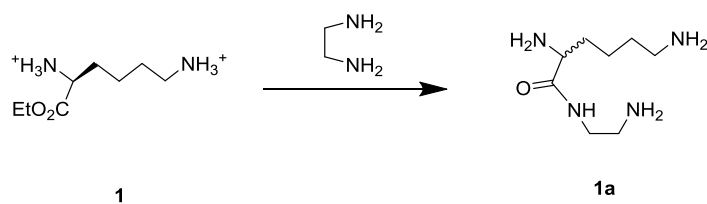


Figure 81: Chiral HPLC trace for **[EuL¹³]**, (CHIRALPAK-ID 4.0 mm × 250 mm, MeOH, 1 mL/min, $\lambda = 268$ nm, 290 K).

Further studies on this system with different C-substituents revealed that the formation of the minor stereoisomer could be traced back to racemisation during the first step of the synthesis of the macrocycle (*Scheme 37*). Racemisation could be avoided by lowering the temperature of the reaction between the amino-acid ester and ethylenediamine (100 °C) and by carrying out the subsequent distillation to remove excess ethylenediamine at lower pressure and temperature. The degree of racemisation was calculated by adding the chiral solvating agent *R*-*O*-acetyl mandelic acid (1.2 eq) to samples of (2*S*)-*N*-(2-aminoethyl)-(2,6-diaminohexanamide) dissolved in CDCl₃.¹²⁶ The amide peak shifted to higher frequency and split. Examination of the integral ratios revealed that the enantiomeric purity was > 90 %, under this conditions.



Scheme 37: Possible racemisation occurring during the first step of the synthesis.

The CPL spectrum of **[EuL¹³]** was recorded (*Figure 83*) and compared to the CPL spectra recorded for the two enantiomers of the parent derivative, **[EuL^{13a}]** (*Figure 82*). These complexes had been resolved earlier in Durham by Dr Nick Evans and had allowed the assignment of the absolute configuration. In this case, for **[EuL¹³]** the major stereoisomer is assigned as *S*(Lys)-*RRR*-*A*($\delta\delta\delta$).

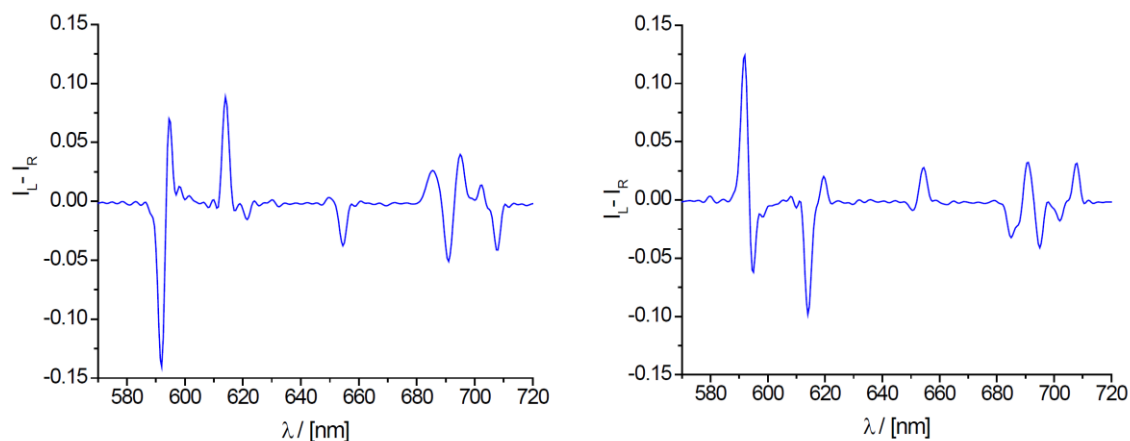


Figure 82: Circularly polarised luminescence spectra of the Δ -enantiomer of $[\text{EuL}^{13a}]$ (left) and the Λ -enantiomer (right), (H_2O , $\lambda_{ex} = 268$ nm, 295 K).

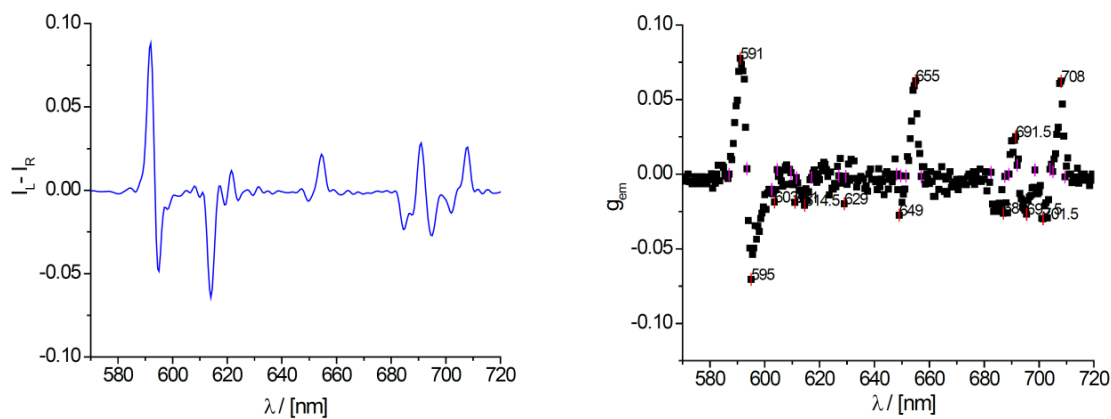


Figure 83: Circularly polarised luminescence spectrum (left) of $[\text{EuL}^{13}]$, (H_2O , $\lambda_{ex} = 268$ nm, 295 K). Emission dissymmetry factor for $[\text{EuL}^{13}]$ as a function of wavelength (right).

Large values of emission dissymmetry factors, g_{em} , were found especially in the $\Delta J = 1$ region (Table 23).

$$g_{em} = \frac{2(I_L - I_R)}{I_L + I_R} \quad [13]$$

Table 23: Emission dissymmetry factors, g_{em} , for $[\text{EuL}^{13}]$ and for the Δ -enantiomer of $[\text{EuL}^{13a}]$.

	$[\text{EuL}^{13}]$ $S(\text{Lys})\text{-RRR-}\Lambda(\delta\delta\delta)$				
λ / nm	591	595	655	691	708
g_{em}	0.08	-0.07	0.06	0.02	0.05
$g_{em} [\text{EuL}^{13a}]$ (Δ)	0.10	-0.07	0.07	0.03	0.06

The diastereomeric excess of $[\text{EuL}^{13}]$ can also be estimated by comparing g_{em} values for the same transitions, as the g_{em} value scales directly with the percentage of diastereomeric purity. The value for the transition at 591 nm (0.08 compared to 0.10 for the enantiopure complex) confirmed an optical purity of 80 %.

Rationalisation of the induced stereoselectivity was provided by consideration of the X-ray structure of the $SSS-\Delta-(\lambda\lambda\lambda)$ enantiomer of $[\text{EuL}^{13a}]$ (Figure 84).¹²⁵ The pro-*R* ring protons (*red*) sit in a pseudo-equatorial position that is directed away from the steric bulk of the pyridyl arms; a C-substitution in this position will be more favourable due to less steric hindrance. In the same way, the chirality induced by the stereocentre of lysine (*S*) will be $RRR-\Lambda-(\delta\delta\delta)$, consistent with a less hindered complex, and in agreement with the configuration obtained for $[\text{EuL}^{13}]$.

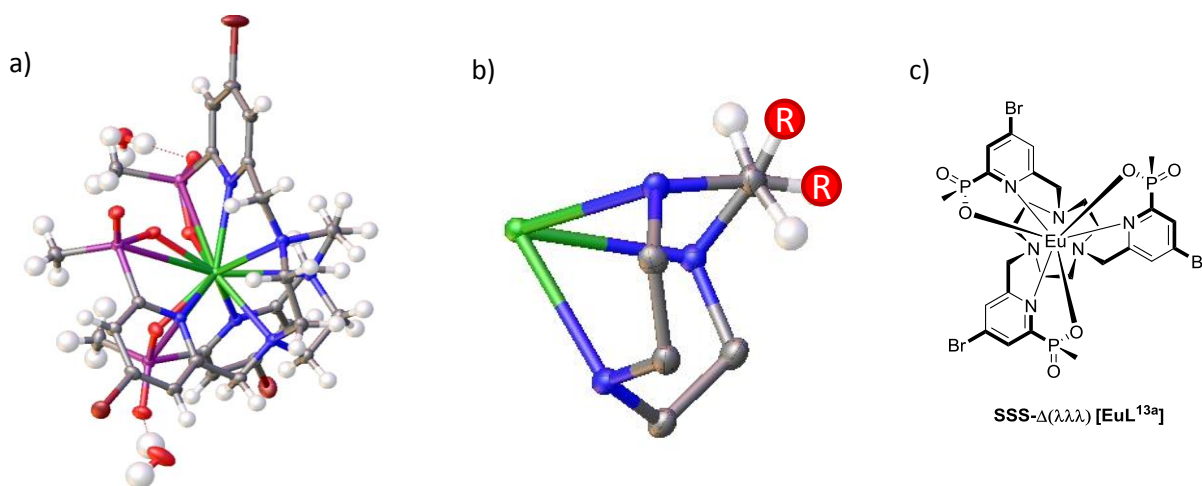
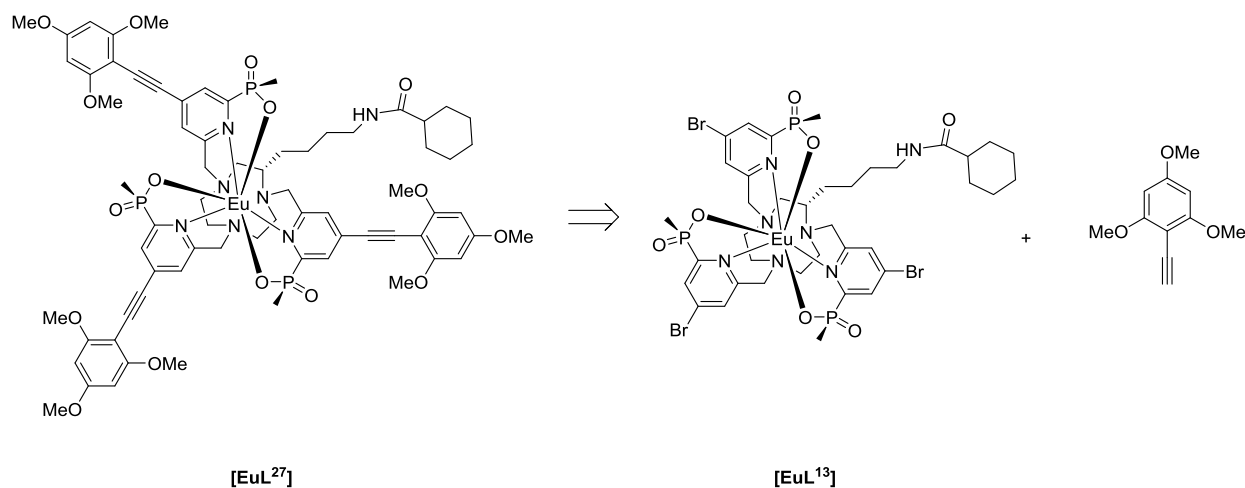
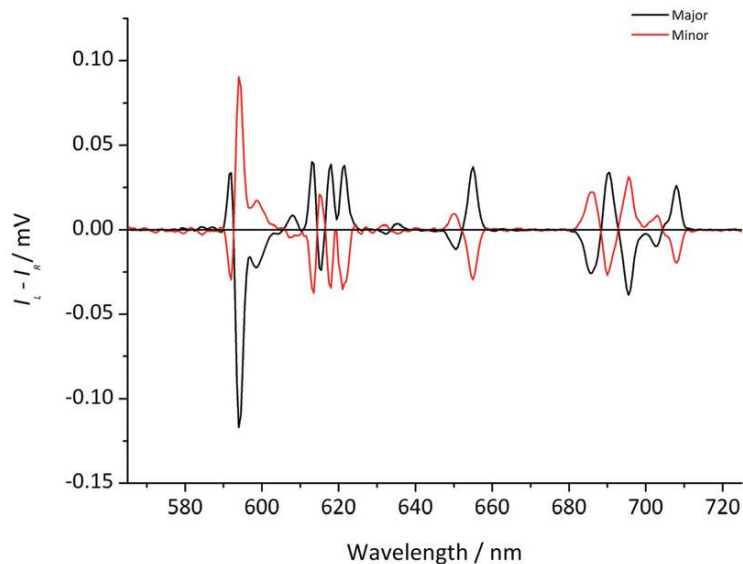


Figure 84: X-ray structure of Δ -[EuL^{13a}] (a), part of the crystal structure illustrating the pseudo-equatorial positions of the pro-*R* hydrogens (*red*) on the 9-N₃ ring (b), structure of Δ -[EuL^{13a}] (c).¹²⁵

5.4.1 The C-substituted systems bearing the alkynyl chromophore

The chiroptical properties for the complexes bearing the extended chromophore were analysed. The complex $[\text{EuL}^{27}]$ was synthesised using a Sonogashira cross coupling reaction from the 80 % diastereomerically pure precursor, $[\text{EuL}^{13}]$, by Dr Stephen Butler.⁷⁹ The two stereoisomers were separated and their CPL spectra recorded.

Scheme 38: Retrosynthetic approach for the synthesis of **[EuL²⁷]**.Figure 85: Circularly polarised luminescence spectra of **S-RRR-Δ-[EuL²⁷]** (black) and **S-SSS-Δ-[EuL²⁷]** (red), (MeOH, λ_{ex} = 355 nm, 295 K).

Due to the brightness of this complex ($B = 30 \text{ mM}^{-1} \text{ cm}^{-1}$ at 355 nm in MeOH) and the $|g_{em}|$ values in the range from 0.1 to 0.3 (Table 24), this complex gave the strongest CPL signal yet observed for any lanthanide complex in solution, allowing the spectrum to be acquired with good signal intensity over a period of 20 minutes, using a 3 μM solution of the complex.

Table 24: Emission dissymmetry factors, g_{em} , for the diastereopure **Δ-[EuL²⁷]**.

[EuL²⁷]	S(Lys)-RRR-Δ(δδδ)		
λ / nm	598	655	708
g_{em}	-0.11	0.17	0.30

The CPL spectrum was recorded for different complexes bearing the alkynyl-based chromophore; strong CPL signals were observed in each case (Figure 87).

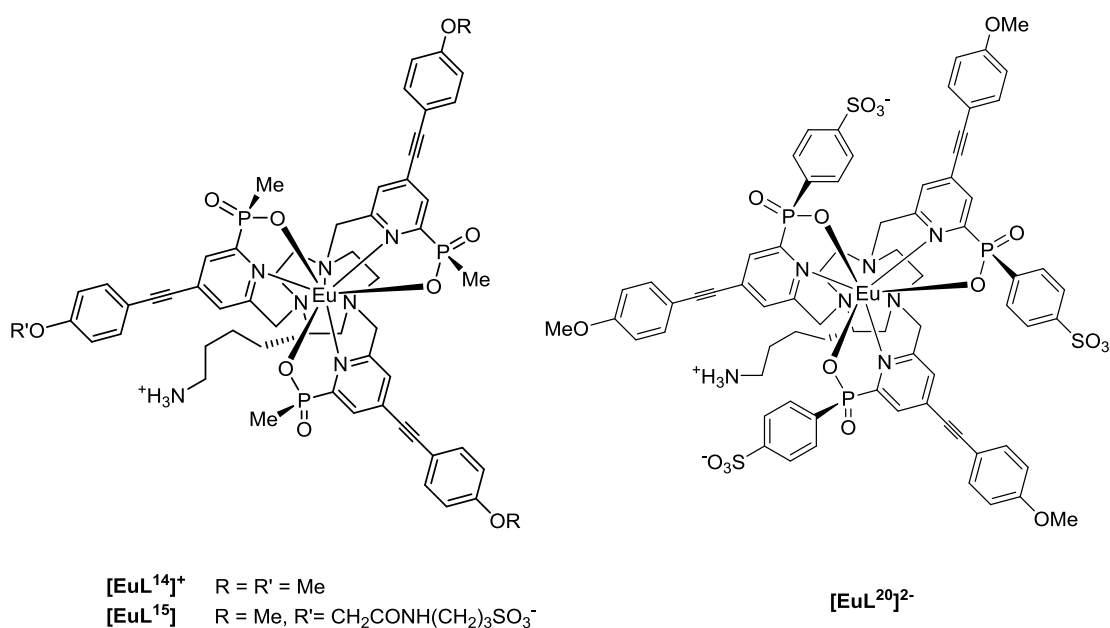


Figure 86: Structures of the complexes analysed using CPL spectroscopy.

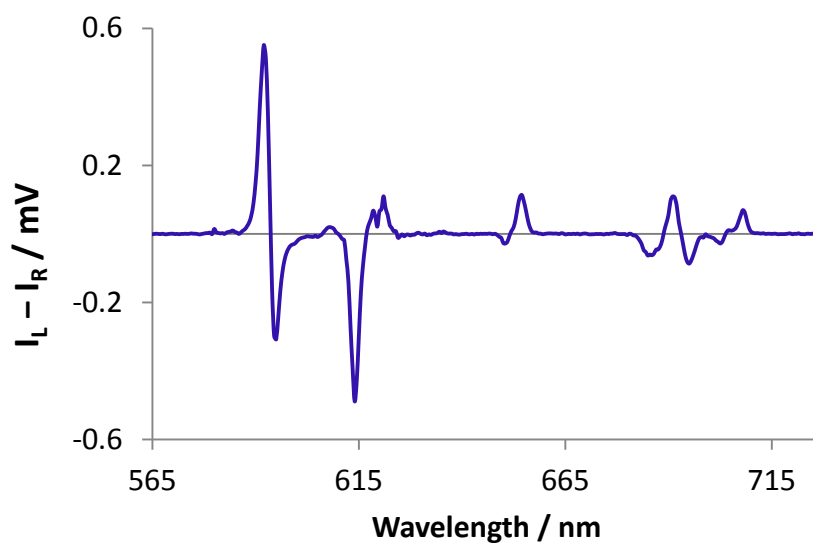


Figure 87: Circularly polarised emission spectrum of *S-RRR-A*- $[\text{EuL}^{20}]^{2-}$, (H_2O , $\lambda_{\text{ex}} = 332 \text{ nm}$, 295 K).

The chiral HPLC analysis of these charged complexes was found not to be amenable using the standard conditions as for the neutral analogue $[\text{EuL}^{27}]$ (aqueous methanol gradients). However, the enantiomeric purity of the three complexes was estimated by comparing g_{em} values for the same transitions (Table 25). Similar values of g_{em} were found for the

diastereomerically pure complex **[EuL²⁷]** and the three complexes analysed. Given that the experimental error associated with measurement of g_{em} is ($\pm 10\%$), it seemed reasonable to assume that the values refer to samples with a diastereomeric excess of $> 90\%$.

Table 25: Emission dissymmetry factors, g_{em} , for the akynyl complexes (H₂O, $\lambda_{ex} = 332$ nm, 295 K).

		598 nm	655 nm	708 nm
g_{em} ^a	[EuL²⁷]	-0.11	0.17	0.30
g_{em}	[EuL¹⁴]	-0.10	0.16	0.25
g_{em}	[EuL¹⁵]	-0.10	0.22	0.27
g_{em}	[EuL²⁰]	-0.10	0.18	0.25

^a values recorded in MeOH.

5.5 Conclusions

Pyridyl derivatives of 9-N₃ complexes exist as a pair of enantiomers that can be separated at room temperature with chiral HPLC, due to the high energy of racemisation.

The mono substitution at a carbon atom on the macrocyclic ring provided complete control of the stereochemistry of the final complex. Direct and selective formation of chiral complexes was observed with $> 90\%$ optical purity. Due to the high brightness of these compounds, an intense CPL signal could be recorded during a short period of time (20 min). Such behaviour can be exploited for the preparation of bright and enantiopure emissive complexes that have the potential to form the basis of responsive chiral probes for CPL spectroscopy and microscopy.

6 Conclusions and future work

6.1 General conclusions

The Eu(III) complexes based on the triazacyclononane ligand tri-substituted with different examples of pyridyl-alkynyl-aryl moieties are the brightest examples of europium complexes reported in the literature ($B = 30 \text{ mM}^{-1} \text{ cm}^{-1}$ at 332 nm in MeOH). Their photophysical properties are very well suited to fluorescence microscopy studies: a broad absorption band with a maximum typically around 330 - 340 nm, a long luminescence lifetime, and good stability in a biological medium.

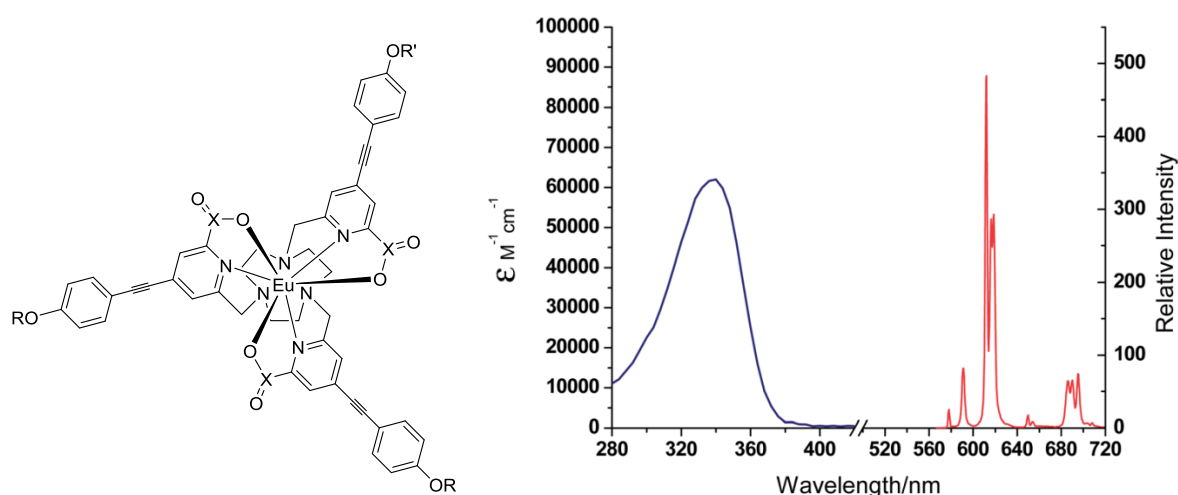


Figure 88: General structure of a series of highly emissive europium complexes (left), ($X = \text{C}$ or $\text{P-R}''$). Absorption (blue) and emission (red) spectra for these Eu(III) complexes (right).

The complexes possess a very intense set of $\Delta J = 2$ transitions (610 - 620 nm) that is of fundamental importance for the use of these complexes as donors in FRET based experiments. This particularly favourable emission spectral form resulted in improved properties, compared to earlier Eu(III) cryptates, when these complexes are used as donors in energy transfer studies with the cyanine dye acceptor **Dy647-NH₂**. Faster rates of energy transfer and bigger spectral overlaps were measured, compared to the commercially available donors, **Eu(TBP)** and **Lumi4-Tb**.

Taking the structure of these complexes as starting point, the synthetic work focused on the introduction of a linkage point for conjugation with biomolecules and on the improvement of the water solubility of these systems. The introduction of a linkage point was achieved with an aliphatic chain on the azamacrocycle, terminally substituted with a primary amine. The

synthesis of a C-substituted macrocyclic core was optimised; the C-substitution on the ring did not affect the emissive properties and created a useful intermediate that can be easily functionalised for a variety of applications. The introduction of negatively charged moieties (e.g. carboxylate and sulfonate) onto the antenna made these complexes fully water soluble ($\log P = -2.2$) and did not affect the energy transfer properties of the original neutral complex.

This first generation of P-Me phosphinate C-substituted complexes was evaluated for FRET experiments *in cellulo*. The introduction of carboxylate or sulfonate functionalities into the ligand system, in addition to the enhanced water solubility, inhibits the non-specific internalisation of these complexes in living cells. The selective targeting of G-protein coupled membrane receptors of living HEK cells was therefore possible, due to the low non-specific interactions of these complexes. The TR-FRET binding assays were performed on two GPCRs (dopamine-d2 and cholecystinin-2 receptors) in living cells with promising results for the use of this technology in high-throughput screening assays. In addition, the visualisation of these systems with confocal and TR-FRET microscopy was possible and required very small quantities of material (nM concentrations), due to the high brightness of these complexes.

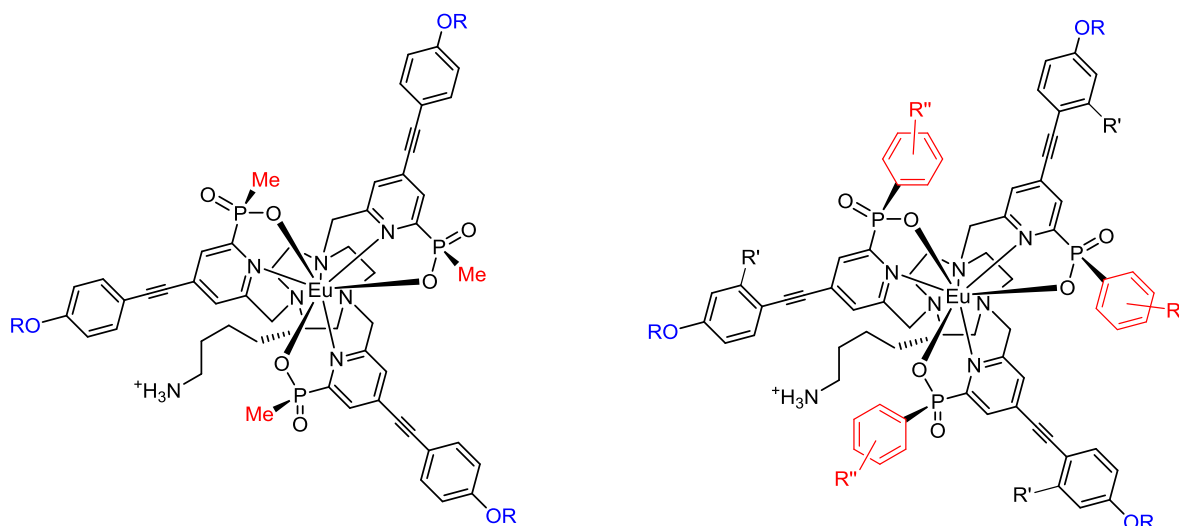


Figure 89: General structures of first (*left*) and second (*right*) generation of C-substituted Eu(III) complexes.

A second generation of highly water soluble sulfonated Eu(III) complexes was designed and synthesised. The introduction of the P-Ph phosphinates made these complexes amongst the brightest Eu(III) complexes in aqueous solution (typically $B = 20 \text{ mM}^{-1} \text{ cm}^{-1}$ at 332 nm in water). The high quantum yields allowed the calculation of a low limit of detection, ten times

lower than for the **Lumi4-Tb** under the same conditions. The Eu(III) emission lifetime increased by about 10 % compared to the first generation P-Me analogues, as a consequence of the presence of the phenyl ring. Faster rate of energy transfer to the cyanine dye donor were also observed; this enhancement was most well-defined for the P-Ph-SO₃⁻ series. The presence of the sulfonate moieties was sufficient to achieve a high degree of water solubility, even in the presence of the lipophilic phenyl rings. Suppression of non-specific binding to hydrophobic pockets in proteins, interactions with the cell membranes and inhibition of internalisation within the cell were also observed for those complexes. This behaviour was exploited for the visualisation of a near-IR emitting acousto-optical probe on the NDMA-2B surface receptors on astrocytes.

To achieve these multifunctional sulfonated ligands, new synthetic methodologies were applied. Different sulfonate protecting groups were considered and the utility of a trifluoroethylsulfonate group was emphasised, in more complex examples than those previously reported in the literature. These TFE-sulfonates were proved to be stable towards vigorous reaction conditions, including treatment with an acyl bromide, mCPBA oxidation, acid-catalysed trans-esterification and palladium catalysed coupling reactions. Moreover, the release of the trifluoroethyl ester under basic conditions, in the final deprotection step, permitted easy handling and purification of the intermediates up to that point. Aliphatic sulfonates were synthesised in a “one-pot” reaction, resulting in the introduction of a TFE protected sulfonic acid from a bromo alkane precursor.

The utility of these C-substituted complexes was evaluated also as potential chiral CPL emitting probes. In fact, the monosubstitution at a carbon atom on the macrocyclic ring provided complete control of the stereochemistry of the final complex. This synthesis led to the direct and selective formation of chiral complexes with > 90 % enantiomeric purity. An intense CPL signal was recorded for these complexes during a short period of time (20 min) resulting in the strongest CPL signal yet observed for any lanthanide complex in solution.

6.2 Future work

The second generation of P-Ph phosphinate complexes is under evaluation in *in vivo* TR-FRET assays. The benzyl-guanine labelled complexes have been prepared and they will be used for GPCRs binding assays.

The preparation of the NHS active ester of these complexes is also under investigation (Figure 90). These reactive compounds will be used for the direct labelling of antibodies, which will be used for a variety of immunoassays (currently under investigation at Cisbio Bioassays).¹²⁷

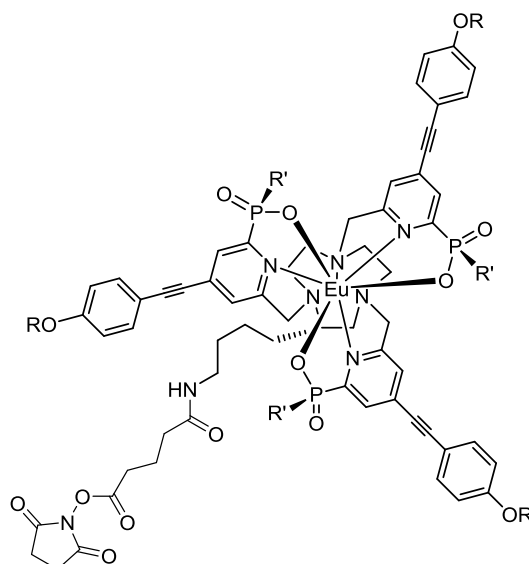


Figure 90: NHS active ester of the a general Eu(III) complex.

Many examples of these Eu(III) complexes have been prepared and evaluated in various biological assays. Two patents, which describe the preparation of all these different complexes, are available.⁷⁴⁻⁷⁸ The sulfonate complex [EuL¹⁹] seems to report the best results for the *in vivo* TR-FRET assays, due to the high water solubility and the suppression of the non-specific binding. A systematic analysis of the different examples of complexes in different HTRF bioassays will permit the selection of one (or more) target complexes for the commercialization of these systems. The technology evaluated for the GPCRs assay is showing promising results and can be further developed to provide access to general high-throughput screening assays.

The low non-specific interactions of these complexes will be also of great advantage to the development of novel bioassays, where specific biological interactions are studied. The easy and accessible conjugation of these complexes with biologically relevant molecules may permit the targeting of different receptors on the cell surface. For example, the conjugation of these complexes with folic acid might be a feasible method to target cancer cells, where folate receptors are overexpressed.¹²⁸ Internalisation of the folate-conjugated complex might

occur upon interaction with the receptor. Another possibility will be the conjugations of these complexes with known small organic molecules to selective target the dopamine receptors, overexpressed on the surface of cancer stem cells.¹²⁹

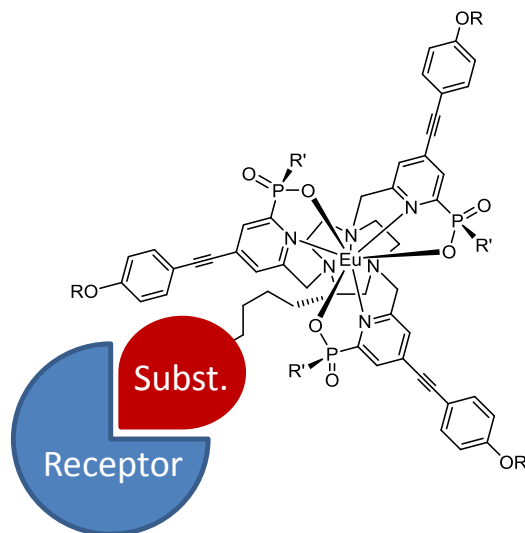


Figure 91: Targeting of a receptor with a specific vector.

Having suppressed the internalisation of these complexes through the micropinocytosis mechanism,⁸⁷ it will might be also possible to attach these complexes to specific targeting sequences, which use different internalisation pathways (*e.g.* cell penetrating peptides),¹³⁰ to send the complexes to specific organelles or to the nucleus.

Towards the use of lanthanide complexes as stains for fluorescence microscopy, some assessments can be made regarding the use of different excitation sources. The use of less powerful (red shifted) excitation wavelengths results in low phototoxicity and reduced background fluorescence from the endogenous chromophores.¹³¹ Due to the high brightness of these complexes, the use of pulsed excitation at 365 nm is possible; in addition, the use of a phase-modulation method to improve the intrinsic resolution (130 nm for $\lambda_{ex} = 365$ nm) has allowed microscopic resolution of 65 nm to be achieved.⁸⁷ By introducing different electron-donating moieties on the aryl ring, the development of chromophores whose electronic absorption bands are bathochromically shifted is possible, due to the perturbation of the ICT band for the sensitisation of the Eu(III). This change also has an effect on the quantum yield of the complex; in fact, the perturbation of the ICT band can cause back energy transfer resulting in a decrease in the emission quantum yield. A good balance was achieved with the tri-methoxy derivative **[EuL²⁷]** ($\lambda_{ex} = 355$ nm, $\Phi_{em} = 55$ % in MeOH).

These bright complexes have also been used as responsive probes for the monitoring of the local changes in the anion concentration.¹³² Five bis-substituted systems (P-Me or P-Ph phosphinate donors) were studied and reported changes in the emission spectra upon displacement of the bound water molecule with different oxy-anions ($\log K_a = 3$). Following the synthetic methodology developed for the production of the P-Ph-SO₃⁻ system, different R' substituents can be introduced in order to have stronger binding affinity or increased binding selectivity (*e.g.* hydrogen bond donors that increase the overall electrostatic interactions and lead to some directionality in the binding).¹³³

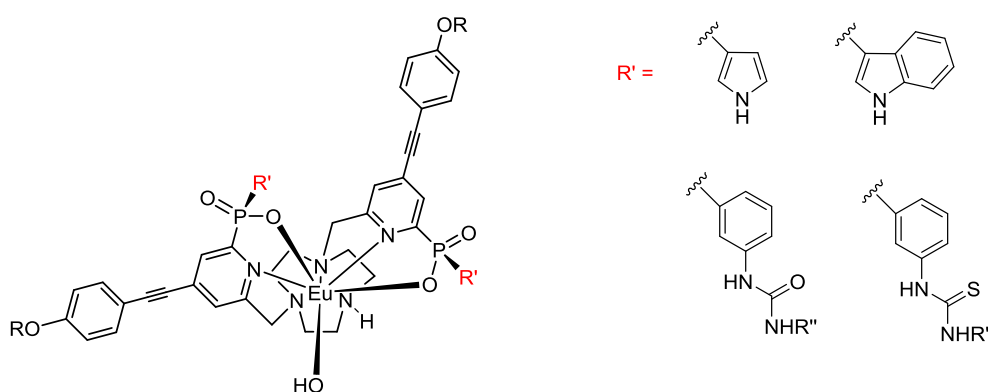


Figure 92: Bis-substituted Eu(III) complex that binds anions.

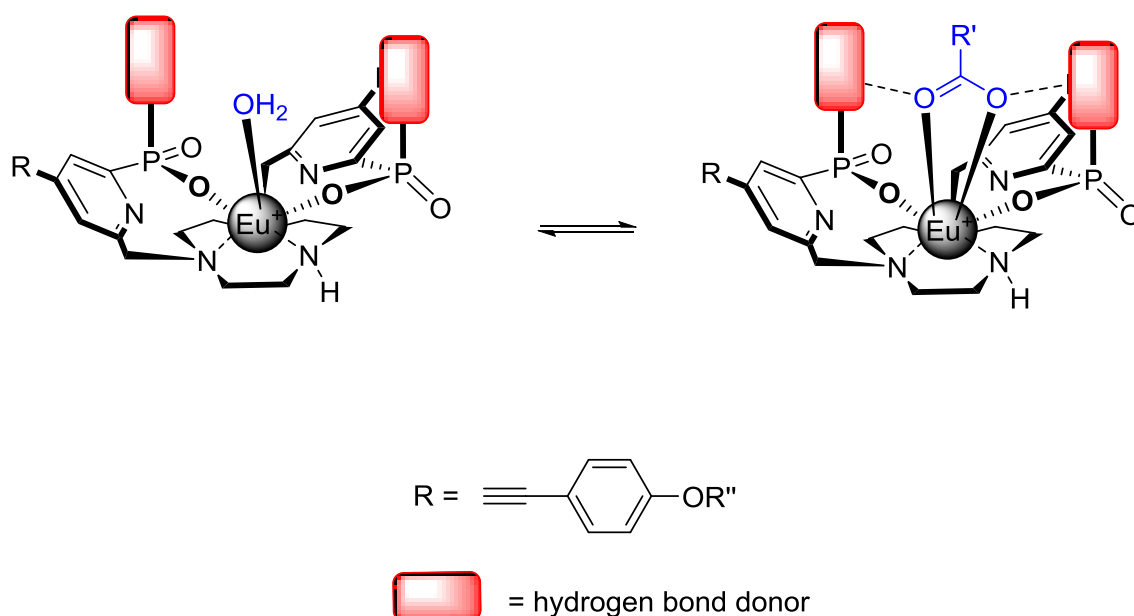


Figure 93: Cartoon explaining the mechanism of anion binding stabilisation.

The application of these complexes as chiral probes for CPL spectroscopy and microscopy is also a possibility. The stereoselectivity of the synthesis allowed for the formation of chiral

complexes with > 90 % optical purity that reported a very intense CPL emission. New examples of enantiomerically pure probes that report changes in their chiral environment can be envisaged.

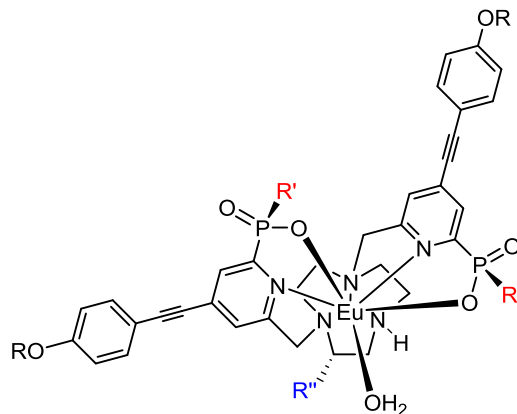


Figure 94: Bis-substituted enantiopure Eu(III) complex.

7 Experimental

7.1 General experimental

7.1.1 General procedures

All **reagents** were used as received from their respective suppliers. Solvents were laboratory grade and were dried over appropriate drying agents when necessary. Air sensitive reactions were carried out under an atmosphere of argon using Schlenk-line techniques.

Isolated **yields** for the Eu(III) complexes are based on the measured absorbance as the isolated amount of material was small and the extinction coefficients are particularly high and were assumed to be the same for the precursor ligand and the complex. Such behaviour has been observed previously for related series of complexes with strong ICT bands, ($\epsilon = 60000 \text{ M}^{-1} \text{ cm}^{-1}$ in MeOH). The structure reported for the Eu(III) complexes represents the species present in water at neutral pH, although most complexes were isolated as a salt (details in the synthetic procedure).

Thin-layer **chromatography** was carried out on silica plates (Merck 5554) and visualised under UV irradiation (254/365 nm). Preparative column chromatography was carried out using silica (Merck Silica Gel 60, 230 – 400 mesh).

Electrospray mass spectra were obtained on a TQD mass spectrometer equipped with an Acquity UPLC, an electrospray ion source and an Acquity photodiode array detector (Waters Ltd, UK). Methanol was used as the carrier solvent. For LC-MS analyses a 2.1 x 50 mm 1.7 micron Acquity UPLC BEH C18 column was used.

Accurate masses were recorded on a QTOF Premier mass spectrometer equipped with an Acquity UPLC, a lock-mass electrospray ion source and an Acquity photodiode array detector (Waters Ltd, UK). Methanol was used as the carrier solvent.

^1H , ^{19}F , ^{31}P and ^{13}C NMR spectra were obtained at 295 K on Varian spectrometers operating at 4.7, 9.4, 11.7, 14.1, 16.5 Tesla, specifically on a Mercury 200 (^1H at 200.06 MHz, ^{19}F at 188.24 MHz, ^{31}P at 80.99 MHz, ^{13}C at 50.30 MHz), a Mercury 400 spectrometer (^1H at 399.97 MHz, ^{19}F at 376.33 MHz, ^{31}P at 161.91 MHz, ^{13}C at 100.61 MHz), a Varian Inova-500 spectrometer (^1H at 499.78 MHz, ^{19}F at 470.32 MHz, ^{31}P at 202.34 MHz, ^{13}C at 155.69 MHz),

a Varian VNMRS-600 spectrometer (^1H at 599.94 MHz, ^{19}F at 564.51 MHz, ^{31}P at 242.86 MHz, ^{13}C at 150.86 MHz) and a Varian VNMRS-700 spectrometer (^1H at 700.00 MHz, ^{19}F at 658.66 MHz, ^{31}P at 283.37 MHz, ^{13}C at 175.95 MHz). Commercially available deuterated solvents were used. All chemical shifts are given in ppm with coupling constants in Hz.

Melting points were recorded using a Sanyo Gallenkamp Melting Point Apparatus and are uncorrected.

7.1.2 HPLC analysis

HPLC analysis and purifications was performed at 295 K with three different set-ups:

- *Waters Mass Directed Auto Preparation (MDAP) system*: Waters 575 pump, Waters "System Fluidics Organizer", Waters 2545 "Binary Gradient Module", Waters 2767 "Sample Manager", Waters Fraction Collector III, Waters 2998 Photodiode Array Detector and Waters 3100 Mass Detector.
- *Perkin Elmer system*: Perkin Elmer Series 200 pump, Perkin Elmer Series 200 auto-sampler, Perkin Elmer Series 200 UV/Vis detector and Perkin Elmer Series 200 fluorescence detector.
- *Shimadzu system*: Degassing Unit (DGU-20A5R), a Prominence Preparative Liquid Chromatograph (LC-20AP), a Prominence UV/Vis Detector (SPD-20A) and a Communications Bus Module (CBM-20A).

Various chromatographic systems were employed for analytical and preparative HPLC:

- *Method A*: (XBridge C_{18} OBD, 19 x 100 mm, i.d. 5 μm) flow rate of 17 mL / min with H_2O (0.1% formic acid) – 10 % MeOH (0.1% formic acid) as eluents [linear gradient to 100 % MeOH (0.1% formic acid) (15 min)].
- *Method B*: (XBridge C_{18} OBD, 4.6 x 100 mm, i.d. 5 μm) flow rate of 1 mL / min with H_2O (0.1% formic acid) – 10 % MeOH (0.1% formic acid) as eluents [linear gradient to 100 % MeOH (0.1% formic acid) (15 min)].
- *Method C*: (XBridge C_{18} OBD, 4.6 x 100 mm, i.d. 5 μm) flow rate of 1 mL / min with H_2O (0.1% formic acid) – 30 % MeOH (0.1% formic acid) as eluents [linear gradient to 100 % MeOH (0.1% formic acid) (10 min), isocratic 100 % MeOH (0.1% formic acid) (5 min)].

- *Method D:* (XBridge C18 OBD 10 x 100 mm, i.d. 3.5 μ M) flow rate of 4.4 mL / min with H₂O (0.05 M ammonium bicarbonate) – 30 % MeOH as eluents [linear gradient to 100 % MeOH (15 min)].
- *Method E:* (XBridge C18 OBD 10 x 100 mm, i.d. 3.5 μ M) flow rate of 4.4 mL / min with H₂O (0.1% formic acid) – 40 % MeOH (0.1% formic acid) as eluents [linear gradient to 100 % MeOH (0.1% formic acid) (15 min)].
- *Method F:* (XBridge C₁₈ OBD, 19 x 100 mm, i.d. 5 μ m) flow rate of 20 mL / min with H₂O (0.1% formic acid) – 30 % MeOH (0.1% formic acid) as eluents [linear gradient to 100 % MeOH (0.1% formic acid) (20 min)].
- *Method G:* (XBridge C₁₈ OBD, 19 x 100 mm, i.d. 5 μ m) flow rate of 20 mL / min with H₂O (25 mM triethylammonium acetate buffer, pH = 7) – 2 % CH₃CN as eluents [linear gradient to 40 % CH₃CN (20 min)].
- *Method H:* (XBridge C₁₈ OBD, 19 x 100 mm, i.d. 5 μ m) flow rate of 20 mL / min with H₂O (0.1% formic acid) – 10 % CH₃CN (0.1% formic acid) as eluents [linear gradient to 60 % CH₃CN (0.1% formic acid) (19 min)].
- *Method I:* (XBridge C₁₈ OBD, 4.6 x 100 mm, i.d. 5 μ m) flow rate of 1 mL / min with H₂O (0.1% formic acid) – 30 % MeOH (0.1% formic acid) as eluents [linear gradient to 100 % MeOH (0.1% formic acid) (15 min), isocratic 100 % MeOH (0.1% formic acid) (5 min)].
- *Method J:* (XBridge C₁₈ column, 19 x 100 mm, i.d. 5 μ m) flow rate of 17 mL / min with H₂O (0.1 % formic acid) – 30 % MeOH (0.1 % formic acid) as eluents (3 min) [linear gradient to 100 % MeOH (15 min)].
- *Method K:* (XBridge C₁₈ column, 19 x 100 mm, i.d. 5 μ m) flow rate of 17 mL / min with H₂O (25 mM triethylammonium acetate buffer, pH = 7) – 2 % CH₃CN as eluents (3 min) [linear gradient to 40 % MeOH (15 min), linear gradient to 100 % MeOH (3 min)].
- *Method L:* (XBridge C₁₈ column, 4.6 x 100 mm, i.d. 5 μ m) flow rate of 2 mL / min with H₂O (25 mM triethylammonium acetate buffer, pH = 7) – 2 % CH₃CN as eluents (3 min) [linear gradient to 40 % MeOH (15 min), linear gradient to 100 % MeOH (3 min)].
- *Method M:* Performed on the QTOF Premier mass spectrometer described above. Solvent system H₂O (25 mM triethylammonium acetate buffer, pH = 7) – 2 % CH₃CN as eluents [linear gradient to 40 % CH₃CN (6 min), linear gradient to 100 % CH₃CN (4 min), isocratic 100 % MeOH (2 min)].

- *Method N*: Performed on the TQD mass spectrometer described above. Solvent system H₂O + 0.1% formic acid – 5 % MeOH [linear gradient to 95 % MeOH (0.1% formic acid) (5 min)].

Chiral HPLC was performed on the Perkin Elmer system described above using analytical CHIRALPAK-IC 250 x 4.6 mm 5 μM or CHIRALPAK-ID 250 x 4.6 mm 5 μM chiral columns with an isocratic solvent system of MeOH.

7.1.3 Optical techniques

UV/Vis absorbance spectra were recorded on a Perkin Elmer Lambda 900 UV/Vis/NIR spectrometer. **Emission spectra** were recorded on a ISA Jobin-Yvon Spex Fluorolog-3 luminescence spectrometer. **Lifetime measurements** were carried out using a Perkin Elmer LS55 spectrometer using FL Winlab software. Quantum yields were calculated by comparison with two standards, as reported in literature.⁴⁴

CPL was measured with a home-built (modular) spectrometer. The excitation source was a broad band (200 – 1000 nm) laser-driven light source EQ 99 (Elliot Scientific). The excitation wavelength was selected by feeding the broadband light into an Acton SP-2155 monochromator (Princeton Instruments); the collimated light was focused into the sample cell (1 cm quartz cuvette). Sample PL emission was collected perpendicular to the excitation direction with a lens ($f = 150$ mm). The emission was fed through a photoelastic modulator (PEM) (Hinds Series II/FS42AA) and through a linear sheet polariser (Comar). The light was then focused into a second scanning monochromator (Acton SP-2155) and subsequently on to a photomultiplier tube (PMT) (Hamamatsu H10723 series). The detection of the CPL signal was achieved using the field modulation lock-in technique. The electronic signal from the PMT was fed into a lock-in amplifier (Hinds Instruments Signaloc Model 2100). The reference signal for the lock-in detection was provided by the PEM control unit. The monochromators, PEM control unit and lock-in amplifier were interfaced to a desktop PC and controlled by a Labview code. The lock-in amplifier provided two signals, an *AC* signal corresponding to $(I_L - I_R)$ and a *DC* signal corresponding to $(I_L + I_R)$ after background subtraction. The emission dissymmetry factor was therefore readily obtained from the experimental data, as $2 AC/DC$.

Spectral calibration of the scanning monochromator was performed using a Hg-Ar calibration lamp (Ocean Optics). A correction factor for the wavelength dependence of the detection

system was constructed using a calibrated lamp (Ocean Optics). The measured raw data was subsequently corrected using this correction factor. The validation of the CPL detection systems was achieved using light emitting diodes (LEDs) at various emission wavelengths. The LED was mounted in the sample holder and the light from the LED was fed through a broad band polarising filter and 1/4 wave plate (Ocean Optics) to generate circularly polarised light. Prior to all measurements, the $\lambda/4$ plate and a LED were used to set the phase of the lock-in amplifier correctly. The emission spectra were recorded with 0.5 nm step size and the slits of the detection monochromator were set to a slit width corresponding to a spectral resolution of 0.25 nm. CPL spectra (as well as total emission spectra) were obtained through an averaging procedure of several scans. The CPL spectra have been smoothed using Savitzky-Golay smoothing (polynomial order 5, window size 9 with reflection at the boundaries) to enhance visual appearance; all calculations were carried out using raw spectral data. Analysis of smoothed vs raw data was used to help to estimate the uncertainty in the stated g_{em} factors, which was typically $\pm 10\%$.

7.1.4 Cellular studies and microscopy

The Tag-lite labelling medium (LABMED), the SNAP-CCK2 plasmid for transient transfection of CCK2 receptors (PSNAP-CCK2), the SNAP-Dopamine D2 plasmid for transient transfection of dopamine-d2 receptors (PSNAPD2), the red-fluorescent red-CCK(26-33) agonist (L0013RED) and the red-NAPS antagonist (L002RED) were obtained from Cisbio Bioassays. The CCK2 receptor antagonist PD135158 was purchased from Tocris. CCK(26-33) was obtained from Almac (Craigavon, UK). The 96-well plates were purchased from Greiner Bio-One (ref. 655086, Monroe, NC).

HEK293 wild-type cells were cultured in Dulbecco's modified Eagle's medium (DMEM) glutaMAX (1966-021; Invitrogen, Carlsbad, CA) supplemented with fetal bovine serum (10 %), non-essential amino acids (1 %), penicillin/streptomycin (1 %), and HEPES (2 mM).

Transient transfection was performed in 96-well plates using 100,000 cells per well according to a previously described procedure.⁹⁶ Prior to cell seeding, the wells of the plates were pre-coated with poly-L-ornithine (50 μ L) for 30 min at 37 °C. The transfection mixture (per individual well) was prepared by adding the SNAP-tag-CCK2 plasmid (100 ng) to optiMEM medium (49 μ L), and Lipofectamine 2000 (0.8 μ L; Invitrogen) and incubating for 20 min at room temperature prior to the addition to the plates. Subsequently, HEK293 cells

(100 μL) at a density of 10^6 cell mL^{-1} were distributed in each well of the plates. The plates were incubated overnight at 37°C under 5% CO_2 .

For the labelling of SNAP-CCK2-expressed HEK293 cells, with the Eu(III) complexes, a previously described procedure was used.⁹⁶ A concentration series ranging from 0–500 nM was prepared in Tag-lite labelling medium. After incubation, the transfection mixture was removed from 96-well plates, and cells were treated with the prepared solutions (50 μL) and incubated for 1 h at 37°C under 5% CO_2 . The residual compounds were removed by washing each well four times with Tag-lite labelling medium (100 μL).

The affinity of red-CCK(26-33) for the CCK2 receptors was determined by incubating labelled cells with increasing concentrations of the fluorescent ligand. The non-specific signal for each ligand concentration was determined by adding an excess of the corresponding unlabelled CCK(26-33) compound (10 μM). The unlabelled CCK(26-33) compound (20 μL) was added to plates containing labelled cells with Tag-lite labelling medium (100 μL), followed by the addition of the fluorescent red- CCK(26-33) agonist (20 μL). Plates were incubated at room temperature for 2 h before signal detection.

In competitive binding experiments, a fixed concentration of the fluorescent red-CCK(26-33) agonist (10 nM) was used in the presence of increasing concentrations of antagonist PD135158. PD135158 (20 μL) was added to plates containing labelled cells with Tag-lite labelling medium (100 μL), followed by the addition of the fluorescent red-CCK(26-33) agonist (10 μL). Plates were incubated at room temperature for 4 h before signal detection.

Signal detection was performed on PHERAstar FS plate reader (BMG LABTECH, Champigny-sur-Marne, France) at $\lambda = 620$ nm and $\lambda = 665$ nm (in TR mode: $\tau_{\text{delay}} = 60$ μs ; $\tau_{\text{gate}} = 400$ μs) upon $\lambda = 337$ nm laser excitation. Recorded data were analysed using GraphPad Prism (GraphPad Software, Inc., San Diego, CA). Specific binding was determined by subtracting the non-specific signal from the total signal. K_d values of the fluorescent ligand were obtained from the saturation curve of the specific binding. K_i values were calculated from competition assay experiments according to the Cheng and Prusoff equation.¹³⁴

A Lab-Tek 8 chamber slide system was pre-coated with poly-L-ornithine (200 μL) and incubated for 30 minutes at 37 $^{\circ}\text{C}$. The slide was washed with PBS (200 μL) and HEK293 cells were plated at a density of 5×10^4 cells per well (c/w) and incubated overnight at 37 $^{\circ}\text{C}$ under 5% CO_2 . The following day, transfection was performed with optiMEM medium (100 μL), Lipofectamine 2000 (0.8 μL), and SNAP-CCK2 plasmid (1.2 μg per well). The Lab-Tek slide was further incubated for 2 days at 37 $^{\circ}\text{C}$ under 5% CO_2 . After removal of the medium, SNAP-CCK2 receptors were labelled with the Eu(III) complex (200 nM) for 1 h at 37 $^{\circ}\text{C}$ and washed twice with Tag-lite medium. The fluorescent red-CCK(26-33) ligand (10 nM) was added for the FRET signal detection. Hoechst 33342 (2 mg mL^{-1} per well) was added and after 20 min incubation at room temperature and washing twice with Tag-lite medium, the Lab-Tek slide was observed with a Zeiss oil immersion objective (40 x magnification, 1.3 F-Fluar) on the Zeiss Axiovert 200M TR-FRET inverted microscope equipped with a pulsed nitrogen laser ($\lambda = 337$ nm, 30 Hz) and a cooled intensified CCD camera PI Max 1024X1024 GenIII. For the luminescence images, a $\lambda = 615 \pm 10$ nm band-pass filter was used with $\tau_{\text{delay}} = 100$ μs , $\tau_{\text{gate}} = 2000$ μs , and at 60 gates per exposure. TR-FRET images were collected with a $\lambda = 670 \pm 20$ nm band-pass filter using the same procedure. The recorded data were analysed using ImageJ software.

For the d2-dopamine receptors, the same procedure described for CCK2 receptors was used.

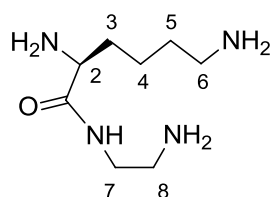
Confocal microscopy images were obtained using a Leica SP5 II microscope. In order to achieve excitation with maximal probe emission, the microscope was coupled by an optical fibre to a Coherent 355nm CW (Nd:YAG) laser, operating at 12mW power. The microscope was equipped with a triple channel imaging detector, comprising two conventional PMT systems and a HyD hybrid avalanche photodiode detector. The latter part of the detection system, when operated in the BrightRed mode, is capable of improving imaging sensitivity above 550 nm by 25%, reducing signal to noise by a factor of 5. The pinhole was always determined by the Airy disc size, calculated from the objective in use, using the lowest excitation wavelength. Scanning speed was adjusted to 100 Hz in a unidirectional mode, to ensure both sufficient light exposure and time to collect the emitted light from the lanthanide based optical probes. Spectral imaging on this Leica system is possible with the $xy\lambda$ -scan function, using the smallest allowed spectral band-pass (5 nm) and step-size (3 nm) settings.

NSC-34 cells were cultured in a 1:1 mixture of Dulbecco's modified Eagle's (DMEM) and F12 medium supplemented with fetal bovine serum (FBS, 10% v/v), non essential amino acids (0.5%) and Penicillin/Streptomycin (0.1%). At approximately 90% confluence after 3 healthy passages, cells were sub-cultured into a different growth medium, which contained a mixture of DMEM/Ham's F12 (1:1), FBS (1%), non-essential amino acids (1%) and Penicillin/Streptomycin (0.1%). Cells were allowed to proliferate over a period of several days to allow for the growth of functional NMDA receptors.

Cell Microscopy and spectral imaging of **NS155** in cells was achieved using a custom built microscope (modified Zeiss Axiovert 200M), using a Zeiss APOCHROMAT 63x/1.40 NA objective combined with a low voltage 365 nm pulsed UV LED focused, collimated excitation source (1.2W). For rapid spectral acquisition the microscope was equipped at the X1 port with a Peltier cooled 2D-CCD detector (Ocean Optics) used in an inverse 100 Hz time gated sequence. Probe lifetimes were measured on the same microscope platform using a novel cooled PMT detector (Hamamatsu H7155) interchangeable on the X1 port. Both the control and detection algorithm were written in LabView2011.

7.2 Synthetic procedures

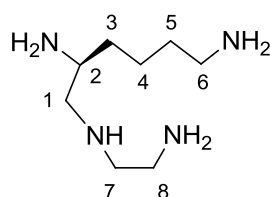
(2*S*)-*N*-(2-aminoethyl)-(2,6-diaminohexanamide), **1a**



(2*S*)-Lysine ethyl ester hydrochloride, **1** (5.0 g, 20 mmol) was added in small portions over 1 h to ethylenediamine (50 mL) at 80 °C, under argon, with continuous stirring. The reaction was heated to 120 °C for 3 h, after which time, the ethylenediamine was removed by distillation under reduced pressure. The orange oil was taken into aqueous sodium hydroxide (4 M, 10 mL), the solvent was evaporated and the residue was dissolved in MeOH (20 mL). The solution was filtered and the filtrate was added to DCM (50 mL) and passed down a pad of Celite. The combined filtrates were evaporated to give a yellow oil (3.2 g, 85 %); δ_{H} (CDCl₃) 7.57 (1H, br, NH), 3.35-3.32 (1H, m, H²), 3.28 (2H, q, ³*J*_{H-H} 6 Hz, H⁷), 2.80 (2H, t, ³*J*_{H-H} 6 Hz, H⁸), 2.68 (2H, t, ³*J*_{H-H} 6 Hz, H⁶), 1.85 (2H, m, H³), 1.46-1.30 (10H, m, NH₂ and H⁴⁻⁵); δ_{C} (CDCl₃) 188.6 (CO), 55.2 (C²), 41.9, 41.7, 41.5 (C⁶⁻⁷⁻⁸), 35.0, 33.5, 23.2 (C³⁻⁴⁻⁵), NMR data are in good agreement with those previously reported;⁸⁰ *m/z* (ESI) 211.3 [M + Na]⁺.

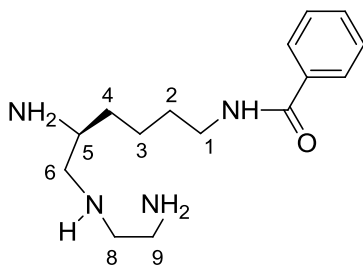
Racemisation may occur in this step, but it can be suppressed by lowering the temperature of the reaction between the amino-acid ester and ethylenediamine (100 °C) and the bath temperature in the subsequent distillation. The degree of racemization was calculated by adding the chiral solvating agent *R*-*O*-acetyl mandelic acid (1.2 eq) to samples of (2*S*)-*N*-(2-aminoethyl)-(2,6-diaminohexanamide) dissolved in CDCl₃.¹²⁶ The amide peak shifted to higher frequencies and split ($\delta_{\text{H}(\text{major})} = 8.09$ ppm, $\delta_{\text{H}(\text{minor})} = 8.32$ ppm, CDCl₃, 295 K). From the integral ratios, an enantiomeric purity of > 90 % was established.

(5*S*)-1,5,9-Triamino-3-azanonane, **2**



(2*S*)-*N*-(2-Aminoethyl)-(2,6-diaminohexanamide) **1a**, (3.2 g, 17 mmol) was boiled under reflux (70 °C) in BH₃-THF (100 mL, 100 mmol) for 24 h. The reaction was quenched with methanol (100 mL) at 0 °C and the solvents were evaporated. Reaction completion was confirmed by IR which revealed disappearance of the amide carbonyl group. The resulting white solid was boiled under reflux overnight in HCl (2 M, 50 mL). Evaporation of the solvent, followed by treatment of the residue with MeOH (50 mL) followed by evaporation (three times), gave the tetra-hydrochloride salt as a white solid (5.5 g, quantitative yield); δ_{H} (D₂O) 3.64-3.58 (1H, m, H²), 3.38-3.30 (6H, m, H¹⁻⁷⁻⁸), 2.93 (2H, t, ³J_{H-H} 8 Hz, H⁶), 1.73-1.38 (6H, m, H³⁻⁴⁻⁵); δ_{C} (D₂O) 49.3, 48.6, 45.3, 39.2, 35.5 (C¹⁻²⁻⁶⁻⁷⁻⁸), 30.0, 26.5, 21.5 (C³⁻⁴⁻⁵), NMR data were in good agreement with those previously reported;⁸⁰ *m/z* (ESI) 175.2 [M + H]⁺.

(5*S*)-*N*-(5,9-Diamino-7-azanonyl)benzamide, 3



First procedure:

The tetra-hydrochloride salt of (5*S*)-1,5,9-triamino-3-azanonane, **2** (1.0 g, 3.1 mmol) was dissolved in water (15 mL) and converted into the free tetra-amine by addition of aqueous potassium hydroxide solution (to pH = 7). Addition of basic copper carbonate Cu(CO₃)Cu(OH)₂ (0.4 g, 1.8 mmol) to the stirred solution gave an intense blue colour. The mixture was heated to 50 °C for 30 min. Benzoyl chloride (470 μ L, 4.1 mmol) was added over 1 h to the cooled solution (0 °C), and the pH was maintained between 8 and 9 by periodic addition of small KOH pellets. The reaction was allowed to warm to RT and stirring was continued for 1 h. The solution was filtered and the filtrate was treated with H₂S over 5 min. After filtration of the dark solid, the solution was pale yellow. The filtrate was washed with DCM and the aqueous layer was reduced to half the initial volume. The pH was increased up to 11 and the solution was extracted repeatedly with DCM. The organic layer was concentrated to give a colourless oil (130 mg, 15 %).

Second procedure:

The tetra-hydrochloride salt of (5*S*)-1,5,9-triamino-3-azanonane, **2** (1.0 g, 3.1 mmol) was dissolved in water (20 mL) and converted into the free tetra-amine by addition of potassium hydroxide (to pH = 7). Addition of copper carbonate $\text{Cu}(\text{CO}_3)\text{Cu}(\text{OH})_2$ (0.4 mg, 1.8 mmol) to the stirred solution gave an intense blue colour. The mixture was heated to 50 °C for 30 min. The solution was cooled to RT, the pH was adjusted to 9 with KOH pellets and the benzoic acid NHS active ester (0.9 g, 4.0 mmol) was added. The reaction was heated to 40 °C with efficient stirring for 2 h, the solution was filtered and the filtrate treated with H_2S over 5 min. After filtration of the dark solid, the solution was pale yellow. The filtrate was washed with DCM and the aqueous layer was reduced to half the initial volume. The pH was increased up to 11 and the solution was extracted repeatedly with DCM. The organic layer was concentrated to give a colourless oil (170 mg, 20 %).

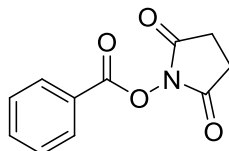
Third procedure:

The tetra-hydrochloride salt of (5*S*)-1,5,9-triamino-3-azanonane, **2** was converted into the free tetra-amine (1.0 g, 5.7 mmol) by anion exchange chromatography using DOWEX 1x2-200 resin. The free amine was dried under reduced pressure and then dissolved in anhydrous dibutyl ether (60 mL) and the solution degassed using a freeze-pump-thaw cycles. $\text{Mo}(\text{CO})_6$ (1.5 g, 5.7 mmol) was added and the solution was heated to 140 °C for 2 h in which a yellow precipitate formed. After cooling to RT, the solvent was removed with a syringe and dry DMF (40 mL) previously degassed with freeze-thaw cycles was added. 2,5-dioxopyrrolidin-1-yl benzoate (1.6 g, 7.3 mmol) was added quickly and the solution was stirred at RT for 1 h. The reaction was monitored by observing the disappearance of the active ester by TLC ($R_f = 0.34$ silica, Hex: EtOAc 1 : 1). The solvent was removed and the brown residue was taken up in dilute HCl (10 %, 12 mL) and stirred in air at RT for 18 h. The solution was centrifuged and the red solution was decanted and washed with DCM (2 x 30 mL). The pH was raised to 7 and the solution was washed with DCM (2 x 30 mL). The pH was raised to 12 and the solution was extracted repeatedly with DCM. The solvent was removed to give a colourless oil (870 mg, 52 %).

δ_{H} (CDCl_3) 7.80-7.77 (2H, m, ArH), 7.51-7.43 (3H, m, ArH), 6.33 (1H, br, CONH), 2.82 (2H, t, $^3J_{\text{H-H}}$ 4 Hz H^1), 2.72-2.66 (6H, m, H^{6-8-9}), 2.41 (1H, m, H^5), 1.67-1.53 (11H, m, NH_2 and H^{2-3-4}); δ_{C} (CDCl_3) 166.6 (CO), 133.8, 130.3, 127.5, 125.9 (Ar), 55.6 (C^5), 51.6, 50.0, 40.8 (C^{6-8-9}).

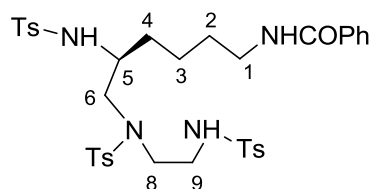
⁹), 38.7 (C¹), 28.7, 23.7, 22.5 (C²⁻³⁻⁴), NMR data were in good agreement with those previously reported;⁸⁰ *m/z* (ESI) 279.4 [M + H]⁺.

2,5-Dioxopyrrolidin-1-yl benzoate



Triethylamine (5.7 mL, 41 mmol) was added to a solution of benzoic acid (5.0 g, 41 mmol) in dry DCM (70 mL) under argon. EDC (7.8 g, 41 mmol) was added and a white solid precipitated. After 10 min of vigorous stirring, *N*-hydroxysuccinimide (4.7 g, 41 mmol) was added and the solution became colourless. After stirring for 4 h at RT, the solution was washed with water, dried over MgSO₄, filtered and evaporated. The white solid was purified by crystallization from diethyl ether to give a white solid (5.2 g, 60 %); m.p. 138 – 140 °C [lit.¹³⁵ 137 – 138 °C]; δ_H (CDCl₃) 8.16 (2H, d, ³*J*_{H-H} 4 Hz, *o*-H), 7.71 (1H, dd, ³*J*_{H-H} 4 Hz, ³*J*_{H-H} 2 Hz, *p*-H), 7.54 (2H, dd, ³*J*_{H-H} 4 Hz, ³*J*_{H-H} 2 Hz, *m*-H), 2.93 (4H, s, 2CH₂); *R*_f = 0.26 (silica, Hex : EtOAc 1 : 1).

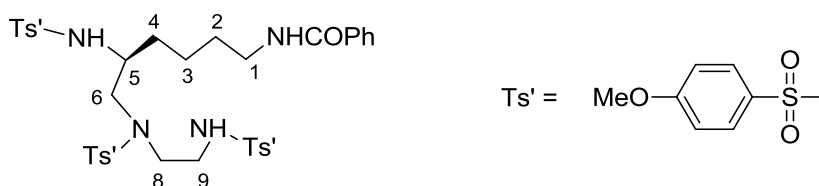
(5*S*)-*N*-(5,9-Bis-*p*-toluenesulphonamido-7-*p*-toluenesulphonyl-7-azanonyl)benzamide, 4a



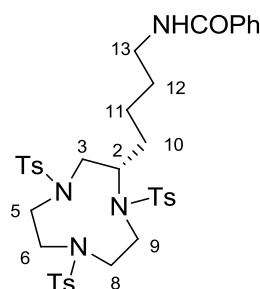
A solution of tosyl chloride (1.6 g, 8.4 mmol) in DCM (20 mL) was added dropwise to a solution of (5*S*)-*N*-(5,9-diamino-7-azanonyl)benzamide, **3** (660 mg, 2.4 mmol) and Et₃N (1.5 mL, 10.8 mmol) in DCM (20 mL) with stirring over a period of 1 h. The reaction mixture was stirred at RT overnight, after which time, the mixture was washed with water (2 x 20 mL). The water layer was extracted with EtOAc and the combined organic layers were concentrated. DCM (30 mL) was added to the brown oil and a white precipitate formed. The solid was isolated and the filtrate was concentrated and purified by column chromatography (silica, DCM : EtOAc 100 : 0 to 70 : 30) to give a white solid (800 mg, 46 %); m.p. 148 – 150 °C [lit.⁸⁰ 149 – 151 °C]; δ_H (CDCl₃) 7.86 (2H, d, ³*J*_{H-H} 8 Hz, ArH), 7.78 (3H, m, ArH), 7.70 (2H, d, ³*J*_{H-H} 8 Hz, ArH), 7.53 (1H, m, ArH), 7.44 (2H, m, ArH), 7.02-6.99 (5H, m, ArH), 6.90 (2H, m, ArH), 6.48 (1H, br, CONH), 5.30-5.26 (2H, m, NHTs), 3.35-3.04 (9H, m, H¹⁻⁵⁻⁶⁻

⁸⁻⁹), 2.73 (6H, s, CH₃), 2.25 (3H, s, CH₃), 1.71(1H, m, H⁴), 1.50-1.35 (3H, m, H²⁻⁴), 1.02-0.98 (2H, m, H³); δ_C (CDCl₃) 166.8 (CO), 143.2, 142.6, 136.1, 135.8, 133.3, 130.4, 129.0, 128.8, 128.7, 127.5, 126.4, 126.3, 126.1 (Ar), 55.0 (C⁵), 52.4, 51.6, 50.1 (C⁶⁻⁸⁻⁹), 41.7 (C¹), 38.0, 30.1, 27.7 (C²⁻³⁻⁴), 20.5 (CH₃), 5 signals obscured or overlapping; *m/z* (ESI) 763.4 [M + Na]⁺; *R_f* = 0.16 (silica, DCM : EtOAc 9 : 1).

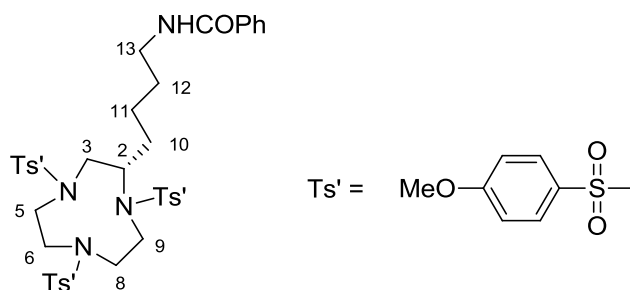
(S)-N-(6-(4-Methoxy-N-(2-(4-methoxyphenylsulfonamido)ethyl)phenylsulfonamido)-5-(4-methoxyphenylsulfonamido)hexyl)benzamide, 4b



A solution of *p*-methoxybenzenesulfonyl chloride (1.2 g, 5.7 mmol) in DCM (15 mL) was added dropwise to a solution of (5S)-N-(5,9-diamino-7-azanonyl)benzamide, **3** (440 mg, 1.6 mmol) and Et₃N (1.0 mL, 7.3 mmol) in DCM (35 mL) with stirring over a period of 1 h. The reaction mixture was stirred at RT overnight, after which time, it was washed with water, dried over MgSO₄, filtered and evaporated. The brown residue was purified by column chromatography (silica, DCM: EtOAc 100 : 0 to 70 : 30) to give a white solid (470 mg, 38 %); m.p. 145 – 148 °C; anal. calc. for C₃₆H₄₄N₄O₁₀S₃: C, 54.81; H, 5.62; N, 7.10 %; found: C, 54.90; H, 5.55; N, 7.13 %; δ_H (CDCl₃) 7.76 (2H, d, ³J_{H-H} 8 Hz, ArH), 7.65 (3H, m, ArH), 7.54 (2H, d, ³J_{H-H} 8 Hz, ArH), 7.40 (1H, m, ArH), 7.35 (2H, m, ArH), 7.26-7.19 (5H, m, ArH), 7.13-7.11 (2H, m, ArH), 6.40 (1H, br, CONH), 5.22-5.18 (2H, m, NHTs'), 3.90 (6H, s, CH₃), 3.79 (3H, s, CH₃), 3.35-3.04 (9H, m, H¹⁻⁵⁻⁶⁻⁸⁻⁹), 1.71(1H, m, H⁴), 1.50-1.35 (3H, m, H²⁻⁴), 1.02-0.98 (2H, m, H³); δ_C (CDCl₃) 166.8 (CO), 143.2, 142.6, 136.1, 135.8, 133.3, 130.4, 129.0, 128.8, 128.7, 127.5, 126.4, 126.3, 126.1 (Ar), 55.0 (C⁵), 52.4, 51.6, 50.1 (C⁶⁻⁸⁻⁹), 41.7 (C¹), 38.0 (CH₃), 30.1, 28.7 21.9 (C²⁻³⁻⁴), 5 signals obscured or overlapping; *m/z* (ESI) 811.8 [M + Na]⁺; *R_f* = 0.21 (silica, DCM : EtOAc 8 : 2).

(S)-2-(4-Benzamidobutyl)-1,4,7-tris(*p*-toluenesulfonyl)-1,4,7-triazacyclononane, 5a

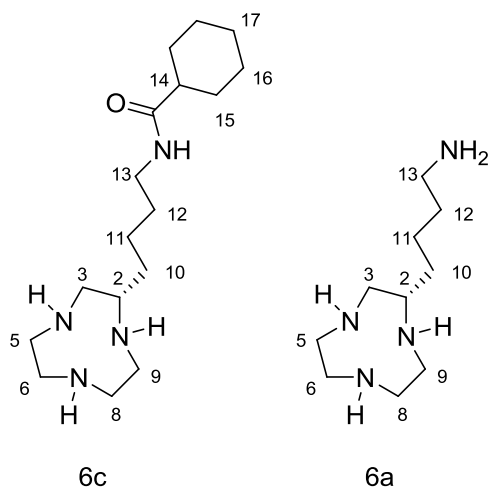
Caesium carbonate (1.0 g, 3.3 mmol) was added to a solution of the tritosylamide, **4a** (750 mg, 1 mmol), in anhydrous DMF (45 mL) under argon. A solution of ethylene glycol bis(toluene-*p*-sulphonate) (412 mg, 1.1 mmol) in anhydrous DMF (20 mL) was added dropwise over a period of 2 h, with efficient stirring. After stirring for 16 h, the temperature was raised to 65 °C for 5 h. The solvent was removed under reduced pressure and the residue was dissolved in chloroform (50 mL) and washed with water. The organic layer was dried over MgSO₄, filtered and evaporated. The yellow oil was purified by column chromatography (silica, DCM: EtOAc 100 : 0 to 80 : 20) to give a white solid (495 mg, 66 %); m.p. 107 – 109 °C [lit.⁸⁰ 106 – 108 °C]; δ_{H} (CDCl₃) 7.84-7.82 (2H, d, ³J_{H-H} 8 Hz, ArH), 7.75 (2H, m, ArH), 7.63 (2H, m, ArH), 7.61 (2H, m, ArH), 7.39-7.27 (9H, m, ArH), 6.59 (1H, br, CONH), 3.61-3.10 (13H, m, H²⁻³⁻⁵⁻⁶⁻⁸⁻⁹⁻¹³), 2.45-2.39 (9H, m, CH₃), 1.54-1.24 (6H, m, H¹⁰⁻¹¹⁻¹²); δ_{C} (CDCl₃) 166.5 (CO), 143.2, 143.1, 142.9, 133.6, 113.4, 133.2, 130.3, 129.0, 128.9, 128.8, 127.5, 127.0, 126.7, 126.6, 126.5, 126.3, 126.0 (Ar), 59.4 (C²), 52.7, 51.6, 49.7, 45.3 (C³⁻⁵⁻⁶⁻⁸⁻⁹), 38.7 (C¹³), 38.5, 28.0, 23.0, (C¹⁰⁻¹¹⁻¹²), 20.5 (CH₃), 2 signals obscured or overlapping; *m/z* (ESI) 789.4 [M + Na]⁺; *R*_f = 0.47 (silica, DCM : EtOAc 8 : 2).

(S)-N-(4-(1,4,7-Tris(4-methoxyphenylsulfonyl)-1,4,7-triazacyclononan-2-yl)butyl)benzamide, 5b

Caesium carbonate (140 mg, 0.43 mmol) was added to a solution of the tritosylamide, **4b** (100 mg, 0.13 mmol), in anhydrous DMF (10 mL) under argon. A solution of ethylene glycol bis(toluene-*p*-sulphonate) (61 mg, 0.17 mmol) in anhydrous DMF (10 mL) was added

dropwise over a period of 2 h, with efficient stirring. After stirring overnight RT, the temperature of the mixture was raised to 65 °C for 5 h. The solvent was removed under reduced pressure and the residue was dissolved in chloroform (25 mL) and washed with water. The organic layer was dried over MgSO₄, filtered and evaporated. The yellow oil was purified by column chromatography (silica, DCM: EtOAc 100 : 0 to 80 : 20) to give the a white solid (67 mg, 63 %); m.p. 104 – 106 °C; anal. calc. for C₃₈H₄₆N₄O₁₀S₃: C, 56.00; H, 5.69; N, 6.87 %; found: C, 56.50; H, 5.78; N, 6.82 %; δ_H (CDCl₃) 7.85-7.82 (2H, d, ³J_{H-H} 8 Hz, ArH), 7.76 (2H, m, ArH), 7.68 (2H, m, ArH), 7.44 (2H, m, ArH), 7.01-6.98 (9H, m, ArH), 6.43 (1H, br, CONH), 3.90-3.87 (9H, m, CH₃), 3.61-3.10 (13H, m, H²⁻³⁻⁵⁻⁶⁻⁸⁻⁹⁻¹³), 1.54-1.24 (6H, m, H¹⁰⁻¹¹⁻¹²); δ_C (CDCl₃) 166.5 (CO), 143.2, 143.1, 142.9, 133.6, 113.4, 133.2, 130.3, 129.0, 128.9, 128.8, 127.5, 127.0, 126.7, 126.6, 126.5, 126.3, 126.0 (Ar), 59.4 (C²), 52.7, 51.6, 49.7, 45.3 (C³⁻⁵⁻⁶⁻⁸⁻⁹), 38.7 (C¹³), 38.5 (CH₃), 28.0, 23.0, 20.5 (C¹⁰⁻¹¹⁻¹²), 2 signals obscured or overlapping; *m/z* (ESI) 837.8 [M + Na]⁺; *R_f* = 0.34 (silica, DCM : EtOAc 9 : 1).

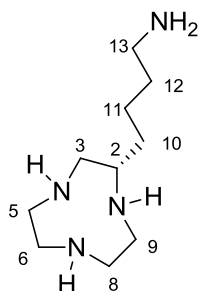
(S)-N-(4-(1,4,7-Triazacyclononan-2-yl)butyl)cyclohexanecarboxamide, 6c



Ammonia (40 mL) was condensed into a solution of the tritosylamide, **5a** (450 mg, 0.55 mmol) in a mixture of dry THF (20 mL) and dry EtOH (1.5 mL) whilst stirring under argon at -78 °C. Lithium (350 mg, excess) was added in small portions to the solution and a strong blue colour developed. The solution was slowly warmed to RT overnight; during this period the solution turned colourless and the ammonia gas was allowed to evaporate through an anti-suck back apparatus. Water (20 mL) was added slowly to the solution and the solvent was removed. The residue was dissolved in HCl (18 mL, 2 M) and washed with ether. The aqueous layer was concentrated, and the residue was dissolved in aqueous KOH solution (15 mL, 6 M) and extracted with DCM (3 x 20 mL). The organic layer was concentrated to give a

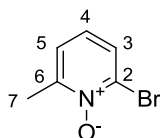
yellow oil (100 mg). The presence of the ligand **6c** was confirmed by MS, which also revealed the presence of compound **6a**. Completion of reaction was confirmed by $^1\text{H-NMR}$, observing the disappearance of the aromatic signals and by $^{13}\text{C-NMR}$ observing the appearance of the cyclohexyl peak at 24 and 28 ppm. The product was taken on without further purification and used for the alkylation step; m/z (HRMS^+) 311.2801 $[\text{M} + \text{H}]^+$ ($\text{C}_{17}\text{H}_{35}\text{N}_4\text{O}$ requires 311.2811) for **6c** and 201.2068 $[\text{M} + \text{H}]^+$ ($\text{C}_{10}\text{H}_{25}\text{N}_4$ requires 201.2079) for **6a**.

(S)-4-(1,4,7-Triazacyclononan-2-yl)butan-1-amine, 6a



2-(4-Cyclohexylamidobutyl)-1,4,7-triazacyclononane, **6c** (65 mg, 0,21 mmol) was dissolved in HCl (6 M, 3 mL) and stirred at 100 °C for 72 h. After completion the reaction was diluted with H_2O (3 mL) and washed with diethyl ether (3 x 10 mL). The aqueous layer was concentrated to give the tetrahydrochloride salt (100 mg, quantitative yield). δ_{H} (D_2O): 3.42-3.13 (10H, m, $\text{H}^{3-5-6-9-9}$), 3.96-2.87 (3H, m, H^{2-13}), 1.64-1.37 (6H, m, $\text{H}^{10-11-12}$); δ_{C} (D_2O): 53.3 (C^2), 46.1, 43.2, 41.8, 39.2, 39.1, 39.0 ($\text{C}^{3-5-6-8-9-13}$), 30.6, 26.5, 22.1, ($\text{C}^{10-11-12}$); m/z (HRMS^+) 201.2068 $[\text{M} + \text{H}]^+$ ($\text{C}_{10}\text{H}_{25}\text{N}_4$ requires 201.2079).

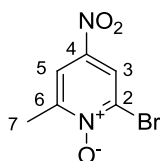
2-Bromo-6-methylpyridine-1-oxide, 8



2-Bromo-6-methylpyridine, **7** (10.0 g, 0.58 mol) was dissolved in CHCl_3 (150 mL). *m*CPBA (20.1 g, 1.16 mol) was added and the solution was stirred at 65 °C under argon for 18 h. The volume of the solution was reduced to 75 mL by removal of the solvent under reduced pressure. The solution was cooled to 0 °C overnight causing precipitation of 3-chlorobenzoic acid, which was removed by filtration. From the remaining filtrate, the solvent was removed under reduced pressure to give a yellow oil, which was dissolved in aqueous NaOH solution

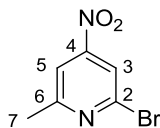
(1 M, 50 mL) and extracted with DCM (3 × 50 mL). The organic extracts were combined, dried over MgSO₄, filtered and the solvent removed under reduced pressure to give a yellow solid (6.0 g, 55 %); m.p. 54 – 57 °C [lit.⁷⁸ 48 – 55 °C];^b δ_H (CDCl₃) 7.55 (1H, dd, ³J_{H-H} 8 Hz, ⁴J_{H-H} 1.5 Hz, H³), 7.23 (1H, dd, ³J_{H-H} 8 Hz, ⁴J_{H-H} 1.5 Hz, H⁵), 7.01 (1H, t, ³J_{H-H} 8 Hz, H⁴), 2.57 (3H, s, H⁷); δ_C (CDCl₃) 151.2 (s, C²), 133.5 (s, C⁶), 128.7 (s, C³), 125.3 (s, C⁵), 125.2 (s, C⁴), 19.3 (s, C⁷); *m/z* (HRMS⁺) 187.9698 [M + H]⁺ (C₆H₇NO⁷⁹Br requires 187.9711); *Rf* = 0.16 (silica, DCM : 2 % MeOH).

2-Bromo-6-methyl-4-nitropyridine-1-oxide, 9



2-Bromo-6-methylpyridine-1-oxide, **8** (15.0 g, 80.0 mmol) was dissolved in concentrated H₂SO₄ (98%, 23 mL). The solution was stirred at 0 °C and HNO₃ (70 %, 26 mL, 0.38 mol) was added dropwise. The mixture was heated to 100 °C for 16 h. The yellow solution was dropped onto stirred ice (150 g) causing a pale yellow solid to precipitate. After 1 h the precipitate was filtered and dried under high vacuum to afford a pale yellow solid (12.0 g, 65 %); m.p. 138 – 139 °C [lit.⁷⁸ 137 – 138 °C];^c δ_H (CDCl₃) 8.40 (1H, d, ⁴J_{H-H} 3 Hz, H³), 8.09 (1H, d, ⁴J_{H-H} 3 Hz, H⁵), 2.62 (3H, s, H⁷); δ_C (CDCl₃) 151.8 (s, C⁴), 140.7 (s, C²), 134.0 (s, C⁶), 122.8 (s, C³), 118.9 (s, C⁵), 19.6 (s, C⁷); *m/z* (HRMS⁺) 232.9564 [M + H]⁺ (C₆H₆N₂O₃⁷⁹Br requires 232.9556); *Rf* = 0.53 (silica, DCM : 2% MeOH).

2-Bromo-6-methyl-4-nitropyridine, 10



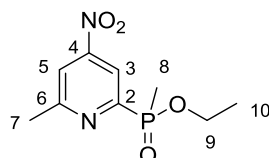
2-Bromo-6-methyl-4-nitropyridine-1-oxide, **9** (2.0 g, 8.6 mmol) was dissolved in CHCl₃ (50 mL) and PBr₃ (2.4 mL, 25.8 mmol) was added dropwise. The mixture was stirred at 60 °C under argon for 48 h. The solvent was removed under reduced pressure to give a yellow oil. Aqueous NaOH solution (2 M, 100 mL) was added cautiously and the solution was extracted with DCM (3 × 100 mL). The organic extracts were combined, dried over MgSO₄ and the

^b This compound is commercially available, <http://www.acespharma.com>

^c This compound is commercially available, <http://www.acccorporation.com>

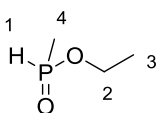
solvent removed under reduced pressure to give a yellow oil, which was purified by column chromatography on silica (DCM) to yield a pale yellow oil (1.6 g, 78 %); δ_{H} (CDCl_3) 8.02 (1H, d, $^4J_{\text{H-H}}$ 3 Hz, H^3), 7.83 (1H, d, $^4J_{\text{H-H}}$ 3 Hz, H^5), 2.70 (3H, s, H^7); δ_{C} (CDCl_3) 162.9 (s, C^4), 154.9 (s, C^2), 142.4 (s, C^6), 118.4 (s, C^3), 115.0 (s, C^5), 24.6 (s, C^7); m/z (HRMS^+) 216.9621 [$\text{M} + \text{H}$] $^+$ ($\text{C}_6\text{H}_6\text{N}_2\text{O}_2^{79}\text{Br}$ requires 216.9613); R_f = 0.75 (silica, DCM : 2 % MeOH).

Ethyl (6-methyl-4-nitropyridin-2-yl)(methyl)phosphinate, **11**



Neat ethyl methylphosphinate (570 mg, 3.67 mmol), containing one equivalent of ethanol, was added to degassed (freeze-thaw cycle) toluene (10 mL), followed by 2-bromo-6-methyl-4-nitropyridine, **10** (660 mg, 3.06 mmol) and freshly distilled triethylamine (1.49 mL, 10.70 mmol). Argon was bubbled through the yellow solution for 30 min, then $\text{PdCl}_2(\text{dppf})\cdot\text{DCM}$ (50 mg, 0.061 mmol) was added, and the mixture stirred at 125 °C for 16 h under argon, during which time the mixture turned black. The solvent was removed under reduced pressure, with purification of the resulting black oil by column chromatography (silica, EtOAc : Hex 1:1 to 3:1) giving an off-white oil (510 mg, 67 %); δ_{H} (CDCl_3) 8.54-8.56 (1H, m, H^3), 7.96-8.01 (1H, m, H^5), 3.68-4.44 (2H, m, H^9), 2.79 (3H, s, H^7), 1.83 (3H, d, $^2J_{\text{H-P}}$ 15 Hz, H^8), 1.31 (3H, t, $^3J_{\text{H-H}}$ 7 Hz, H^{10}); δ_{C} (CDCl_3) 163.2 (d, $^3J_{\text{C-P}}$ 21 Hz, C^4), 158.1 (d, $^1J_{\text{C-P}}$ 157 Hz, C^2), 154.3 (d, $^3J_{\text{C-P}}$ 157 Hz, C^6), 117.9 (d, $^4J_{\text{C-P}}$ 3 Hz, C^5), 117.2 (d, $^2J_{\text{C-P}}$ 23 Hz, C^3), 61.6 (d, $^3J_{\text{C-P}}$ 7 Hz, C^9), 24.9 (s, C^7), 16.6 (d, $^4J_{\text{C-P}}$ 6 Hz, C^{10}), 13.5 (d, $^1J_{\text{C-P}}$ 105 Hz, C^8); δ_{P} (CDCl_3) + 37.2; m/z (HRMS^+) 267.0527 [$\text{M} + \text{Na}$] $^+$ ($\text{C}_9\text{H}_{13}\text{N}_2\text{O}_4\text{PNa}$ requires 267.0511); R_f = 0.14 (silica, EtOAc : Hex 1 : 3).

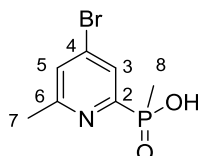
Ethyl methylphosphinate



Neat diethyl methylphosphonite (2.0 g, 14.7 mmol) was stirred under argon at RT and H_2O (264 μL , 14.7 mmol) was added. The mixture was stirred for 18 h. ^1H - and ^{31}P -NMR were used to confirm formation of the product, which was used *in situ* without further purification. The reaction mixture also contains one equivalent of ethanol as a by-product (100 %

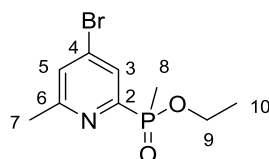
conversion by $^1\text{H-NMR}$); δ_{H} (CDCl_3) 7.22 (1H, dq, $^1J_{\text{H-P}}$ 536, $^2J_{\text{H-H}}$ 2 Hz, H^1), 4.11 (2H, dqd, $^2J_{\text{H-H}}$ 36 Hz $^3J_{\text{H-H}}$ 7 Hz $^3J_{\text{H-P}}$ 4 Hz, H^2), 1.54 (3H, dd, $^2J_{\text{H-P}}$ 15 Hz $^3J_{\text{H-H}}$ 2 Hz, H^4), 1.23 (3H, $^3J_{\text{H-H}}$ 7 Hz, H^3); δ_{P} (CDCl_3) +34.5; δ_{C} (CDCl_3) 62.3 (d, $^2J_{\text{C-P}}$ 7 Hz, C^2), 16.1 (s, C^3), 14.9 (d, $^1J_{\text{C-P}}$ 95 Hz, C^4); m/z (HRMS $^+$) 109.0414 [$\text{M} + \text{H}$] $^+$ ($\text{C}_3\text{H}_{10}\text{O}_2\text{P}$ requires 109.0418).

(4-Bromo-6-methylpyridin-2-yl)(methyl)phosphinic acid, **11a**



Ethyl (6-methyl-4-nitropyridin-2-yl)(methyl)phosphinate, **11** (750 mg, 3.07 mmol) was dissolved in acetyl bromide (6.8 mL, 92 mmol) and the mixture stirred at 70 °C for 16 h under argon. A pale brown precipitate formed. Both precipitate and solution were dropped cautiously into MeOH (30 mL) stirred at 0 °C. The solvent was removed under reduced pressure to yield a pale brown solid. The material, containing minor impurities, was used in the next step without further purification, assuming quantitative conversion to the bromophosphinic acid; δ_{H} (CD_3OD) 8.25-8.28 (1H, m, H^3), 8.17-8.18 (1H, m, H^5), 2.76 (3H, s, H^7), 1.80 (3H, d, $^2J_{\text{H-P}}$ 16 Hz, H^8); δ_{P} (CD_3OD) +28.6; m/z (HRMS $^+$) 249.9627 [$\text{M} + \text{H}$] $^+$ ($\text{C}_7\text{H}_{10}\text{NO}_2^{79}\text{BrP}$ requires 249.9627); R_f = 0.01 (silica, DCM : MeOH 95 : 5).

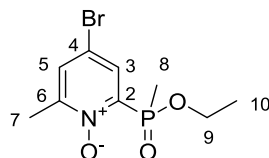
Ethyl (4-bromo-6-methylpyridin-2-yl)(methyl)phosphinate, **12**



Crude (4-bromo-6-methylnitropyridin-2-yl)(methyl)phosphinic acid, **11a** (768 mg, 3.07 mmol) was added to $\text{HC}(\text{OCH}_2\text{CH}_3)_3$ (25 mL) and the mixture stirred at 140 °C for 72 h under argon. The solvent was removed under reduced pressure and the resulting residue was purified by column chromatography (silica, DCM : MeOH 1 to 2 %) to yield a yellow oil (660 mg, 77 % over two steps); δ_{H} (CDCl_3) 8.04 (1H, dd $^3J_{\text{H-P}}$ 6 Hz $^4J_{\text{H-H}}$ 2 Hz, H^3), 7.46 (1H, app s, H^5), 3.82-4.16 (2H, m, H^9), 2.59 (3H, s, H^7), 1.77 (3H, d, $^2J_{\text{H-P}}$ 15 Hz, H^8), 1.28 (3H, t, $^3J_{\text{H-H}}$ 7 Hz, H^{10}); δ_{C} (CDCl_3) 161.1 (d, $^3J_{\text{C-P}}$ 21 Hz, C^4), 155.4 (d, $^1J_{\text{C-P}}$ 156 Hz, C^2), 133.6 (d, $^3J_{\text{C-P}}$ 14 Hz, C^6), 128.9 (d, $^4J_{\text{C-P}}$ 3 Hz, C^5), 128.2 (d, $^2J_{\text{C-P}}$ 22 Hz, C^3), 61.3 (d, $^3J_{\text{C-P}}$ 6 Hz, C^9),

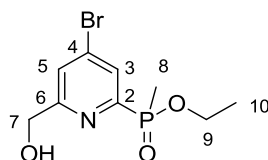
24.4 (s, C⁷), 16.5 (d, ⁴J_{C-P} 6 Hz, C¹⁰), 13.6 (d, ¹J_{C-P} 104 Hz, C⁸); δ_P (CDCl₃) + 38.0; *m/z* (HRMS⁺) 277.9973 [M + H]⁺ (C₉H₁₄NO₂⁷⁹BrP requires 277.9946); *R_f* = 0.33 (silica, DCM : MeOH 95 : 5).

Ethyl (4-bromo-6-methylpyridin-1-oxide-2-yl)(methyl)phosphinate, **13**



Ethyl (4-bromo-6-methylpyridin-2-yl)(methyl)phosphinate, **12** (250 mg, 1.10 mmol) was dissolved in CH₃CN (5 mL). 3-Chloroperbenzoic acid (378 mg, 2.19 mmol) was added and the solution stirred at 65 °C for 16 h. The solvent was then removed under reduced pressure, with the resulting material being re-dissolved in DCM (10 mL), and washed with aqueous NaHCO₃ (0.5 M, 10 mL). The aqueous layer was re-extracted with DCM (3 × 10 mL), the organic extracts combined, dried over MgSO₄, and the solvent removed under reduced pressure, with purification of the resulting yellow oil by column chromatography (silica, DCM : MeOH 0 to 3 %) giving a colourless oil (256 mg, 79 %); δ_H (CDCl₃) 8.04 (1H, dd ³J_{H-P} 8 Hz ⁴J_{H-H} 3 Hz, H³), 7.54 (1H, dd ⁴J_{H-H} 3 Hz, H⁵), 3.89-4.22 (2H, m, H⁹), 2.48 (3H, s, H⁷), 1.97 (3H, d, ²J_{H-P} 17 Hz, H⁸), 1.31 (3H, t, ³J_{H-H} 7 Hz, H¹⁰); δ_C (CDCl₃) 151.1 (d, ³J_{C-P} 4 Hz, C⁴), 143.8 (d, ¹J_{C-P} 136 Hz, C²), 133.4 (d, ³J_{C-P} 11 Hz, C⁶), 132.3 (d, ⁴J_{C-P} 2 Hz, C⁵), 118.0 (d, ²J_{C-P} 12 Hz, C³), 62.1 (d, ³J_{C-P} 7 Hz, C⁹), 17.5 (s, C⁷), 16.6 (d, ⁴J_{C-P} 6 Hz, C¹⁰), 14.5 (d, ¹J_{C-P} 111 Hz, C⁸); δ_P (CDCl₃) + 32.2; *m/z* (HRMS⁺) 293.9909 [M + H]⁺ (C₉H₁₄NO₃⁷⁹BrP requires 293.9895); *R_f* = 0.27 (silica, DCM : MeOH 95 : 5).

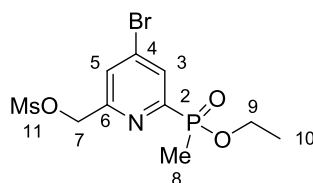
Ethyl (4-bromo-6-hydroxymethylpyridin-2-yl)(methyl)phosphinate, **14**



Trifluoroacetic anhydride (5 mL) was added to a solution of ethyl (4-bromo-6-methylpyridin-1-oxide-2-yl)(methyl)phosphinate, **13** (557 mg, 2.00 mmol) in dry CH₃CN (15 mL). The reaction mixture was heated to 60 °C for 3 h under argon. The solvent was removed under reduced pressure and the resulting oil was dissolved in EtOH (15 mL) and H₂O (15 mL) and stirred for 16 h. After this time, the solution was concentrated (ca. 10 mL) and extracted with

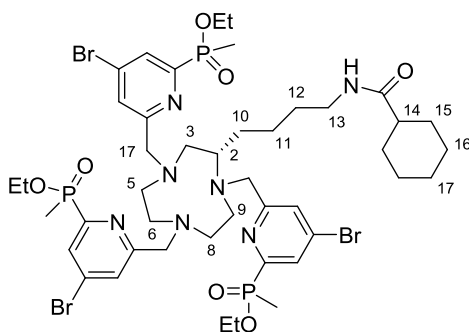
DCM (3 × 30 mL). The organic extracts were combined, dried over MgSO₄, and the solvent removed under reduced pressure, with purification of the resulting oil by column chromatography (silica, DCM : MeOH 1 to 3 %) giving a golden oil (470 mg, 80 %); δ_{H} (CDCl₃) 8.13 (1H, dd ³J_{H-P} 6 Hz ⁴J_{H-H} 1.8 Hz, H³), 7.63 (1H, app s, H⁵), 4.80 (2H, s, H⁷), 3.70-4.20 (2H, m, H⁹), 3.26 (1H, br s, OH), 1.76 (3H, d, ²J_{H-P} 15 Hz, H⁸), 1.27 (3H, t, ³J_{H-H} 7 Hz, H¹⁰); δ_{C} (CDCl₃) 162.8 (d, ³J_{C-P} 20 Hz, C⁴), 154.8 (d, ¹J_{C-P} 154 Hz, C²), 134.5 (d, ³J_{C-P} 13 Hz, C⁶), 129.5 (d, ²J_{C-P} 22 Hz, C³), 126.3 (d, ⁴J_{C-P} 3 Hz, C⁵), 64.2 (s, C⁷), 61.5 (d, ³J_{C-P} 6 Hz, C⁹), 16.5 (d, ⁴J_{C-P} 6 Hz, C¹⁰), 13.6 (d, ¹J_{C-P} 105 Hz, C⁸); δ_{P} (CDCl₃) + 38.0; *m/z* (HRMS⁺) 315.9729 [M + Na]⁺ (C₉H₁₃NO₃⁷⁹BrPNa requires 315.9714); *R_f* = 0.24 (silica, DCM : MeOH 95 : 5).

(4-Bromo-6-(ethoxy(methyl)phosphoryl)pyridin-2-yl)methyl methanesulfonate, **15**



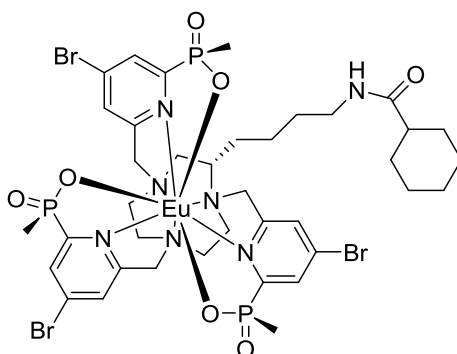
Ethyl (4-bromo-6-hydroxymethylpyridin-2-yl)(methyl)phosphinate, **14** (330 mg, 1.12 mmol) was dissolved in dry THF (15 mL) under argon. Et₃N (250 μ L, 3.37 mmol) was added and the solution was cooled to 0 °C. Methanesulfonyl chloride (130 μ L, 1.68 mmol) was added and the stirring was continued for 15 min, the progress of the reaction being monitored by TLC (silica, DCM : 3 % MeOH, *R_f*(product) = 0.50, *R_f*(reactant) = 0.24). The solvent was removed and the resulting oil was dissolved in DCM (20 mL) and washed with brine. The aqueous layers were extracted with DCM; the organic layers were combined, reduced in volume (20 mL), washed with brine, dried over MgSO₄, and the solvent removed under reduced pressure giving a pale yellow solid (320 mg, 75 %); the material was used without purification for the next step; δ_{H} (CDCl₃) 8.14 (1H, dd ³J_{H-P} 6 Hz ⁴J_{H-H} 2 Hz, H³), 7.72 (1H, app s, H⁵), 5.29 (2H, s, H⁷), 3.78-4.10 (2H, m, H⁹), 3.09 (3H, br s, H¹¹), 1.71 (3H, d, ²J_{H-P} 15 Hz, H⁸), 1.22 (3H, t, ³J_{H-H} 7 Hz, H¹⁰); *R_f* = 0.50 (silica, DCM : 3 % MeOH).

Triethyl 6,6',6''-((*S*)-2-(4-(cyclohexanecarboxamido)butyl)-1,4,7-triazacyclononane-1,4,7-triyl)tris(methylene)tris(4-bromopyridine-6,2-diyl)tris(methylphosphinate), **16**



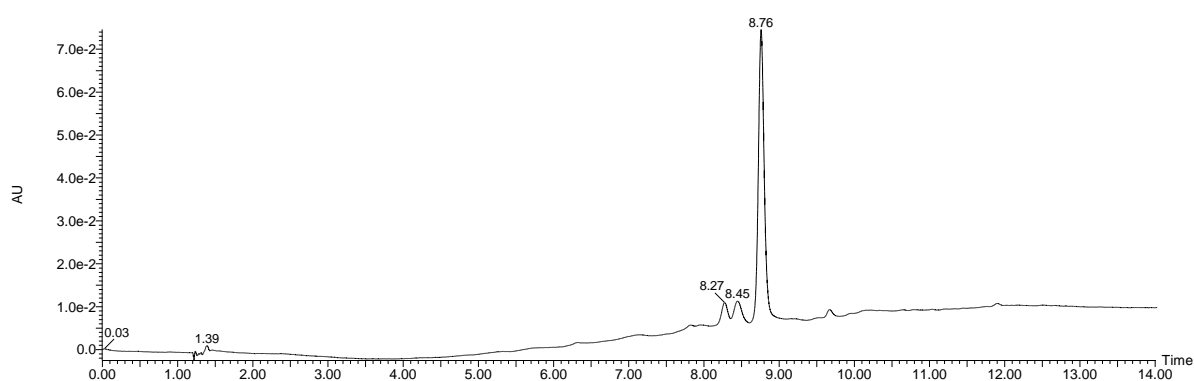
(*S*)-*N*-(4-(1,4,7-Triazacyclononan-2-yl)butyl)cyclohexanecarboxamide **6c** (75 mg, 0.24 mmol), containing traces of (*S*)-4-(1,4,7-triazonon-2-yl)butan-1-amine **6a**, was added to a solution of (4-bromo-6-(ethoxy(methyl)phosphoryl)pyridin-2-yl)methyl methanesulfonate (320 mg, 0.86 mmol) and K_2CO_3 (198 mg, 1.47 mmol) in dry CH_3CN (15 mL) and stirred under argon at 65 °C. After 6 h the solution was allowed to cool to RT and filtered. The filtrate was concentrated and purified by HPLC (*Method A*, $t_R = 8.5$ min) to give a yellow oil (65 mg, 25 %); δ_H ($CDCl_3$) 8.20-7.82 (6H, m, Py), 6.45 (1H, br, CONH), 4.17-3.87 (12H, m, $POCH_2$ and $H^{17-17'-17''}$), 3.23-2.59 (13H, m, $H^{2-3-5-6-8-9-13}$), 1.82-1.76 (9H, m, PCH_3), 1.76-1.26 (26H, m, $CH_3(Et)$ and $H^{10-11-12-14-15-16-17}$); δ_P ($CDCl_3$) + 37.76; m/z (HRMS⁺) 1138.191 [$M + H$]⁺ ($C_{44}H_{68}^{79}Br_3N_7O_7P_3$ requires 1138.193).

Europium (III) complex of (*R,R,R*)-6,6',6''-((*S*)-2-(4-(cyclohexanecarboxamido)butyl)-1,4,7-triazacyclononane-1,4,7-triyl)tris(methylene)tris(4-bromopyridine-6,2-diyl)tris(methylphosphinate), [EuL¹³]



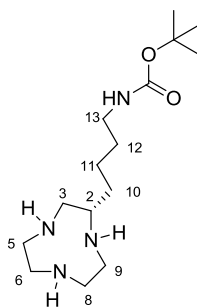
Triethyl 6,6',6''-((*S*)-2-(4-(cyclohexanecarboxamido)butyl)-1,4,7-triazacyclononane-1,4,7-triyl)tris(methylene)tris(4-bromopyridine-6,2-diyl)tris(methylphosphinate), **16** (10.0 mg, 8.8 μ mol) was dissolved in CD_3OD (3 mL) and a solution of NaOH in D_2O (0.1 M, 1 mL) was

added. The mixture was heated to 90 °C under argon and monitored with ^{31}P -NMR [$\delta_{\text{P}}(\text{reactant}) = 38.8$, ($\delta_{\text{P}}(\text{product}) = 25.9$]. After 5 h the solution was cooled to RT and the pH was adjusted to 7 with HCl. $\text{Eu}(\text{AcO})_3\text{H}_2\text{O}$ (3.2 mg, 9.7 μmol) was added and the mixture heated to 65 °C overnight under argon. The solvent was removed under reduced pressure and the product purified by column chromatography (silica, DCM : MeOH : NH_3 9 : 1: 0.1) giving a white solid (3.0 mg, 30 %); δ_{P} (CD_3OD) 43.4, 40.7, 37.5 ; m/z (HRMS^+) 1203.995 [$\text{M} + \text{H}^+$] ($\text{C}_{38}\text{H}_{53}^{79}\text{Br}_3^{153}\text{EuN}_7\text{O}_7\text{P}_3$ requires 1203.995); $R_f = 0.32$ (silica, DCM : MeOH : NH_3 9 : 1: 0.1); $\tau_{\text{MeOH}} = 1.50$ ms; $\lambda_{\text{max}}(\text{MeOH}) = 272$ nm, $\varepsilon = 8$ $\text{mM}^{-1} \text{cm}^{-1}$.



Method B, $t_{\text{R}} = 8.8$ min

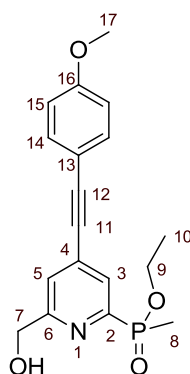
(*S*)-*tert*-Butyl 4-(1,4,7-triazacyclononane-2-yl)butylcarbamate, **17**



The tetrahydrochloride salt of (*S*)-4-(1,4,7-triazacyclononane-2-yl)butan-1-amine, **6a** was converted into the free tetra-amine (66 mg, 0.33 mmol) by anion exchange chromatography using DOWEX 1x2-200 resin (hydroxide form). The free amine was dissolved in MeOH (4 mL) and $\text{CuCl}_2\cdot\text{H}_2\text{O}$ (56 mg, 1.33 mmol) was added, resulting in an intense green mixture. The mixture was stirred at RT under argon for 2 h, after which the solvent was removed and the green solid was dissolved in H_2O (2 mL). A solution of di-*tert*-butyl-dicarbonate (140 mg, 0.66 mmol) in dioxane (2 mL) was added and the solution was stirred at RT. After 3 h another

equivalent of di-*tert*-butyl-dicarbonate (70 mg) was added and the reaction was stirred for 16 h. At this time, LC-MS revealed complete consumption of starting material. The blue solution was treated with H₂S over 5 min and the mixture was centrifuged to remove the dark precipitate. The supernatant was washed with DCM and the pH was adjusted to 11 before extracting repeatedly with DCM. The organic layer was concentrated to give a colourless oil (54 mg, 55 %); δ_{H} (CDCl₃): 6.46 (1H, br, CONH), 3.13 (2H, m, H¹³), 2.89-2.47 (10H, m, H³⁻⁵⁻⁶⁻⁸⁻⁹), 2.79 (1H, m, H²), 2.35 (3H, br, NH), 1.47 (9H, s, CH₃(Boc)), 1.49-1.35 (6H, m, H¹⁰⁻¹¹⁻¹²); δ_{C} (CDCl₃): 156.3 (CO), 79.3 (C(Boc)), 55.2 (C²), 49.9, 46.2, 45.3, 44.3, 40.6 (C³⁻⁵⁻⁶⁻⁸⁻⁹), 40.3(C¹³), 33.9, 30.4, 23.7, (C¹⁰⁻¹¹⁻¹²), 28.6 (CH₃(Boc)); (HRMS⁺) 301.2603 [M + H]⁺ (C₁₅H₃₃N₄O₂ requires 301.2604). Analysis of the enantiomeric purity of this amine by ¹H-NMR using *R*-O-acetyl mandelic acid (CDCl₃, 500 MHz, 295 K) as a chiral solvating agent;¹²⁶ the analysis of the shift of the H² proton at 2.84 ppm, (that resolved into two signals for a sample that was scalemic) confirmed the enantiomeric purity to be > 98 %.

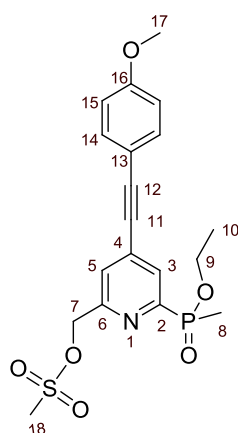
Ethyl(6-(hydroxymethyl)-4-[2-(4-methoxyphenyl)ethynyl]pyridin-2-yl)(methyl)phosphinate, 18



Ethyl (6-(hydroxymethyl)-4-(bromopyridin-2-yl)(methyl)phosphinate, **14** (100 mg, 0.34 mmol) was dissolved in dry THF (2 mL) and the solution was degassed (freeze-thaw cycle) three times. 4-Ethynylanisole (67 mg, 0.51 mmol) and NEt₃ (0.2 mL) were added and the solution degassed once more. [1,1'-Bis(diphenylphosphino)ferrocene]palladium(II) chloride (28 mg, 0.034 mmol) and CuI (13 mg, 0.068 mmol) were added and the solution was degassed a further three times. The solution was stirred at 65 °C under argon for 12 h, solvent was removed under reduced pressure and the crude material purified by column chromatography (silica, DCM : MeOH 0 to 3 %) to give a dark yellow oil (113 mg, 96 %); δ_{H} (CDCl₃) 7.95 (1H, bs, H³), 7.51 (1H, bs, H⁵), 7.42 (2H, d, ³J_{H-H} 9 Hz, H¹⁴), 6.84 (2H, d, ³J_{H-H} 9 Hz, H¹⁵), 4.78 (2H, s, H⁷), 4.10 – 4.04 (1H, m, H⁹), 3.86 – 3.81 (1H, m, H⁹), 3.78 (3H, s,

H¹⁷), 1.73 (3H, d, ²J_{H-P} 15 Hz, H⁸), 1.23 (3H, t, ³J_{H-H} 7 Hz, H¹⁰); δ_C (CDCl₃) 161.2 (d, ³J_{C-P} 18 Hz, C⁶), 160.6 (s, C¹⁶), 153.1 (d, ¹J_{C-P} 156 Hz, C²), 133.6 (s, C¹⁴), 132.9 (d, ²J_{C-P} 12 Hz, C⁴), 127.7 (d, ³J_{C-P} 19 Hz, C³), 124.1 (d, ⁴J_{C-P} 4 Hz, C⁵), 114.2 (s, C¹⁵), 114.0 (s, C¹³), 96.0 (s, C¹²), 85.3 (s, C¹¹), 64.2 (s, C⁷), 61.2 (d, ²J_{C-P} 6 Hz, C⁹), 55.3 (s, C¹⁷), 16.4 (d, ³J_{C-P} 6 Hz, C¹⁰), 13.4 (d, ¹J_{C-P} 104 Hz, C⁸); δ_P (CDCl₃) +38.6; *m/z* (HRMS⁺) 346.1228 [M + H]⁺ (C₁₈H₂₁O₄NP requires 346.1208); *R_f* = 0.20 (silica, DCM : 10 % MeOH).

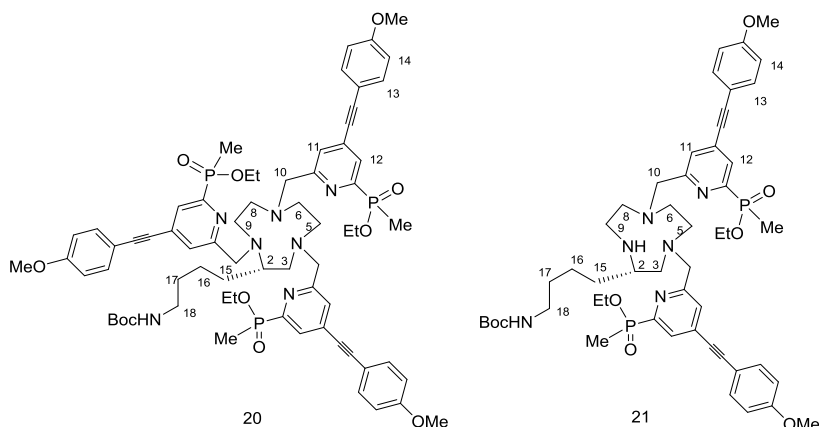
Ethyl(6-(ethyl-methanesulfonate)-4-[2-(4-methoxyphenyl)ethynyl]pyridin-2-yl)(methyl)phosphinate, 19



Ethyl(6-(hydroxymethyl)-4-[2-(4-methoxyphenyl)ethynyl]pyridine-2-yl)(methyl)phosphinate, **18** (128 mg, 0.37 mmol) was dissolved in anhydrous THF (3 mL) and NEt₃ (0.18 mL, 1.3 mmol) was added. The mixture was stirred at 5 °C and methanesulfonyl chloride (43 μL, 0.56 mmol) was added. The reaction was monitored by TLC (silica, DCM : 10 % MeOH, *R_f*(product) = 0.65, *R_f*(reactant) = 0.20) and stopped after 15 min. The solvent was removed under reduced pressure and the residue dissolved in DCM (15 mL) and washed with NaCl solution (saturated, 10 mL). The aqueous layer was re-extracted with DCM (3 × 10 mL) and the organic layers combined, dried over MgSO₄ and the solvent removed under reduced pressure to leave a colourless oil (128 mg, 81 %); δ_H (CDCl₃) 8.11 (1H, dd, ³J_{H-P} 6 Hz, ⁴J_{H-H} 1.5, H³), 7.65 (1H, bs, H⁵), 7.52 (2H, d, ³J_{H-H} 9 Hz, H¹⁴), 6.93 (2H, d, ³J_{H-H} 9 Hz, H¹⁵), 5.39 (2H, s, H⁷), 4.20 – 4.10 (1H, m, H⁹), 3.95 – 3.88 (1H, m, H⁹), 3.86 (3H, s, H¹⁷), 3.16 (3H, s, H¹⁸) 1.80 (3H, d, ²J_{H-P} 15 Hz, H⁸), 1.31 (3H, t, ³J_{H-H} 7 Hz, H¹⁰); *m/z* (HRMS⁺) 446.0804 [M + Na]⁺ (C₁₉H₂₂O₆SNPNa requires 446.0803); *R_f* = 0.65 (silica, DCM : 10 % MeOH).

tert*-Butyl 4-((*S*)-1,4,7-tris((6-(ethoxy(methyl)phosphoryl)-4-((4-methoxyphenyl)ethynyl)pyridin-2-yl)methyl)-1,4,7-triazacyclononan-2-yl)butylcarbamate, **20*

tert*-butyl 4-((*S*)-4,7-bis((6-(ethoxy(methyl)phosphoryl)-4-((4-methoxyphenyl)ethynyl)pyridin-2-yl)methyl)-1,4,7-triazacyclononan-2-yl)butylcarbamate, **21*



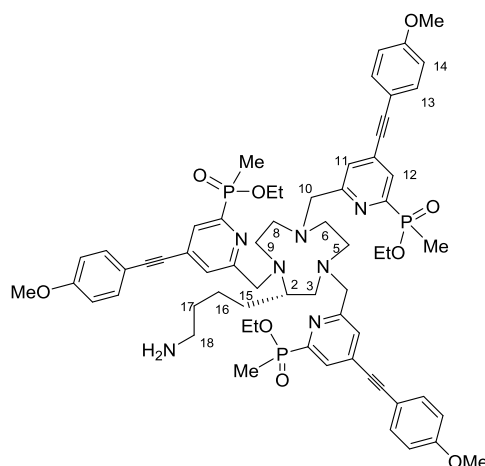
(*S*)-*tert*-Butyl 4-(1,4,7-triazacyclononan-2-yl)butylcarbamate, **16** (21 mg, 0.071 mmol) and ethyl(6-(ethyl-methanesulfonate)-4-[2-(4-methoxyphenyl)ethynyl]pyridin-2-yl)(methyl)phosphinate, **19** (90 mg, 0.21 mmol) were dissolved in anhydrous CH₃CN (4 mL) and K₂CO₃ (30 mg, 0.21 mmol) was added. The mixture was stirred under argon at 60 °C. After 24 h, MS showed the formation of the di-alkylated and tri-alkylated compounds in equal amount. The reaction was cooled and the solution decanted from excess potassium salts. The solvent was removed under reduced pressure and the crude material purified by column chromatography (silica, DCM : MeOH 0 to 20 %) to give *tert*-butyl 4-((*S*)-1,4,7-tris((6-(ethoxy(methyl)phosphoryl)-4-((4-methoxyphenyl)ethynyl)pyridin-2-yl)methyl)-1,4,7-triazacyclononan-2-yl)butylcarbamate as a yellow oil (18 mg, 20 %) and *tert*-butyl 4-((*S*)-4,7-bis((6-(ethoxy(methyl)phosphoryl)-4-((4-methoxyphenyl)ethynyl)pyridin-2-yl)methyl)-1,4,7-triazacyclononan-2-yl)butylcarbamate as a yellow oil (14 mg, 20 %).

tert-Butyl-4-((*S*)-1,4,7-tris((6-(ethoxy(methyl)phosphoryl)-4-((4-methoxyphenyl)ethynyl)pyridin-2-yl)methyl)-1,4,7-triazacyclononan-2-yl)butylcarbamate, **20**: δ_H (CDCl₃) 7.96 (3H, m, H¹²), 7.46 (9H, m H¹¹ and H¹³), 6.88 (6H, m, H¹⁴), 5.04 (1H, br, CONH), 4.11-3.84 (12H, m, P-OCH₂ and H¹⁰), 3.80 (9H, m, OMe), 3.09-2.74 (13H, m, H²⁻³⁻⁵⁻⁶⁻⁸⁻⁹⁻¹⁸), 1.77-1.70 (9H, m, P-Me), 1.39 (9H, s, Boc), 1.42-1.23 (7H, H¹⁵⁻¹⁶⁻¹⁷ and NH), 1.25

(9H, m, CH₃(Et)); δ_P (CDCl₃) +39.2; m/z (HRMS+) 1282.570 [M + H]⁺ (C₆₉H₈₇N₇O₁₁P₃ requires 1282.568); R_f = 0.54 (silica, DCM : 20% MeOH).

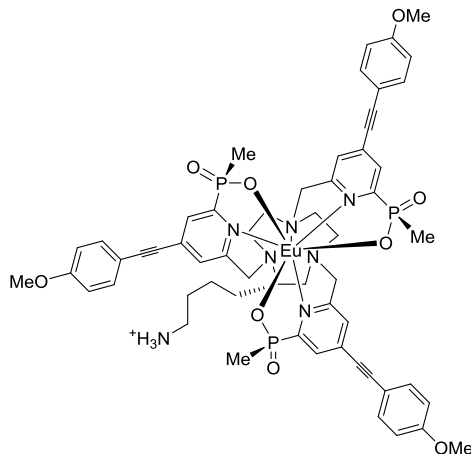
tert-Butyl-4-((*S*)-4,7-bis((6-(ethoxy(methyl)phosphoryl)-4-((4-methoxyphenyl)ethynyl)pyridin-2-yl)methyl)-1,4,7-triazacyclononan-2-yl)butylcarbamate, **21**: δ_H (CDCl₃) 7.87 (2H, m, H¹²), 7.40 (6H, m H¹¹ and H¹³), 6.82 (4H, m, H¹⁴), 5.04 (1H, br, CONH), 4.09-3.98 (8H, m, P-OCH₂ and H¹⁰), 3.75 (6H, m, OMe), 3.08-2.60 (13H, m, H²⁻³⁻⁵⁻⁶⁻⁸⁻⁹⁻¹⁸), 1.82-1.69 (6H, m, P-Me), 1.35 (9H, s, Boc), 1.51-1.20 (7H, H¹⁵⁻¹⁶⁻¹⁷ and NH), 1.22 (6H, m, CH₃(Et)); δ_P (CDCl₃) +39.4; m/z (HRMS+) 955.4622 [M + H]⁺ (C₅₁H₆₉N₆O₈P₂ requires 955.4652); R_f = 0.51 (silica, DCM : 20% MeOH).

Triethyl-6,6',6''-((*S*)-2-(4-aminobutyl)-1,4,7-triazacyclononan-1,4,7-triyl)tris(methylene)tris(4-((4-methoxyphenyl)ethynyl)pyridine-6,2-diyl)tris(methylphosphinate), 20a

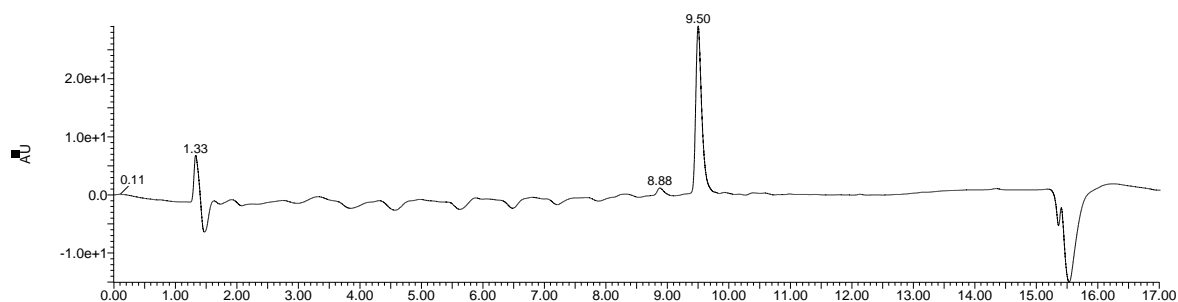


tert-Butyl-4-((*S*)-1,4,7-tris((6-(ethoxy(methyl)phosphoryl)-4-((4-methoxyphenyl)ethynyl)pyridin-2-yl)methyl)-1,4,7-triazacyclononan-2-yl)butylcarbamate, **20** (12.0 mg, 9.4 μ mol) was dissolved in dry DCM (0.8 mL). Argon was bubbled for 10 min after which time TFA (0.2 mL) was added. The solution was stirred for 15 min and the solvent was removed under reduced pressure to give the trifluoroacetate salt as a sticky yellow oil (12.0 mg, quantitative yield); δ_H (CDCl₃) 7.93 (3H, m, H¹²), 7.46 (9H, m H¹¹ and H¹³), 6.88 (6H, m, H¹⁴), 4.15-3.84 (12H, m, P-OCH₂ and H¹⁰), 3.76 (9H, m, OMe), 3.00-2.71 (13H, m, H²⁻³⁻⁵⁻⁶⁻⁸⁻⁹⁻¹⁸), 1.80-1.75 (9H, m, P-Me), 1.42-1.23 (7H, H¹⁵⁻¹⁶⁻¹⁷ and NH), 1.25 (9H, m, CH₃(Et)); δ_P (CDCl₃) +39.7; m/z (HRMS+) 1182.518 [M + H]⁺ (C₆₄H₇₉N₇O₉P₃ requires 1182.515).

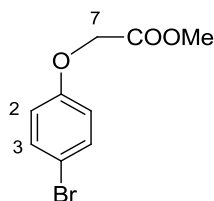
Europium (III) complexes of (*R,R,R*)-6,6',6''-((*S*)-2-(4-aminobutyl)-1,4,7-triazacyclononane-1,4,7-triyl)tris(methylene)tris(4-((4-methoxyphenyl)ethynyl)pyridine-6,2-diyl)tris(methylphosphinate), [EuL¹⁴]⁺



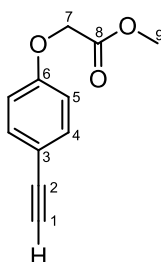
Triethyl 6,6',6''-((*S*)-2-(4-aminobutyl)-1,4,7-triazacyclononane-1,4,7-triyl)tris(methylene)tris(4-((4-methoxyphenyl)ethynyl)pyridine-6,2-diyl)tris(methylphosphinate), **20a** (25.0 mg, 21 μmol) was dissolved in CD_3OD (3 mL) and a solution of NaOH in D_2O (0.1 M, 1 mL) was added. The mixture was heated to 60 $^\circ\text{C}$ under argon and monitored with ^{31}P -NMR [δ_{P} (reactant) = + 39.7, δ_{P} (product) = + 27.8]. After 5 h the solution was cooled to RT and the pH was adjusted to 7 with HCl. $\text{Eu}(\text{AcO})_3\text{H}_2\text{O}$ (7.6 mg, 23 μmol) was added and the mixture heated to 65 $^\circ\text{C}$ overnight under argon. The solvent was removed under reduced pressure and the product purified by purified by HPLC (*Method A*, t_{R} = 9.2 min) giving a white solid (8.0 mg, 30 %); δ_{P} (CD_3OD) 43.5, 40.3, 36.6; m/z (HRMS+) 1246.321 [M]⁺ ($\text{C}_{58}\text{H}_{64}^{153}\text{EuN}_7\text{O}_9\text{P}_3$ requires 1246.318); $\tau_{\text{H}_2\text{O}}$ = 1.00 ms; $\lambda_{\text{max}}(\text{H}_2\text{O})$ = 328 nm; ε = 58 $\text{mM}^{-1} \text{cm}^{-1}$.



Method B, t_{R} = 9.5 min

Methyl 2-(4-bromophenoxy)acetate, 22

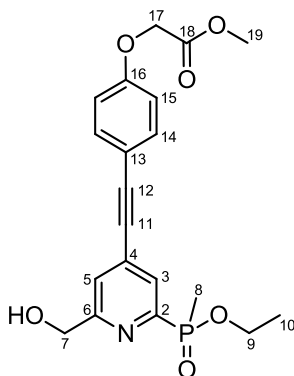
2-(4-Bromophenoxy)acetic acid, **22a** (1.0 g, 4.3 mmol) was dissolved in methanolic HCl (3 M, 3 mL) and stirred at RT for 20 h. The solvent was removed under reduced pressure, the resulting oil was dissolved in DCM (15 mL) and sequentially washed with H₂O, saturated aqueous NaHCO₃ and H₂O, then dried over MgSO₄, filtered and the solvent removed under reduced pressure giving a clear oil (1.0 mg, 95 %); δ_{H} (CDCl₃) 7.31 (2H, d, $^3J_{\text{H-H}}$ 8.5 Hz, H³), 6.78 (2H, d, $^3J_{\text{H-H}}$ 8.5 Hz, H²), 4.55 (2H, s, H⁷), 3.80 (3H, s, Me), NMR data are in good agreement with those previously reported; $^{136}\text{R}_f = 0.65$ (silica, EtOAc : Hex 1 : 1).

Methyl 2-(4-ethynylphenoxy)acetate, 23

Methyl-(4-bromophenoxy)acetate, **22** (1.20 g, 4.89 mmol) was dissolved in anhydrous THF (2 mL) and the solution was degassed (freeze-thaw cycle) three times. Ethynyltrimethylsilane (0.83 mL, 5.87 mmol) and triethylamine (3.40 mL, 24.5 mmol) were added and the solution was degassed (2 freeze-thaw cycles) once more. [1,1-Bis(diphenylphosphino)ferrocene]dichloropalladium(II) (0.41 g, 0.489 mmol) and CuI (93 mg, 0.489 mmol) were added and the resulting brown solution was stirred at 65 °C under argon for 24 h. The solvent was removed under reduced pressure and the resulting brown oil was purified by column chromatography (silica, Hex : DCM 3 : 1 to 1 : 1) to give methyl 2-(4-((trimethylsilyl)ethynyl)phenoxy)acetate as a yellow oil (0.76 g, 60 %); $R_f = 0.47$ (silica, Hex : EtOAc 4 : 1). This material (140 mg, 0.54 mmol) was dissolved in anhydrous THF (2 mL) and triethylamine trihydrofluoride (0.870 mL, 5.35 mmol) was added. The mixture was stirred at 35 °C under argon for 24 h. The solvent was removed under reduced pressure to give a yellow oil which was subjected to column chromatography (silica, Hex : DCM 3 : 1),

giving a colourless oil (89 mg, 87 %); δ_{H} (CDCl_3) 7.43 (2H, d, $^3J_{\text{H-H}}$ 9 Hz, H^4), 6.85 (2H, d, $^3J_{\text{H-H}}$ 9 Hz, H^5), 4.64 (2H, s, H^7), 3.80 (3H, s, H^9), 3.00 (1H, s, H^1); δ_{C} (CDCl_3) 169.1 (s, C^8), 158.2 (s, C^6), 133.8 (s, C^4), 115.6 (s, C^3), 114.7 (s, C^5), 83.4 (s, C^2), 76.3 (s, C^1), 65.3 (s, C^7), 52.5 (s, C^9); MS (ESI) m/z 189 $[\text{M-H}]^-$; $R_f = 0.39$ (silica, Hex : EtOAc 4 : 1).

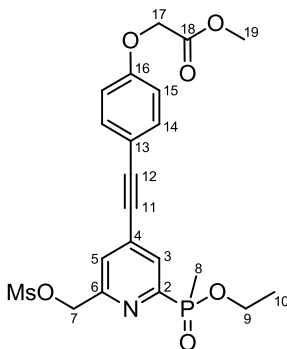
Methyl 2-(4-((2-(ethoxy(methyl)phosphoryl)-6-(hydroxymethyl)pyridin-4-yl)ethynyl)phenoxy)acetate, **24**



To a stirred degassed solution of ethyl (6-(hydroxymethyl)-4-(bromopyridin-2-yl)(methyl)phosphinate, **14** (103 mg, 0.351 mmol) in anhydrous THF (1 mL) was added methyl 2-(4-ethynylphenoxy)acetate, **23** (80 mg, 0.421 mmol) and triethylamine (0.245 mL, 1.75 mmol), and the solution was degassed (freeze-thaw cycle) three times. [1,1-Bis(diphenylphosphino)ferrocene]dichloropalladium(II) (30 mg, 0.035 mmol) and CuI (7 mg, 0.035 mmol) were added and the resulting brown solution was stirred at 65 °C under argon for 18 h. The solvent was removed under reduced pressure and the brown residue was purified by column chromatography (silica, DCM : MeOH 1 to 3%) to afford a yellow oil (122 mg, 87 %); δ_{H} (CDCl_3) 7.98 (1H, br s, H^3), 7.50 (1H, br s, H^5), 7.45 (2H, d, $^3J_{\text{H-H}}$ 9 Hz, H^{14}), 6.88 (2H, d, $^3J_{\text{H-H}}$ 9 Hz, H^{15}), 4.80 (2H, s, H^7), 4.65 (2H, s, H^{17}), 4.09 (1H, m, H^9), 3.99 (1H, br s, CH_2OH), 3.86 (1H, m, H^9), 3.79 (3H, s, H^{19}), 1.76 (3H, d, $^2J_{\text{H-P}}$ 15 Hz, H^8), 1.26 (3H, t, $^3J_{\text{H-H}}$ 7 Hz, H^{10}); δ_{C} (CDCl_3) 168.9 (s, C^{18}), 161.0 (d, $^3J_{\text{C-P}}$ 19 Hz, C^6), 158.8 (s, C^{16}), 153.3 (d, $^1J_{\text{C-P}}$ 155 Hz, C^2), 133.8 (s, C^{14}), 132.9 (d, $^3J_{\text{C-P}}$ 12 Hz, C^4), 128.1 (d, $^2J_{\text{C-P}}$ 22 Hz, C^3), 124.2 (s, C^5), 115.1 (s, C^{13}), 115.0 (s, C^{15}), 95.7 (s, C^{12}), 85.6 (s, C^{11}), 65.2 (s, C^{17}), 64.3 (s, C^7), 61.3 (d, $^2J_{\text{C-P}}$ 5 Hz, C^9), 52.5 (s, C^{19}), 16.5 (d, $^3J_{\text{C-P}}$ 4 Hz, C^{10}), 13.5 (d, $^1J_{\text{C-P}}$ 104 Hz, C^8); δ_{P} (CDCl_3) +39.5; m/z (HRMS+) 426.1063 $[\text{M} + \text{Na}]^+$ ($\text{C}_{20}\text{H}_{22}\text{NO}_6\text{PNa}$ requires 426.1082); $R_f = 0.44$ (silica, DCM : 10% MeOH).

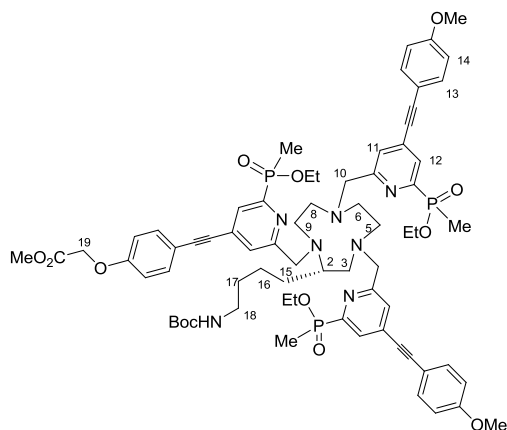
^d HRMS could not be obtained due to low ionisation

Methyl 2-(4-((2-(ethoxy(methyl)phosphoryl)-6-((methylsulfonyloxy)methyl)pyridin-4-yl)ethynyl)phenoxy)acetate, **25**



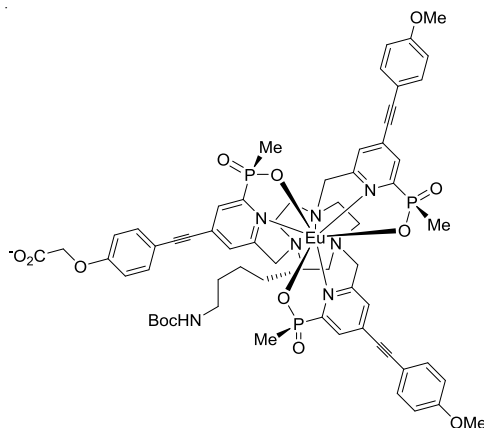
Methyl 2-(4-((2-(ethoxy(methyl)phosphoryl)-6-(hydroxymethyl)pyridin-4-yl)ethynyl)phenoxy)acetate, **24** (122 mg, 0.30 mmol) was dissolved in anhydrous THF (3 mL) and NEt_3 (0.15 mL, 1.0 mmol) was added. The mixture was stirred at 5 °C and methanesulfonyl chloride (35 μL , 0.45 mmol) was added. The reaction was monitored by TLC (silica; DCM : 10 % MeOH, $R_f(\text{product}) = 0.70$, $R_f(\text{reactant}) = 0.44$) and stopped after 15 min. The solvent was removed under reduced pressure and the residue dissolved in DCM (15 mL) and washed with NaCl solution (saturated, 10 mL). The aqueous layer was re-extracted with DCM (3×10 mL) and the organic layers combined, dried over MgSO_4 and the solvent removed under reduced pressure to leave a colourless oil (115 mg, 80 %); δ_{H} (CDCl_3) 8.08 (1H, br s, H^3), 7.63 (1H, br s, H^5), 7.48 (2H, d, $^3J_{\text{H-H}} 9$ Hz, H^{14}), 6.90 (2H, d, $^3J_{\text{H-H}} 9$ Hz, H^{15}), 5.35 (2H, s, H^7), 4.66 (2H, s, H^{17}), 4.12 (1H, m, H^9), 3.87 (1H, m, H^9), 3.80 (3H, s, H^{19}), 3.10 (3H, s, H^{20}), 1.76 (3H, d, $^2J_{\text{H-P}} 15$ Hz, H^8), 1.26 (3H, t, $^3J_{\text{H-H}} 7$ Hz, H^{10}); δ_{P} (CDCl_3) +38.2; m/z (HRMS+) 504.0859 [$\text{M} + \text{Na}$] $^+$ ($\text{C}_{21}\text{H}_{24}\text{NO}_8\text{PSNa}$ requires 504.0858); $R_f = 0.56$ (silica, DCM : 10% MeOH).

Methyl 2-(4-((2-(((S)-2-(4-(*tert*-butoxycarbonylamino)butyl)-4,7-bis((6-(ethoxy(methyl)phosphoryl)-4-((4-methoxyphenyl)ethynyl)pyridin-2-yl)methyl)-1,4,7-triazacyclononan-1-yl)methyl)-6-(ethoxy(methyl)phosphoryl)pyridin-4-yl)ethynyl)phenoxy)acetate, **26**



Methyl 2-(4-((2-(ethoxy(methyl)phosphoryl)-6-((methylsulfonyloxy)methyl)pyridin-4-yl)ethynyl)phenoxy)acetate, **25** (8.0 mg, 17 μ mol) and *tert*-butyl 4-(((S)-4,7-bis((6-(ethoxy(methyl)phosphoryl)-4-((4-methoxyphenyl)ethynyl)pyridin-2-yl)methyl)-1,4,7-triazacyclononan-2-yl)butyl)carbamate, **21** (14.0 mg, 15 μ mol) were dissolved in anhydrous CH_3CN (0.7 mL) and K_2CO_3 (2.0 mg, 17 μ mol) was added. The mixture was stirred under argon at 60 $^\circ\text{C}$ for 24 h, after which time, the reaction was cooled and the solution decanted from excess potassium salts. The solvent was removed under reduced pressure to give a yellow oil that was used in the next step without further purification (19.0 mg, 95 %); δ_{H} (CDCl_3) 7.92 (3H, m, H^{12}), 7.43 (9H, m H^{11} and H^{13}), 6.83 (6H, m, H^{14}), 5.04 (1H, br, CONH), 4.59 (2H, s, H^{19}), 4.06-3.77 (12H, m, P-OCH₂ and H^{10}), 3.75 (9H, m, OMe and CO₂Me), 3.00-2.55 (13H, m, $\text{H}^{2-3-5-6-8-9-18}$), 1.74-1.66 (9H, m, P-Me), 1.33 (9H, s, Boc), 1.35-1.16 (6H, $\text{H}^{15-16-17}$), 1.19 (9H, m, CH₃(Et)); δ_{P} (CDCl_3) +41.1; m/z (HRMS+) 1340.573 [$\text{M} + \text{H}$]⁺ ($\text{C}_{71}\text{H}_{89}\text{N}_7\text{O}_{13}\text{P}_3$ requires 1340.573).

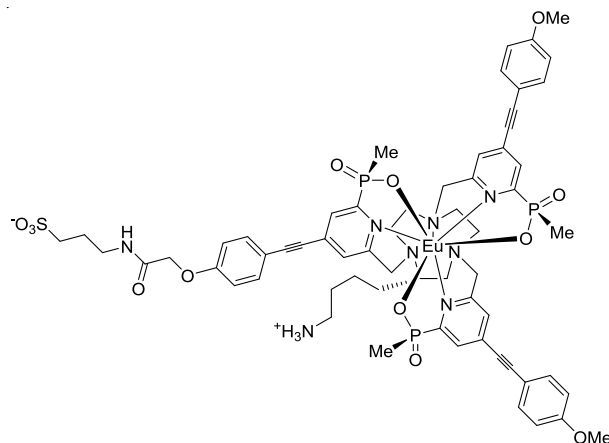
Europium (III) complex of 2-(4-((2-(((S)-2-(4-(*tert*-butoxycarbonylamino)butyl)-4,7-bis((6-((R)-hydroxy(methyl)phosphoryl)-4-((4-methoxyphenyl)ethynyl)pyridin-2-yl)methyl)-1,4,7-triazacyclononan-1-yl)methyl)-6-((R)-hydroxy(methyl)phosphoryl)pyridin-4-yl)ethynyl)phenoxy)acetate, **27**



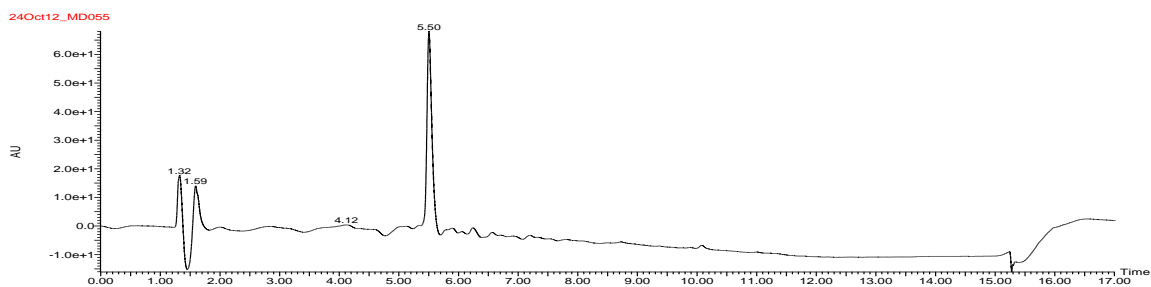
Methyl 2-(4-((2-(((S)-2-(4-(*tert*-butoxycarbonylamino)butyl)-4,7-bis((6-ethoxy(methyl)phosphoryl)-4-((4-methoxyphenyl)ethynyl)pyridin-2-yl)methyl)-1,4,7-triazacyclononan-1-yl)methyl)-6-ethoxy(methyl)phosphoryl)pyridin-4-yl)ethynyl)phenoxy)acetate, **26** (7.0 mg, 5.2 μmol) was dissolved in CD_3OD (1.5 mL) and a solution of NaOH in D_2O (0.1 M, 0.5 mL) was added. The mixture was heated to 60 $^\circ\text{C}$ under argon and monitored using ^{31}P -NMR [δ_{P} (reactant) = + 39.7, (δ_{P} (product) = + 27.8]. After 16 h the solution was cooled to RT and the pH was adjusted to 7 with HCl. $\text{Eu}(\text{AcO})_3\text{H}_2\text{O}$ (1.8 mg, 5.7 μmol) was added and the mixture heated to 65 $^\circ\text{C}$ overnight under argon. The solvent was removed under reduced pressure and the product purified by HPLC (*Method D*, t_{R} = 8.6 min) giving the ammonium salt as white solid (2.2 mg, 30 %); m/z (ESI) 1390.4 [$\text{MH} + \text{H}$] $^{+}$; e $\tau_{\text{H}_2\text{O}}$ = 1.06 ms; $\lambda_{\text{max}}(\text{H}_2\text{O})$ = 328 nm; ε = 58 $\text{mM}^{-1} \text{cm}^{-1}$.

^e HRMS could not be obtained due to low ionisation

Europium (III) complex of 3-(2-(4-((2-(((S)-2-(4-aminobutyl)-4,7-bis((6-((R)-hydroxy(methyl)phosphoryl)-4-((4-methoxyphenyl)ethynyl)pyridin-2-yl)methyl)-1,4,7-triazacyclononan-1-yl)methyl)-6-((R)-hydroxy(methyl)phosphoryl)pyridin-4-yl)ethynyl)phenoxy)acetamido)propane-1-sulfonate, [EuL¹⁵]

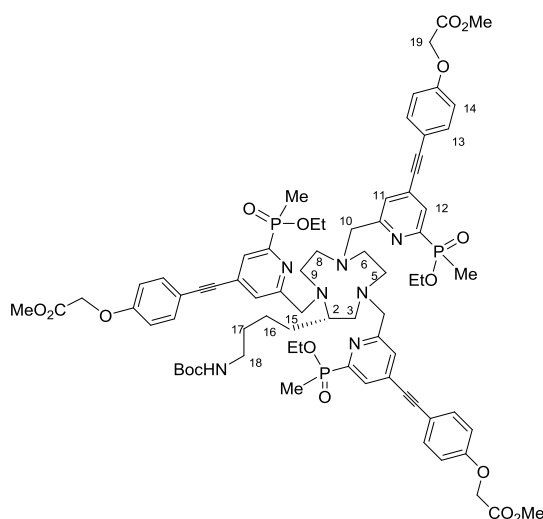


The europium(III) complex of 2-(4-((2-(((S)-2-(4-(*tert*-butoxycarbonylamino)butyl)-4,7-bis((6-(hydroxy(methyl)phosphoryl)-4-((4-methoxyphenyl)ethynyl)pyridin-2-yl)methyl)-1,4,7-triazacyclononan-1-yl)methyl)-6-((hydroxy(methyl)phosphoryl)pyridin-4-yl)ethynyl)phenoxy)acetate, **27** (0.35 mg, 0.25 μmol) was dissolved in dry DMF (50 μL) and 10 μL of a solution of PyBOP (2.00 mg, 3.75 μmol) in dry DMF (100 μL) was added. A solution of DIPEA (2.2 μL , 13 μmol) in DMF (100 μL) was prepared and 5 μL of that solution was added to the reaction. The mixture was stirred for 5 min under argon after which time 10 μL of a solution of homotaurine (0.50 mg, 3.75 μmol) in H₂O (100 μL) was added. After 16 h, the solvent was removed under reduced pressure giving a white solid (quantitative conversion by ESI-MS, m/z 1511 [M]⁻). The white solid was dissolved in dry DCM (95 μL) under argon at 4 °C and TFA (5 μL) was added. The mixture was stirred for 20 min after which time the solvent was removed under reduced pressure. The product was purified by HPLC (*Method E*, t_{R} = 8.5 min) giving a white solid (0.30 mg, 85 %); m/z (HRMS-) 1409.311 [M - H]⁻ (C₆₂H₆₉O₁₃N₈¹⁵¹EuP₃S requires 1409.312); $\tau_{\text{H}_2\text{O}}$ = 1.08 ms; $\lambda_{\text{max(H}_2\text{O)}}$ = 328 nm; ϵ = 58 mM⁻¹ cm⁻¹.



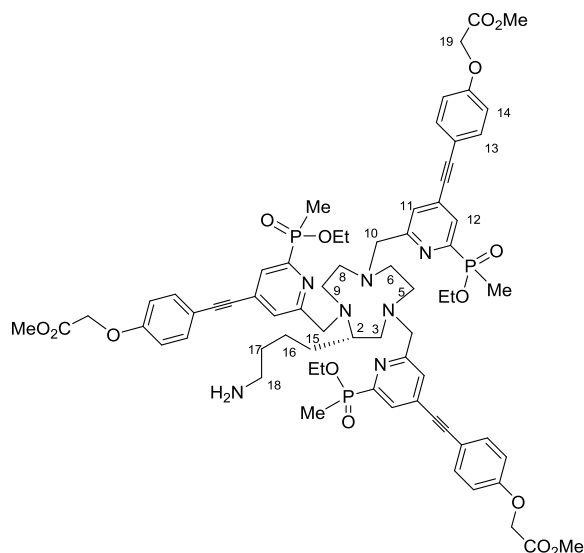
Method B, $t_R = 5.5$ min

Trimethyl 2,2',2''-(4,4',4''-6,6',6''-((*S*)-2-(4-(*tert*-butoxycarbonylamino)butyl)-1,4,7-triazacyclononane-1,4,7-triyl)tris(methylene)tris(2-(ethoxy(methyl)phosphoryl)pyridine-6,4-diyl)tris(ethyne-2,1-diyl)tris(benzene-4,1-diyl)tris(oxy))triacetate, **28**



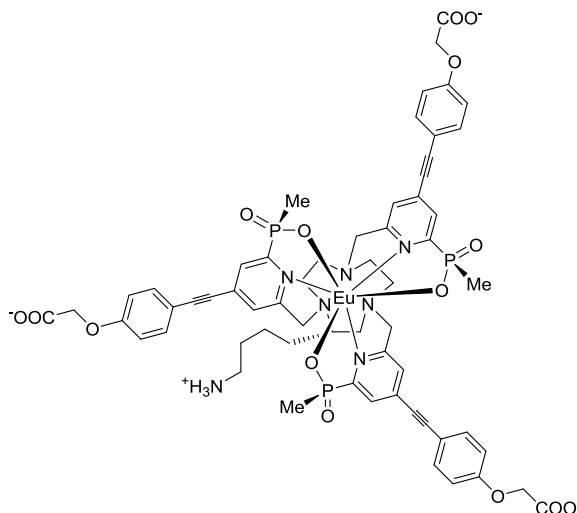
(*S*)-*tert*-Butyl 4-(1,4,7-triazacyclononan-2-yl)butylcarbamate, **17** (23 mg, 0.075 mmol) and methyl 2-(4-((2-(ethoxy(methyl)phosphoryl)-6-((methylsulfonyloxy)methyl)pyridin-4-yl)ethynyl)phenoxy)acetate, **25** (105 mg, 0.22 mmol), were dissolved in anhydrous CH_3CN (4 mL) and K_2CO_3 (32 mg, 0.23 mmol) was added. The mixture was stirred under argon at 60 °C for 18 h. The reaction was cooled and the solution decanted from excess potassium salts. The solvent was removed under reduced pressure and the crude material purified by column chromatography (silica, DCM : MeOH 0 to 20 %) to give a yellow oil (45 mg, 41 %): δ_{H} (CDCl_3) 7.99 (3H, m, H^{12}), 7.49 (9H, m H^{11} and H^{13}), 6.90 (6H, m, H^{14}), 5.10 (1H, br, CONH), 4.67 (6H, s, H^{19}), 4.12-3.86 (12H, m, P-OCH₂ and H^{10}), 3.82 (9H, m, CO₂Me), 3.12-2.90 (13H, m, $\text{H}^{2-3-5-6-8-9-18}$), 1.85-1.70 (9H, m, P-Me), 1.41 (9H, s, Boc), 1.45-1.28 (6H, $\text{H}^{15-16-17}$), 1.27 (9H, m, CH₃(Et)); δ_{P} (CDCl_3) +40.4; m/z (HRMS⁺) 728.7949 [$\text{M} + 2\text{H}$]²⁺ ($\text{C}_{75}\text{H}_{94}\text{N}_7\text{O}_{17}\text{P}_3$ requires 728.7960); $R_f = 0.50$ (silica; DCM : 20% MeOH).

Trimethyl 2,2',2''-(4,4',4''-(6,6',6''-((*S*)-2-(4-aminobutyl)-1,4,7-triazacyclononane-1,4,7-triyl)tris(methylene)tris(2-(ethoxy(methyl)phosphoryl)pyridine-6,4-diyl))tris(ethyne-2,1-diyl)tris(benzene-4,1-diyl))tris(oxy)triacetate, **28a**



Trimethyl 2,2',2''-(4,4',4''-6,6',6''-((*S*)-2-(4-(*tert*-butoxycarbonylamino)butyl)-1,4,7-triazacyclononane-1,4,7-triyl)tris(methylene)tris(2-(ethoxy(methyl)phosphoryl)pyridine-6,4-diyl)tris(ethyne-2,1-diyl)tris(benzene-4,1-diyl)tris(oxy))triacetate, **28** (30 mg, 20 μmol), was dissolved in dry DCM (1.8 mL). Argon was bubbled for 10 min after which time TFA (0.2 mL) was added at 4 $^{\circ}\text{C}$. The solution was allowed to warm up to RT and stirred for 15 min. The solvent was removed under reduced pressure to give the trifluoroacetate salt as a yellow oil (27 mg, quantitative yield); δ_{H} (CDCl_3) 7.91 (3H, m, H^{12}), 7.51 (9H, m H^{11} and H^{13}), 6.92 (6H, m, H^{14}), 4.67 (6H, s, H^{19}), 4.16-3.97 (12H, m, P-OCH₂ and H^{10}), 3.81 (9H, m, CO₂Me), 3.12-2.90 (13H, m, $\text{H}^{2-3-5-6-8-9-18}$), 1.89-1.75 (9H, m, P-Me), 1.45-1.32 (8H, $\text{H}^{15-16-17}$ and NH₂), 1.29 (9H, m, CH₃(Et)); δ_{P} (CDCl_3) +41.2; m/z (HRMS⁺) 1356.533 [$\text{M} + \text{H}$]⁺ (C₇₀H₈₅O₁₅N₇P₃ requires 1356.531).

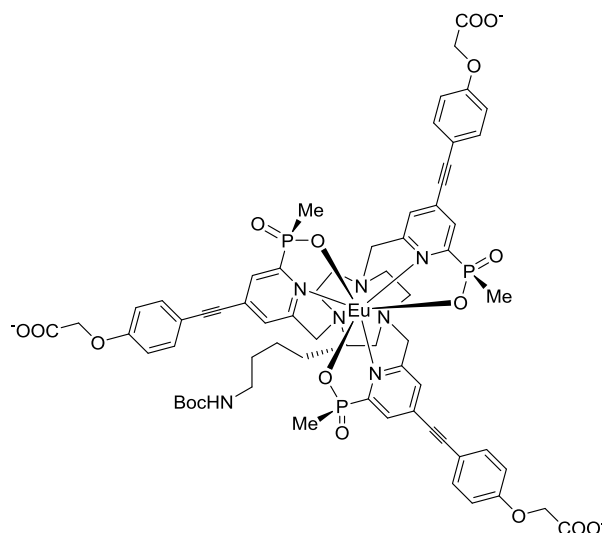
Eu(III) complex of (*R,R,R*)-6,6',6''-((*S*)-2-(4-aminobutyl)-1,4,7-triazacyclononane-1,4,7-triyl)tris(methylene)tris(4-((4-(carboxymethoxy)phenyl)ethynyl)pyridine-6,2-diyl)tris(methylphosphinate), [EuL¹⁶]²⁻



Trimethyl 2,2',2''-(4,4',4''-6,6',6''-((*S*)-2-(4-aminobutyl)-1,4,7-triazacyclononane-1,4,7-triyl)tris(methylene)tris(2-((ethoxy(methyl)phosphoryl)pyridine-6,4-diyl)tris(ethyne-2,1-diyl)tris(benzene-4,1-diyl)tris(oxy)triacetate, **28a** (27 mg, 20 μmol) was dissolved in CD_3OD (3 mL) and a solution of NaOH in D_2O (0.1 M, 1.5 mL) was added. The mixture was heated to 60 $^\circ\text{C}$ under argon and monitored with ^{31}P -NMR [δ_{P} (reactant) = + 41.2, (δ_{P} (product) = + 25.6]. After 5 h the solution was cooled to RT and the pH was adjusted to 7 with HCl. $\text{Eu}(\text{AcO})_3\text{H}_2\text{O}$ (7 mg, 21 μmol) was added and the mixture heated to 65 $^\circ\text{C}$ overnight under argon. The solvent was removed under reduced pressure and the product purified by HPLC (*Method F*, t_{R} = 9.6 min) giving a white solid (11 mg, 40 %); m/z (ESI) 690.6 [$\text{MH}_2 + 2\text{H}$]²⁺,^f $\tau_{\text{H}_2\text{O}}$ = 1.05 ms; $\lambda_{\text{max}}(\text{H}_2\text{O})$ = 330 nm; ε = 57 $\text{mM}^{-1} \text{cm}^{-1}$.

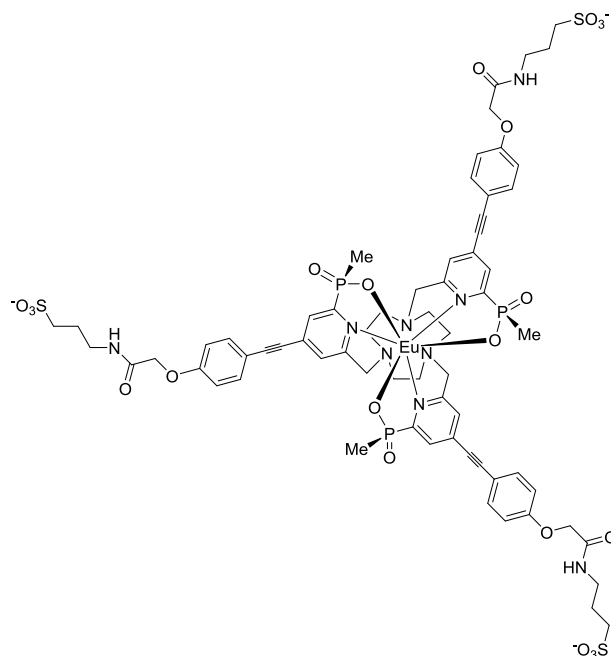
^f HRMS could not be obtained due to low ionisation

Eu(III) complex of (*R,R,R*)-6,6',6''-((*S*)-2-(4-(*tert*-butoxycarbonylamino)butyl)-1,4,7-triazacyclononane-1,4,7-triyl)tris(methylene)tris(4-((4-(carboxymethoxy)phenyl)ethynyl)pyridine-6,2-diyl)tris(methylphosphinate), **29**



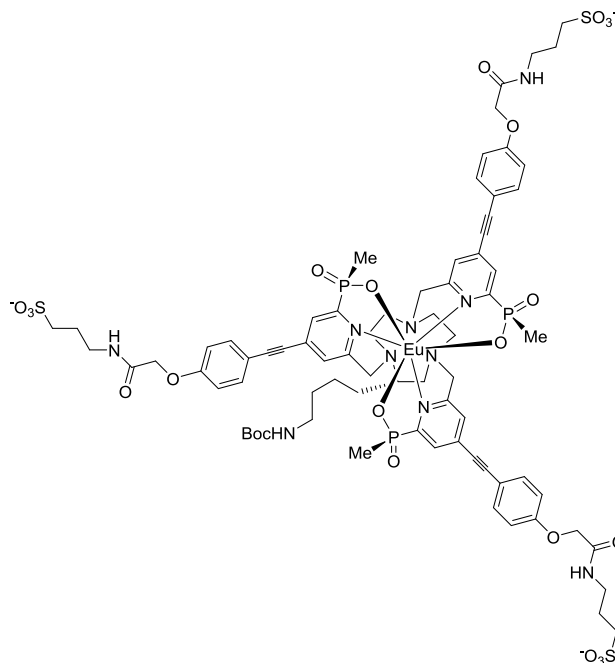
Trimethyl 2,2',2''-(4,4',4''-6,6',6''-((*S*)-2-(4-(*tert*-butoxycarbonylamino)butyl)-1,4,7-triazacyclononane-1,4,7-triyl)tris(methylene)tris(2-(ethoxy(methyl)phosphoryl)pyridine-6,4-diyl)tris(ethyne-2,1-diyl)tris(benzene-4,1-diyl)tris(oxy))triacetate, **28** (10.0 mg, 6.8 μmol) was dissolved in CD_3OD (2 mL) and a solution of NaOH in D_2O (0.1 M, 1 mL) was added. The mixture was heated to 60 $^\circ\text{C}$ under argon and monitored with ^{31}P -NMR [δ_{P} (reactant) = + 40.4, (δ_{P} (product) = + 26.7]. After 5 h the solution was cooled to RT and the pH was adjusted to 7 with HCl. $\text{Eu}(\text{AcO})_3\text{H}_2\text{O}$ (1.8 mg, 5.7 μmol) was added and the mixture heated to 65 $^\circ\text{C}$ overnight under argon. The solvent was removed under reduced pressure and the product purified by HPLC (*Method F*, t_{R} = 11.8 min) giving a white solid (6.0 mg, 59 %); m/z (ESI) 740.2 [$\text{MH}_3 + 2\text{H}$] $^{2+}$; $\tau_{\text{H}_2\text{O}}$ = 1.05 ms; $\lambda_{\text{max}}(\text{H}_2\text{O})$ = 330 nm; ε = 57 $\text{mM}^{-1} \text{cm}^{-1}$.

Eu(III) complex of 6,6',6''-(1,4,7-triazacyclononane-1,4,7-triyl)tris(methylene)tris(4-((4-(2-oxo-2-(3-sulfopropylamino)ethoxy)phenyl)ethynyl)pyridine-6,2-diyl)tris(methylphosphinate), [EuL^{17a}]³⁻



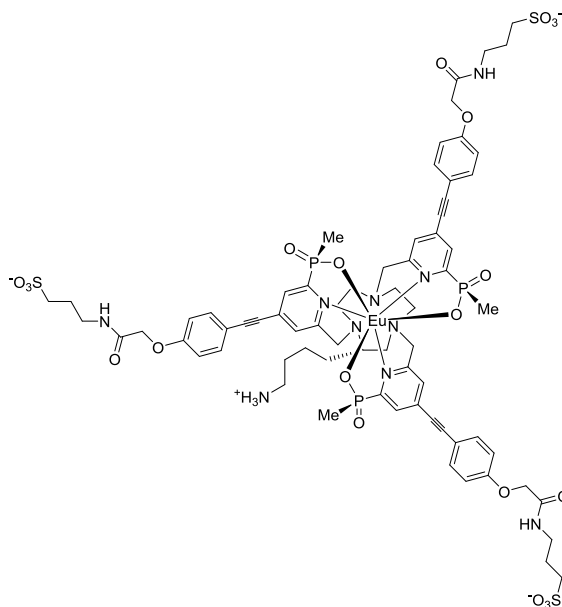
The Eu(III) complex of 6,6',6''-(1,4,7-triazacyclononane-1,4,7-triyl)tris(methylene)tris(4-((4-(carboxymethoxy)phenyl)ethynyl)pyridine-6,2-diyl)tris(methylphosphinate), [EuL⁴]³⁻ (0.5 mg, 0.38 μmol) and homotaurine (0.32 mg, 2.3 μmol) were dissolved in a mixture of DMSO (0.2 mL) and H₂O (20 μL). HATU (1.2 mg, 2.3 μmol) and DIPEA (0.7 μL , 3.8 μmol) were added to the reaction and the mixture was stirred for 24 h under argon after which time LC-MS showed complete conversion. The product was purified by HPLC (*Method K*, $t_{\text{R}} = 13.0$ min) giving the triethylammonium salt as a white solid (0.4 mg, 67 %); m/z (HRMS-) 834.6254 [MH]²⁻ (C₆₆H₇₃¹⁵³EuN₉O₂₁P₃S₃ requires 834.6257); $\tau_{\text{H}_2\text{O}} = 1.01$ ms; $\lambda_{\text{max}}(\text{H}_2\text{O}) = 328$ nm; $\varepsilon = 57$ mM⁻¹ cm⁻¹.

Eu(III) complex of (*R,R,R*)-6,6',6''-((*S*)-2-(4-(*tert*-butoxycarbonylamino)butyl)-1,4,7-triazacyclononane-1,4,7-triyl)tris(methylene)tris(4-((4-(2-oxo-2-(3-sulfopropylamino)ethoxy)phenyl)ethynyl)pyridine-6,2-diyl)tris(methylphosphinate), 30

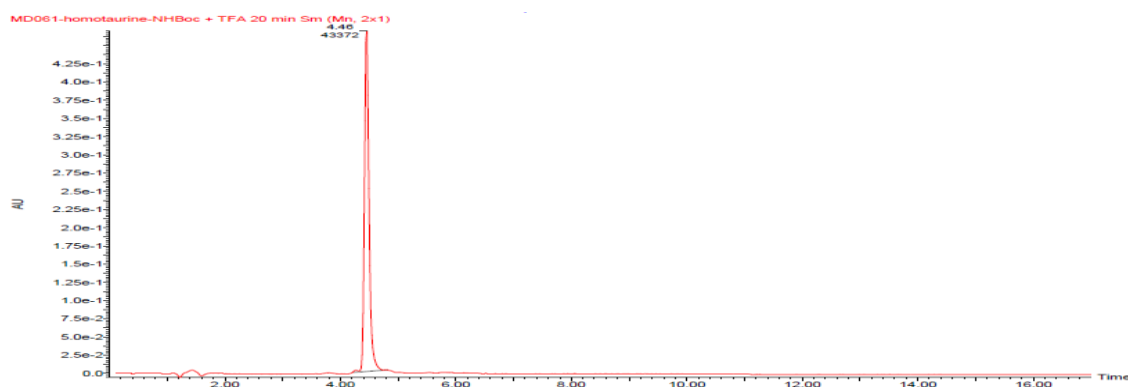


The Eu(III) complex of (*R,R,R*)-6,6',6''-((*S*)-2-(4-(*tert*-butoxycarbonylamino)butyl)-1,4,7-triazacyclononane-1,4,7-triyl)tris(methylene)tris(4-((4-(carboxymethoxy)phenyl)ethynyl)pyridine-6,2-diyl)tris(methylphosphinate), **29** (7.1 mg, 4.8 μmol) and homotaurine (4.0 mg, 28.8 μmol) were dissolved in dry DMSO (1 mL). HATU (5.4 mg, 14.4 μmol) and DIPEA (9 μL , 48 μmol) were added to the reaction and the mixture was stirred for 1 h under argon after which time LC-MS showed complete conversion. The product was purified by HPLC (*Method G*, $t_{\text{R}} = 14.9$ min) giving the triethylammonium salt as a white solid (6.6 mg, 70 %); m/z (HRMS+) 922.2045 [$\text{MH}_3 + 2\text{H}$] $^{2+}$ ($\text{C}_{75}\text{H}_{94}^{153}\text{EuN}_{10}\text{O}_{23}\text{P}_3\text{S}_3$ requires 922.2039). $\tau_{\text{H}_2\text{O}} = 1.01$ ms; $\lambda_{\text{max}}(\text{H}_2\text{O}) = 328$ nm; $\varepsilon = 57$ mM^{-1} cm^{-1} .

Eu(III) complex of (*R,R,R*)-6,6',6''-((*S*)-2-(4-aminobutyl)-1,4,7-triazacyclononane-1,4,7-triyl)tris(methylene)tris(4-((4-(2-oxo-2-(3-sulfopropylamino)ethoxy)phenyl)ethynyl)pyridine-6,2-diyl)tris(methylphosphinate), [EuL¹⁷]²⁻

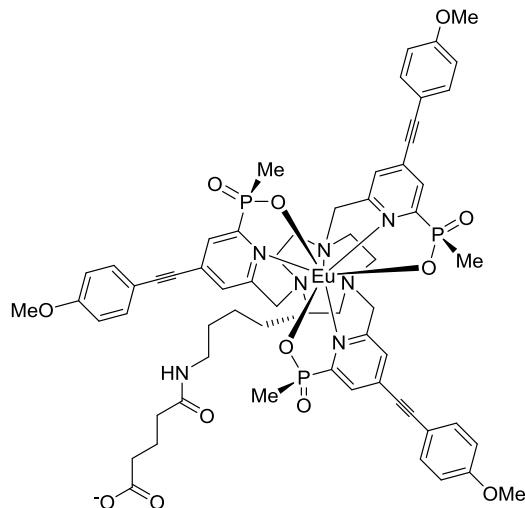


The Eu(III) complex of (*R,R,R*)-6,6',6''-((*S*)-2-(4-(tert-butoxycarbonylamino)butyl)-1,4,7-triazacyclononane-1,4,7-triyl)tris(methylene)tris(4-((4-(2-oxo-2-(3-sulfopropylamino)ethoxy)phenyl)ethynyl)pyridine-6,2-diyl)tris(methylphosphinate), **30** (6.6 mg, 3.6 μmol) was dissolved in dry DCM (0.8 mL). TFA (0.2 mL) was added and the mixture was stirred at RT for 20 min. The solvent was removed under reduced pressure to give the triethylammonium salt as a white solid (6.4 mg, quantitative yield); m/z (HRMS⁺) 872.1781 [$\text{MH}_2 + 2\text{H}$]²⁺ ($\text{C}_{70}\text{H}_{86}^{153}\text{EuN}_{10}\text{O}_{21}\text{P}_3\text{S}_3$ requires 872.1776); $\tau_{\text{H}_2\text{O}} = 1.00$ ms; $\lambda_{\text{max}}(\text{H}_2\text{O}) = 328$ nm; $\varepsilon = 57 \text{ mM}^{-1} \text{ cm}^{-1}$.



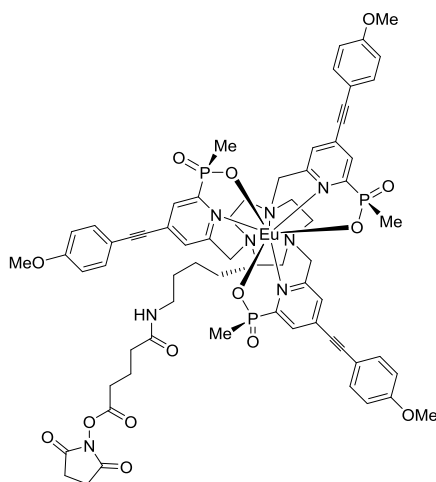
Method G, $t_{\text{R}} = 4.5$ min

Eu(III) complex of (*R,R,R*)-6,6',6''-((*S*)-2-(4-(4-carboxybutanamido)butyl)-1,4,7-triazacyclononane-1,4,7-triyl)tris(methylene)tris(4-((4-methoxyphenyl)ethynyl)pyridine-6,2-diyl)tris(methylphosphinate), [EuL¹⁴]-glu⁻



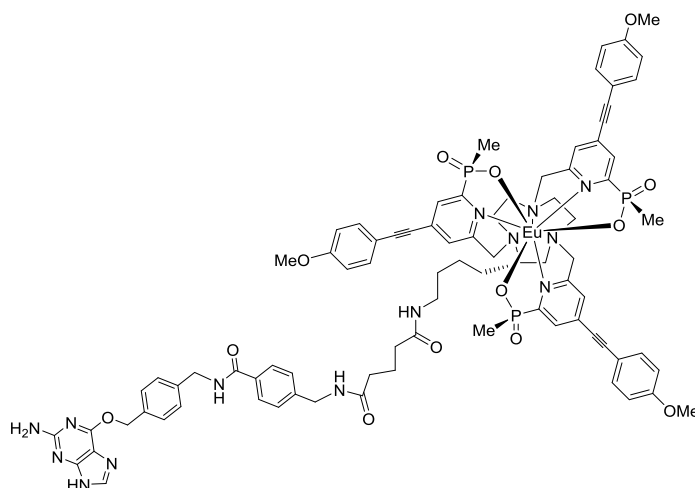
The Eu(III) complex of (*R,R,R*)-6,6',6''-((*S*)-2-(4-aminobutyl)-1,4,7-triazacyclononane-1,4,7-triyl)tris(methylene)tris(4-((4-methoxyphenyl)ethynyl)pyridine-6,2-diyl)tris(methylphosphinate), [EuL¹⁴]⁺ (0.80 mg, 0.65 μmol), was dissolved in dry DMF (400 μL). Glutaric anhydride (0.10 mg, 0.65 μmol) and DIPEA (4 μL) were added and the reaction was stirred at RT for 1 h. The product was purified by HPLC (*Method H*, $t_{\text{R}} = 14.2$ min) giving a white solid (0.54 mg, 61 %); m/z (ESI) 1361.9 [MH + H]⁺.

Eu(III) complex of (*R,R,R*)-6,6',6''-((*S*)-2-(4-(5-(2,5-dioxopyrrolidin-1-yloxy)-5-oxopentanamido)butyl)-1,4,7-triazacyclononane-1,4,7-triyl)tris(methylene)tris(4-((4-methoxyphenyl)ethynyl)pyridine-6,2-diyl)tris(methylphosphinate), [EuL¹⁴]-glu-NHS



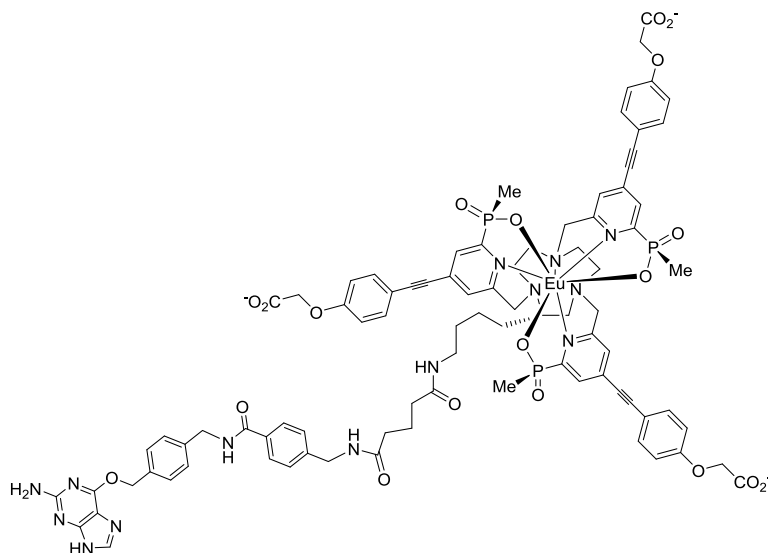
The Eu(III) complex of (*R,R,R*)-6,6',6''-((*S*)-2-(4-(4-carboxybutanamido)butyl)-1,4,7-triazacyclononane-1,4,7-triyl)tris(methylene)tris(4-((4-methoxyphenyl)ethynyl)pyridine-6,2-diyl)tris(methylphosphinate), [**EuL¹⁴**]-**glu⁻** (0.54 mg, 0.40 μmol) was dissolved in dry DMF (400 μL). TSTU (0.15 mg, 0.48 μmol) and DIPEA (4 μL) were added and the reaction was stirred at RT for 15 min. The product was purified by HPLC (*Method H*, t_{R} = 15.2 min) giving a white solid (0.38 mg, 65 %); m/z (ESI) 1458.3 [$\text{M} + \text{H}$]⁺.

Eu(III) complex of (*R,R,R*)-6,6',6''-((*S*)-2-(4-(5-(4-(4-((2-Amino-9H-purin-6-yloxy)methyl)benzylcarbamoyl)benzylamino)-5-oxopentanamido)butyl)-1,4,7-triazacyclononane-1,4,7-triyl)tris(methylene)tris(4-((4-methoxyphenyl)ethynyl)pyridine-6,2-diyl)tris(methylphosphinate), [EuL¹⁴**]-**glu-MB-BG****



To a solution of the Eu(III) complex of (*R,R,R*)-6,6',6''-((*S*)-2-(4-(5-(2,5-dioxopyrrolidin-1-yloxy)-5-oxopentanamido)butyl)-1,4,7-triazacyclononane-1,4,7-triyl)tris(methylene)tris(4-((4-methoxyphenyl)ethynyl)pyridine-6,2-diyl)tris(methylphosphinate), [**EuL¹⁴**]-**glu-NHS** (0.20 mg, 140 nmol) in dry DMSO (100 μL) was added **BG-MB-NH₂** (0.26 mg, 500 nmol) and DIPEA (1 μL). The mixture was stirred at room temperature for 1 h. After this period, the reaction was completed. The mixture was purified by preparative HPLC (*Method H*, t_{R} = 11.9 min) to give a white solid (50 nmol, 37 %). m/z (HRMS⁺) 874.2626 [$\text{M} + 2\text{H}$]²⁺ ($\text{C}_{84}\text{H}_{90}^{153}\text{EuN}_{14}\text{O}_{13}\text{P}_3$ requires 874.2618).

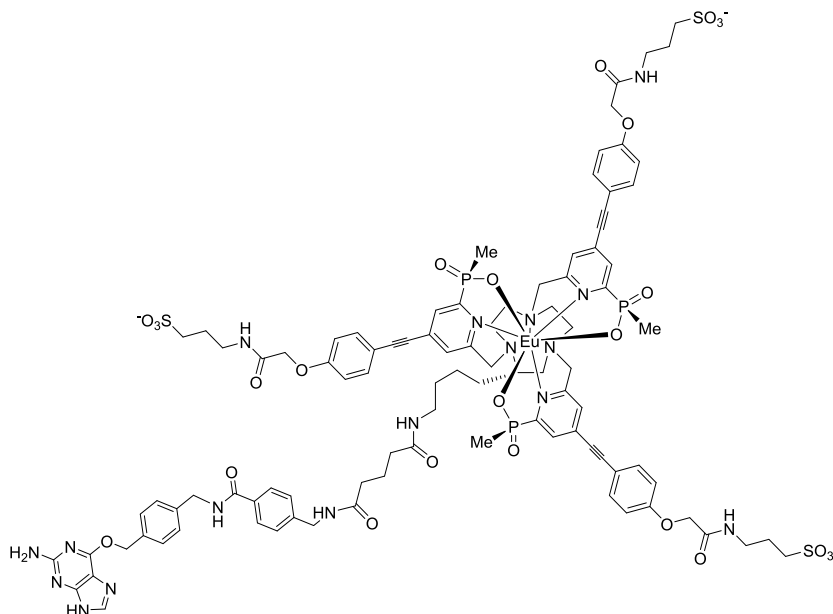
Eu(III) complex of (*R,R,R*)-6,6',6''-((*S*)-2-(4-(5-(4-(4-((2-Amino-9H-purin-6-yloxy)methyl)benzylcarbonyl)benzylamino)-5-oxopentanamido)butyl)-1,4,7-triazacyclononane-1,4,7-triyl)tris(methylene)tris(4-((4-(carboxymethoxy)phenyl)ethynyl)pyridine-6,2-diyl)tris(methylphosphinate), [EuL¹⁶]-glu-MB-BG



The Eu(III) complex of (*R,R,R*)-6,6',6''-((*S*)-2-(4-aminobutyl)-1,4,7-triazacyclononane-1,4,7-triyl)tris(methylene)tris(4-((4-(carboxymethoxy)phenyl)ethynyl)pyridine-6,2-diyl)tris(methylphosphinate), [EuL¹⁶]²⁻ (0.27 mg, 0.20 μmol) and BG-MB-glu-NHS (0.12 mg, 0.20 μmol) were dissolved in DMSO (0.7 mL) and DIPEA (2 μL) was added. The reaction was stirred at RT for 1 h, after which time, more BG-MB-glu-NHS (0.30 mg, 0.50 μmol) was added. After 1 h the same addition BG-MB-glu-NHS (0.30 mg, 0.50 μmol) was repeated and the reaction was stirred for 1 h after which time LC-MS showed complete conversion. The product was purified by HPLC (*Method G*, $t_{\text{R}} = 9.3$ min) giving a white solid (0.30 mg, 80 %); m/z (ESI) 940.4 [MH₃ + 2H]²⁺.^g

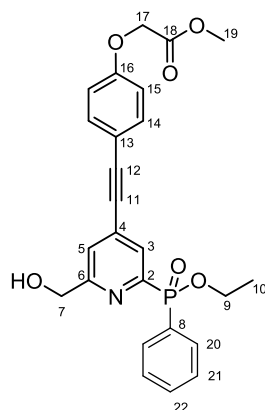
^g HRMS could not be obtained due to low ionisation

Eu(III) complex of (*R,R,R*)-6,6',6''-((*S*)-2-(4-(5-(4-(4-((2-Amino-9H-purin-6-yloxy)methyl)benzylcarbamoylethyl)amino)-5-oxopentanamido)butyl)-1,4,7-triazacyclononane-1,4,7-triyl)tris(methylene)tris(4-((4-(2-oxo-2-(3-sulfopropylamino)ethoxy)phenyl)ethynyl)pyridine-6,2-diyl)tris(methylphosphinate), [EuL¹⁷]-glu-MB-BG



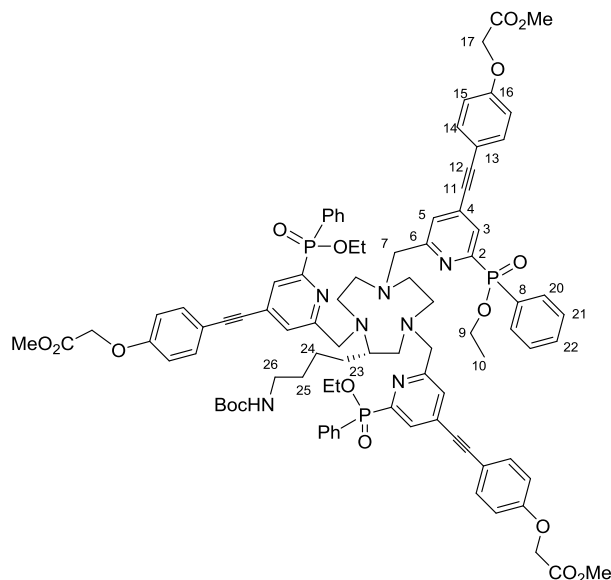
The Eu(III) complex of (*R,R,R*)-6,6',6''-((*S*)-2-(4-aminobutyl)-1,4,7-triazacyclononane-1,4,7-triyl)tris(methylene)tris(4-((4-(2-oxo-2-(3-sulfopropylamino)ethoxy)phenyl)ethynyl)pyridine-6,2-diyl)tris(methylphosphinate), [EuL¹⁷]²⁻ (0.90 mg, 0.52 μmol) and BG-MB-glu-NHS (0.30 mg, 0.50 μmol) were dissolved in phosphate buffer (0.05 M, pH = 8, 0.7 mL) and DMSO (0.3 mL). The reaction was stirred overnight after which time LC-MS showed 85 % conversion. The product was purified by HPLC (*Method H*, $t_R = 7.5$ min) giving a white solid (0.99 mg, 85 %); m/z (HRMS+) 748.1867 [MH₃ + 3H]³⁺ (C₉₆H₁₁₂¹⁵³EuN₁₇O₂₅P₃S₃ requires 748.1866).

Methyl 2-(4-((2-(ethoxy(phenyl)phosphoryl)-6-(hydroxymethyl)pyridin-4-yl)ethynyl)phenoxy)acetate, **32**



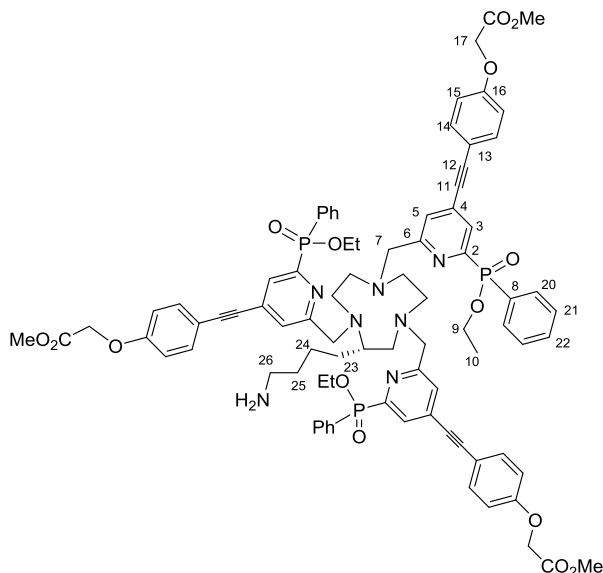
To a stirred degassed solution of ethyl (6-(hydroxymethyl)-4-(bromopyridin-2-yl)(phenyl)phosphinate, **31** (234 mg, 0.650 mmol) in anhydrous THF (2.5 mL) was added methyl 2-(4-ethynylphenoxy)acetate, **23** (185 mg, 0.980 mmol) and triethylamine (1.5 mL), and the solution was degassed (freeze-thaw cycle) three times. [1,1-Bis(diphenylphosphino)ferrocene]dichloropalladium(II) (62 mg, 0.065 mmol) and CuI (10 mg, 0.065 mmol) were added and the resulting brown solution was stirred at 65 °C under argon for 18 h. The solvent was removed under reduced pressure and the brown residue was purified by column chromatography (silica, DCM : MeOH 1 to 2%) to afford a yellow oil (226 mg, 75 %); δ_{H} (CDCl₃) 8.06 (1H, d, $^3J_{\text{H-P}}$ 6 Hz, H³), 7.95 (2H, dd, $^3J_{\text{H-P}}$ 12 Hz, $^3J_{\text{H-H}}$ 7.5 Hz, H²⁰), 7.53 (1H, t, $^3J_{\text{H-H}}$ 7.5 Hz, H²²), 7.45 (4H, m, H¹⁴⁻²¹), 7.39 (1H, s, H⁵), 6.87 (2H, d, $^3J_{\text{H-H}}$ 9 Hz, H¹⁵), 4.75 (2H, s, H⁷), 4.66 (2H, s, H¹⁷), 4.16 (2H, m, H⁹), 3.80 (3H, s, H¹⁹), 3.54 (1H, br, OH), 1.37 (3H, t, $^3J_{\text{H-H}}$ 7 Hz, H¹⁰); δ_{C} (CDCl₃) 168.8 (s, C¹⁸), 161.3 (d, $^3J_{\text{C-P}}$ 19 Hz, C⁶), 158.7 (s, C¹⁶), 153.3 (d, $^1J_{\text{C-P}}$ 164 Hz, C²), 133.7 (s, C¹⁴), 132.9 (d, $^3J_{\text{C-P}}$ 12 Hz, C⁴), 132.8 (d, $^4J_{\text{C-P}}$ 3 Hz, C²²), 132.6 (d, $^4J_{\text{C-P}}$ 2.5 Hz, C²⁰), 129.6 (d, $^1J_{\text{C-P}}$ 140.5 Hz, C⁸), 128.7 (d, $^2J_{\text{C-P}}$ 22 Hz, C³), 128.5 (d, $^3J_{\text{C-P}}$ 13 Hz, C²¹), 125.8 (s, C¹³), 123.9 (s, C⁵), 115.0 (s, C¹⁵), 95.6 (s, C¹²), 85.5 (s, C¹¹), 65.1 (s, C¹⁷), 63.8 (s, C⁷), 61.9 (d, $^2J_{\text{C-P}}$ 6 Hz, C⁹), 52.4 (C¹⁹), 16.5 (d, $^3J_{\text{C-P}}$ 6 Hz, C¹⁰); δ_{P} (CDCl₃) +25.4; m/z (HRMS+) 466.1398 [M + H]⁺ (C₂₅H₂₅NO₆P requires 466.1420); R_f = 0.50 (silica; DCM : 3 % MeOH).

Trimethyl 2,2',2''-(4,4',4''-6,6',6''-((*S*)-2-(4-(*tert*-butoxycarbonylamino)butyl)-1,4,7-triazacyclononane-1,4,7-triyl)tris(methylene)tris(2-(ethoxy(phenyl)phosphoryl)pyridine-6,4-diyl)tris(ethyne-2,1-diyl)tris(benzene-4,1-diyl)tris(oxy))triacetate, **34**



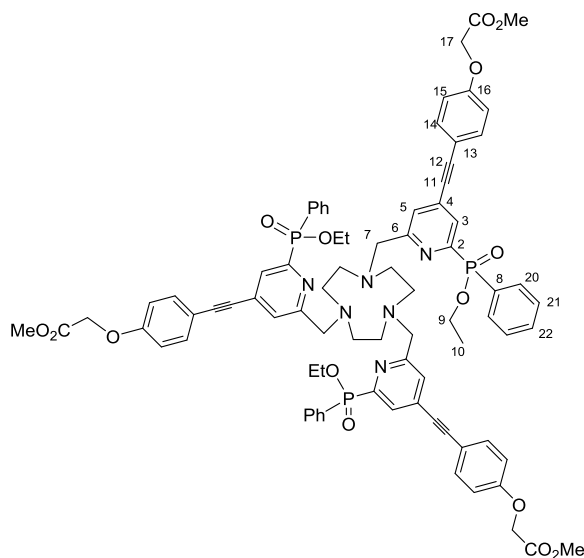
(*S*)-*tert*-Butyl 4-(1,4,7-triazacyclononan-2-yl)butylcarbamate, **17** (24 mg, 0.08 mmol) and methyl 2-(4-((2-(ethoxy(phenyl)phosphoryl)-6-((methylsulfonyloxy)methyl)pyridin-4-yl)ethynyl)phenoxy)acetate, **33** (130 mg, 0.24 mmol), were dissolved in anhydrous CH₃CN (4 mL) and K₂CO₃ (33 mg, 0.24 mmol) was added. KI (0.1 mg) was added to the reaction and the mixture was stirred under argon at 60 °C for 3 h. The reaction was cooled and the solution decanted from excess potassium salts to give a yellow oil (68 mg, 52 %): δ_{H} (CDCl₃) 8.02 (9H, m, H³⁻²⁰), 7.53 (18H, m, H⁵⁻¹⁴⁻²¹⁻²²), 6.94 (6H, m, H¹⁵), 5.10 (1H, br, CONH), 4.64 (6H, s, H¹⁷), 4.11 (6H, m, H⁹), 3.96 (6H, s, H⁷), 3.79 (9H, s, CO₂Me), 2.82 (14H, br, 9N₃ and H²⁶), 1.41 (9H, s, Boc), 1.45-1.28 (6H, H²³⁻²⁴⁻²⁵), 1.39 (9H, m, H¹⁰); δ_{P} (CDCl₃) +25.3; *m/z* (HRMS⁺) 1642.627 [M + H]⁺ (C₉₀H₉₈N₇O₁₇P₃ requires 1642.631).

Trimethyl 2,2',2''-(4,4',4''-(6,6',6''-((*S*)-2-(4-aminobutyl)-1,4,7-triazacyclononane-1,4,7-triyl)tris(methylene)tris(2-(ethoxy(phenyl)phosphoryl)pyridine-6,4-diyl))tris(ethyne-2,1-diyl))tris(benzene-4,1-diyl))tris(oxy)triacetate, **35**



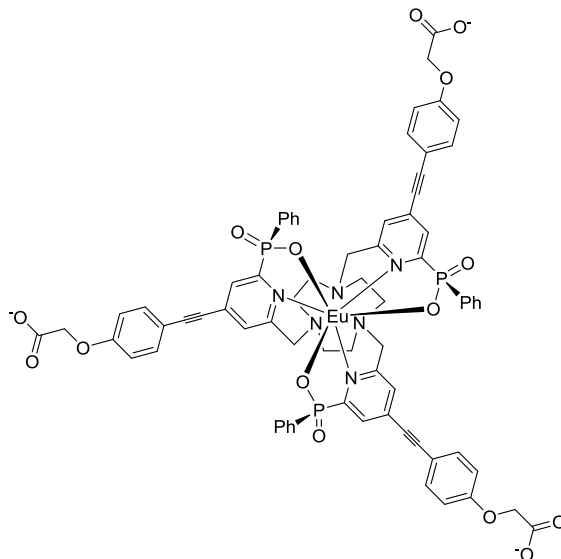
Trimethyl 2,2',2''-(4,4',4''-(6,6',6''-((*S*)-2-(4-(*tert*-butoxycarbonylamino)butyl)-1,4,7-triazacyclononane-1,4,7-triyl)tris(methylene)tris(2-(ethoxy(phenyl)phosphoryl)pyridine-6,4-diyl))tris(ethyne-2,1-diyl))tris(benzene-4,1-diyl))tris(oxy)triacetate, **34** (23 mg, 14 μmol), was dissolved in dry DCM (1.8 mL). Argon was bubbled for 10 min after which time TFA (0.2 mL) was added at 4 °C. The solution was allowed to warm up to RT and stirred for 15 min. The solvent was removed under reduced pressure to give the trifluoroacetate salt as a yellow oil (21 mg, 97 %); δ_{H} (CDCl_3) 8.05 (9H, m, H^{3-20}), 7.56 (18H, m, $\text{H}^{5-14-21-22}$), 6.99 (6H, m, H^{15}), 4.67 (6H, s, H^{17}), 4.11 (6H, m, H^9), 3.96 (6H, s, H^7), 3.81 (9H, s, CO_2Me), 2.95 (14H, br, 9 N_3 and H^{26}), 1.45-1.28 (8H, $\text{H}^{23-24-25}$ and NH_2), 1.34 (9H, m, H^{10}); δ_{P} (CDCl_3) +26.6; m/z (HRMS⁺) 771.7914 [$\text{M} + 2\text{H}$]²⁺ ($\text{C}_{85}\text{H}_{90}\text{N}_7\text{O}_{15}\text{P}_3$ requires 771.7932).

Trimethyl 2,2',2''-(4,4',4''-(6,6',6''-(1,4,7-triazacyclononane-1,4,7-triyl)tris(methylene)tris(2-(ethoxy(phenyl)phosphoryl)pyridine-6,4-diyl))tris(ethyne-2,1-diyl))tris(benzene-4,1-diyl))tris(oxy)triacetate, **36**



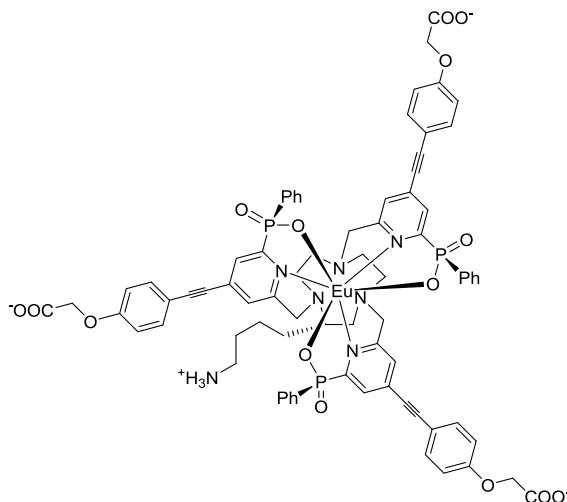
1,4,7-Triazacyclononane trihydrochloride (1.8 mg, 7.6 μmol) and methyl 2-(4-((2-(ethoxy(phenyl)phosphoryl)-6-((methylsulfonyloxy)methyl)pyridin-4-yl)ethynyl)phenoxy)acetate, **33** (12 mg, 22 μmol), were dissolved in anhydrous CH_3CN (1 mL) and K_2CO_3 (6.3 mg, 44 μmol) was added. KI (0.1 mg) was added to the reaction and the mixture was stirred under argon at 60 $^\circ\text{C}$ for 3 h. The reaction was cooled and the solution decanted from excess potassium salts to give a yellow oil (10 mg, 89 %); δ_{H} (CDCl_3) 8.03 (9H, m, H^{3-20}), 7.53 (18H, m, $\text{H}^{5-14-21-22}$), 6.92 (6H, d, $^3J_{\text{H-H}}$ 9 Hz, H^{15}), 4.67 (6H, s, H^{17}), 4.16 (6H, m, H^9), 3.96 (6H, s, H^7), 3.82 (9H, s, CO_2Me), 2.82 (12H, br, 9N_3), 1.37 (9H, t, $^3J_{\text{H-H}}$ 7 Hz, H^{10}); δ_{C} (CDCl_3) 168.9 (s, C^{18}), 160.3 (s, C^6), 158.6 (s, C^{16}), 153.3 (d, $^1J_{\text{C-P}}$ 163 Hz, C^2), 133.7 (s, C^{14}), 132.9 (s, C^4), 132.8 (s, C^{22}), 132.5 (s, C^{20}), 129.2 (d, $^1J_{\text{C-P}}$ 140.5 Hz, C^8), 128.9 (d, $^2J_{\text{C-P}}$ 16 Hz, C^3), 128.5 (s, C^{21}), 125.4 (s, C^{13}), 124.0 (s, C^5), 115.0 (s, C^{15}), 95.6 (s, C^{12}), 85.6 (s, C^{11}), 65.1 (s, C^{17}), 63.8 (s, C^7), 61.5 (s, C^9), 55.4-54.7 (br, 9N_3), 52.3 (CO_2Me), 16.5 (ds, C^{10}); δ_{P} (CDCl_3) +25.4; m/z (HRMS+) 1471.504 [$\text{M} + \text{H}$] $^+$ ($\text{C}_{81}\text{H}_{82}\text{N}_6\text{O}_{15}\text{P}_3$ requires 1471.501).

Eu(III) complex of 2,2',2''-(4,4',4''-(6,6',6''-(1,4,7-triazacyclononane-1,4,7-triyl)tris(methylene)tris(2-(hydroxy(phenyl)phosphoryl)pyridine-6,4-diyl))tris(ethyne-2,1-diyl)tris(benzene-4,1-diyl))tris(oxy)triacetate, [EuL^{18a}]³⁻

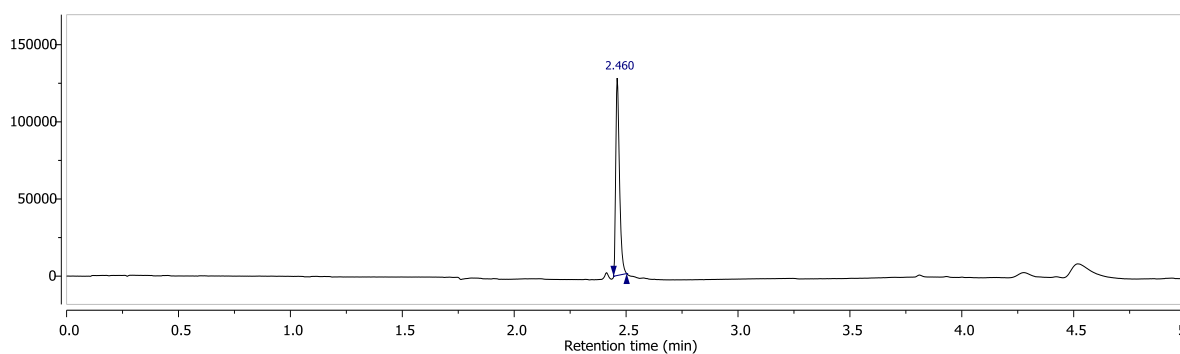


Trimethyl 2,2',2''-(4,4',4''-(6,6',6''-(1,4,7-triazacyclononane-1,4,7-triyl)tris(methylene)tris(2-(ethoxy(phenyl)phosphoryl)pyridine-6,4-diyl))tris(ethyne-2,1-diyl)tris(benzene-4,1-diyl))tris(oxy)triacetate, **36** (7.0 mg, 4.8 μmol) was dissolved in CD_3OD (1 mL) and a solution of NaOH in D_2O (0.1 M, 0.5 mL) was added. The mixture was heated to 60 $^\circ\text{C}$ under argon and reaction monitored by ^{31}P -NMR [δ_{P} (reactant) = + 25.4, (δ_{P} (product) = + 14.9]. After 3 h the solution was cooled to RT and the pH was adjusted to 7 with HCl. $\text{Eu}(\text{OAc})_3\text{H}_2\text{O}$ (1.7 mg, 5 μmol) was added and the mixture heated to 65 $^\circ\text{C}$ overnight under argon. The solvent was removed under reduced pressure and the product purified by HPLC (*Method J*, t_{R} = 14.4 min) giving a white solid (4.8 mg, 67 %); m/z (HRMS⁺) 747.1342 [$\text{MH}_3 + 2\text{H}$]²⁺ ($\text{C}_{72}\text{H}_{60}^{151}\text{EuN}_6\text{O}_{15}\text{P}_3$ requires 747.1342); $\tau_{\text{H}_2\text{O}}$ = 1.11 ms; $\lambda_{\text{max}}(\text{H}_2\text{O})$ = 330 nm; ϵ = 58 $\text{mM}^{-1}\text{cm}^{-1}$.

Eu(III) complex of (*R,R,R*)-6,6',6''-((*S*)-2-(4-aminobutyl)-1,4,7-triazacyclononane-1,4,7-triyl)tris(methylene)tris(4-((4-(carboxymethoxy)phenyl)ethynyl)pyridine-6,2-diyl)tris(phenylphosphinate), [EuL¹⁸]²⁻

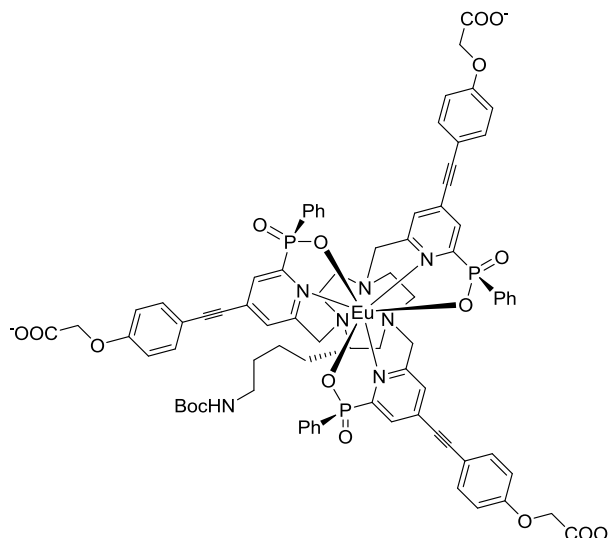


Trimethyl 2,2',2''-(4,4',4''-(6,6',6''-((*S*)-2-(4-aminobutyl)-1,4,7-triazacyclononane-1,4,7-triyl)tris(methylene)tris(2-((ethoxy(phenyl)phosphoryl)pyridine-6,4-diyl)tris(ethyne-2,1-diyl)tris(benzene-4,1-diyl)tris(oxy)triacetate, **35** (7 mg, 4.5 μmol) was dissolved in CD_3OD (3 mL) and a solution of NaOH in D_2O (0.1 M, 1.5 mL) was added. The mixture was heated to 60 °C under argon and reaction monitored by ^{31}P -NMR [δ_{P} (reactant) = + 26.6, (δ_{P} (product) = + 16.2]. After 5 h the solution was cooled to RT and the pH was adjusted to 7 with HCl. $\text{Eu}(\text{AcO})_3\text{H}_2\text{O}$ (1.6 mg, 5.0 μmol) was added and the mixture heated to 65 °C overnight under argon. The solvent was removed under reduced pressure and the product purified by HPLC (*Method J*, t_{R} = 13.5 min) giving a white solid (3 mg, 43 %); m/z (HRMS+) 783.6727 [$\text{MH}_2 + 2\text{H}$]²⁺ ($\text{C}_{76}\text{H}_{69}^{153}\text{EuN}_7\text{O}_{15}\text{P}_3$ requires 783.6724); $\tau_{\text{H}_2\text{O}}$ = 1.10 ms; $\lambda_{\text{max}}(\text{H}_2\text{O})$ = 330 nm; ε = 58 $\text{mM}^{-1}\text{cm}^{-1}$.



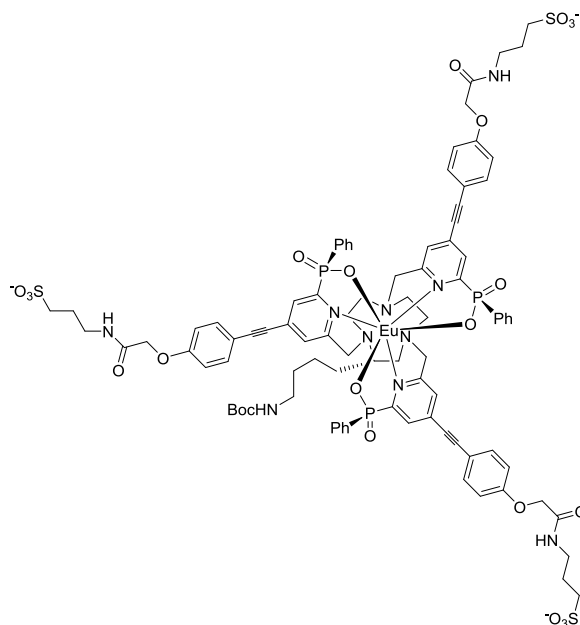
Method N, t_{R} = 2.5 min

Eu(III) complex of (*R,R,R*)-6,6',6''-((*S*)-2-(4-(*tert*-butoxycarbonylamino)butyl)-1,4,7-triazacyclononane-1,4,7-triyl)tris(methylene)tris(4-((4-(carboxymethoxy)phenyl)ethynyl)pyridine-6,2-diyl)tris(phenylphosphinate), **37**



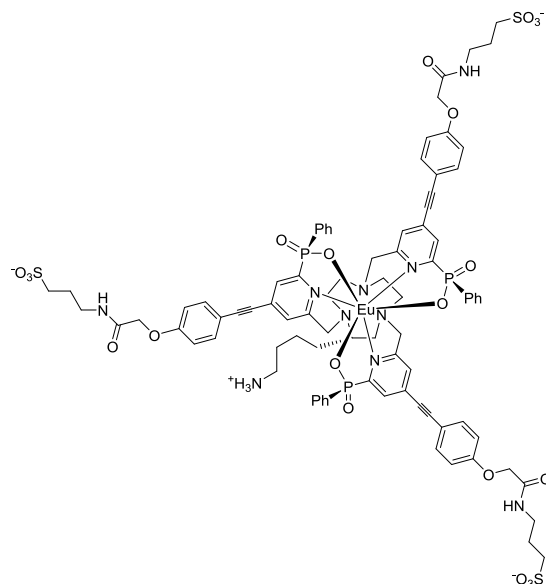
Trimethyl 2,2',2''-(4,4',4''-6,6',6''-((*S*)-2-(4-(*tert*-butoxycarbonylamino)butyl)-1,4,7-triazacyclononane-1,4,7-triyl)tris(methylene)tris(2-(ethoxy(phenyl)phosphoryl)pyridine-6,4-diyl)tris(ethyne-2,1-diyl)tris(benzene-4,1-diyl)tris(oxy))triacetate, **34** (16.0 mg, 10 μ mol) was dissolved in CD₃OD (2 mL) and a solution of NaOH in D₂O (0.1 M, 1 mL) was added. The mixture was heated to 60 °C under argon and the reaction monitored by ³¹P-NMR [$\delta_P(\text{reactant}) = +25.3$, ($\delta_P(\text{product}) = +14.9$]. After 3 h, the solution was cooled to RT and the pH was adjusted to 7 with HCl. Eu(AcO)₃H₂O (3.6 mg, 10.1 μ mol) was added and the mixture heated to 65 °C overnight under argon. The solvent was removed under reduced pressure and the product purified by HPLC (*Method J*, $t_R = 14.7$ min) giving a white solid (8.8 mg, 53 %); m/z (HRMS+) 1666.388 [$\text{MH}_3 + \text{H}^+$] ($\text{C}_{81}\text{H}_{77}^{153}\text{EuN}_7\text{O}_{17}\text{P}_3$ requires 1666.389); $\tau_{\text{H}_2\text{O}} = 1.12$ ms; $\lambda_{\text{max}}(\text{H}_2\text{O}) = 330$ nm; $\varepsilon = 58$ mM⁻¹ cm⁻¹.

Eu(III) complex of (*R,R,R*)-6,6',6''-((*S*)-2-(4-(*tert*-butoxycarbonylamino)butyl)-1,4,7-triazacyclononane-1,4,7-triyl)tris(methylene)tris(4-((4-(2-oxo-2-(3-sulfopropylamino)ethoxy)phenyl)ethynyl)pyridine-6,2-diyl)tris(phenylphosphinate), **38**

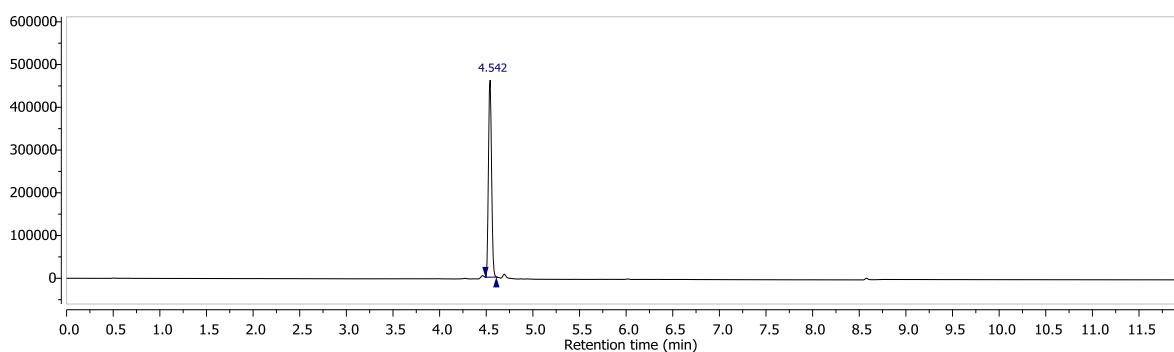


Eu(III) complex of (*R,R,R*)-6,6',6''-((*S*)-2-(4-(*tert*-butoxycarbonylamino)butyl)-1,4,7-triazacyclononane-1,4,7-triyl)tris(methylene)tris(4-((4-(carboxymethoxy)phenyl)ethynyl)pyridine-6,2-diyl)tris(phenylphosphinate), **37** (8.8 mg, 5.3 μmol) and homotaurine (4.4 mg, 31.8 μmol) were dissolved a mixture of DMSO (1 mL) and H₂O (50 μL). HATU (12.0 mg, 31.8 μmol) and DIPEA (9 μL , 53 μmol) were added to the reaction and the mixture was stirred for 3 h under argon, after which time LC-MS showed complete conversion. The product was purified by HPLC (*Method K*, $t_{\text{R}} = 17.3$ min) giving the triethylammonium salt as a white solid (8.1 mg, 76 %); m/z (HRMS-) 1013.211 [MH]²⁻ (C₉₀H₉₈¹⁵³EuN₁₀O₂₃P₃S₃ requires 1013.213); $\tau_{\text{H}_2\text{O}} = 1.11$ ms; $\lambda_{\text{max}}(\text{H}_2\text{O}) = 328$ nm; $\varepsilon = 57$ mM⁻¹ cm⁻¹.

Eu(III) complex of (*R,R,R*)-6,6',6''-((*S*)-2-(4-aminobutyl)-1,4,7-triazacyclononane-1,4,7-triyl)tris(methylene)tris(4-((4-(2-oxo-2-(3-sulfopropylamino)ethoxy)phenyl)ethynyl)pyridine-6,2-diyl)tris(phenylphosphinate), [EuL¹⁹]²⁻

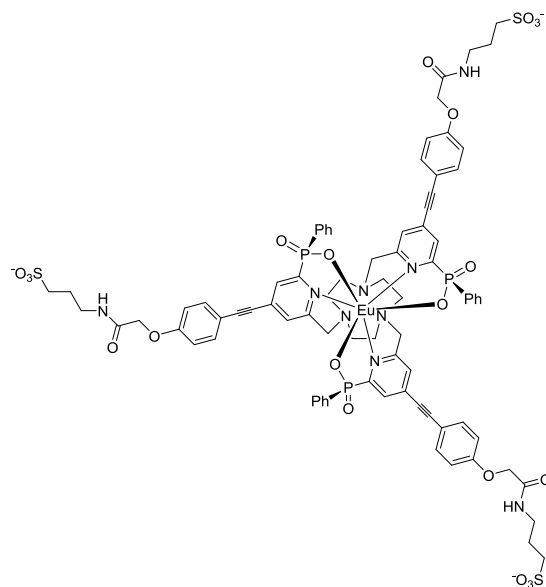


Eu(III) complex of (*R,R,R*)-6,6',6''-((*S*)-2-(4-(*tert*-butoxycarbonylamino)butyl)-1,4,7-triazacyclononane-1,4,7-triyl)tris(methylene)tris(4-((4-(2-oxo-2-(3-sulfopropylamino)ethoxy)phenyl)ethynyl)pyridine-6,2-diyl)tris(phenylphosphinate), **38** (21 mg, 10 μmol) was dissolved in dry DCM (1.7 mL). TFA (0.3 mL) was added and the mixture was stirred at RT for 20 min. The solvent was removed under reduced pressure and the product was purified by HPLC (*Method K*, $t_{\text{R}} = 16.4$ min) giving the triethylammonium salt as a white solid (18 mg, 93 %); m/z (HRMS-) 963.1838 [M]²⁻ ($\text{C}_{85}\text{H}_{90}^{153}\text{EuN}_{10}\text{O}_{21}\text{P}_3\text{S}_3$ requires 963.1862); $\tau_{\text{H}_2\text{O}} = 1.11$ ms; $\lambda_{\text{max}}(\text{H}_2\text{O}) = 328$ nm; $\varepsilon = 57$ $\text{mM}^{-1} \text{cm}^{-1}$.

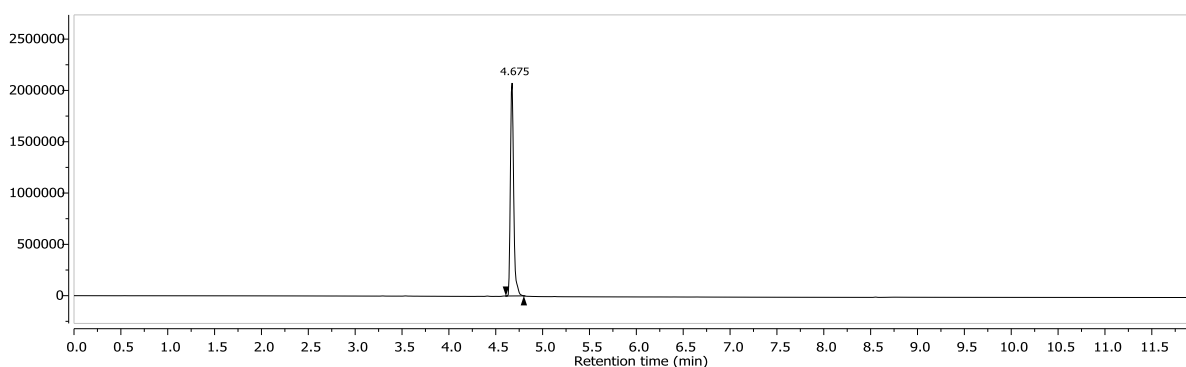


Method M, $t_{\text{R}} = 4.5$ min

Eu(III) complex of 6,6',6''-(1,4,7-triazacyclononane-1,4,7-triyl)tris(methylene)tris(4-((4-(2-oxo-2-(3-sulfopropylamino)ethoxy)phenyl)ethynyl)pyridine-6,2-diyl)tris(phenylphosphinate), [EuL^{19a}]³⁻

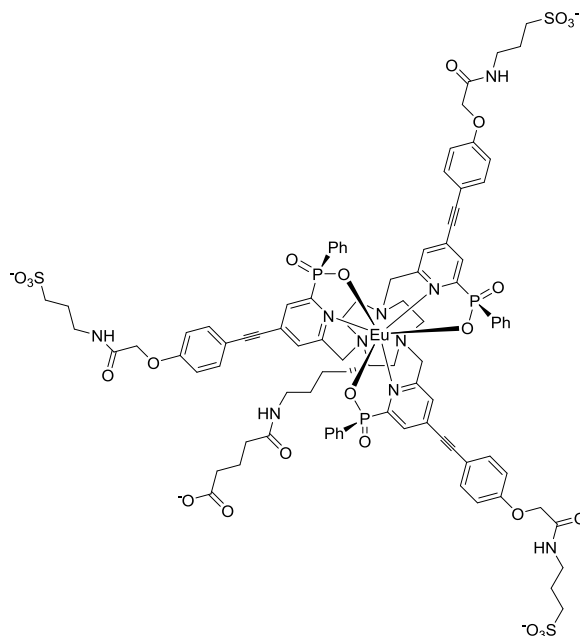


The Eu(III) complex of 2,2',2''-(4,4',4''-(6,6',6''-(1,4,7-triazacyclononane-1,4,7-triyl)tris(methylene)tris(2-(hydroxy(phenyl)phosphoryl)pyridine-6,4-diyl))tris(ethyne-2,1-diyl)tris(benzene-4,1-diyl))tris(oxy)triacetate, [EuL^{18a}]³⁻ (3.2 mg, 2.0 μmol) and homotaurine (1.8 mg, 18 μmol) were dissolved in a mixture of DMSO (1 mL) and H₂O (100 μL). HATU (4.5 mg, 18 μmol) and DIPEA (3.5 μL , 20 μmol) were added to the reaction and the mixture was stirred for 3 h under argon, after which time, LC-MS showed complete conversion. The product was purified by HPLC (*Method K*, $t_{\text{R}} = 17.4$ min) giving a the triethylammonium salt as a white solid (2.3 mg, 62 %); m/z (HRMS⁻) 927.6472 [MH]²⁻ (C₈₁H₈₁¹⁵³EuN₉O₂₁P₃S₃ requires 927.6494); $\tau_{\text{H}_2\text{O}} = 1.12$ ms; $\lambda_{\text{max}}(\text{H}_2\text{O}) = 328$ nm; $\varepsilon = 57$ mM⁻¹ cm⁻¹.

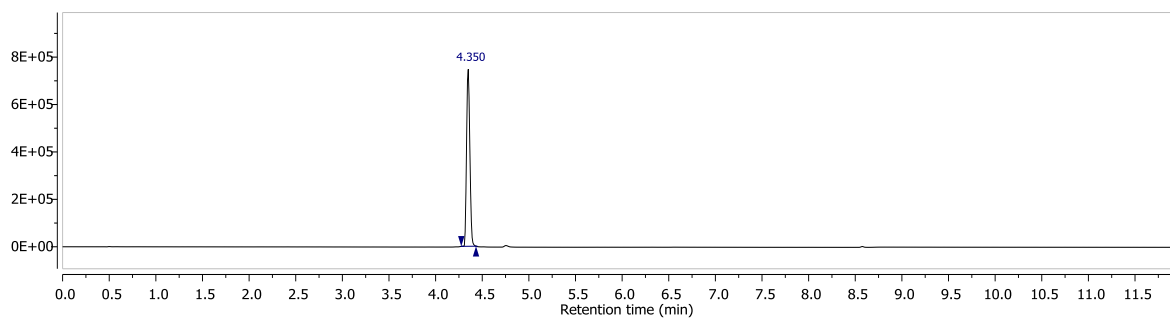


Method M, $t_{\text{R}} = 4.7$ min

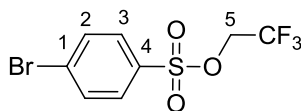
Eu(III) complex of (*R,R,R*)-6,6',6''-((*S*)-2-(4-(4-carboxybutanamido)butyl)-1,4,7-triazacyclononane-1,4,7-triyl)tris(methylene)tris(4-((4-(2-oxo-2-(3-sulfopropylamino)ethoxy)phenyl)ethynyl)pyridine-6,2-diyl)tris(phenylphosphinate), [EuL¹⁹]-glu⁴⁻



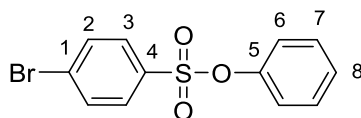
The Eu(III) complex of (*R,R,R*)-6,6',6''-((*S*)-2-(4-aminobutyl)-1,4,7-triazacyclononane-1,4,7-triyl)tris(methylene)tris(4-((4-(2-oxo-2-(3-sulfopropylamino)ethoxy)phenyl)ethynyl)pyridine-6,2-diyl)tris(phenylphosphinate), [EuL¹⁹]²⁻ (17.0 mg, 8.8 μ mol), was dissolved in dry DMF (1 mL). Glutaric anhydride (1.0 mg, 8.8 μ mol) and DIPEA (10 μ L, 52.8 μ mol) were added and the reaction was stirred at RT for 1 h. The product was purified by HPLC (*Method K*, t_R = 16.5 min) giving the triethylammonium salt as a white solid (16.5 mg, 92 %); m/z (HRMS-) 1020.202 [M - 2H]²⁻ (C₉₀H₉₆¹⁵³EuN₁₀O₂₄P₃S₃ requires 1020.202).



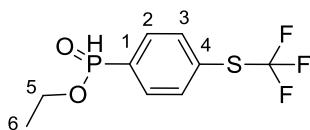
Method M, t_R = 4.4 min

2,2,2-Trifluoroethyl 4-bromobenzenesulfonate, 43

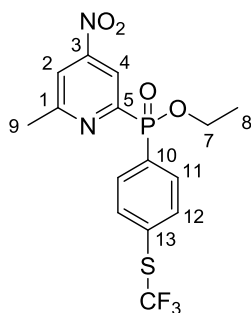
4-Bromobenzenesulfonyl chloride, **42** (3.00 g, 11.7 mmol) was dissolved in DCM (20 mL) and trifluoroethanol (840 μ L, 11.7 mmol) was added. A solution of DABCO (1.50 g, 13.4 mmol) in DCM (10 mL) was added resulting in precipitate formation. The reaction was stirred for 1 h at RT, after which time a solution of aqueous NaOH (1 M, 3 mL) was added. The reaction was diluted in EtOAc (100 mL) and washed with 0.5 M NaHCO₃, 0.1 M HCl, water and brine. The organic layer was dried over MgSO₄ and the solvent removed under reduced pressure to give a white solid (3.40 g, 91 %); m.p. 105 – 107 °C; anal. calc. for C₈H₆F₃BrO₃S: C, 30.11; H, 1.90 %; found: C, 30.15; H, 1.88 %; δ_{H} (CDCl₃) 7.77 (4H, m, H²⁻³), 4.40 (2H, q, ³J_{H-F} 8 Hz, H⁵); δ_{C} (CDCl₃) 134.1 (C¹), 133.1 (C³), 130.3 (C⁴), 129.7 (C²), 122.0 (q, ¹J_{C-F} 278 Hz, CF₃), 65.0 (q, ²J_{C-F} 38 Hz, C⁵); δ_{F} (CDCl₃) -74.2 (t, ³J_{F-H} 7 Hz); *m/z* (HRMS⁺) 340.9077 [M + Na]⁺ (C₈H₆O₃S⁷⁹BrF₃Na requires 340.9071); *R_f* = 0.58 (silica, EtOAc : Hex 2 : 8).

Phenyl 4-bromobenzenesulfonate, 44

4-Bromobenzenesulfonyl chloride, **42** (10.0 g, 39 mmol), was dissolved in DCM (40 mL) and phenol (3.7 g, 39 mmol) was added. A solution of DABCO (5.2 g, 46 mmol) in DCM (30 mL) was added resulting in precipitate formation. The reaction was stirred for 30 min at RT, after which time a solution of aqueous NaOH (1 M, 20 mL) was added. The reaction was diluted in EtOAc (250 mL) and washed successively with 0.5 M aq. NaHCO₃, 0.1 M HCl, water and brine. The organic layer was dried over MgSO₄ and the solvent removed under reduced pressure to give a white solid (11.5 g, 95 %); m.p. 116 – 117 °C [lit.¹³⁷ 116 – 117 °C]; δ_{H} (CDCl₃) 7.66 (4H, m, H²⁻³), 7.30 (2H, m, H⁷), 7.26 (1H, m, H⁸), 6.99 (2H, m, H⁶); δ_{C} (CDCl₃) 149.4 (s, C⁵), 134.4 (s, C¹), 132.8 (s, C³), 129.9 (s, C²), 129.8 (s, C⁷), 129.6 (s, C⁴), 127.3 (s, C⁸), 122.2 (s, C⁶); *m/z* (ESI) 311.0 [M - H]⁻; *R_f* = 0.47 (silica, EtOAc : Hex 1 : 9).

Ethyl 4-(trifluoromethylthio)phenylphosphinate, 48

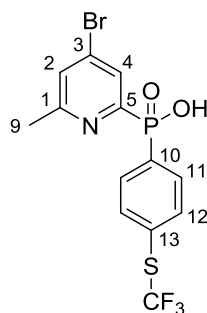
1-Bromo-4-(trifluoromethylthio)benzene, **46** (5.00 g, 19.5 mmol) was dissolved in dry THF (30 mL); 2 mL of this solution was added to magnesium turnings (0.70 g, 0.29 mmol) previously activated by heating for 2 h in the oven and 15 min under vacuum. A few drops of dibromoethane were added to the mixture and the rest of the solution was added dropwise under argon. The mixture was stirred for 1 h, after which time, diethylchlorophosphite (1.7 mL, 11.7 mmol) was added to the dark solution. The mixture was stirred at RT overnight after which time the solvent was removed and hexane (50 mL) was added to the brown oil. The reaction was stirred for 10 min and decanted in order to remove the brown solid. This procedure was repeated another 3 times. The organic fractions were combined and the solvent was removed under reduced pressure giving the aryl phosphonite, **47** as an orange oil (^{31}P -NMR δ_{P} (product) = 153.7]. The oil was dissolved in EtOH (3 mL) and 1 eq of 1 M HCl was added. The solvent was removed under pressure giving an orange oil (1 g, 32 %). The product was taken on without further purification and used in the next step; δ_{H} (CDCl_3) 7.61 (1H, d, $^1J_{\text{H-P}}$ 536 Hz, PH), 7.78-7.40 (4H, m, H^{2-3}), 4.16 (2H, m, H^5), 1.39 (3H, t, $^3J_{\text{H-H}}$ 7 Hz, H^6); δ_{F} (CDCl_3) -42.0; δ_{P} (CDCl_3) +22.4; m/z (HRMS+) 271.0161 [$\text{M} + \text{H}$] $^+$ ($\text{C}_9\text{H}_{11}\text{O}_2\text{F}_3\text{PS}$ requires 271.0169).

Ethyl 6-methyl-4-nitropyridin-2-yl(4-(trifluoromethylthio)phenyl)phosphinate, 49

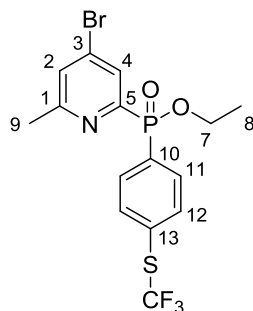
Ethyl 4-(trifluoromethylthio)phenylphosphinate, **48** (0.70 g, 2.60 mmol) was added to degassed toluene (10 mL), followed by 2-bromo-6-methyl-4-nitropyridine, **10** (0.56 g, 2.60 mmol), and freshly distilled triethylamine (1.2 mL, 9.10 mmol). Argon was bubbled through the yellow solution for 30 min, then $\text{PdCl}_2(\text{dppf}) \cdot \text{DCM}$ (60 mg, 0.05 mmol) was added, and

the mixture stirred at 125 °C for 16 h under argon, during which time the mixture turned black. The solvent was removed under reduced pressure, with purification of the resulting black oil by column chromatography (silica, EtOAc : Hex 1:1 to 3:1) giving a clear oil (0.32 g, 30 %); δ_{H} (CDCl₃) 8.60 (1H, dd, $^3J_{\text{H-P}}$ 6 Hz, $^4J_{\text{H-H}}$ 1.5 Hz, H⁴), 8.05 (2H, dd, $^3J_{\text{H-P}}$ 12 Hz, $^3J_{\text{H-H}}$ 8.5 Hz, H¹¹), 7.95 (1H, s, H²), 7.74 (2H, dd, $^3J_{\text{H-H}}$ 8.5 Hz, $^4J_{\text{H-P}}$ 3 Hz, H¹²), 4.31 – 3.87 (2H, m, H⁷), 2.75 (3H, s, H⁹), 1.40 (3H, t, $^3J_{\text{H-H}}$ 7 Hz, H⁸); δ_{C} (CDCl₃) 163.3 (d, $^5J_{\text{C-P}}$ 21 Hz, C¹), 157.3 (d, $^1J_{\text{C-P}}$ 169 Hz, C⁵), 154.1 (d, $^3J_{\text{C-P}}$ 14 Hz, C³), 135.3 (d, $^3J_{\text{C-P}}$ 14 Hz, C¹²), 133.4 (d, $^2J_{\text{C-P}}$ 10 Hz, C¹¹), 132.0 (d, $^1J_{\text{C-P}}$ 140 Hz, C¹⁰), 130.1 (s, C¹³), 129.2 (q, $^1J_{\text{C-F}}$ 309 Hz, CF₃), 117.9 (d, $^4J_{\text{C-P}}$ 13 Hz, C²), 117.8 (d, $^2J_{\text{C-P}}$ 9 Hz, C⁴), 62.5 (d, $^2J_{\text{C-P}}$ 6 Hz, C⁷), 24.9 (s, C⁹), 16.5 (d, $^3J_{\text{C-P}}$ 6 Hz, C⁸); δ_{F} (CDCl₃) -42.0; δ_{P} (CDCl₃) + 22.1; m/z (HRMS⁺) 407.0435 [M + H]⁺ (C₁₅H₁₅N₂O₄F₃PS requires 407.0442); R_f = 0.70 (silica, EtOAc : Hex 2 : 1).

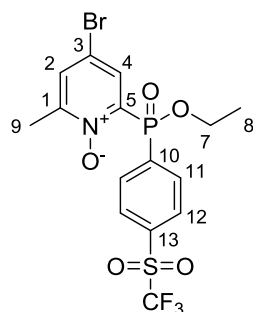
4-Bromo-6-methylpyridin-2-yl(4-(trifluoromethylthio)phenyl)phosphinic acid, 49a



Ethyl 6-methyl-4-nitropyridin-2-yl(4-(trifluoromethylthio)phenyl)phosphinate, **49** (380 mg, 0.94 mmol) was dissolved in acetyl bromide (2.1 mL, 28.2 mmol) and the mixture stirred at 70 °C for 16 h under argon. The brown solution was dropped cautiously into MeOH (30 mL) stirred at 0 °C. The solvent was removed under reduced pressure to yield a pale brown solid. The resulting material, containing unidentified contaminants, was used without further purification, assuming quantitative conversion to the bromo-phosphinic acid; δ_{H} (CDCl₃) 8.21 (2H, dd, $^3J_{\text{H-P}}$ 12 Hz, $^3J_{\text{H-H}}$ 8.5 Hz, H¹¹), 8.06-7.91 (2H, m, H^{4,2}), 7.80 (2H, s, H¹²), 3.07 (3H, s, H⁹); δ_{C} (CDCl₃) 157.8 (s, C¹), 149.8 (d, $^1J_{\text{C-P}}$ 106 Hz, C⁵), 144.2 (s, C³), 135.7 (d, $^3J_{\text{C-P}}$ 14 Hz, C¹²), 133.8 (d, $^2J_{\text{C-P}}$ 12 Hz, C¹¹), 133.5 (s, C²), 131.9 (s, C¹³), 131.8 (s, C⁴), 131.1 (q, $^1J_{\text{C-F}}$ 308 Hz, CF₃), 131.0 (d, $^1J_{\text{C-P}}$ 140 Hz, C¹⁰), 21.2 (s, C⁹); δ_{F} (CDCl₃) -41.5; δ_{P} (CDCl₃) + 12.5; m/z (HRMS⁺) 411.9383 [M + H]⁺ (C₁₃H₁₁NO₂F₃PS⁷⁹Br requires 411.9384).

Ethyl 4-bromo-6-methylpyridin-2-yl(4-(trifluoromethylthio)phenyl)phosphinate, 50

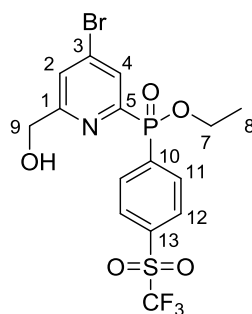
4-Bromo-6-methylpyridin-2-yl(4-(trifluoromethylthio)phenyl)phosphinic acid, **49a** (670 mg, 1.62 mmol) was added to $\text{HC}(\text{OCH}_2\text{CH}_3)_3$ (25 mL) and the mixture stirred at 140 °C for 72 h under argon. The solvent was removed under reduced pressure and the resulting residue was purified by column chromatography (silica, DCM : 1 % MeOH) to yield a clear oil (475 mg, 68 % over two steps); δ_{H} (CDCl_3) 8.09 (1H, dd, $^3J_{\text{H-P}}$ 6 Hz, $^4J_{\text{H-H}}$ 1.5 Hz, H^4), 8.03 (2H, dd, $^3J_{\text{H-P}}$ 12 Hz, $^3J_{\text{H-H}}$ 8 Hz, H^{11}), 7.72 (2H, dd, $^3J_{\text{H-H}}$ 8, $^4J_{\text{H-P}}$ 3 Hz, H^{12}), 7.43 (1H, s, H^2), 4.40 – 3.87 (2H, m, H^7), 2.55 (3H, s, H^9), 1.37 (3H, t, $^3J_{\text{H-H}}$ 7 Hz, H^8); δ_{C} (CDCl_3) 161.2 (d, $^5J_{\text{C-P}}$ 22 Hz, C^1), 154.5 (d, $^1J_{\text{C-P}}$ 168 Hz, C^5), 135.2 (d, $^3J_{\text{C-P}}$ 13.5 Hz, C^{12}), 133.5 (d, $^3J_{\text{C-P}}$ 15.5 Hz, C^3), 133.3 (d, $^2J_{\text{C-P}}$ 10 Hz, C^{11}), 132.7 (d, $^1J_{\text{C-P}}$ 138 Hz, C^{10}), 129.6 (s, C^{13}), 129.3 (q, $^1J_{\text{C-F}}$ 314 Hz, CF_3), 128.9 (d, $^4J_{\text{C-P}}$ 2 Hz, C^2), 129.7 (d, $^2J_{\text{C-P}}$ 6 Hz, C^4), 62.3 (d, $^2J_{\text{C-P}}$ 6 Hz, C^7), 24.3 (s, C^9), 16.5 (d, $^3J_{\text{C-P}}$ 6 Hz, C^8); δ_{F} (CDCl_3) -41.9; δ_{P} (CDCl_3) +22.6; m/z (HRMS^+) 439.9697 [$\text{M} + \text{H}]^+$ ($\text{C}_{15}\text{H}_{15}\text{O}_2\text{N}^{79}\text{BrF}_3\text{PS}$ requires 439.9691); R_f = 0.41 (silica, DCM : MeOH 96 : 4).

4-Bromo-2-(ethoxy(4-(trifluoromethylsulfonyl)phenyl)phosphoryl)-6-methylpyridine 1-oxide, 51

Ethyl 4-bromo-6-methylpyridin-2-yl(4-(trifluoromethylthio)phenyl)phosphinate, **50** (475 mg, 1.08 mmol) was dissolved in CHCl_3 (10 mL). 3-Chloroperbenzoic acid (1.10 g, 6.48 mmol) was added and the solution stirred at 65 °C for 16 h. The solvent was removed under reduced

pressure, with the resulting material being re-dissolved in DCM (10 mL), and washed with aqueous NaHCO₃ (0.5 M, 10 mL). The aqueous layer was re-extracted with DCM (3 × 10 mL), the organic extracts combined, dried over MgSO₄, and the solvent removed under reduced pressure. Purification of the resulting yellow oil was undertaken by column chromatography (silica, DCM : MeOH 0 to 2 %) giving a colourless oil (250 mg, 48 %); δ_{H} (CDCl₃) 8.30 (2H, dd, $^3J_{\text{H-P}}$ 13 Hz, $^3J_{\text{H-H}}$ 8.5 Hz, H¹¹), 8.12 (1H, dd, $^3J_{\text{H-P}}$ 8 Hz, $^4J_{\text{H-H}}$ 2.5 Hz, H⁴), 8.08 (2H, dd, $^3J_{\text{H-H}}$ 8.5 Hz, $^4J_{\text{H-P}}$ 3.0 Hz, H¹²), 7.55 (1H, d, $^4J_{\text{H-H}}$ 3 Hz, H²), 4.35 – 4.26 (2H, m, H⁷), 2.35 (3H, s, H⁹), 1.39 (3H, t, $^3J_{\text{H-H}}$ 7 Hz, H⁸); δ_{C} (CDCl₃) 151.0 (d, $^5J_{\text{C-P}}$ 4.5 Hz, C¹), 142.5 (d, $^1J_{\text{C-P}}$ 154 Hz, C⁵), 138.4 (d, $^1J_{\text{C-P}}$ 150 Hz, C¹⁰), 135.0 (s, C¹³), 134.3 (d, $^3J_{\text{C-P}}$ 11.5 Hz, C¹¹), 133.3 (d, $^2J_{\text{C-P}}$ 11 Hz, C⁴), 132.9 (d, $^4J_{\text{C-P}}$ 1.5 Hz, C²), 130.1 (d, $^2J_{\text{C-P}}$ 14.5 Hz, C¹²), 119.1 (q, $^1J_{\text{C-F}}$ 317 Hz, CF₃), 118.2 (d, $^3J_{\text{C-P}}$ 13 Hz, C³), 63.1 (d, $^2J_{\text{C-P}}$ 6 Hz, C⁷), 17.2 (s, C⁹), 16.4 (d, $^3J_{\text{C-P}}$ 6.5 Hz, C⁸); δ_{F} (CDCl₃) -77.9; δ_{P} (CDCl₃) + 16.8; m/z (HRMS⁺) 487.9544 [M + H]⁺ (C₁₅H₁₅O₅N⁷⁹BrF₃PS requires 487.9539); R_f = 0.45 (silica, DCM : MeOH 97 : 3).

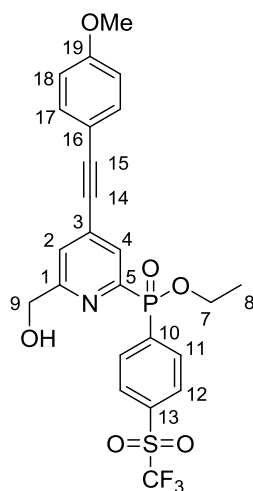
Ethyl-4-bromo-6-(hydroxymethyl)pyridin-2-yl(4-(trifluoromethylsulfonyl)phenyl)phosphinate, 52



Trifluoroacetic anhydride (1.4 mL) was added to a solution of 4-bromo-2-(ethoxy(4-(trifluoromethylsulfonyl)phenyl)phosphoryl)-6-methylpyridine 1-oxide, **51** (240 mg, 0.49 mmol), in dry CHCl₃ (10 mL). The reaction mixture was heated to 60 °C for 3 h under argon. The solvent was removed under reduced pressure and the resulting oil was dissolved in EtOH (10 mL) and H₂O (10 mL) and stirred for 1 h. After this time the solution was concentrated (ca. 10 mL) and extracted with DCM (3 × 30 mL). The organic extracts were combined, dried over MgSO₄, and the solvent removed under reduced pressure, giving a clear oil (220 mg, 92 %); δ_{H} (CDCl₃) 8.25 (2H, dd, $^3J_{\text{H-P}}$ 11.5 Hz, $^3J_{\text{H-H}}$ 8.5 Hz, H¹¹), 8.15 (1H, d, $^3J_{\text{H-P}}$ 5.0 Hz, H⁴), 8.08 (2H, m, H¹²), 7.75 (1H, s, H²), 6.47 (1H, br, OH), 4.76 (2H, s, H⁹), 4.18 (2H, m, H⁷), 1.37 (3H, t, $^3J_{\text{H-H}}$ 7 Hz, H⁸); δ_{C} (CDCl₃) 163.3 (d, $^5J_{\text{C-P}}$ 21 Hz, C¹), 152.6 (d, $^1J_{\text{C-P}}$ 169.5 Hz,

C⁵), 138.5 (d, ¹J_{C-P} 136.5 Hz, C¹⁰), 135.3 (s, C¹³), 134.6 (d, ³J_{C-P} 15 Hz, C³), 133.6 (d, ³J_{C-P} 10 Hz, C¹¹), 130.4 (d, ²J_{C-P} 13 Hz, C¹²), 130.3 (d, ²J_{C-P} 11.5 Hz, C⁴), 126.8 (d, ⁴J_{C-P} 3 Hz, C²), 119.6 (q, ¹J_{C-F} 327 Hz, CF₃), 64.1 (s, C⁹), 63.3 (d, ²J_{C-P} 6.5 Hz, C⁷), 16.4 (d, ³J_{C-P} 6 Hz, C⁸); δ_F (CDCl₃) -78.3; δ_P (CDCl₃) + 21.6; *m/z* (HRMS⁺) 487.9558 [M + H]⁺ (C₁₅H₁₅O₅N⁷⁹BrF₃PS requires 487.9544); *R_f* = 0.31 (silica, DCM : MeOH 97 : 3).

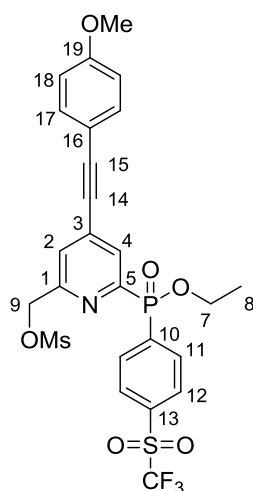
Ethyl 6-(hydroxymethyl)-4-((4-methoxyphenyl)ethynyl)pyridin-2-yl(4-(trifluoromethylsulfonyl)phenyl)phosphinate, 53



Ethyl 4-bromo-6-(hydroxymethyl)pyridin-2-yl(4-(trifluoromethylsulfonyl)phenyl)phosphinate, **52** (100 mg, 0.20 mmol), was dissolved in dry THF (2 mL) and the solution was degassed (freeze-thaw cycle) three times. 4-Ethynylanisole (45 mg, 0.30 mmol) and NEt₃ (0.65 mL) were added and the solution degassed once more. [1,1'-Bis(diphenylphosphino)ferrocene]palladium(II) chloride (27 mg, 0.02 mmol) and CuI (4 mg, 0.02 mmol) were added and the solution was degassed a further three times. The solution was stirred at 65 °C under argon for 16 h, solvent was removed under reduced pressure and the crude material purified by column chromatography (silica, DCM : MeOH 0 to 2 %) to give a dark yellow oil (80 mg, 68 %); δ_H (CDCl₃) 8.27 (2H, dd, ³J_{H-P} 11.1 Hz, ³J_{H-H} 8.5 Hz, H¹¹), 8.12 (3H, m, H⁴⁻¹²), 7.50 (1H, s, H²), 7.47 (2H, d, ³J_{H-H} 8.4 Hz, H¹⁷), 6.90 (2H, d, ³J_{H-H} 8.5 Hz, H¹⁸), 4.78 (2H, s, H⁹), 4.40-4.00 (2H, m, H⁷), 3.83 (3H, s, OMe), 3.49 (1H, br, OH), 1.40 (3H, t, ³J_{H-H} 7 Hz, H⁸); δ_C (CDCl₃) 161.2 (d, ⁵J_{C-P} = 19 Hz, C¹), 160.8 (s, C¹⁹), 151.6 (d, ¹J_{C-P} 169 Hz, C⁵), 139.5 (d, ¹J_{C-P} 135 Hz, C¹⁰), 135.0 (s, C¹³), 133.7 (d, ³J_{C-P} 18 Hz, C¹⁷), 133.5 (d, ³J_{C-P} 15 Hz, C¹¹), 133.4 (s, C³), 130.4 (s, C¹²), 129.1 (d, ²J_{C-P} 26 Hz, C⁴), 126.8 (d, ⁴J_{C-P} 13 Hz, C²), 118.4 (q, ¹J_{C-F} 329 Hz, CF₃), 114.3 (d, ²J_{C-P} 3 Hz, C¹⁸), 113.4 (s, C¹⁶), 96.8

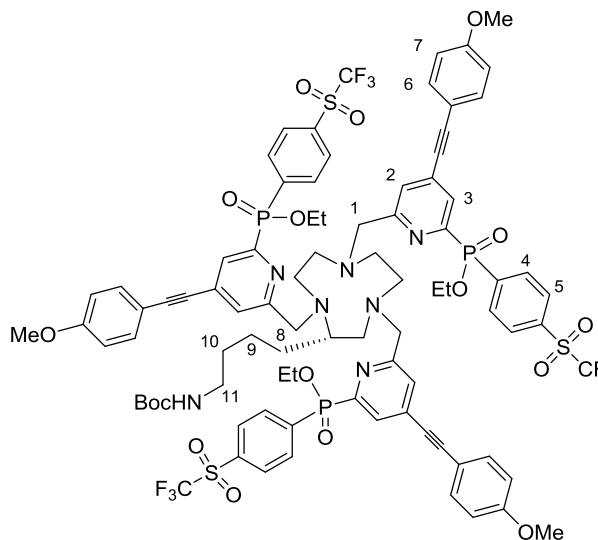
(s, C¹⁵), 85.0 (s, C¹⁴), 64.1 (s, C⁹), 62.7 (d, ²J_{C-P} 6.5 Hz, C⁷), 55.4 (d, ¹¹J_{C-P} 15 Hz, OMe), 16.5 (d, ³J_{C-P} 4.5 Hz, C⁸); δ_F (CDCl₃) -77.9; δ_P (CDCl₃) + 22.1; *m/z* (HRMS⁺) 540.0856 [M + H]⁺ (C₂₄H₂₂NO₆F₃PS requires 540.0858); *R_f* = 0.46 (silica, DCM : MeOH 95 : 5).

(6-(Ethoxy(4-(trifluoromethylsulfonyl)phenyl)phosphoryl)-4-((4-methoxyphenyl)ethynyl)pyridin-2-yl)methyl methanesulfonate, 54



Ethyl 6-(hydroxymethyl)-4-((4-methoxyphenyl)ethynyl)pyridin-2-yl(4-(trifluoromethylsulfonyl)phenyl)phosphinate, **53** (130 mg, 0.24 mmol), was dissolved in anhydrous THF (5 mL) and NEt₃ (0.10 mL, 0.72 mmol) was added. The mixture was stirred at 5 °C and methanesulfonyl chloride (28 μL, 0.36 mmol) was added. The reaction was monitored by TLC (silica; DCM : 3 % MeOH, *R_f*(product) = 0.50, *R_f*(reactant) = 0.31) and stopped after 15 min. The solvent was removed under reduced pressure and the residue dissolved in DCM (15 mL) and washed with saturated brine (10 mL). The aqueous layer was re-extracted with DCM (3 × 10 mL) and the organic layers combined, dried over MgSO₄ and the solvent removed under reduced pressure to leave a colourless oil (140 mg, 95 %); δ_H (CDCl₃) 8.30 (2H, dd, ³J_{H-P} 11.5 Hz, ³J_{H-H} 8.4 Hz, H¹¹), 8.18 (1H, d, ³J_{H-H} 6.5 Hz, H⁴), 8.13 (2H, m, H¹²), 7.62 (1H, s, H²), 7.49 (2H, d, ³J_{H-H} 9 Hz, H¹⁷), 6.91 (2H, d, ³J_{H-H} 9 Hz, H¹⁸), 5.25 (2H, m, H⁹), 4.18 (2H, m, H⁷), 3.84 (3H, s, OMe), 3.08 (3H, s, Ms), 1.39 (3H, t, ³J_{H-H} 7 Hz, H⁸); δ_F (CDCl₃) -78.3; δ_P (CDCl₃) + 22.4; *m/z* (HRMS⁺) 618.0649 [M + H]⁺ (C₂₅H₂₄NO₈F₃PS₂ requires 618.0633); *R_f* = 0.31 (silica, DCM : MeOH 97 : 3).

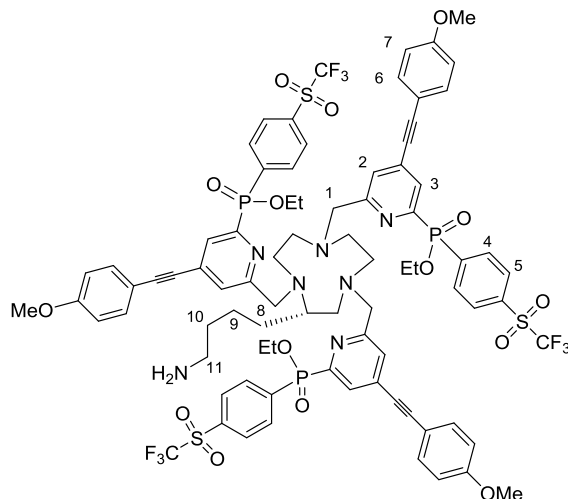
tert*-Butyl 4-((*S*)-1,4,7-tris((6-(ethoxy(4-(trifluoromethylsulfonyl)phenyl)phosphoryl)-4-((4-methoxyphenyl)ethynyl)pyridin-2-yl)methyl)-1,4,7-triazacyclononan-2-yl)butylcarbamate, **55*



(*S*)-*tert*-Butyl 4-(1,4,7-triazacyclononan-2-yl)butylcarbamate, **17** (23 mg, 0.078 mmol) and (6-(ethoxy(4-(trifluoromethylsulfonyl)phenyl)phosphoryl)-4-((4-methoxyphenyl)ethynyl)pyridin-2-yl)methyl methanesulfonate, **54** (140 mg, 0.22 mmol), were dissolved in anhydrous CH₃CN (4 mL) and K₂CO₃ (32 mg, 0.23 mmol) was added. The mixture was stirred under argon at 60 °C for 2 h. The reaction was cooled and the solution decanted from excess potassium salts. The solvent was removed under reduced pressure to give an orange oil (58 mg, 40 %); δ_H (CDCl₃) 8.28 (6H, m, H⁴), 8.11 (3H, m, H³), 8.06 (6H, m, H⁵), 7.57 (3H, m, H²), 7.45 (6H, m, H⁶), 6.88 (6H, m, H⁷), 5.04 (1H, br, CONH), 4.16 (6H, m, P-OCH₂), 3.82 (15H, m, H¹ and OMe), 3.00-2.61 (13H, m, 9N₃ and H¹¹), 1.37 (9H, s, Boc), 1.45-1.23 (6H, m, H¹⁰⁻⁹⁻⁸), 1.35 (9H, m, CH₃(Et)); δ_F (CDCl₃) -78.3, -78.4, -78.5; δ_P (CDCl₃) +22.1; m/z (ESI) 1864.5 [M + H]⁺.^h

^h HRMS could not be obtained due the mass out of the calibration range.

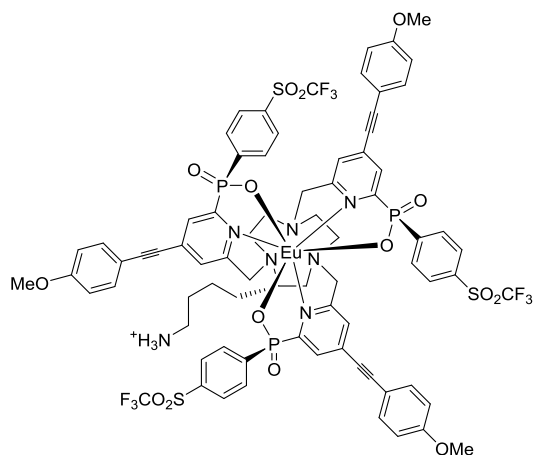
Triethyl 6,6',6''-((S)-2-(4-aminobutyl)-1,4,7-triazacyclononane-1,4,7-triyl)tris(methylene)tris(4-((4-methoxyphenyl)ethynyl)pyridine-6,2-diyl)tris(4-(trifluoromethylsulfonyl)phenylphosphinate), 56



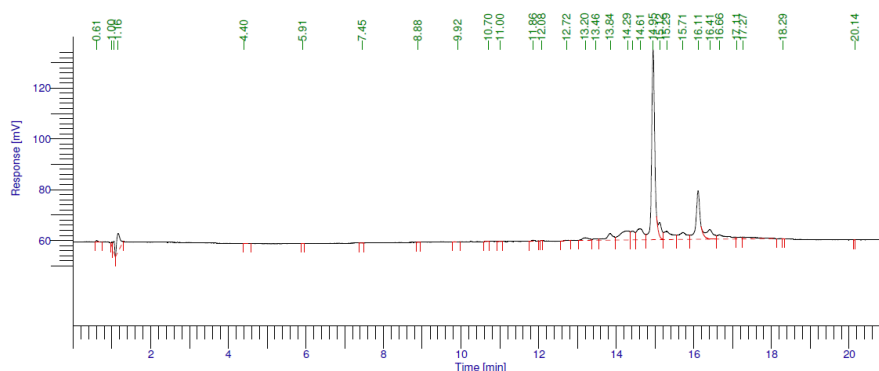
tert-Butyl 4-((*S*)-1,4,7-tris((6-(ethoxy(4-(trifluoromethylsulfonyl)phenyl)phosphoryl)-4-((4-methoxyphenyl)ethynyl)pyridin-2-yl)methyl)-1,4,7-triazacyclononan-2-yl)butylcarbamate, **55** (57 mg, 30 μ mol) was dissolved in dry DCM (1.8 mL). Argon was bubbled for 10 min after which time TFA (0.2 mL) was added. The solution was stirred for 15 min and the solvent was removed under reduced pressure to give the trifluoroacetate salt as a yellow oil (60 mg, quantitative yield); δ_{H} (CD_3OD) 8.26 (6H, m, H^4), 8.09 (3H, m, H^4), 8.04 (6H, m, H^5), 7.62 (3H, m, H^2), 7.55 (6H, m, H^6), 6.98 (6H, m, H^7), 4.12 (6H, m, P-OCH₂), 3.82 (15H, m, H^1 and OMe), 3.10-2.75 (13H, m, 9N₃ and H^{11}), 1.45-1.23 (7H, H^{10-9-8}), 1.41 (9H, m, CH₃(Et)); δ_{F} (CD_3OD) -80.2, -80.3, -80.4; δ_{P} (CD_3OD) + 22.5; m/z (ESI) 1764.4 [$\text{M} + \text{H}$]⁺.ⁱ

ⁱ HRMS could not be obtained due the mass out of the calibration range.

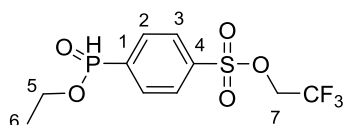
Eu(III) complex of (*R,R,R*)-6,6',6''-((*S*)-2-(4-aminobutyl)-1,4,7-triazacyclononane-1,4,7-triyl)tris(methylene)tris(4-((4-methoxyphenyl)ethynyl)pyridine-6,2-diyl)tris(4-(trifluoromethylsulfonyl)phenylphosphinate), [EuL²¹]⁺



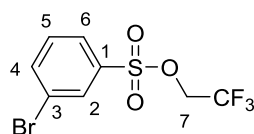
Triethyl 6,6',6''-((*S*)-2-(4-aminobutyl)-1,4,7-triazacyclononane-1,4,7-triyl)tris(methylene)tris(4-((4-methoxyphenyl)ethynyl)pyridine-6,2-diyl)tris(4-(trifluoromethylsulfonyl)phenylphosphinate) (3.0 mg, 1.7 μmol) was dissolved in dry MeOH (2 mL) and Na (2 mg, excess) was added. The reaction was stirred under argon at $-20\text{ }^{\circ}\text{C}$ and monitored by ^{19}F -NMR [δ_{F} (reactant) = -80.3 , (δ_{F} (product) = -80.7] and ^{31}P -NMR [δ_{P} (reactant) = $+25.5$, (δ_{P} (product) = $+11.7$]. After 16 h, the ethylphosphinate esters were completely hydrolysed. The reaction was allowed to warm to RT, water (1 mL) was added to the reaction and the pH was adjusted to 7 with HCl. Eu(AcO)₃H₂O (0.6 mg, 1.7 μmol) was added and the mixture heated to $65\text{ }^{\circ}\text{C}$ overnight under argon. The solvent was removed under reduced pressure giving a white solid (1.4 mg, 45 %); m/z (HRMS⁺) 915.6102 [$\text{M} + \text{H}$]²⁺ (C₇₆H₆₈¹⁵³EuF₉N₇O₁₅P₃S₃ requires 915.6113); $\tau_{\text{MeOH}} = 1.10\text{ ms}$; $\lambda_{\text{max}}(\text{MeOH}) = 342\text{ nm}$; $\varepsilon = 58\text{ mM}^{-1}\text{ cm}^{-1}$.



Method 1, $t_{\text{R}} = 15.0\text{ min}$

2,2,2-Trifluoroethyl 4-(ethoxyhydrophosphoryl)benzenesulfonate, 57

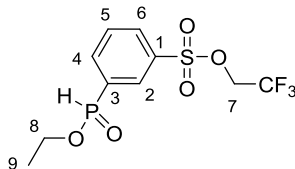
To a suspension of anilinium hypophosphite (1.00 g, 6.29 mmol) in dry toluene was added 2,2,2-trifluoroethyl 4-bromobenzenesulfonate, **43** (1.60 g, 5.02 mmol). Argon was bubbled through the solution for 30 min, then aminopropyltriethoxysilane (1.48 mL, 6.30 mmol) was added, and argon was bubbled through the solution for an additional 30 min. PdCl₂(dppf)·DCM (220 mg, 0.27 mmol) was added, and the mixture stirred at 100 °C for 45 min under argon. The reaction was monitored by ³¹P-NMR [$\delta_P(\text{reactant}) = 7.4$, $\delta_P(\text{product}) = 20.8$, $\delta_P(\text{diaryl phosphinate}) = 25.5$]. The solvent was removed under reduced pressure, dilute HCl (1 M, 10 mL) was added and the mixture extracted with EtOAc (3 x 20 mL). The organic fractions were combined, dried over MgSO₄ and concentrated to give a pale orange oil. The crude product was used in the next step without further purification; δ_H (CDCl₃) 8.03 (4H, m, H²⁻³), 7.76 (1H, d, ¹J_{P-H} 576 Hz, PH), 4.43 (2H, q, ³J_{F-H} 10 Hz, H⁷), 4.21 (2H, m, H⁵), 1.40 (3H, t, ³J_{H-H} 7.0 Hz, H⁶); δ_F (CDCl₃) -74.2 (t, ³J_{F-H} 8 Hz); δ_P (CDCl₃) +20.8; *m/z* (HRMS+) 333.0167 [M + H]⁺ (C₁₀H₁₃O₅SF₃P requires 333.0173).

2,2,2-Trifluoroethyl 3-bromobenzenesulfonate, 60

3-Bromobenzenesulfonyl chloride, **59** (5.00 g, 19.5 mmol) was dissolved in DCM (25 mL) and trifluoroethanol (1.40 mL, 19.5 mmol) was added. A solution of DABCO (2.60 g, 23.4 mmol) in DCM (15 mL) was added resulting in precipitate formation. The reaction was stirred for 1 h at RT, after which time a solution of 1 M NaOH (8 mL) was added. The reaction was diluted in EtOAc (100 mL) and washed successively with 0.5 M aq. NaHCO₃, 0.1 M HCl, water and brine. The organic layer was dried over MgSO₄ and the solvent removed under reduced pressure to give a clear oil (5.50 g, 88 %); δ_H (CDCl₃) 8.06 (1H, d, ⁴J_{H-H} 2 Hz, H²), 7.86 (1H, dd, ³J_{H-H} 8 Hz, ⁴J_{H-H} 1.5 Hz, H⁴), 7.84 (1H, d, ³J_{H-H} 8 Hz, ⁴J_{H-H} 1.5 Hz, H⁶), 7.48 (1H, t, ³J_{H-H} 8 Hz, H⁵), 4.41 (2H, q, ³J_{H-F} 8 Hz, H⁷); δ_C (CDCl₃) 137.7 (C⁶), 136.7 (C³), 131.0 (C⁵), 130.8 (C²), 126.5 (C⁴), 123.4 (C¹), 121.7 (q, *J* 278 Hz, C⁵), 64.8 (q, *J* 38 Hz, CF₃); δ_F (CDCl₃)

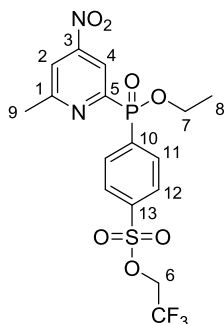
-73.8 (t, $^3J_{\text{F-H}}$ 7.0 Hz); m/z (HRMS+) 340.9078 $[\text{M} + \text{Na}]^+$ ($\text{C}_8\text{H}_6\text{O}_3\text{S}^{79}\text{BrF}_3\text{Na}$ requires 340.9071); $R_f = 0.58$ (silica, EtOAc : Hex 2 : 8).

2,2,2-Trifluoroethyl 4-(ethoxyhydrophosphoryl)benzenesulfonate, **61**



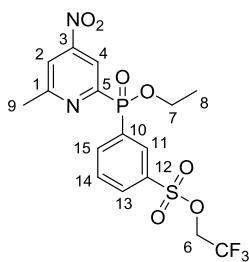
To a suspension of anilinium hypophosphite (1.20 g, 7.54 mmol) in dry toluene was added 2,2,2-trifluoroethyl 3-bromobenzenesulfonate, **60** (2.00 g, 6.27 mmol). Argon was bubbled through the solution for 30 min, then aminopropyltriethoxysilane (1.80 mL, 7.65 mmol) was added, and argon was bubbled through the solution for an additional 30 min. $\text{PdCl}_2(\text{dppf}) \cdot \text{DCM}$ (270 mg, 0.33 mmol) was added, and the mixture stirred at 100 °C for 30 min under argon. The reaction was monitored by ^{31}P -NMR [$\delta_{\text{P}}(\text{reactant}) = 7.4$, $\delta_{\text{P}}(\text{product}) = 20.2$, $\delta_{\text{P}}(\text{diaryl phosphinate}) = 24.9$]. The solvent was removed under reduced pressure, dilute HCl (1 M, 12 mL) was added and the mixture extracted with EtOAc (3 x 30 mL). The organic fractions were combined, dried over MgSO_4 and concentrated to give a pale orange oil. The crude product was used for the next step without further purification; δ_{H} (CDCl_3) 8.32 (1H, m, H^2), 8.12 (2H, m, H^4 and H^6), 7.48 (1H, t, $^3J_{\text{H-H}} = 8$ Hz, H^5), 7.67 (1H, d, $^1J_{\text{P-H}} = 576$ Hz, PH), 4.45 (2H, q, $^3J_{\text{F-H}} = 9$ Hz, H^7), 4.23 (2H, m, H^5), 1.42 (3H, t, $^3J_{\text{H-H}} = 7.0$ Hz, H^6); δ_{F} (CDCl_3) -74.2 (t, $^3J_{\text{F-H}} = 8$ Hz); δ_{P} (CDCl_3) +20.2; m/z (HRMS+) 333.0170 $[\text{M} + \text{H}]^+$ ($\text{C}_{10}\text{H}_{13}\text{O}_5\text{SF}_3\text{P}$ requires 333.0173).

2,2,2-Trifluoroethyl 4-(ethoxy(6-methyl-4-nitropyridin-2-yl)phosphoryl)benzenesulfonate, **62**



2,2,2-Trifluoroethyl 4-(ethoxyhydrophosphoryl)benzenesulfonate, **57** (1.60 g, 4.82 mmol) was added to degassed toluene (40 mL), followed by 2-bromo-6-methyl-4-nitropyridine, **10** (1.00 g, 4.61 mmol) and freshly distilled triethylamine (2.30 mL, 16.8 mmol). Argon was bubbled through the yellow solution for 30 min, then PdCl₂(dppf)·DCM (110 mg, 0.13 mmol) was added, and the mixture stirred at 120 °C for 2 h under argon, during which time the mixture turned brown. The solvent was removed under reduced pressure, with purification of the resulting black oil by column chromatography (silica, EtOAc : Hex 1:3 to 1:1) giving a colourless oil (902 mg, 40 %); δ_{H} (CDCl₃) 8.63 (1H, dd, ³J_{H-P} 6.5 ⁴J_{H-H} 1.5 Hz, H⁴), 8.24 (2H, dd, ³J_{H-P} 11.5 Hz, ³J_{H-H} 8.5 Hz, H¹¹), 8.02 (2H, dd, ³J_{H-H} 8.5 Hz, ⁴J_{H-P} 3 Hz, H¹²), 7.79 (1H, s, H²), 4.42 (2H, q, ³J_{F-H} 8 Hz, H⁶), 4.27 – 4.09 (2H, m, H⁷), 2.74 (3H, s, H⁹), 1.40 (3H, t, ³J_{H-H} 7.0 Hz, H⁸); δ_{C} (CDCl₃) 163.5 (d, ⁵J_{C-P} 21.5 Hz, C¹), 156.5 (d, ¹J_{C-P} 171 Hz, C⁵), 154.2 (d, ³J_{C-P} 13.5 Hz, C³), 138.9 (d, ⁵J_{C-P} 3.5 Hz, C¹³), 136.5 (d, ¹J_{C-P} 138 Hz, C¹⁰), 133.7 (d, ²J_{C-P} 10 Hz, C¹¹), 127.7 (d, ³J_{C-P} 13.5 Hz, C¹²), 122.1 (q, ¹J_{C-F} 281 Hz, CF₃), 118.2 (s, C²), 118.0 (d, ²J_{C-P} 9 Hz, C⁴), 64.8 (q, ²J_{C-F} 38.5 Hz, C⁶), 62.9 (d, ²J_{C-P} 6.5 Hz, C⁷), 24.8 (s, C⁹), 16.5 (d, ³J_{C-P} 6 Hz, C⁸); δ_{F} (CDCl₃) -74.2 (t, ³J_{F-H} 7 Hz); δ_{P} (CDCl₃) +20.7; *m/z* (HRMS⁺) 469.0444 [M + H]⁺ (C₁₆H₁₇N₂O₇SF₃P requires 469.0446); *R_f* = 0.70 (silica, EtOAc : Hex 2 : 1).

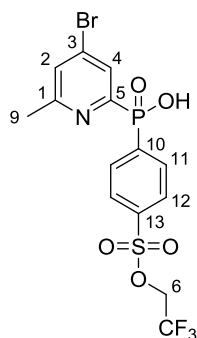
2,2,2-Trifluoroethyl 3-(ethoxy(6-methyl-4-nitropyridin-2-yl)phosphoryl)benzenesulfonate, 63



2,2,2-Trifluoroethyl-3-(ethoxyhydrophosphoryl)benzenesulfonate, **61** (1.60 g, 4.82 mmol) was added to degassed toluene (40 mL), followed by 2-bromo-6-methyl-4-nitropyridine, **10** (1.00 g, 4.61 mmol) and freshly distilled triethylamine (2.30 mL, 16.8 mmol). Argon was bubbled through the yellow solution for 30 min, then PdCl₂(dppf)·DCM (110 mg, 0.13 mmol) was added, and the mixture stirred at 120 °C overnight under argon, during which time the mixture turned brown. The solvent was removed under reduced pressure, with purification of the resulting black oil by column chromatography (silica, EtOAc : Hex 1:3 to 1:1) giving a clear oil (850 mg, 38 %); δ_{H} (CDCl₃) 8.61 (1H, dd, ³J_{H-P} 6.5 ⁴J_{H-H} 2 Hz, H⁴), 8.57 (1H, d,

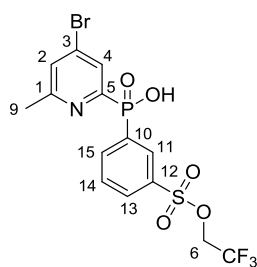
$^3J_{\text{H-P}}$ 12 Hz, H¹¹), 8.33 (1H, dd, $^3J_{\text{H-P}}$ 12 Hz, $^3J_{\text{H-H}}$ 7.5 Hz, H¹⁵), 8.09 (1H, d, $^3J_{\text{H-H}}$ 7 Hz, H¹³), 7.94 (1H, s, H²), 7.72 (1H, m, H¹⁴), 4.41 (2H, q, $^3J_{\text{F-H}}$ 8 Hz, H⁶), 4.24 – 4.11 (2H, m, H⁷), 2.71 (3H, s, H⁹), 1.38 (3H, t, $^3J_{\text{H-H}}$ 7.0 Hz, H⁸); δ_{C} (CDCl₃) 163.5 (d, $^5J_{\text{C-P}}$ 21.5 Hz, C¹), 156.5 (d, $^1J_{\text{C-P}}$ 171.5 Hz, C⁵), 154.2 (d, $^3J_{\text{C-P}}$ 14 Hz, C³), 138.4 (d, $^2J_{\text{C-P}}$ 9.5 Hz, C¹⁵), 135.7 (d, $^3J_{\text{C-P}}$ 14 Hz, C¹²), 132.1 (d, $^2J_{\text{C-P}}$ 10.5 Hz, C¹¹), 132.0 (d, $^1J_{\text{C-P}}$ 142 Hz, C¹⁰), 131.7 (d, $^4J_{\text{C-P}}$ 2.5 Hz, C¹³), 129.8 (d, $^3J_{\text{C-P}}$ 13 Hz, C¹⁴), 121.7 (q, $^1J_{\text{C-F}}$ 278 Hz, CF₃), 118.1 (d, $^4J_{\text{C-P}}$ 3 Hz, C²), 118.0 (d, $^2J_{\text{C-P}}$ 24.5 Hz, C⁴), 64.8 (q, $^2J_{\text{C-F}}$ 38.5 Hz, C⁶), 62.8 (d, $^2J_{\text{C-P}}$ 6 Hz, C⁷), 24.7 (s, C⁹), 16.4 (d, $^3J_{\text{C-P}}$ 6 Hz, C⁸); δ_{F} (CDCl₃) -74.2 (t, $^3J_{\text{F-H}}$ 7 Hz); δ_{P} (CDCl₃) + 20.4; m/z (HRMS⁺) 469.0443 [M + H]⁺ (C₁₆H₁₇N₂O₇SF₃P requires 469.0446); R_f = 0.70 (silica, EtOAc : Hex 2 : 1).

4-Bromo-6-methylpyridin-2-yl(4-(2,2,2-trifluoroethoxysulfonyl)phenyl)phosphinic acid, **62a**



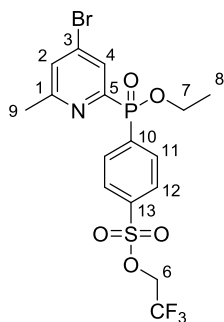
2,2,2-Trifluoroethyl 4-(ethoxy(6-methyl-4-nitropyridin-2-yl)phosphoryl)benzenesulfonate, **62** (600 mg, 1.28 mmol) was dissolved in acetyl bromide (3.0 mL, 39 mmol) and the mixture stirred at 70 °C for 16 h under argon. The brown solution was dropped cautiously into MeOH (30 mL) stirred at 0 °C. The solvent was removed under reduced pressure to yield a pale brown solid. The resulting material, containing unidentified contaminants, was used without further purification, assuming quantitative conversion to the bromophosphinic acid; δ_{H} (CDCl₃) 8.42 (1H, d, $^3J_{\text{H-P}}$ 7, H⁴), 8.31 (1H, s, H²), 8.24 (2H, dd, $^3J_{\text{H-P}}$ 12.5 Hz, $^3J_{\text{H-H}}$ 8.5 Hz, H¹¹), 8.09 (2H, dd, $^3J_{\text{H-H}}$ 8.5 Hz, $^4J_{\text{H-P}}$ 2 Hz, H¹²), 4.66 (2H, q, $^3J_{\text{F-H}}$ 8 Hz, H⁶), 2.81 (3H, s, H⁹); δ_{C} (CDCl₃) 158.0 (d, $^5J_{\text{C-P}}$ 8 Hz, C¹), 151.0 (d, $^1J_{\text{C-P}}$ 134 Hz, C⁵), 143.5 (d, $^3J_{\text{C-P}}$ 10.5 Hz, C³), 138.9 (s, C¹³), 138.8 (d, $^1J_{\text{C-P}}$ 155 Hz, C¹⁰), 133.4 (s, C²), 133.3 (d, $^2J_{\text{C-P}}$ 11 Hz, C¹¹), 131.5 (d, $^2J_{\text{C-P}}$ 12 Hz, C⁴), 128.0 (d, $^3J_{\text{C-P}}$ 14 Hz, C¹²), 122.2 (q, $^1J_{\text{C-F}}$ 277 Hz, CF₃), 65.1 (q, $^2J_{\text{C-F}}$ 37.5 Hz, C⁶), 19.0 (s, C⁹); δ_{F} (CDCl₃) -76.0 (t, $^3J_{\text{F-H}}$ 7 Hz); δ_{P} (CDCl₃) + 8.1; m/z (HRMS⁺) 473.9390 [M + H]⁺ (C₁₄H₁₃NO₅F₃PS⁷⁹Br requires 473.9388).

4-Bromo-6-methylpyridin-2-yl(3-(2,2,2-trifluoroethoxysulfonyl)phenyl)phosphinic acid, 63a



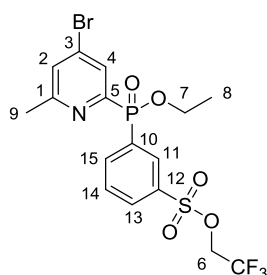
2,2,2-Trifluoroethyl-3-(ethoxy(6-methyl-4-nitropyridin-2-yl)phosphoryl)benzenesulfonate, **63** (300 mg, 0.64 mmol) was dissolved in acetyl bromide (2 mL) and the mixture stirred at 70 °C for 16 h under argon. The brown solution was dropped cautiously into MeOH (20 mL) stirred at 0 °C. The solvent was removed under reduced pressure to yield a pale brown solid. The resulting material, containing unidentified contaminants, was used without further purification, assuming quantitative conversion to the bromo-phosphinic acid; δ_{H} (CD_3OD) 8.53 (1H, d, $^3J_{\text{H-P}}$ 13, H^{11}), 8.46 (1H, d, $^3J_{\text{H-P}}$ 6.5 Hz, H^4), 8.40 (1H, m, H^{15}), 8.38 (1H, s, H^2), 8.18 (1H, d, $^3J_{\text{H-H}}$ 7.5 Hz, H^{13}), 7.91 (1H, td, $^3J_{\text{H-H}}$ 8 Hz, $^4J_{\text{H-P}}$ 3 Hz, H^{14}), 4.70 (2H, q, $^3J_{\text{F-H}}$ 8 Hz, H^6), 2.88 (3H, s, H^9); δ_{C} (CD_3OD) 158.1 (d, $^5J_{\text{C-P}}$ 7.5 Hz, C^1), 149.9 (d, $^1J_{\text{C-P}}$ 131 Hz, C^5), 144.2 (d, $^3J_{\text{C-P}}$ 11 Hz, C^3), 138.3 (d, $^2J_{\text{C-P}}$ 11 Hz, C^{15}), 135.8 (d, $^3J_{\text{C-P}}$ 15 Hz, C^{12}), 134.7 (C^2), 133.6 (d, $^1J_{\text{C-P}}$ 148 Hz, C^{10}), 132.1 (d, $^4J_{\text{C-P}}$ 2.5 Hz, C^{13}), 131.8 (d, $^2J_{\text{C-P}}$ 11.5 Hz, C^4), 131.3 (d, $^2J_{\text{C-P}}$ 12 Hz, C^{11}), 130.9 (d, $^3J_{\text{C-P}}$ 13.5 Hz, C^{14}), 122.3 (q, $^1J_{\text{C-F}}$ 277 Hz, CF_3), 65.4 (q, $^2J_{\text{C-F}}$ 37.5 Hz, C^6), 19.4 (s, C^9); δ_{F} (CD_3OD) -76.0 (t, $^3J_{\text{F-H}}$ 7 Hz); δ_{P} (CD_3OD) + 8.0; m/z (HRMS^+) 473.9388 [$\text{M} + \text{H}$] $^+$ ($\text{C}_{14}\text{H}_{13}\text{NO}_5\text{F}_3\text{PS}^{79}\text{Br}$ requires 473.9388).

2,2,2-Trifluoroethyl 4-((4-bromo-6-methylpyridin-2-yl)(ethoxy)phosphoryl)benzenesulfonate, 64



4-Bromo-6-methylpyridin-2-yl(4-(2,2,2-trifluoroethoxysulfonyl)phenyl)phosphinic acid, **62a** (606 mg, 1.28 mmol) was added to $\text{HC}(\text{OCH}_2\text{CH}_3)_3$ (25 mL) and the mixture stirred at 140 °C for 16 h under argon. The solvent was removed under reduced pressure and the resulting residue was purified by column chromatography (silica, DCM : 1 % MeOH) to yield a yellow oil (530 mg, 81 % over two steps); δ_{H} (CDCl_3) 8.22 (2H, dd, $^3J_{\text{H-P}}$ 11.5 Hz, $^3J_{\text{H-H}}$ 8.5 Hz, H^{11}), 8.11 (1H, dd, $^3J_{\text{H-P}}$ 6.5, $^4J_{\text{H-H}}$ 1.5 Hz, H^4), 8.00 (2H, dd, $^3J_{\text{H-H}}$ 8.5 Hz, $^4J_{\text{H-P}}$ 3 Hz, H^{12}), 7.45 (1H, s, H^2), 4.40 (2H, q, $^3J_{\text{F-H}}$ 8 Hz, H^6), 4.23 – 4.08 (2H, m, H^7), 2.54 (3H, s, H^9), 1.37 (3H, t, $^3J_{\text{H-H}}$ 7 Hz, H^8); δ_{C} (CDCl_3) 161.3 (d, $^5J_{\text{C-P}}$ 22 Hz, C^1), 153.8 (d, $^1J_{\text{C-P}}$ 169 Hz, C^5), 138.5 (d, $^5J_{\text{C-P}}$ 3 Hz, C^{13}), 137.3 (d, $^1J_{\text{C-P}}$ 136 Hz, C^{10}), 133.7 (s, C^3), 133.6 (d, $^2J_{\text{C-P}}$ 10 Hz, C^{11}), 129.2 (s, $^4J_{\text{C-P}}$ 3 Hz, C^2), 129.0 (d, $^2J_{\text{C-P}}$ 24 Hz, C^4), 127.5 (d, $^3J_{\text{C-P}}$ 13 Hz, C^{12}), 121.7 (q, $^1J_{\text{C-F}}$ 278 Hz, CF_3), 64.8 (q, $^2J_{\text{C-F}}$ 38.5 Hz, C^6), 62.6 (d, $^2J_{\text{C-P}}$ 6.5 Hz, C^7), 24.3 (s, C^9), 16.4 (d, $^3J_{\text{C-P}}$ 6.5 Hz, C^8); δ_{F} (CDCl_3) -74.2 (t, $^3J_{\text{F-H}}$ 7 Hz); δ_{P} (CDCl_3) +21.5; m/z (HRMS^+) 501.9690 [$\text{M} + \text{H}]^+$ ($\text{C}_{16}\text{H}_{17}\text{NO}_5\text{F}_3\text{PS}^{79}\text{Br}$ requires 501.9701); $R_f = 0.50$ (silica, DCM : MeOH 96 : 4).

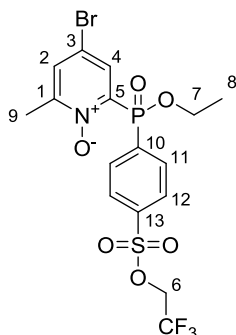
2,2,2-Trifluoroethyl 3-((4-bromo-6-methylpyridin-2-yl)(ethoxy)phosphoryl)benzenesulfonate, 65



4-Bromo-6-methylpyridin-2-yl(3-(2,2,2-trifluoroethoxysulfonyl)phenyl)phosphinic acid, **63a** (300 mg, 0.64 mmol) was added to $\text{HC}(\text{OCH}_2\text{CH}_3)_3$ (13 mL) and the mixture stirred at 140 °C for 16 h under argon. The solvent was removed under reduced pressure and the resulting residue was purified by column chromatography (silica, DCM : 1 % MeOH) to yield a yellow oil (256 mg, 77 % over two steps); δ_{H} (CDCl_3) 8.58 (1H, dt, $^3J_{\text{H-P}}$ 11.5, $^4J_{\text{H-H}}$ 1.5, H^{11}), 8.32 (1H, m, H^{15}), 8.11 (1H, d, $^3J_{\text{H-P}}$ 6.5 Hz, H^4), 8.07 (1H, dd, $^3J_{\text{H-H}}$ 8 Hz, $^4J_{\text{H-H}}$ 2 Hz, H^{13}), 7.69 (1H, td, $^3J_{\text{H-H}}$ 8 Hz, $^4J_{\text{H-P}}$ 3 Hz, H^{14}), 7.43 (1H, s, H^2), 4.40 (2H, qd, $^3J_{\text{F-H}}$ 8 Hz, $^2J_{\text{H-H}}$ 3.5 Hz, H^6), 4.12 (2H, m, H^7), 2.52 (3H, s, H^9), 1.36 (3H, t, $^3J_{\text{H-H}}$ 7 Hz, H^8); δ_{C} (CDCl_3) 161.3 (d, $^5J_{\text{C-P}}$ 22 Hz, C^1), 153.8 (d, $^1J_{\text{C-P}}$ 169.5 Hz, C^5), 138.3 (d, $^2J_{\text{C-P}}$ 9.5 Hz, C^{15}), 135.4 (d, $^3J_{\text{C-P}}$ 14 Hz, C^{12}), 133.6 (d, $^3J_{\text{C-P}}$ 15.5 Hz, C^3), 132.6 (d, $^1J_{\text{C-P}}$ 139 Hz, C^{10}), 132.1 (d, $^2J_{\text{C-P}}$ 10.5 Hz, C^{11}), 131.4 (d, $^4J_{\text{C-P}}$ 2.5 Hz, C^{13}), 129.6 (d, $^3J_{\text{C-P}}$ 12.5 Hz, C^{14}), 129.1 (d, $^4J_{\text{C-P}}$ 3 Hz, C^2), 128.9 (d,

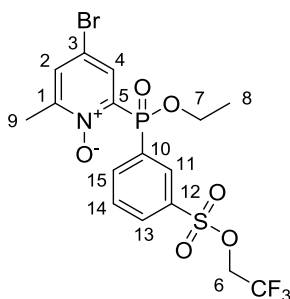
$^2J_{C-P}$ 24 Hz, C^4), 121.7 (q, $^1J_{C-F}$ 278 Hz, CF_3), 64.8 (q, $^2J_{C-F}$ 38 Hz, C^6), 62.5 (d, $^2J_{C-P}$ 6 Hz, C^7), 24.2 (C^9), 16.4 (d, $^3J_{C-P}$ 6 Hz, C^8); δ_F ($CDCl_3$) -74.2 (t, $^3J_{F-H}$ 7 Hz); δ_P ($CDCl_3$) + 21.1; m/z (HRMS $^+$) 501.9693 [$M + H$] $^+$ ($C_{16}H_{17}NO_5F_3PS^{79}Br$ requires 501.9701); R_f = 0.50 (silica, DCM : MeOH 96 : 4).

4-Bromo-2-(ethoxy(4-(2,2,2-trifluoroethoxysulfonyl)phenyl)phosphoryl)-6-methylpyridine 1-oxide, **66**



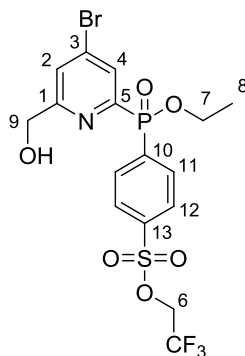
2,2,2-Trifluoroethyl 4-((4-bromo-6-methylpyridin-2-yl)(ethoxy)phosphoryl)benzenesulfonate, **64** (530 mg, 1.06 mmol) was dissolved in $CHCl_3$ (15 mL). 3-Chloroperbenzoic acid (345 mg, 2.01 mmol) was added and the solution stirred at 65 °C for 16 h. The solvent was then removed under reduced pressure, with the resulting material being re-dissolved in DCM (15 mL), and washed with aqueous $NaHCO_3$ (0.5 M, 10 mL). The aqueous layer was re-extracted with DCM (3×10 mL), the organic extracts combined, dried over $MgSO_4$, and the solvent removed under reduced pressure to afford a yellow oil (475 mg, 91 %); δ_H ($CDCl_3$) 8.25 (2H, dd, $^3J_{H-P}$ 13 Hz, $^3J_{H-H}$ 8.5 Hz, H^{11}), 8.12 (1H, dd, $^3J_{H-P}$ 8, $^4J_{H-H}$ 3 Hz, H^4), 7.99 (2H, dd, $^3J_{H-H}$ 8.5 Hz, $^4J_{H-P}$ 3 Hz, H^{12}), 7.55 (1H, d, $^5J_{H-P}$ 2.5 Hz, H^2), 4.40 (2H, q, $^3J_{F-H}$ 8 Hz, H^6), 4.26 – 4.16 (2H, m, H^7), 2.37 (3H, s, H^9), 1.40 (3H, t, $^3J_{H-H}$ 7.0 Hz, H^8); δ_C ($CDCl_3$) 150.9 (s, C^1), 142.8 (d, $^1J_{C-P}$ 153 Hz, C^5), 138.7 (s, C^{13}), 136.3 (d, $^1J_{C-P}$ 151 Hz, C^{10}), 134.2 (d, $^2J_{C-P}$ 11.5 Hz, C^{11}), 133.2 (d, $^2J_{C-P}$ 11 Hz, C^4), 132.7 (s, C^2), 127.4 (d, $^3J_{C-P}$ 14.5 Hz, C^{12}), 124.1 (s, C^3), 121.6 (q, $^1J_{C-F}$ 274 Hz, CF_3), 64.8 (q, $^2J_{C-F}$ 38.5 Hz, C^6), 63.0 (d, $^2J_{C-P}$ 6 Hz, C^7), 17.2 (s, C^9), 16.5 (d, $^3J_{C-P}$ 6 Hz, C^8); δ_F ($CDCl_3$) -74.2 (t, $^3J_{F-H}$ 8 Hz); δ_P ($CDCl_3$) + 17.2; m/z (HRMS $^+$) 517.9650 [$M + H$] $^+$ ($C_{16}H_{17}NO_6PS^{79}BrF_3$ requires 517.9650); R_f = 0.49 (silica, DCM : MeOH 96 : 4).

4-Bromo-2-(ethoxy(3-(2,2,2-trifluoroethoxysulfonyl)phenyl)phosphoryl)-6-methylpyridine 1-oxide, 67



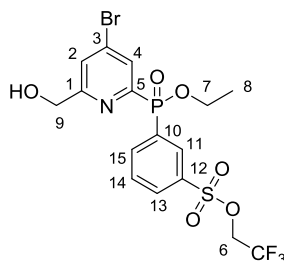
2,2,2-Trifluoroethyl 3-((4-bromo-6-methylpyridin-2-yl)(ethoxy)phosphoryl)benzenesulfonate, **65** (350 mg, 0.70 mmol) was dissolved in CHCl_3 (10 mL). 3-Chloroperbenzoic acid (240 mg, 1.39 mmol) was added and the solution stirred at 65 °C for 16 h. The solvent was removed under reduced pressure, with the resulting material being re-dissolved in DCM (15 mL), and washed with aqueous NaHCO_3 (0.5 M, 10 mL). The aqueous layer was re-extracted with DCM (3×10 mL), the organic extracts combined, dried over MgSO_4 , and the solvent removed under reduced pressure giving a yellow oil (320 mg, 85 %); δ_{H} (CDCl_3) 8.53 (1H, dt, $^3J_{\text{H-P}}$ 13.5, $^4J_{\text{H-H}}$ 1.5, H^{11}), 8.36 (1H, m, H^{15}), 8.09 (1H, dd, $^3J_{\text{H-P}}$ 8 Hz, $^4J_{\text{H-H}}$ 3 Hz, H^4), 8.05 (1H, d, $^3J_{\text{H-H}}$ 8 Hz, H^{13}), 7.68 (1H, td, $^3J_{\text{H-H}}$ 8 Hz, $^4J_{\text{H-P}}$ 3.5 Hz, H^{14}), 7.52 (1H, d, $^4J_{\text{H-H}}$ 3 Hz, H^2), 4.41 (2H, m, H^6), 4.18 (2H, m, H^7), 2.30 (3H, s, H^9), 1.38 (3H, t, $^3J_{\text{H-H}}$ 7 Hz, H^8); δ_{C} (CDCl_3) 150.8 (d, $^5J_{\text{C-P}}$ 4.5 Hz, C^1), 142.7 (d, $^1J_{\text{C-P}}$ 154 Hz, C^5), 139.2 (d, $^2J_{\text{C-P}}$ 10.5 Hz, C^{15}), 134.8 (d, $^3J_{\text{C-P}}$ 15.5 Hz, C^{12}), 133.1 (d, $^2J_{\text{C-P}}$ 11 Hz, C^4), 132.8 (d, $^2J_{\text{C-P}}$ 12.5 Hz, C^{11}), 132.7 (d, $^4J_{\text{C-P}}$ 2 Hz, C^2), 131.8 (d, $^4J_{\text{C-P}}$ 2.5 Hz, C^{13}), 131.4 (d, $^1J_{\text{C-P}}$ 129 Hz, C^{10}), 129.5 (d, $^3J_{\text{C-P}}$ 14 Hz, C^{14}), 121.8 (q, $^1J_{\text{C-F}}$ 278 Hz, CF_3), 117.9 (d, $^3J_{\text{C-P}}$ 13 Hz, C^3), 65.0 (q, $^2J_{\text{C-F}}$ 38 Hz, C^6), 62.9 (d, $^2J_{\text{C-P}}$ 6 Hz, C^7), 17.0 (C^9), 16.4 (d, $^3J_{\text{C-P}}$ 6 Hz, C^8); δ_{F} (CDCl_3) -74.2 (t, $^3J_{\text{F-H}}$ 7 Hz); δ_{P} (CDCl_3) + 17.0; m/z (HRMS⁺) 517.9653 [$\text{M} + \text{H}$]⁺ ($\text{C}_{16}\text{H}_{17}\text{NO}_6\text{PS}^{79}\text{BrF}_3$ requires 517.9650); R_f = 0.49 (silica, DCM : MeOH 96 : 4).

2,2,2-Trifluoroethyl-4-((4-bromo-6-(hydroxymethyl)pyridin-2-yl)(ethoxy)phosphoryl)benzenesulfonate, 68



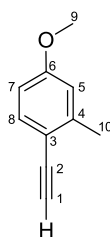
Trifluoroacetic anhydride (2.5 mL) was added to a solution of 4-bromo-2-(ethoxy(4-(2,2,2-trifluoroethoxysulfonyl)phenyl)phosphoryl)-6-methylpyridine 1-oxide, **66** (475 mg, 0.91 mmol) in anhydrous CHCl_3 (20 mL). The reaction mixture was heated to 60 °C for 3 h under argon. The solvent was removed under reduced pressure and the resulting oil was dissolved in EtOH (15 mL) and H_2O (15 mL) and stirred for 1 h. After this time, the solution was concentrated (ca. 15 mL) and extracted with DCM (3 \times 30 mL). The organic extracts were combined, dried over MgSO_4 , and the solvent removed under reduced pressure, giving a clear oil (430 mg, 91 %); δ_{H} (CDCl_3) 8.19-8.13 (3H, m, H^{4-11}), 8.00 (2H, dd, $^3J_{\text{H-H}}$ 8.5 Hz, $^4J_{\text{H-P}}$ 2.5 Hz, H^{12}), 7.72 (1H, s, H^2), 6.83 (1H, br, OH), 4.76 (2H, s, H^9), 4.41 (2H, q, $^3J_{\text{F-H}}$ 8 Hz, H^6), 4.29-4.04 (2H, m, H^7), 1.37 (3H, t, $^3J_{\text{H-H}}$ 7 Hz, H^8); δ_{C} (CDCl_3) 163.1 (s, $^5J_{\text{C-P}}$ 20.5 Hz, C^1), 152.8 (d, $^1J_{\text{C-P}}$ 169 Hz, C^5), 139.0 (d, $^4J_{\text{C-P}}$ 3 Hz C^{13}), 136.2 (d, $^1J_{\text{C-P}}$ 138.5 Hz, C^{10}), 134.6 (d, $^3J_{\text{C-P}}$ 15 Hz, C^3), 133.5 (d, $^2J_{\text{C-P}}$ 10.5 Hz, C^{11}), 130.3 (d, $^2J_{\text{C-P}}$ 23.5 Hz, C^4), 127.8 (d, $^3J_{\text{C-P}}$ 13.5 Hz, C^{12}), 126.8 (d, $^4J_{\text{C-P}}$ 3 Hz, C^2), 122.8 (q, $^1J_{\text{C-F}}$ 274 Hz, CF_3), 64.9 (q, $^2J_{\text{C-F}}$ 38.5 Hz, C^6), 64.0 (s, C^9), 63.2 (d, $^2J_{\text{C-P}}$ 6.5 Hz, C^7), 16.4 (d, $^3J_{\text{C-P}}$ 6 Hz, C^8); δ_{F} (CDCl_3) -74.2 (t, $^3J_{\text{F-H}}$ 8 Hz); δ_{P} (CDCl_3) +22.1; m/z (HRMS^+) 517.9647 [$\text{M} + \text{H}$] $^+$ ($\text{C}_{16}\text{H}_{17}\text{NO}_6\text{PS}^{79}\text{BrF}_3$ requires 517.9650); R_f = 0.56 (silica, DCM : MeOH 96 : 4).

2,2,2-Trifluoroethyl-3-((4-bromo-6-(hydroxymethyl)pyridin-2-yl)(ethoxy)phosphoryl)benzenesulfonate, 69



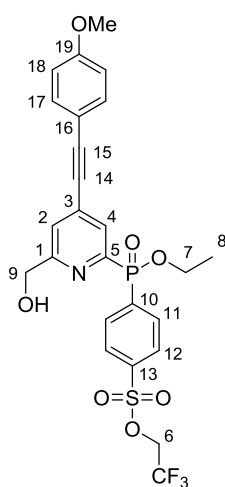
Trifluoroacetic anhydride (1.70 mL) was added to a solution of 4-bromo-2-(ethoxy(3-(2,2,2-trifluoroethoxysulfonyl)phenyl)phosphoryl)-6-methylpyridine 1-oxide, **67** (310 mg, 0.60 mmol) in dry CHCl_3 (15 mL). The reaction mixture was heated to 60 °C for 3 h under argon. The solvent was removed under reduced pressure and the resulting oil was dissolved in EtOH (12 mL) and H_2O (12 mL) and stirred for 1 h. After this time, the solution was concentrated (ca. 15 mL) and extracted with DCM (3×30 mL). The organic extracts were combined, dried over MgSO_4 , the solvent removed under reduced pressure and the resulting residue was purified by column chromatography (silica, DCM : MeOH 100 : 0 to 97 : 3) to yield a clear oil (220 mg, 70 %); δ_{H} (CDCl_3) 8.55 (1H, dt, $^3J_{\text{H-P}}$ 12, $^4J_{\text{H-H}}$ 1.5, H^{11}), 8.29 (1H, m, H^{15}), 8.19 (1H, dd, $^3J_{\text{H-P}}$ 6.5 Hz, $^4J_{\text{H-H}}$ 2 Hz, H^4), 8.08 (1H, d, $^3J_{\text{H-H}}$ 8 Hz, H^{13}), 7.71 (1H, td, $^3J_{\text{H-H}}$ 8 Hz, $^4J_{\text{H-P}}$ 3 Hz, H^{14}), 7.66 (1H, s, H^2), 6.72 (1H, br, OH), 4.75 (2H, s, H^9), 4.43 (2H, m, H^6), 4.16 (2H, m, H^7), 1.37 (3H, t, $^3J_{\text{H-H}}$ 7 Hz, H^6); δ_{C} (CDCl_3) 162.7 (d, $^5J_{\text{C-P}}$ 20.5 Hz, C^1), 153.3 (d, $^1J_{\text{C-P}}$ 168.5 Hz, C^5), 138.2 (d, $^2J_{\text{C-P}}$ 10 Hz, C^{15}), 135.7 (d, $^3J_{\text{C-P}}$ 14 Hz, C^{12}), 134.5 (d, $^3J_{\text{C-P}}$ 14.5 Hz, C^3), 132.0 (d, $^1J_{\text{C-P}}$ 128.5 Hz, C^{10}), 131.9 (d, $^2J_{\text{C-P}}$ 11 Hz, C^{11}), 131.7 (d, $^4J_{\text{C-P}}$ 2.5 Hz, C^{13}), 130.3 (d, $^2J_{\text{C-P}}$ 23.5 Hz, C^4), 129.8 (d, $^3J_{\text{C-P}}$ 12.5 Hz, C^{14}), 126.5 (d, $^4J_{\text{C-P}}$ 3 Hz, C^2), 121.8 (q, $^1J_{\text{C-F}}$ 278 Hz, CF_3), 64.8 (q, $^2J_{\text{C-F}}$ 38 Hz, C^6), 64.0 (C^9), 62.8 (d, $^2J_{\text{C-P}}$ 6 Hz, C^7), 16.4 (d, $^3J_{\text{C-P}}$ 6 Hz, C^8); δ_{F} (CDCl_3) -74.3 (t, $^3J_{\text{F-H}}$ 7 Hz); δ_{P} (CDCl_3) + 21.9; m/z (HRMS⁺) 517.9646 [$\text{M} + \text{H}$]⁺ ($\text{C}_{16}\text{H}_{17}\text{NO}_6\text{PS}^{79}\text{BrF}_3$ requires 517.9650); R_f = 0.56 (silica, DCM : MeOH 96 : 4).

1-Ethynyl-4-methoxy-2-methylbenzene



3-Methyl-4-bromoanisole (700 mg, 3.48 mmol) was dissolved in anhydrous THF (12 mL) and the solution was degassed (freeze-thaw cycle) three times. Ethynyltrimethylsilane (0.74 mL, 5.24 mmol) and triethylamine (2.40 mL, 17.4 mmol) were added and the solution was degassed (freeze-thaw cycle) once more. [1,1-Bis(diphenylphosphino)ferrocene]dichloropalladium(II) (400 mg, 0.49 mmol) and CuI (66 mg, 0.35 mmol) were added and the resulting brown solution was stirred at 65 °C under argon for 16 h. The solvent was removed under reduced pressure and the resulting brown oil was purified by column chromatography (silica, Hex : DCM 10:0 to 10:1) to give (4-methoxy-2-methylphenylethynyl)trimethylsilane as a yellow oil (440 mg, 58 %); $R_f = 0.49$ (silica, Hex : DCM 3:1). This compound (440 mg, 2.0 mmol) was immediately dissolved in anhydrous THF (5 mL) and triethylammonium dihydrofluoride (3.3 mL, 20 mmol) was added. The mixture was stirred at 35 °C under argon for 48 h. The solvent was removed under reduced pressure to give a yellow oil which was subjected to column chromatography (silica, Hex : DCM 3:1), to afford 1-ethynyl-4-methoxy-2-methylbenzene as a colourless oil (200 mg, 68%); δ_H (CDCl₃) 7.39 (1H, d, $^3J_{H-H}$ 8.6 Hz, H⁸), 6.74 (1H, d, $^4J_{H-H}$ 2.6 Hz, H⁵), 6.68 (1H, dd, $^3J_{H-H}$ 8.6 Hz, $^4J_{H-H}$ 2.6 Hz, H⁷), 3.80 (3H, s, H¹⁰), 3.19 (1H, s, H¹), 2.43 (3H, s, H⁹); δ_C (151 MHz, CDCl₃) δ 160.0 (C⁶), 142.7 (C⁴), 134.0 (C⁸), 115.2 (C⁵), 114.3 (C³), 111.3 (C⁷), 82.7 (C²), 79.6 (C¹), 55.4 (C⁹), 21.0 (C¹⁰); (HRMS⁻) m/z 145.0667 [M - H]⁻ (C₁₀H₉O requires 145.0653); $R_f = 0.46$ (silica; Hex : DCM 2 : 1).

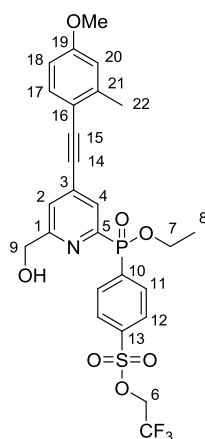
2,2,2-Trifluoroethyl-4-(ethoxy(6-(hydroxymethyl)-4-((4-methoxyphenyl)ethynyl)pyridin-2-yl)phosphoryl)benzenesulfonate, 70



2,2,2-Trifluoroethyl 4-((4-bromo-6-(hydroxymethyl)pyridin-2-yl)(ethoxy)phosphoryl)benzenesulfonate, **68** (200 mg, 0.39 mmol) was dissolved in dry THF

the crude material purified by column chromatography (silica, DCM : MeOH 0 to 2 %) to give an orange oil (140 mg, 49 %); δ_{H} (CDCl_3) 8.57 (1H, d, $^3J_{\text{H-P}}$ 10, H^{11}), 8.31 (1H, m, H^{15}), 8.11 (1H, s, H^4), 8.08 (1H, d, $^3J_{\text{H-H}}$ 7.5 Hz, H^{13}), 7.71 (1H, t, $^3J_{\text{H-H}}$ 8 Hz, H^{14}), 7.47 (3H, m, H^{17-2}), 6.89 (2H, d, $^3J_{\text{H-H}}$ 8.5 Hz, H^{18}), 4.75 (2H, s, H^9), 4.42 (2H, m, H^6), 4.16 (2H, m, H^7), 3.83 (3H, s, OMe), 3.34 (1H, br, OH), 1.39 (3H, t, $^3J_{\text{H-H}}$ 6.5 Hz, H^8); δ_{C} (CDCl_3) 160.8 (s, C^1), 160.7 (s, C^{19}), 151.9 (d, $^1J_{\text{C-P}}$ 169 Hz, C^5), 138.1 (s, C^{12}), 135.6 (d, $^2J_{\text{C-P}}$ 14 Hz, C^{15}), 133.7 (s, C^{17}), 132.7 (d, $^1J_{\text{C-P}}$ 140 Hz, C^{10}), 131.9 (d, $^2J_{\text{C-P}}$ 11 Hz, C^{11}), 131.6 (s, C^3), 131.5 (s, C^{13}), 129.8 (d, $^3J_{\text{C-P}}$ 13 Hz, C^{14}), 128.7 (d, $^2J_{\text{C-P}}$ 23 Hz, C^4), 124.5 (s, C^2), 121.7 (q, $^1J_{\text{C-F}}$ 278 Hz, CF_3), 114.3 (s, C^{18}), 113.5 (s, C^{16}), 96.7 (s, C^{24}), 85.0 (s, C^{23}), 64.9 (q, $^2J_{\text{C-F}}$ 39 Hz, C^6), 64.0 (s, C^9), 62.6 (d, $^2J_{\text{C-P}}$ 6 Hz, C^7), 55.4 (s, OMe), 16.5 (s, C^8); δ_{F} (CDCl_3) -74.2 (t, $^3J_{\text{F-H}}$ 8 Hz); δ_{P} (CDCl_3) + 22.1; m/z (HRMS⁺) 570.0968 [$\text{M} + \text{H}$]⁺ ($\text{C}_{25}\text{H}_{24}\text{F}_3\text{NO}_7\text{PS}$ requires 570.0963); R_f = 0.61 (silica, DCM : MeOH 95 : 5).

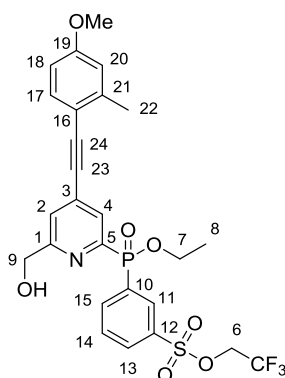
2,2,2-Trifluoroethyl-4-(ethoxy(6-(hydroxymethyl)-4-((4-methoxy-2-methylphenyl)ethynyl)pyridin-2-yl)phosphoryl)benzenesulfonate, 72



2,2,2-Trifluoroethyl 4-((4-bromo-6-(hydroxymethyl)pyridin-2-yl)(ethoxy)phosphoryl)benzenesulfonate, **68** (230 mg, 0.44 mmol) was dissolved in dry THF (2 mL) and the solution was degassed (freeze-thaw cycle) three times. 1-Ethynyl-4-methoxy-2-methylbenzene (100 mg, 0.66 mmol) and NEt_3 (1.2 mL) were added and the solution degassed once more. [1,1'-Bis(diphenylphosphino)ferrocene]palladium(II) chloride (51 mg, 63 μmol) and CuI (8 mg, 42 μmol) were added and the solution was degassed a further three times. The solution was stirred at 65 °C under argon for 16 h, the solvent was removed under reduced pressure and the crude material purified by column chromatography (silica, DCM : MeOH 0 to 2 %) to give a pale orange oil (185 mg, 72 %); δ_{H} (CDCl_3) 8.19 (2H, dd, $^3J_{\text{H-P}}$ 11

Hz, $^3J_{\text{H-H}}$ 8 Hz, H¹¹), 8.08 (1H, s, H⁴), 7.98 (2H, d, $^3J_{\text{H-H}}$ 8 Hz, H¹²), 7.48 (1H, s, H²), 7.41 (1H, d, $^3J_{\text{H-H}}$ 8.5 Hz, H¹⁷), 6.76 (1H, d, $^4J_{\text{H-H}}$ 2.5 Hz, H²⁰), 6.72 (1H, dd, $^3J_{\text{H-H}}$ 8.5 Hz, $^4J_{\text{H-H}}$ 2.5 Hz, H¹⁸), 4.76 (2H, s, H⁹), 4.39 (2H, q, $^3J_{\text{F-H}}$ 8 Hz, H⁶), 4.16 (2H, m, H⁷), 3.80 (3H, s, OMe), 3.57 (1H, br, OH), 2.46 (3H, s, H²²), 1.38 (3H, t, $^3J_{\text{H-H}}$ 7 Hz, H⁸); δ_{C} (CDCl₃) 161.1 (s, C¹), 160.7 (s, C¹⁹), 151.8 (d, $^1J_{\text{C-P}}$ 168 Hz, C⁵), 142.9 (s, C²¹), 138.6 (s, C¹³), 137.3 (d, $^1J_{\text{C-P}}$ 137 Hz, C¹⁰), 134.0 (s, C¹⁷), 133.4 (d, $^2J_{\text{C-P}}$ 9 Hz, C¹¹), 133.3 (s, C³), 128.9 (s, C⁴), 127.6 (d, $^4J_{\text{C-P}}$ 13 Hz, C¹²), 124.3 (s, C²), 121.7 (q, $^1J_{\text{C-F}}$ 279 Hz, CF₃), 115.3 (s, C²⁰), 113.4 (s, C¹⁶), 111.6 (s, C¹⁸), 95.8 (s, C¹⁵), 88.7 (s, C¹⁴), 64.8 (q, $^2J_{\text{C-F}}$ 38.5 Hz, C⁶), 64.1 (s, C⁹), 62.6 (d, $^2J_{\text{C-P}}$ 6 Hz, C⁷), 55.3 (s, OMe), 21.0 (s, C²²), 16.5 (s, C⁸); δ_{F} (CDCl₃) -74.2 (t, $^3J_{\text{F-H}}$ 8 Hz); δ_{P} (CDCl₃) + 22.6; m/z (HRMS⁺) 584.1111 [M + H]⁺ (C₂₆H₂₆F₃NO₇PS requires 584.1120); R_f = 0.52 (silica, DCM : MeOH 97 : 3).

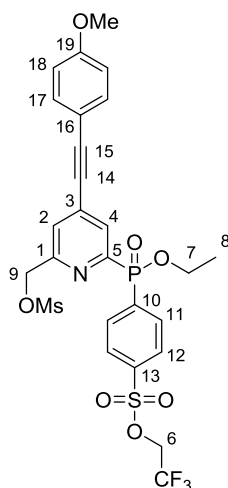
2,2,2-Trifluoroethyl 3-(ethoxy(6-(hydroxymethyl)-4-((4-methoxy-2-methylphenyl)ethynyl)pyridin-2-yl)phosphoryl)benzenesulfonate, 73



2,2,2-Trifluoroethyl 3-((4-bromo-6-(hydroxymethyl)pyridin-2-yl)(ethoxy)phosphoryl)benzenesulfonate, **69** (160 mg, 0.31 mmol) was dissolved in dry THF (1.5 mL) and the solution was degassed (freeze-thaw cycle) three times. 1-Ethynyl-4-methoxy-2-methylbenzene (68 mg, 0.47 mmol) and NEt₃ (0.90 mL) were added and the solution degassed once more. [1,1'-Bis(diphenylphosphino)ferrocene]palladium(II) chloride (36 mg, 58 μmol) and CuI (6 mg, 31 μmol) were added and the solution was degassed a further three times. The solution was stirred at 65 °C under argon for 16 h, the solvent was removed under reduced pressure and the crude material purified by column chromatography (silica, DCM : MeOH 0 – 2 %) to give an orange oil (90 mg, 50 %); δ_{H} (CDCl₃) 8.57 (1H, d, $^3J_{\text{H-P}}$ 11.5, H¹¹), 8.31 (1H, m, H¹⁵), 8.10 (1H, d, $^3J_{\text{H-P}}$ 6 Hz, H⁴), 8.07 (1H, d, $^3J_{\text{H-H}}$ 8 Hz, H¹³), 7.70 (1H, td, $^3J_{\text{H-H}}$ 8 Hz, $^4J_{\text{H-P}}$ 3 Hz, H¹⁴), 7.46 (1H, s, H²) 7.42 (1H, d, $^3J_{\text{H-H}}$ 8.5 Hz, H¹⁷),

6.77 (1H, d, $^4J_{\text{H-H}}$ 2.5 Hz, H²⁰), 6.72 (1H, dd, $^3J_{\text{H-H}}$ 8.5 Hz, $^4J_{\text{H-H}}$ 2.5 Hz, H¹⁸), 4.75 (2H, s, H⁹), 4.35 (2H, m, H⁶), 4.16 (2H, m, H⁷), 3.80 (3H, s, OMe), 3.44 (1H, br, OH), 2.47 (3H, s, H²²), 1.38 (3H, t, $^3J_{\text{H-H}}$ 7 Hz, H⁸); δ_{C} (CDCl₃) 161.0 (d, $^4J_{\text{C-P}}$ 19 Hz, C¹), 160.7 (s, C¹⁹), 151.9 (d, $^1J_{\text{C-P}}$ 169 Hz, C⁵), 142.9 (s, C²¹), 138.1 (d, $^2J_{\text{C-P}}$ 10 Hz, C¹⁵), 135.6 (d, $^3J_{\text{C-P}}$ 14 Hz, C¹²), 134.0 (s, C¹⁷), 132.7 (d, $^1J_{\text{C-P}}$ 140 Hz, C¹⁰), 131.9 (d, $^2J_{\text{C-P}}$ 11 Hz, C¹¹), 131.6 (s, C³), 131.5 (s, C¹³), 129.7 (d, $^3J_{\text{C-P}}$ 13 Hz, C¹⁴), 128.8 (d, $^2J_{\text{C-P}}$ 23 Hz, C⁴), 124.3 (s, C²), 121.7 (q, $^1J_{\text{C-F}}$ 278 Hz, CF₃), 115.3 (s, C²⁰), 113.5 (s, C¹⁶), 111.6 (s, C¹⁸), 95.8 (s, C²⁴), 88.8 (s, C²³), 64.8 (q, $^2J_{\text{C-F}}$ 38.5 Hz, C⁶), 64.0 (s, C⁹), 62.6 (d, $^2J_{\text{C-P}}$ 6 Hz, C⁷), 55.3 (s, OMe), 21.0 (s, C²²), 16.5 (s, $^3J_{\text{C-P}}$ 6 Hz, C⁸); δ_{F} (CDCl₃) -74.2 (t, $^3J_{\text{F-H}}$ 8 Hz); δ_{P} (CDCl₃) + 22.2; m/z (HRMS⁺) 584.1111 [M + H]⁺ (C₂₆H₂₆F₃NO₇PS requires 584.1120); R_f = 0.52 (silica, DCM : MeOH 97 : 3).

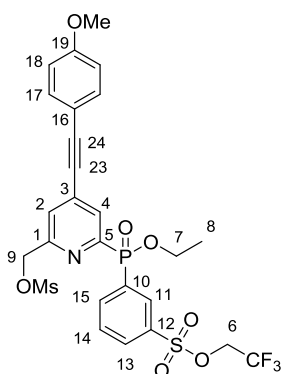
2,2,2-Trifluoroethyl-4-(ethoxy(4-((4-methoxyphenyl)ethynyl)-6-((methylsulfonyloxy)methyl)pyridin-2-yl)phosphoryl)benzenesulfonate, 74



2,2,2-Trifluoroethyl-4-(ethoxy(6-(hydroxymethyl)-4-((4-methoxyphenyl)ethynyl)pyridin-2-yl)phosphoryl)benzenesulfonate, **70** (93 mg, 0.16 mmol) was dissolved in anhydrous THF (4 mL) and NEt₃ (0.07 mL, 0.50 mmol) was added. The mixture was stirred at 5 °C and methanesulfonyl chloride (19 μ L, 0.24 mmol) was added. The reaction was monitored by TLC (silica; DCM : 5 % MeOH, R_f (product) = 0.75, R_f (reactant) = 0.61) and stopped after 30 min. The solvent was removed under reduced pressure and the residue dissolved in DCM (15 mL) and washed with NaCl solution (saturated, 10 mL). The aqueous layer was re-extracted with DCM (3 \times 10 mL) and the organic layers combined, dried over MgSO₄ and the solvent removed under reduced pressure to afford a colourless oil (95 mg, 92 %); δ_{H} (CDCl₃) 8.22 (2H, dd, $^3J_{\text{H-P}}$ 11.5 Hz, $^3J_{\text{H-H}}$ 8.5 Hz, H¹¹), 8.17 (1H, d, $^3J_{\text{H-H}}$ 6.5 Hz, H⁴), 8.02 (2H, dd, $^3J_{\text{H-H}}$

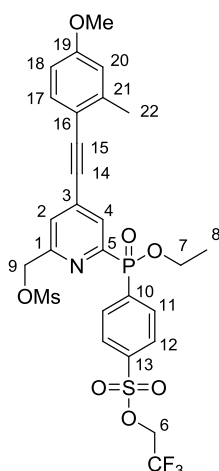
8.5 Hz, $^4J_{\text{H-P}}$ 2.5 Hz, H¹²), 7.62 (1H, s, H²), 7.50 (2H, d, $^3J_{\text{H-H}}$ 9 Hz, H¹⁷), 6.91 (2H, d, $^3J_{\text{H-H}}$ 9 Hz, H¹⁸), 5.32 (2H, m, H⁹), 4.42 (2H, q, $^3J_{\text{F-H}}$ 8 Hz, H⁶), 4.18 (2H, m, H⁷), 3.85 (3H, s, OMe), 3.08 (3H, s, Ms), 1.40 (3H, t, $^3J_{\text{H-H}}$ 7 Hz, H⁸); δ_{F} (CDCl₃) -74.1 (t, $^3J_{\text{F-H}}$ 8 Hz); δ_{P} (CDCl₃) + 21.9; m/z (HRMS⁺) 648.0728 [M + H]⁺ (C₂₆H₂₆F₃NO₉PS₂ requires 648.0739); R_f = 0.75 (silica, DCM : MeOH 95 : 5).

2,2,2-Trifluoroethyl 3-(ethoxy(4-((4-methoxyphenyl)ethynyl)-6-((methylsulfonyloxy)methyl)pyridin-2-yl)phosphoryl)benzenesulfonate, 75



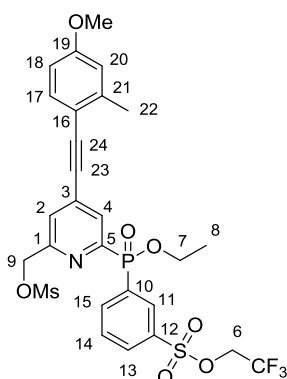
2,2,2-trifluoroethyl 3-(ethoxy(6-(hydroxymethyl)-4-((4-methoxyphenyl)ethynyl)pyridin-2-yl)phosphoryl)benzenesulfonate, **71** (120 mg, 0.21 mmol) was dissolved in anhydrous THF (3 mL) and NEt₃ (87 mL, 0.63 mmol) was added. The mixture was stirred at 5 °C and methanesulfonyl chloride (24 μ L, 0.32 mmol) was added. The reaction was monitored by TLC (silica; DCM : 5 % MeOH, R_f (product) = 0.75, R_f (reactant) = 0.61) and stopped after 30 min. The solvent was removed under reduced pressure and the residue dissolved in DCM (10 mL) and washed with NaCl solution (saturated, 10 mL). The aqueous layer was re-extracted with DCM (3 \times 10 mL) and the organic layers combined, dried over MgSO₄ and the solvent removed under reduced pressure to leave a colourless oil (130 mg, 96 %); δ_{H} (CDCl₃) 8.57 (1H, dd, $^3J_{\text{H-P}}$ 11.5, $^4J_{\text{H-H}}$ 1.5, H¹¹), 8.31 (1H, m, H¹⁵), 8.17 (1H, d, $^3J_{\text{H-P}}$ 6.5, H⁴), 8.08 (1H, d, $^3J_{\text{H-H}}$ 8 Hz, H¹³), 7.71 (1H, td, $^3J_{\text{H-H}}$ 8 Hz, $^4J_{\text{H-H}}$ 1.5 Hz, H¹⁴), 7.60 (1H, s, H¹⁷⁻²), 6.49 (2H, d, $^3J_{\text{H-H}}$ 9 Hz, H¹⁸), 6.90 (2H, d, $^3J_{\text{H-H}}$ 9 Hz, H¹⁸), 5.30 (2H, s, H⁹), 4.43 (2H, q, $^3J_{\text{H-F}}$ 9 Hz, H⁶), 4.16 (2H, m, H⁷), 3.83 (3H, s, OMe), 3.08 (3H, s, Ms), 1.38 (3H, t, $^3J_{\text{H-H}}$ 7 Hz, H⁸); δ_{F} (CDCl₃) -74.1 (t, $^3J_{\text{F-H}}$ 8 Hz); δ_{P} (CDCl₃) + 21.5; m/z (HRMS⁺) 648.0732 [M + H]⁺ (C₂₆H₂₆F₃NO₉PS₂ requires 648.0739); R_f = 0.75 (silica, DCM : MeOH 95 : 5).

2,2,2-Trifluoroethyl-4-(ethoxy(4-((4-methoxy-2-methylphenyl)ethynyl)-6-((methylsulfonyloxy)methyl)pyridin-2-yl)phosphoryl)benzenesulfonate, 76



2,2,2-Trifluoroethyl-4-(ethoxy(6-(hydroxymethyl)-4-((4-methoxy-2-methylphenyl)ethynyl)pyridin-2-yl)phosphoryl)benzenesulfonate, **72** (185 mg, 0.32 mmol) was dissolved in anhydrous THF (5 mL) and NEt_3 (0.14 mL, 0.96 mmol) was added. The mixture was stirred at 5 °C and methanesulfonyl chloride (37 μL , 0.48 mmol) was added. The reaction was monitored by TLC (silica; DCM : 5 % MeOH, $R_f(\text{product}) = 0.75$, $R_f(\text{reactant}) = 0.61$) and stopped after 30 min. The solvent was removed under reduced pressure and the residue dissolved in DCM (15 mL) and washed with NaCl solution (saturated, 10 mL). The aqueous layer was re-extracted with DCM (3×10 mL) and the organic layers combined, dried over MgSO_4 and the solvent removed under reduced pressure to leave a colourless oil (160 mg, 76 %); δ_{H} (CDCl_3) 8.23 (2H, dd, $^3J_{\text{H-P}}$ 11 Hz, $^3J_{\text{H-H}}$ 8 Hz, H^{11}), 8.08 (1H, d, $^4J_{\text{H-H}}$ 2.5 Hz, H^4), 8.03 (2H, d, dd, $^3J_{\text{H-H}}$ 8 Hz, $^4J_{\text{H-P}}$ 2 Hz, H^{12}), 7.59 (1H, s, H^2), 7.44 (1H, d, $^3J_{\text{H-H}}$ 8.5 Hz, H^{17}), 6.78 (1H, s, H^{20}), 6.74 (1H, dd, $^3J_{\text{H-H}}$ 8.5 Hz, $^4J_{\text{H-H}}$ 2.5 Hz, H^{18}), 5.29 (2H, m, H^9), 4.42 (2H, q, $^3J_{\text{F-H}}$ 8 Hz, H^6), 4.18 (2H, m, H^7), 3.82 (3H, s, OMe), 3.07 (3H, s, Ms), 2.48 (2H, s, H^{22}), 1.39 (3H, t, $^3J_{\text{H-H}}$ 7 Hz, H^8); δ_{F} (CDCl_3) -74.1 (t, $^3J_{\text{F-H}}$ 8 Hz); δ_{P} (CDCl_3) +21.9; m/z (HRMS^+) 662.0900 [$\text{M} + \text{H}$] $^+$ ($\text{C}_{27}\text{H}_{28}\text{NO}_9\text{F}_3\text{P}_2$ requires 662.0895); $R_f = 0.75$ (silica, DCM : MeOH 95 : 5).

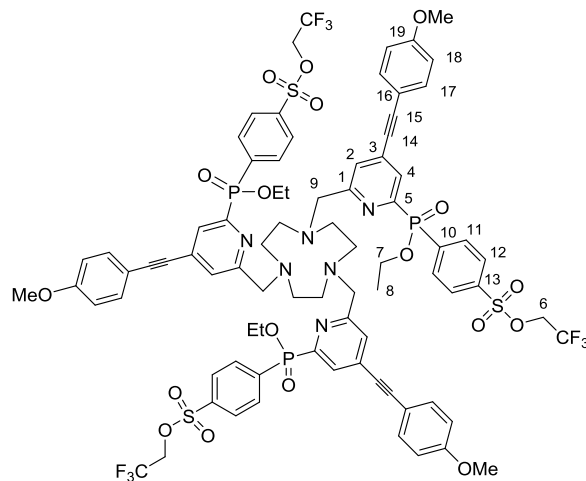
2,2,2-Trifluoroethyl 3-(ethoxy(4-((4-methoxy-2-methylphenyl)ethynyl)-6-((methylsulfonyloxy)methyl)pyridin-2-yl)phosphoryl)benzenesulfonate, 77



2,2,2-Trifluoroethyl 3-(ethoxy(6-(hydroxymethyl)-4-((4-methoxy-2-methylphenyl)ethynyl)pyridin-2-yl)phosphoryl)benzenesulfonate, **73** (45 mg, 78 μmol) was dissolved in anhydrous THF (2.5 mL) and NEt_3 (32 mL, 0.23 mmol) was added. The mixture was stirred at 5 $^\circ\text{C}$ and methanesulfonyl chloride (9 μL , 0.12 mmol) was added. The reaction was monitored by TLC (silica; DCM : 5 % MeOH, $R_f(\text{product}) = 0.75$, $R_f(\text{reactant}) = 0.61$) and stopped after 30 min. The solvent was removed under reduced pressure and the residue dissolved in DCM (10 mL) and washed with NaCl solution (saturated, 10 mL). The aqueous layer was re-extracted with DCM (3×10 mL) and the organic layers combined, dried over MgSO_4 and the solvent removed under reduced pressure to leave a colourless oil (40 mg, 76 %); δ_{H} (CDCl_3) 8.59 (1H, d, $^3J_{\text{H-P}}$ 11.5, H^{11}), 8.36 (1H, m, H^{15}), 8.18 (1H, d, $^3J_{\text{H-P}}$ 6.5 Hz, H^4), 8.10 (1H, d, $^3J_{\text{H-H}}$ 8 Hz, H^{13}), 7.73 (1H, td, $^3J_{\text{H-H}}$ 8 Hz, $^4J_{\text{H-P}}$ 3 Hz, H^{14}), 7.60 (1H, s, H^2), 7.45 (1H, d, $^3J_{\text{H-H}}$ 8.5 Hz, H^{17}), 6.83 (1H, s, H^{20}), 6.73 (1H, d, $^3J_{\text{H-H}}$ 8.5 Hz, H^{18}), 5.29 (2H, m, H^9), 4.44 (2H, q, $^3J_{\text{F-H}}$ 8 Hz, H^6), 4.16 (2H, m, H^7), 3.82 (3H, s, OMe), 3.09 (2H, s, Ms), 2.49 (3H, s, H^{22}), 1.42 (3H, t, $^3J_{\text{H-H}}$ 7 Hz, H^8); δ_{F} (CDCl_3) -74.1 (t, $^3J_{\text{F-H}}$ 8 Hz); δ_{P} (CDCl_3) + 21.5; m/z (HRMS^+) 662.0902 [$\text{M} + \text{H}$] $^+$ ($\text{C}_{27}\text{H}_{28}\text{NO}_9\text{F}_3\text{PS}_2$ requires 662.0895); $R_f = 0.75$ (silica, DCM : MeOH 95 : 5).

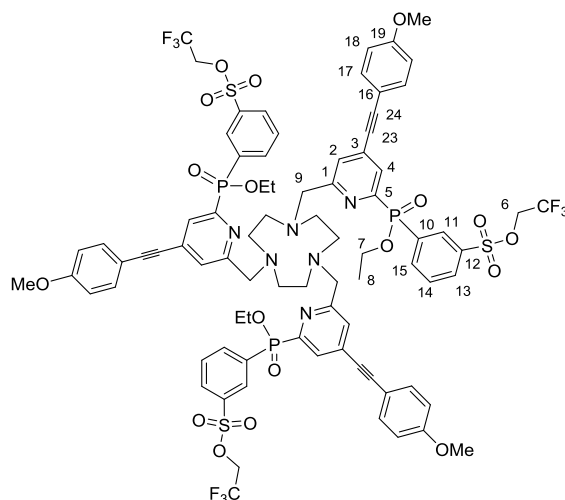
2,2,2-Trifluoroethyl 6,6',6''-(1,4,7-triazacyclononane-1,4,7-triyl)tris(methylene)tris(4-((4-methoxyphenyl)ethynyl)pyridine-6,2-diyl)tris(4-(ethoxyphosphoryl benzenesulfonate)),

78



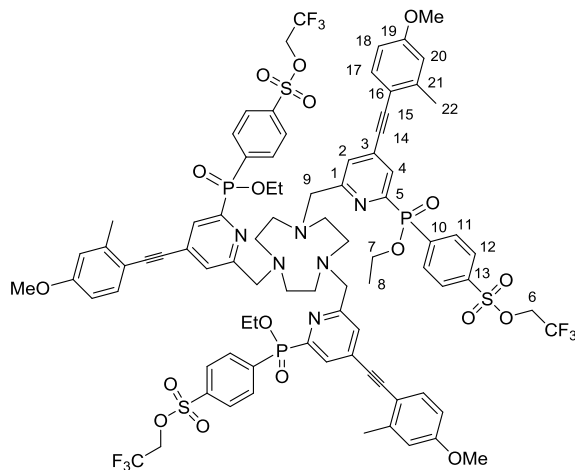
1,4,7-Triazacyclononane trihydrochloride (2.5 mg, 10 μmol) and 2,2,2-trifluoroethyl 4-(ethoxy(4-((4-methoxyphenyl)ethynyl)-6-((methylsulfonyloxy)methyl)pyridin-2-yl)phosphoryl)benzenesulfonate, **74** (20 mg, 29 μmol) were dissolved in anhydrous CH_3CN (1 mL) and K_2CO_3 (8.0 mg, 58 μmol) was added. The mixture was stirred under argon at 60 $^\circ\text{C}$ for 16 h. The reaction was cooled and the solution decanted from excess potassium salts. The solvent was removed under reduced pressure and the crude product purified by HPLC (*Method J*, $t_{\text{R}} = 12.6$ min) to give a pale yellow oil (7.5 mg, 42 %); δ_{H} (CDCl_3) 8.18 (6H, dd, $^3J_{\text{H-P}}$ 11.5 Hz, $^3J_{\text{H-H}}$ 8.5 Hz, H^{11}), 8.05 (3H, d, $^3J_{\text{H-H}}$ 6 Hz, H^4), 7.97 (6H, dd, $^3J_{\text{H-H}}$ 8.5 Hz, $^4J_{\text{H-P}}$ 2 Hz, H^{12}), 7.62 (3H, s, H^2), 7.45 (6H, d, $^3J_{\text{H-H}}$ 9 Hz, H^{17}), 6.88 (6H, d, $^3J_{\text{H-H}}$ 9 Hz, H^{18}), 4.40 (6H, q, $^3J_{\text{F-H}}$ 8 Hz, H^6), 4.20 - 4.06 (6H, m, H^7), 3.87 (6H, s, H^9), 3.82 (9H, s, OMe), 2.81 (12H, br, 9 N_3), 1.34 (9H, t, $^3J_{\text{H-H}}$ 7 Hz, H^8); δ_{C} (CDCl_3) 160.9 (s, C^1), 160.7 (s, C^{19}), 153.0 (d, $^1J_{\text{C-P}}$ 184 Hz, C^5), 138.4 (s, C^{13}), 137.4 (d, $^1J_{\text{C-P}}$ 138 Hz, C^{10}), 133.6 (s, C^{17}), 133.5 (d, $^2J_{\text{C-P}}$ 9.5 Hz, C^{11}), 128.1 (d, $^2J_{\text{C-P}}$ 12 Hz, C^4), 128.2 (s, C^3), 127.5 (d, $^4J_{\text{C-P}}$ 13.5 Hz, C^{12}), 127.0 (s, C^2), 121.7 (q, $^1J_{\text{C-F}}$ 329 Hz, CF_3), 114.3 (s, C^{18}), 113.5 (s, C^{16}), 96.3 (s, C^{15}), 85.0 (s, C^{14}), 64.8 (q, $^2J_{\text{C-F}}$ 37 Hz, C^6), 62.9 (s, C^9), 62.3 (d, $^2J_{\text{C-P}}$ 14 Hz, C^7), 55.5 (OMe), 55.2-54.5 (br, 9 N_3), 16.5 (s, C^8); δ_{F} (CDCl_3) -74.1 (t, $^3J_{\text{F-H}}$ 8 Hz); δ_{P} (CDCl_3) + 22.5; m/z (HRMS $^+$) 1783.362 [$\text{M} + \text{H}$] $^+$ ($\text{C}_{81}\text{H}_{79}\text{F}_9\text{N}_6\text{O}_{18}\text{P}_3\text{S}_3$ requires 1783.368).

2,2,2-Trifluoroethyl-6,6',6''-(1,4,7-triazacyclononane-1,4,7-triyl)tris(methylene)tris(4-((4-methoxyphenyl)ethynyl)pyridine-6,2-diyl)tris(3-(ethoxyphosphoryl)benzenesulfonate), 79



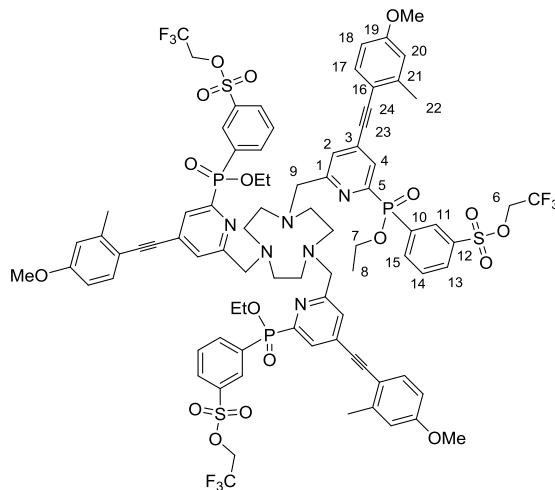
1,4,7-Triazacyclononane trihydrochloride (1.4 mg, 5.9 μmol) and 2,2,2-trifluoroethyl 3-(ethoxy(4-((4-methoxyphenyl)ethynyl)-6-((methylsulfonyloxy)methyl)pyridin-2-yl)phosphoryl)benzenesulfonate, **75** (11 mg, 17 μmol) were dissolved in anhydrous CH_3CN (1 mL) and K_2CO_3 (4.9 mg, 35.4 μmol) was added. KI (0.1 mg) was added to the reaction and the mixture was stirred under argon at 60 $^\circ\text{C}$ for 3 h. The reaction was cooled and the solution decanted from excess potassium salts. The solvent was removed under reduced pressure to give a yellow oil (5.6 mg, 53 %); δ_{H} (CDCl_3) 8.62 (3H, d, $^3J_{\text{H-P}}$ 11.5, H^{11}), 8.37 (3H, m, H^{15}), 8.10 (6H, m, H^{4-13}), 7.71 (6H, m, H^{14-2}), 7.41 (6H, d, $^3J_{\text{H-H}}$ 8.5 Hz, H^{17}), 6.75 (6H, d, $^3J_{\text{H-H}}$ 8.5 Hz, H^{18}), 4.40 (6H, q, $^3J_{\text{F-H}}$ 8 Hz, H^6), 4.20 - 4.03 (6H, m, H^7), 3.82 (6H, s, H^9), 3.78 (9H, s, OMe), 2.81 (12H, br, 9N_3), 1.38 (9H, t, $^3J_{\text{H-H}}$ 7 Hz, H^8); δ_{C} (CDCl_3) 161.0 (d, $^4J_{\text{C-P}}$ 20 Hz, C^1), 160.3 (s, C^{19}), 151.3 (d, $^1J_{\text{C-P}}$ 169 Hz, C^5), 138.0 (d, $^2J_{\text{C-P}}$ 10 Hz, C^{15}), 135.7 (d, $^3J_{\text{C-P}}$ 12 Hz, C^{12}), 134.5 (s, C^{17}), 132.7 (d, $^1J_{\text{C-P}}$ 139 Hz, C^{10}), 131.7 (d, $^2J_{\text{C-P}}$ 11 Hz, C^{11}), 131.4 (s, C^3), 131.2 (s, C^{13}), 129.6 (d, $^3J_{\text{C-P}}$ 14 Hz, C^{14}), 128.6 (d, $^2J_{\text{C-P}}$ 22.5 Hz, C^4), 124.1 (s, C^2), 121.7 (q, $^1J_{\text{C-F}}$ 278 Hz, CF_3), 113.3 (s, C^{16}), 111.2 (s, C^{18}), 95.7 (s, C^{24}), 88.2 (s, C^{23}), 64.8 (q, $^2J_{\text{C-F}}$ 38.5 Hz, C^6), 62.9 (s, C^9), 62.7 (d, $^2J_{\text{C-P}}$ 7 Hz, C^7), 55.3 (s, OMe), 55.2-54.5 (br, 9N_3), 16.5 (s, C^8); δ_{F} (CDCl_3) -74.1 (t, $^3J_{\text{F-H}}$ 8 Hz); δ_{P} (CDCl_3) + 22.3; m/z (HRMS $^+$) 1783.360 [$\text{M} + \text{H}$] $^+$ ($\text{C}_{81}\text{H}_{79}\text{F}_9\text{N}_6\text{O}_{18}\text{P}_3\text{S}_3$ requires 1783.368).

2,2,2-Trifluoroethyl 6,6',6''-(1,4,7-triazacyclononane-1,4,7-triyl)tris(methylene)tris(4-((4-methoxy-2-methylphenyl)ethynyl)pyridine-6,2-diyl)tris(4-(ethoxy phosphoryl benzenesulfonate), 80



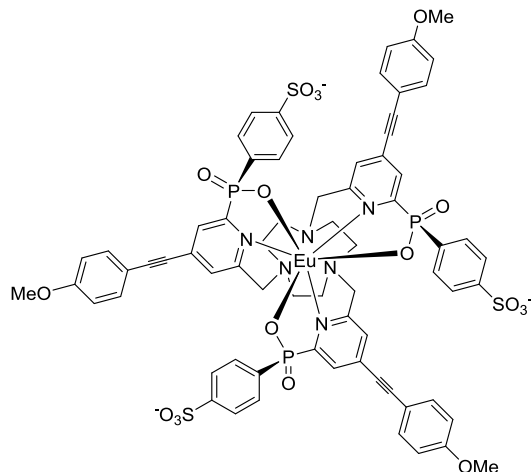
1,4,7-Triazacyclononane trihydrochloride (3.0 mg, 12 μmol) and 2,2,2-trifluoroethyl 4-(ethoxy(4-((4-methoxy-2-methylphenyl)ethynyl)-6-((methylsulfonyloxy)methyl)pyridin-2-yl)phosphoryl)benzenesulfonate, **76** (24 mg, 36 μmol) were dissolved in anhydrous CH_3CN (1 mL) and K_2CO_3 (10 mg, 72 μmol) was added. The mixture was stirred under argon at 60 $^\circ\text{C}$ for 16 h. KI (0.1 mg) was added to the reaction and the mixture was heated for further 1 h. The reaction was cooled and the solution decanted from excess potassium salts. The solvent was removed under reduced pressure to give a yellow oil (15 mg, 69 %); δ_{H} (CDCl_3) 8.21 (6H, dd, $^3J_{\text{H-P}}$ 11 Hz, $^3J_{\text{H-H}}$ 8 Hz, H^{11}), 8.03 (3H, s, H^4), 7.98 (6H, d, $^3J_{\text{H-H}}$ 8 Hz, H^{12}), 7.53 (3H, s, H^2), 7.41 (3H, d, $^3J_{\text{H-H}}$ 8.5 Hz, H^{17}), 6.80 (3H, d, $^4J_{\text{H-H}}$ 2.5 Hz, H^{20}), 6.74 (3H, dd, $^3J_{\text{H-H}}$ 8.5 Hz, $^4J_{\text{H-H}}$ 2.5 Hz, H^{18}), 4.40 (6H, q, $^3J_{\text{F-H}}$ 8 Hz, H^6), 4.20 - 4.06 (6H, m, H^7), 3.85 (6H, s, H^9), 3.80 (9H, s, OMe), 2.46 (9H, s, H^{22}), 2.81 (12H, br, 9N_3), 1.38 (9H, t, $^3J_{\text{H-H}}$ 7 Hz, H^8); δ_{C} (CDCl_3) 161.2 (s, C^1), 160.5 (s, C^{19}), 151.8 (d, $^1J_{\text{C-P}}$ 168 Hz, C^5), 142.7 (s, C^{21}), 138.6 (s, C^{13}), 137.4 (d, $^1J_{\text{C-P}}$ 137 Hz, C^{10}), 134.1 (s, C^{17}), 133.4 (d, $^2J_{\text{C-P}}$ 11 Hz, C^{11}), 133.2 (s, C^3), 128.9 (s, C^4), 127.6 (d, $^4J_{\text{C-P}}$ 13 Hz, C^{12}), 124.2 (s, C^2), 121.7 (q, $^1J_{\text{C-F}}$ 279 Hz, CF_3), 115.1 (s, C^{20}), 113.4 (s, C^{16}), 111.6 (s, C^{18}), 95.8 (s, C^{15}), 88.8 (s, C^{14}), 64.8 (q, $^2J_{\text{C-F}}$ 38.5 Hz, C^6), 62.9 (s, C^9), 62.7 (d, $^2J_{\text{C-P}}$ 14 Hz, C^7), 55.3 (s, OMe), 55.2-54.5 (br, 9N_3), 21.0 (s, C^{22}), 16.5 (s, C^8); δ_{F} (CDCl_3) -74.2 (t, $^3J_{\text{F-H}}$ 8 Hz); δ_{P} (CDCl_3) +22.6; m/z (HRMS^+) 1825.410 [$\text{M} + \text{H}$] $^+$ ($\text{C}_{84}\text{H}_{85}\text{N}_6\text{O}_{18}\text{F}_9\text{P}_3\text{S}_3$ requires 1825.415).

2,2,2-Trifluoroethyl-6,6',6''-(1,4,7-triazacyclononane-1,4,7-triyl)tris(methylene)tris(4-((4-methoxy-2-methylphenyl)ethynyl)pyridine-6,2-diyl)tris(3-(ethoxyphosphoryl)benzenesulfonate), 81

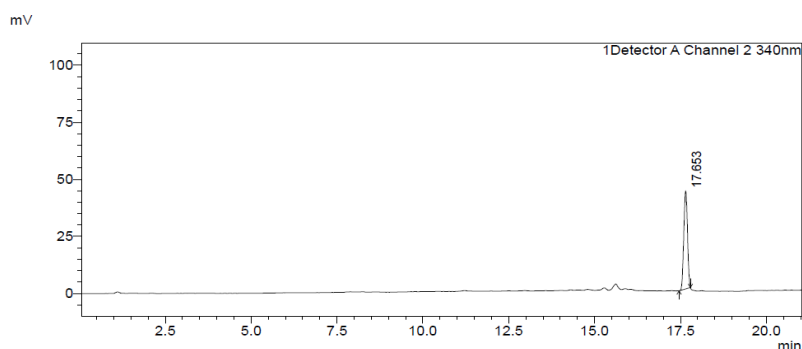


1,4,7-Triazacyclononane trihydrochloride (5.0 mg, 20 μmol) and 2,2,2-trifluoroethyl 3-(ethoxy(4-((4-methoxy-2-methylphenyl)ethynyl)-6-((methylsulfonyloxy)methyl)pyridin-2-yl)phosphoryl)benzenesulfonate, **77** (40 mg, 60 μmol) were dissolved in anhydrous CH_3CN (1.5 mL) and K_2CO_3 (17 mg, 0.12 mmol) was added. KI (catalytical) was added to the reaction and the mixture was stirred under argon at 60 $^\circ\text{C}$ for 1 h. The reaction was cooled and the solution decanted from excess potassium salts. The solvent was removed under reduced pressure to give a yellow oil (18 mg, 51 %); δ_{H} (CDCl_3) 8.61 (3H, d, $^3J_{\text{H-P}}$ 11.5, H^{11}), 8.37 (3H, m, H^{15}), 8.12 (6H, m, H^{4-13}), 7.72 (6H, m, H^{14-2}), 7.41 (3H, d, $^3J_{\text{H-H}}$ 8.5 Hz, H^{17}), 6.83 (3H, s, H^{20}), 6.78 (3H, d, $^3J_{\text{H-H}}$ 8.5 Hz, H^{18}), 4.40 (6H, q, $^3J_{\text{F-H}}$ 8 Hz, H^6), 4.20 - 4.06 (6H, m, H^7), 3.83 (6H, s, H^9), 3.80 (9H, s, OMe), 2.48 (9H, s, H^{22}), 2.81 (12H, br, 9N_3), 1.38 (9H, t, $^3J_{\text{H-H}}$ 7 Hz, H^8); δ_{C} (CDCl_3) 161.0 (d, $^4J_{\text{C-P}}$ 20 Hz, C^1), 160.3 (s, C^{19}), 151.4 (d, $^1J_{\text{C-P}}$ 169 Hz, C^5), 142.4 (s, C^{21}), 138.1 (d, $^2J_{\text{C-P}}$ 10 Hz, C^{15}), 135.7 (d, $^3J_{\text{C-P}}$ 12 Hz, C^{12}), 134.0 (s, C^{17}), 132.7 (d, $^1J_{\text{C-P}}$ 140 Hz, C^{10}), 131.9 (d, $^2J_{\text{C-P}}$ 11 Hz, C^{11}), 131.6 (s, C^3), 131.4 (s, C^{13}), 129.7 (d, $^3J_{\text{C-P}}$ 13 Hz, C^{14}), 128.6 (d, $^2J_{\text{C-P}}$ 23 Hz, C^4), 124.2 (s, C^2), 121.7 (q, $^1J_{\text{C-F}}$ 278 Hz, CF_3), 115.1 (s, C^{20}), 113.6 (s, C^{16}), 111.6 (s, C^{18}), 95.8 (s, C^{24}), 88.2 (s, C^{23}), 64.8 (q, $^2J_{\text{C-F}}$ 38.5 Hz, C^6), 62.9 (s, C^9), 62.7 (d, $^2J_{\text{C-P}}$ 7 Hz, C^7), 55.3 (s, OMe), 55.2-54.5 (br, 9N_3), 21.0 (s, C^{22}), 16.5 (s, C^8); δ_{F} (CDCl_3) -74.1 (t, $^3J_{\text{F-H}}$ 8 Hz); δ_{P} (CDCl_3) + 22.3; m/z (HRMS^+) 1825.417 [$\text{M} + \text{H}$] $^+$ ($\text{C}_{84}\text{H}_{85}\text{N}_6\text{O}_{18}\text{F}_9\text{P}_3\text{S}_3$ requires 1825.415).

Eu(III) complex of 6,6',6''-(1,4,7-triazacyclononane-1,4,7-triyl)tris(methylene)tris(4-((4-methoxyphenyl)ethynyl)pyridine-6,2-diyl)tris(4-(hydroxyphosphoryl benzenesulfonate), [EuL^{20a}]³⁻

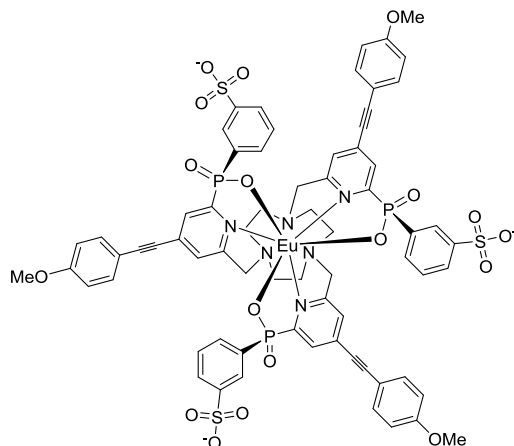


2,2,2-Trifluoroethyl 6,6',6''-(1,4,7-triazacyclononane-1,4,7-triyl)tris(methylene)tris(4-((4-methoxyphenyl)ethynyl)pyridine-6,2-diyl)tris(4-(ethoxyphosphoryl benzenesulfonate), **78** (3.0 mg, 1.7 μmol) was dissolved in CD_3OD (1 mL) and a solution of NaOH in D_2O (0.1 M, 0.5 mL) was added. The mixture was heated to 60 $^\circ\text{C}$ under argon and monitored with ^{19}F -NMR [$\delta_{\text{F}}(\text{reactant}) = -76.0$, $\delta_{\text{F}}(\text{product, trifluoroethanol}) = -78.0$] and ^{31}P -NMR [$\delta_{\text{P}}(\text{reactant}) = +23.1$, $\delta_{\text{P}}(\text{product}) = +14.9$]. After 3 h the solution was cooled to RT and the pH was adjusted to 7 with HCl. $\text{Eu}(\text{Cl})_3 \cdot 6\text{H}_2\text{O}$ (0.7 mg, 1.7 μmol) was added and the mixture heated to 65 $^\circ\text{C}$ overnight under argon. The solvent was removed under reduced pressure and the product purified by HPLC (*Method K*, $t_{\text{R}} = 17.7$ min) giving the triethylammonium salt as a white solid (2.0 mg, 75 %); (HRMS⁻) 1599.146 [MH_2]⁻ ($\text{C}_{69}\text{H}_{59}^{151}\text{EuN}_6\text{O}_{18}\text{P}_3\text{S}_3$ requires 1599.146); $\tau_{\text{H}_2\text{O}} = 1.11$ ms; $\lambda_{\text{max}}(\text{H}_2\text{O}) = 332$ nm; $\varepsilon = 58$ $\text{mM}^{-1} \text{cm}^{-1}$.

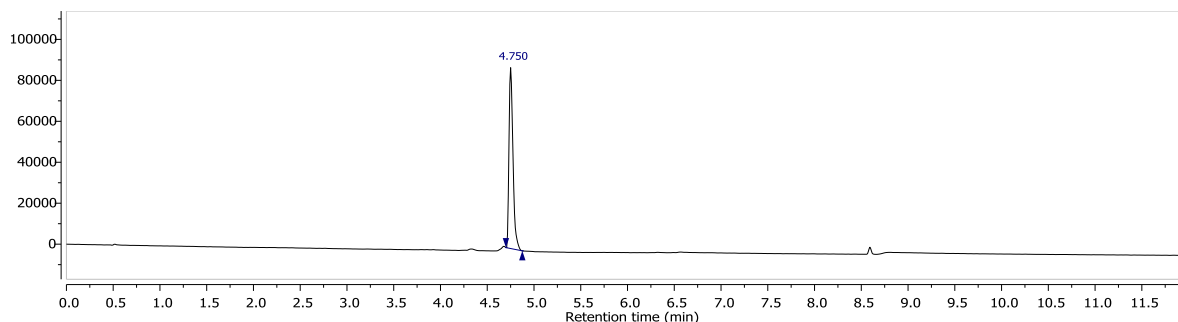


Method L, $t_{\text{R}} = 17.7$ min

Eu(III) complex of 6,6',6''-(1,4,7-triazacyclononane-1,4,7-triyl)tris(methylene)tris(4-((4-methoxyphenyl)ethynyl)pyridine-6,2-diyl)tris(3-(hydroxyphosphoryl benzenesulfonate), [EuL^{23a}]³⁻

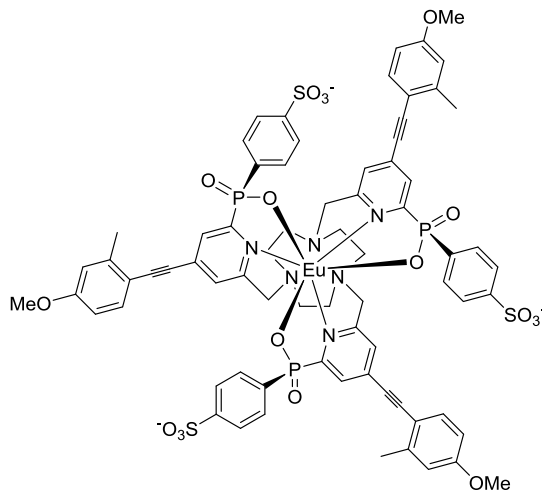


2,2,2-Trifluoroethyl-6,6',6''-(1,4,7-triazacyclononane-1,4,7-triyl)tris(methylene)tris(4-((4-methoxyphenyl)ethynyl)pyridine-6,2-diyl)tris(3-(ethoxyphosphoryl benzenesulfonate), **79** (9 mg, 5.0 μmol) was dissolved in CD_3OD (1.5 mL) and a solution of NaOH in D_2O (0.1 M, 0.8 mL) was added. The mixture was heated to 60 $^\circ\text{C}$ under argon and monitored with ^{19}F -NMR [δ_{F} (reactant) = - 75.3, δ_{F} (product, trifluoroethanol) = - 78.0] and ^{31}P -NMR [δ_{P} (reactant) = + 22.3, δ_{P} (product) = + 13.3]. After 3 h the solution was cooled to RT and the pH was adjusted to 7 with HCl. $\text{Eu}(\text{Ac})_3\text{H}_2\text{O}$ (1.8 mg, 5.5 μmol) was added and the mixture heated to 65 $^\circ\text{C}$ overnight under argon. The solvent was removed under reduced pressure and the product purified by HPLC (*Method K*, t_{R} = 18.2 min) giving the triethylammonium salt as a white solid (4.8 mg, 59 %); (HRMS⁻) 1599.148 [MH_2^-] ($\text{C}_{69}\text{H}_{59}^{151}\text{EuN}_6\text{O}_{18}\text{P}_3\text{S}_3$ requires 1599.146); $\tau_{\text{H}_2\text{O}}$ = 1.10 ms; $\lambda_{\text{max}}(\text{H}_2\text{O})$ = 332 nm; ε = 58 $\text{mM}^{-1} \text{cm}^{-1}$.

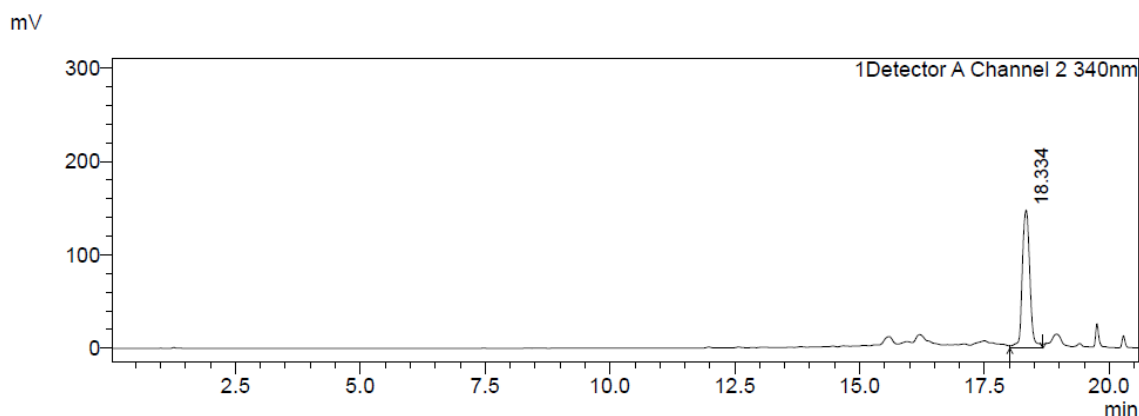


Method M, t_{R} = 4.8 min

Eu(III) complex of 6,6',6''-(1,4,7-triazacyclononane-1,4,7-triyl)tris(methylene)tris(4-((4-methoxy-2-methylphenyl)ethynyl)pyridine-6,2-diyl)tris(4-(hydroxyphosphoryl)benzenesulfonate), [EuL^{24a}]³⁻

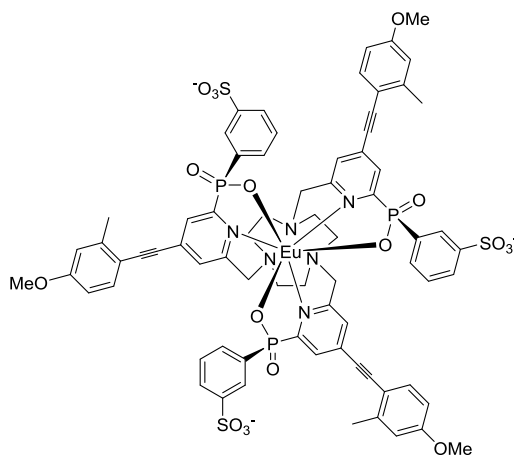


2,2,2-Trifluoroethyl 6,6',6''-(1,4,7-triazacyclononane-1,4,7-triyl)tris(methylene)tris(4-((4-methoxy-2-methylphenyl)ethynyl)pyridine-6,2-diyl)tris(4-(ethoxyphosphoryl)benzenesulfonate), **80** (5.0 mg, 2.7 μmol) was dissolved in CD_3OD (1.5 mL) and a solution of NaOH in D_2O (0.1 M, 0.8 mL) was added. The mixture was heated to 60 $^\circ\text{C}$ under argon and monitored with ^{19}F -NMR [δ_{F} (reactant) = - 76.2, δ_{F} (product, trifluoroethanol) = - 78.0] and ^{31}P -NMR [δ_{P} (reactant) = + 22.3, δ_{P} (product) = + 13.1]. After 3 h the solution was cooled to RT and the pH was adjusted to 7 with HCl. $\text{Eu}(\text{Cl})_3 \cdot 6\text{H}_2\text{O}$ (1.0 mg, 2.9 μmol) was added and the mixture heated to 65 $^\circ\text{C}$ overnight under argon. The solvent was removed under reduced pressure and the product purified by HPLC (*Method K*, t_{R} = 19.8 min) giving the triethylammonium salt as a white solid (2.6 mg, 60 %); (HRMS⁻) 1644.205 [MH_2]⁻ ($\text{C}_{72}\text{H}_{65}^{153}\text{EuN}_6\text{O}_{18}\text{P}_3\text{S}_3$ requires 1644.202); $\tau_{\text{H}_2\text{O}}$ = 1.09 ms; $\lambda_{\text{max}}(\text{H}_2\text{O})$ = 340 nm; ε = 58 $\text{mM}^{-1}\text{cm}^{-1}$.



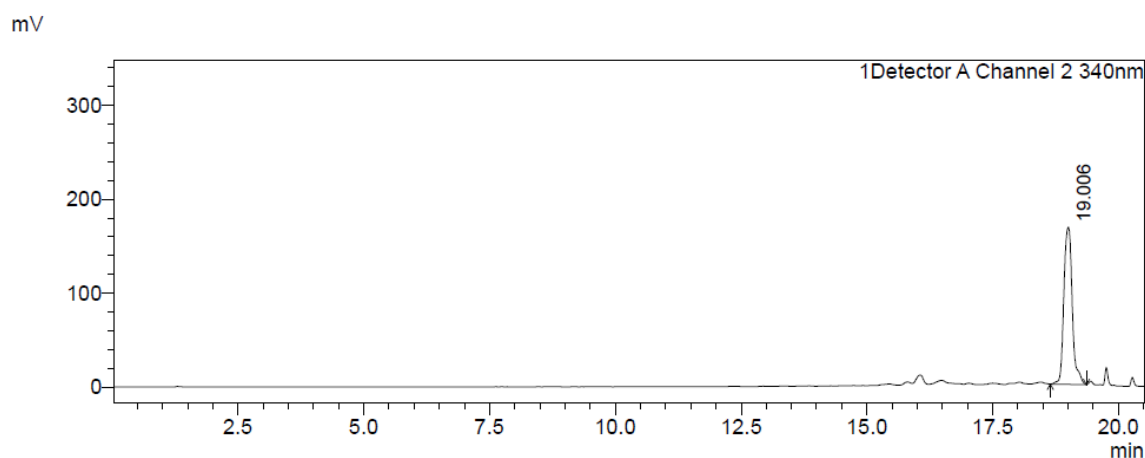
Method L, $t_R = 18.3$ min

Eu(III) complex of 6,6',6''-(1,4,7-triazacyclononane-1,4,7-triyl)tris(methylene)tris(4-((4-methoxy-2-methylphenyl)ethynyl)pyridine-6,2-diyl)tris(3-(hydroxyphosphoryl) benzenesulfonate), [EuL^{25a}]³⁻



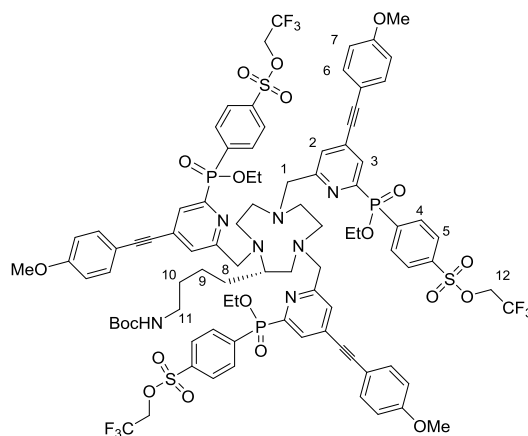
2,2,2-Trifluoroethyl-6,6',6''-(1,4,7-triazacyclononane-1,4,7-triyl)tris(methylene)tris(4-((4-methoxy-2-methylphenyl)ethynyl)pyridine-6,2-diyl)tris(3-(ethoxyphosphoryl) benzenesulfonate), **81** (5.0 mg, 2.7 μmol) was dissolved in CD_3OD (1.5 mL) and a solution of NaOH in D_2O (0.1 M, 0.8 mL) was added. The mixture was heated to 60 $^\circ\text{C}$ under argon and monitored with ^{19}F -NMR [δ_{F} (reactant) = - 76.1, δ_{F} (product, trifluoroethanol) = - 78.0] and ^{31}P -NMR [δ_{P} (reactant) = + 22.3, δ_{P} (product) = + 12.9]. After 3 h the solution was cooled to RT and the pH was adjusted to 7 with HCl. $\text{Eu}(\text{Cl})_3 \cdot 6\text{H}_2\text{O}$ (1.0 mg, 2.9 μmol) was added and the mixture heated to 65 $^\circ\text{C}$ overnight under argon. The solvent was removed under reduced pressure and the product purified by HPLC (*Method K*, $t_R = 19.2$ min) giving the triethylammonium salt as a white solid (2.5 mg, 58 %); (HRMS⁻) 1644.200 [MH_2]⁻

($C_{72}H_{65}^{153}EuN_6O_{18}P_3S_3$ requires 1644.202); $\tau_{H_2O} = 1.12$ ms; $\lambda_{max}(H_2O) = 340$ nm; $\epsilon = 58$ mM $^{-1}$ cm $^{-1}$.



Method L, $t_R = 19.0$ min

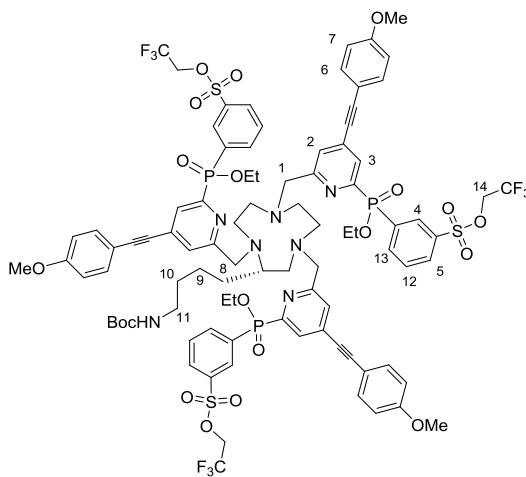
tert*-Butyl-4-((*S*)-1,4,7-tris((6-(ethoxy(4-(2,2,2-trifluoroethyl)phosphoryl)benzenesulfonate)-4-((4-methoxyphenyl)ethynyl)pyridin-2-yl)methyl)-1,4,7-triazacyclononane-2-yl)butylcarbamate, **82*



(*S*)-*tert*-Butyl 4-(1,4,7-triazacyclononane-2-yl)butylcarbamate, **17** (15 mg, 0.05 mmol) and 2,2,2-trifluoroethyl-4-(ethoxy(4-((4-methoxyphenyl)ethynyl)-6-((methylsulfonyloxy)methyl)pyridin-2-yl)phosphoryl)benzenesulfonate, **74** (95 mg, 0.15 mmol), were dissolved in anhydrous CH_3CN (2 mL) and K_2CO_3 (21 mg, 0.15 mmol) was added. The mixture was stirred under argon at 60 °C for 16 h. The reaction was cooled and the solution decanted from excess potassium salts. The solvent was removed under reduced pressure and the crude product purified by HPLC (*Method J*, $t_R = 14.1$ min) to give a pale

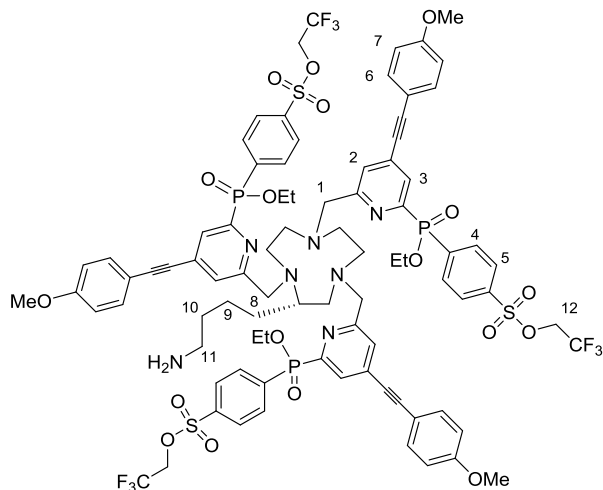
yellow oil (32 mg, 33 %); δ_{H} (CDCl_3) 8.18 (6H, m, H^4), 8.04 (3H, m, H^3), 7.96 (6H, m, H^5), 7.48 (3H, m, H^2), 7.44 (6H, m, H^6), 6.88 (6H, m, H^7), 5.08 (1H, br, CONH), 4.40 (6H, q, $^3J_{\text{F-H}}$ 7.5 Hz, H^{12}), 4.14 (6H, m, P-OCH₂), 3.83 (15H, m, H^1 and OMe), 3.00-2.56 (13H, m, 9N₃ ring protons and H^{11}), 1.38 (9H, s, Boc), 1.45-1.30 (6H, m, H^{10-9-8}), 1.35 (9H, m, CH₃(Et)); δ_{F} (CDCl_3) -74.2 (t, $^3J_{\text{F-H}}$ 8 Hz); δ_{P} (CDCl_3) + 22.6; m/z (HRMS⁺) 977.7515 [$\text{M} + 2\text{H}$]²⁺ (C₉₀H₉₇F₉N₇O₂₀P₃S₃ requires 977.7510).

tert*-Butyl-4-((*S*)-1,4,7-tris((6-(ethoxy(3-(2,2,2-trifluoroethyl)phosphoryl)benzenesulfonate)-4-((4-methoxyphenyl)ethynyl)pyridin-2-yl)methyl)-1,4,7-triazacyclononane-2-yl)butylcarbamate, **83*



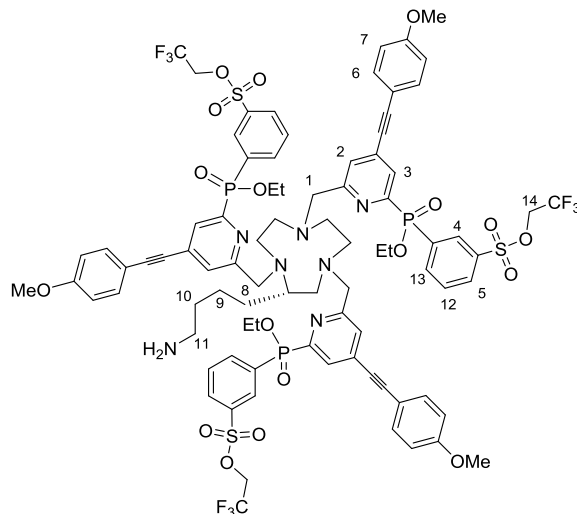
(*S*)-*tert*-Butyl 4-(1,4,7-triazacyclononan-2-yl)butylcarbamate, **17** (17.5 mg, 58 μmol) and 2,2,2-Trifluoroethyl 3-(ethoxy(4-((4-methoxyphenyl)ethynyl)-6-((methylsulfonyloxy)methyl)pyridin-2-yl)phosphoryl)benzenesulfonate, **75** (110 mg, 174 μmol), were dissolved in anhydrous CH₃CN (4 mL) and K₂CO₃ (23 mg, 174 μmol) was added. The mixture was stirred under argon at 60 °C for 16 h. The reaction was cooled and the solution decanted from excess potassium salts. The solvent was removed to give a yellow oil (34 mg, 30 %); δ_{H} (CDCl_3) 8.53 (3H, m, H^4), 8.33 (3H, m, H^{13}), 8.05 (6H, m, H^{5-3}), 7.74 (3H, m, H^{12}), 7.48 (3H, m, H^2), 7.42 (6H, m, H^6), 6.86 (6H, m, H^7), 5.00 (1H, br, CONH), 4.40 (6H, q, $^3J_{\text{F-H}}$ 7.5 Hz, H^{14}), 4.12 (6H, m, P-OCH₂), 3.81 (15H, m, H^1 and OMe), 3.05-2.59 (13H, m, 9N₃ ring protons and H^{11}), 1.39 (9H, s, Boc), 1.42-1.29 (6H, m, H^{10-9-8}), 1.34 (9H, m, CH₃(Et)); δ_{F} (CDCl_3) -74.2 (t, $^3J_{\text{F-H}}$ 8 Hz); δ_{P} (CDCl_3) + 22.3; m/z (HRMS⁺) 977.7517 [$\text{M} + 2\text{H}$]²⁺ (C₉₀H₉₇F₉N₇O₂₀P₃S₃ requires 977.7510).

2,2,2-Trifluoroethyl-6,6',6''-((S)-2-(4-aminobutyl)-1,4,7-triazacyclononane-1,4,7-triyl)tris(methylene)tris(4-((4-methoxyphenyl)ethynyl)pyridine-6,2-diyl)tris(4-(ethoxy phosphoryl benzenesulfonate), **82a**



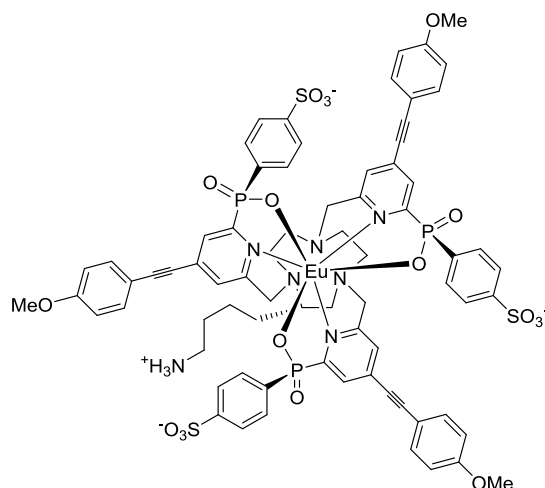
tert-Butyl 4-((*S*)-1,4,7-tris((6-(ethoxy(4-(2,2,2-trifluoroethyl)phosphoryl benzenesulfonate)-4-((4-methoxyphenyl)ethynyl)pyridin-2-yl)methyl)-1,4,7-triazacyclononane-2-yl)butylcarbamate, **82** (30 mg, 15 μ mol) was dissolved in dry DCM (1.8 mL). Argon was bubbled for 10 min after which time TFA (0.2 mL) was added. The solution was stirred for 20 min and the solvent was removed under reduced pressure to give the trifluoroacetate salt as a yellow oil (16 mg, 60 %); δ_{H} (CD_3OD) 8.11 (6H, m, H^4), 8.04 (3H, m, H^3), 8.01 (6H, m, H^5), 7.61 (3H, m, H^2), 7.57 (6H, m, H^6), 6.93 (6H, m, H^7), 4.65 (6H, m, H^{12}), 4.17 (6H, m, P-OCH_2), 3.96 (15H, m, H^1 and OMe), 3.82-3.60 (13H, m, 9N_3 and H^{11}), 1.61-1.47 (6H, m, H^{10-9-8}), 1.46 (9H, m, $\text{CH}_3(\text{Et})$); δ_{F} (CD_3OD) -76.0 (br); δ_{P} (CD_3OD) +23.6; m/z (HRMS^+) 1854.437 [$\text{M} + \text{H}$] $^+$ ($\text{C}_{85}\text{H}_{88}\text{N}_7\text{O}_{18}\text{F}_9\text{P}_3\text{S}_3$ requires 1854.442).

2,2,2-Trifluoroethyl 6,6',6''-((S)-2-(4-aminobutyl)-1,4,7-triazacyclononane-1,4,7-triyl)tris(methylene)tris(4-((4-methoxyphenyl)ethynyl)pyridine-6,2-diyl)tris(3-(ethoxy phosphoryl benzenesulfonate), 83a

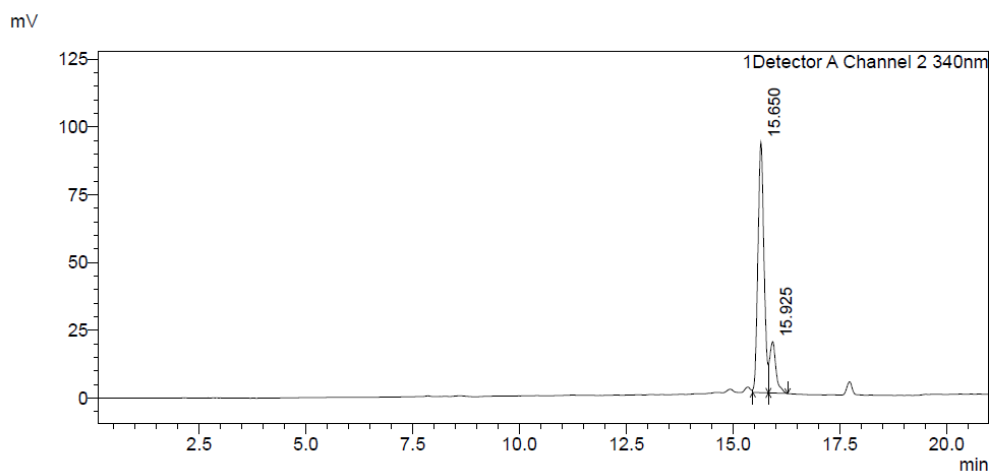


tert-Butyl 4-((*S*)-1,4,7-tris((6-(ethoxy(3-(2,2,2-Trifluoroethyl)phosphoryl benzenesulfonate)-4-((4-methoxyphenyl)ethynyl)pyridin-2-yl)methyl)-1,4,7-triazacyclononan-2-yl)butylcarbamate, **83** (20.0 mg, 10 μ mol) was dissolved in dry DCM (1.8 mL). Argon was bubbled for 10 min after which time TFA (0.2 mL) was added. The solution was stirred for 20 min and the solvent was removed under reduced pressure to give the trifluoroacetate salt as a yellow oil (5.7 mg, 30 %); δ_{H} (CDCl_3) 8.43 (3H, m, H^4), 8.30 (3H, m, H^{13}), 7.88 (6H, m, H^{5-3}), 7.61 (3H, m, H^{12}), 7.52 (3H, m, H^2), 7.43 (6H, m, H^6), 6.93 (6H, m, H^7), 4.65 (6H, q, $^3J_{\text{F-H}}$ 7.5 Hz, H^{14}), 4.15 (6H, m, P-OCH₂), 3.95 (15H, m, H^1 and OMe), 3.78-3.34 (13H, m, 9N₃ ring protons and H^{11}), 1.62-1.49 (6H, m, H^{10-9-8}), 1.43 (9H, m, CH₃(Et)); δ_{F} (CD_3OD) -76.2 (br); δ_{P} (CD_3OD) + 22.0; m/z (HRMS⁺) 1854.439 [$\text{M} + \text{H}$]⁺ ($\text{C}_{85}\text{H}_{88}\text{N}_7\text{O}_{18}\text{F}_9\text{P}_3\text{S}_3$ requires 1854.442).

Eu(III) complex of (*R,R,R*)-6,6',6''-((*S*)-2-(4-aminobutyl)-1,4,7-triazacyclononane-1,4,7-triyl)tris(methylene)tris(4-((4-methoxyphenyl)ethynyl)pyridine-6,2-diyl)tris(4-(hydroxyphosphoryl benzenesulfonate), [EuL²⁰]²⁻

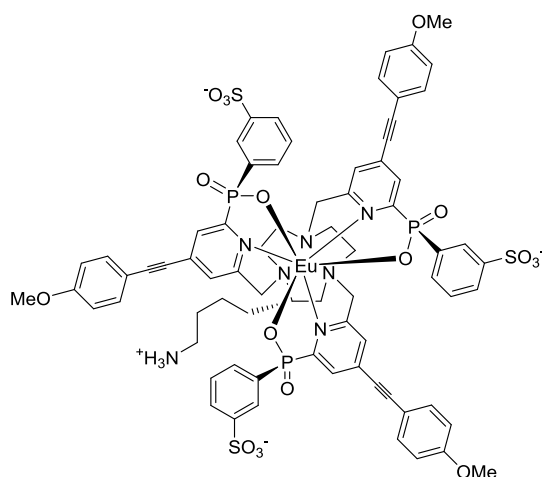


2,2,2-Trifluoroethyl 6,6',6''-((*S*)-2-(4-aminobutyl)-1,4,7-triazacyclononane-1,4,7-triyl)tris(methylene)tris(4-((4-methoxyphenyl)ethynyl)pyridine-6,2-diyl)tris(4-(ethoxy phosphoryl benzenesulfonate), **82a** (5.0 mg, 2.7 μmol) was dissolved in CD_3OD (1 mL) and a solution of NaOH in D_2O (0.1 M, 0.5 mL) was added. The mixture was heated to 60 $^\circ\text{C}$ under argon and monitored with ^{19}F -NMR [δ_{F} (reactant) = - 76.0, δ_{F} (product, trifluoroethanol) = - 78.0] and ^{31}P -NMR [δ_{P} (reactant) = + 23.6, δ_{P} (product) = + 15.1]. After 3 h the solution was cooled to RT and the pH was adjusted to 7 with HCl. $\text{Eu}(\text{Cl})_3\cdot 6\text{H}_2\text{O}$ (1.0 mg, 2.7 μmol) was added and the mixture heated to 65 $^\circ\text{C}$ overnight under argon. The solvent was removed under reduced pressure and the product purified by HPLC (*Method K*, t_{R} = 16.1 min) giving the triethylammonium salt as a white solid (2.8 mg, 63 %); (HRMS⁻) 1671.237 [MH_2]⁻ ($\text{C}_{73}\text{H}_{68}^{151}\text{EuN}_7\text{O}_{18}\text{P}_3\text{S}_3$ requires 1671.238); $\tau_{\text{H}_2\text{O}}$ = 1.13 ms; $\lambda_{\text{max}}(\text{H}_2\text{O})$ = 332 nm; ε = 58 $\text{mM}^{-1}\text{cm}^{-1}$.



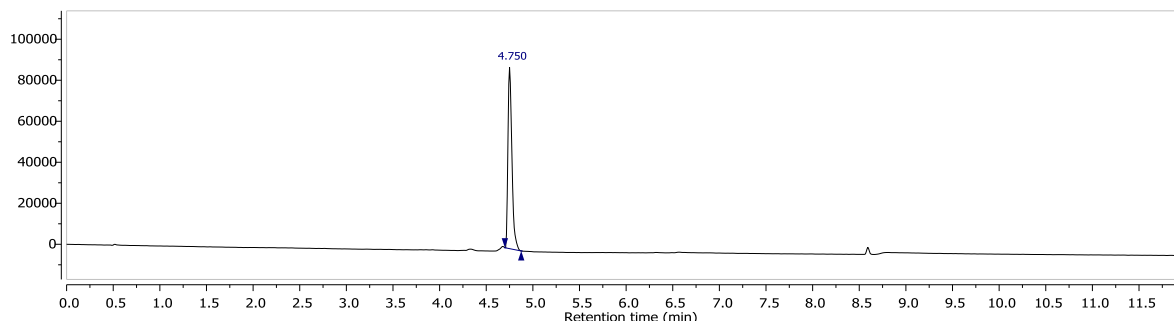
Method L, $t_R = 15.7$ min

Eu(III) complex of (*R,R,R*)-6,6',6''-((*S*)-2-(4-aminobutyl)-1,4,7-triazacyclononane-1,4,7-triyl)tris(methylene)tris(4-((4-methoxyphenyl)ethynyl)pyridine-6,2-diyl)tris(3-(hydroxyphosphoryl benzenesulfonate), [EuL²³]²⁻



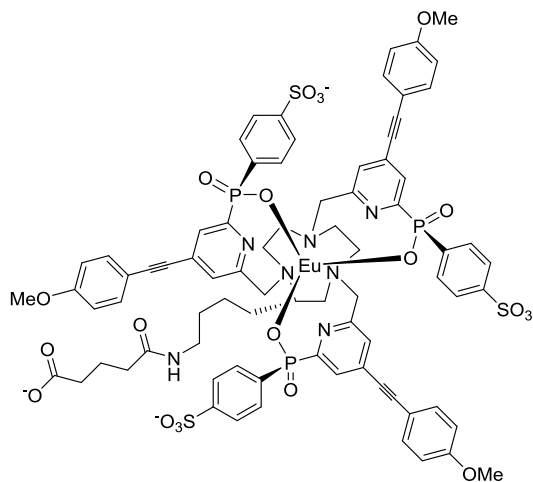
2,2,2-Trifluoroethyl 6,6',6''-((*S*)-2-(4-aminobutyl)-1,4,7-triazacyclononane-1,4,7-triyl)tris(methylene)tris(4-((4-methoxyphenyl)ethynyl)pyridine-6,2-diyl)tris(3-(4-methoxyphosphoryl benzenesulfonate), **83a** (7 mg, 4.2 μmol) was dissolved in CD_3OD (1 mL) and a solution of NaOH in D_2O (0.1 M, 0.5 mL) was added. The mixture was heated to 60 °C under argon and monitored with ^{19}F -NMR [δ_{F} (reactant) = - 76.2, δ_{F} (product, trifluoroethanol) = - 78.0] and ^{31}P -NMR [δ_{P} (reactant) = + 22.0, δ_{P} (product) = + 13.7]. After 3 h the solution was cooled to RT and the pH was adjusted to 7 with HCl. $\text{Eu}(\text{Ac})_3\text{H}_2\text{O}$ (1.4 mg, 4.2 μmol) was added and the mixture heated to 65 °C overnight under argon. The solvent was removed under reduced pressure and the product purified by HPLC (Method K, $t_R = 16.6$ min) giving the

triethylammonium salt as a white solid (3.0 mg, 42 %); (HRMS⁺) 1671.239 [MH]⁺ (C₇₃H₆₈¹⁵¹EuN₇O₁₈P₃S₃ requires 1671.238); $\tau_{\text{H}_2\text{O}} = 1.10$ ms; $\lambda_{\text{max}}(\text{H}_2\text{O}) = 332$ nm; $\varepsilon = 58$ mM⁻¹ cm⁻¹.



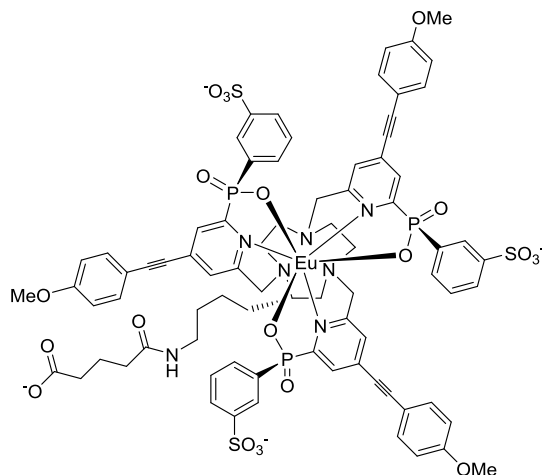
Method M, $t_{\text{R}} = 4.8$ min

Eu(III) complex of (*R,R,R*)-6,6',6''-((*S*)-2-(4-(4-carboxybutanamido) butyl))-1,4,7-triazacyclonane-1,4,7-triyl)tris(methylene)tris(4-((4-methoxyphenyl)ethynyl)pyridine-6,2-diyl)tris(4-(hydroxyphosphoryl benzenesulfonate), [EuL²⁰]-glu⁴⁻



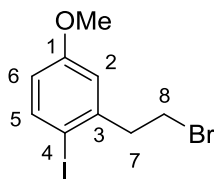
The Eu(III) complex of (*R,R,R*)-6,6',6''-((*S*)-2-(4-aminobutyl)-1,4,7-triazacyclonane-1,4,7-triyl)tris(methylene)tris(4-((4-methoxyphenyl)ethynyl)pyridine-6,2-diyl)tris(4-(hydroxyphosphoryl benzenesulfonate), [EuL²⁰]²⁻ (0.4 mg, 0.24 μmol), was dissolved in dry DMF (300 μL). Glutaric anhydride (0.03 mg, 0.24 μmol) and DIPEA (2 μL) were added and the reaction was stirred at RT for 1 h. The product was purified by HPLC (*Method K*, $t_{\text{R}} = 18.4$ min) giving the triethylammonium salt as a white solid (0.4 mg, 93 %); (HRMS⁺) 1786.255 [MH₃]⁺ (C₇₈H₇₄¹⁵³EuN₇O₂₁P₃S₃ requires 1786.254).

Eu(III) complex of (*R,R,R*)-6,6',6''-((*S*)-2-(4-(4-carboxybutanamido) butyl))-1,4,7-triazacyclonane-1,4,7-triyl)tris(methylene)tris(4-((4-methoxyphenyl)ethynyl)pyridine-6,2-diyl)tris(3-(hydroxyphosphoryl benzenesulfonate), [EuL²³]-glu⁴⁻



The Eu(III) complex of (*R,R,R*)-6,6',6''-((*S*)-2-(4-aminobutyl)-1,4,7-triazacyclonane-1,4,7-triyl)tris(methylene)tris(4-((4-methoxyphenyl)ethynyl)pyridine-6,2-diyl)tris(3-(hydroxyphosphoryl benzenesulfonate), [EuL²³]²⁻ (0.3 mg, 0.18 μmol), was dissolved in dry DMF (400 μL). Glutaric anhydride (0.03 mg, 0.18 μmol) and DIPEA (2 μL) were added and the reaction was stirred at RT for 1 h. The product was purified by HPLC (*Method K*, *t_R* = 16.1 min) giving the triethylammonium salt as a white solid (0.3 mg, 93 %); (HRMS⁻) 1786.258 [MH₃]⁻ (C₇₈H₇₄¹⁵³EuN₇O₂₁P₃S₃ requires 1786.254).

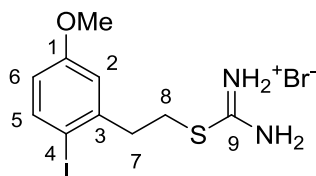
2-(2-Bromoethyl)-1-iodo-4-methoxybenzene, 86



3-Methoxyphenethyl bromide (1.9 g, 8.7 mmol), was dissolved in MeOH (30 mL) and ICl (2.8 g, 17.4 mmol) was added to the solution. The mixture was stirred at RT for 3 h, after which time 10 % solution of Na₂S₂O₃ (90 mL) was added causing the formation of a white solid. The solvent was removed under reduced pressure, the crude product re-dissolved in DMC (50 mL) and washed with 10 % solution of Na₂S₂O₃. The organic layer was dried over MgSO₄ and the solvent removed under reduced pressure. The crude material was purified by column chromatography (silica, Hex : DCM 10 : 0 to 10 : 1) to give a clear oil (1.5 mg, 51

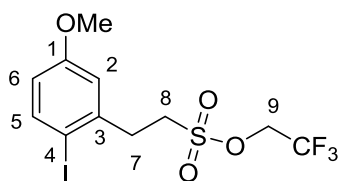
); δ_{H} (CDCl_3) 7.78 (1H, d, $^3J_{\text{H-H}}$ 9 Hz, H⁵), 6.83 (1H, d, $^4J_{\text{H-H}}$ 3 Hz, H²), 6.56 (1H, dd, $^3J_{\text{H-H}}$ 9 Hz, $^4J_{\text{H-H}}$ 3, H⁶) 3.78 (3H, s, OMe), 3.55 (2H, t, $^3J_{\text{H-H}}$ 8 Hz, H⁸), 3.23 (2H, t, $^3J_{\text{H-H}}$ 7.5 Hz, H⁷), NMR data are in good agreement with those previously reported¹³⁸, $R_f = 0.41$ (silica, Hex : DMC 3 : 1).

2-(2-Iodo-5-methoxyphenethyl)isothiuronium bromide, **87**



2-(2-Bromoethyl)-1-iodo-4-methoxybenzene, **86** (1.50 g, 4.40 mmol) was added to EtOH (25 mL), followed by thiourea (335 mg, 4.70 mmol). The mixture was refluxed for 16 h, after which time the solvent was removed under reduced pressure. The crude compound was washed with Et₂O (2 x 5 mL) giving a white solid (1.63 g, 89 %); m.p. = 183 - 186 °C; δ_{H} (CD_3OD) 7.69 (1H, d, $^3J_{\text{H-H}}$ 8.5 Hz, H⁵), 6.96 (1H, d, $^4J_{\text{H-H}}$ 3 Hz, H²), 6.63 (1H, dd, $^3J_{\text{H-H}}$ 8.5 Hz, $^4J_{\text{H-H}}$ 3 Hz, H⁶), 3.78 (3H, s, OMe), 3.42 (2H, t, $^3J_{\text{H-H}}$ 7.5 Hz, H⁸), 3.10 (2H, t, $^3J_{\text{H-H}}$ 7.5 Hz, H⁷); δ_{C} (CD_3OD) 171.2 (s, C⁹), 160.4 (s, C¹), 141.8 (s, C³), 140.0 (s, C⁵), 115.9 (s, C²), 114.7 (s, C⁶), 87.8 (s, C⁴), 54.6 (s, OMe), 38.9 (s, C⁷), 30.9 (s, C⁸); m/z (HRMS+) 336.9878 [$\text{M}]^+$ ($\text{C}_{10}\text{H}_{14}\text{N}_2\text{OSI}$ requires 336.9872).

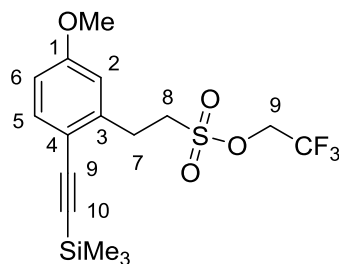
2,2,2-Trifluoroethyl 2-(2-iodo-5-methoxyphenyl)ethanesulfonate, **88**



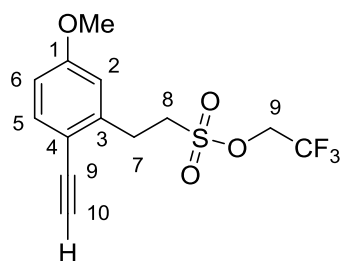
6 M H₂SO₄ (0.8 mL) and Et₂O (9 mL) were added to 2-(2-iodo-5-methoxyphenethyl)isothiuronium bromide, **87** (750 mg, 1.80 mmol) at 0 °C. A solution of bleach (5 %, 10.5 mL) was added dropwise to the resultant suspension under vigorous stirring keeping the temperature below 20 °C. After the addition, the mixture was stirred for 30 min at RT after which time the reaction was transferred into a separating funnel and the two layers partitioned. The organic layer was washed with brine (2 x 10 mL) and 10 % solution of Na₂S₂O₃ (2 x 20 mL), dried over MgSO₄ and the solvent removed under reduced pressure giving the sulfonyl chloride compound as a yellow oil. Without further purification the

compound was dissolved in DCM (12 mL). Trifluoroethanol (130 μ L, 1.8 mmol) was added to the solution, followed by Et₃N (300 mg, 2.1 mmol). The mixture was stirred at RT for 1 h after which time the solvent was removed under reduced pressure. The crude compound was purified by column chromatography (silica, Hex : DCM 4 : 1 to 1 : 1) to yield a clear oil (297 mg, 39 %); δ_{H} (CDCl₃) 7.68 (1H, d, ³J_{H-H} 8.5 Hz, H⁵), 6.83 (1H, d, ⁴J_{H-H} 3 Hz, H²), 6.57 (1H, dd, ³J_{H-H} 8.5 Hz, ⁴J_{H-H} 3 Hz, H⁶), 4.52 (2H, q, ³J_{H-F} 8 Hz, H⁹), 3.77 (3H, s, OMe), 3.45 (2H, m, H⁸), 3.24 (2H, m, H⁷); δ_{C} (CDCl₃) 160.3 (s, C¹), 140.4 (s, C⁵), 140.3 (s, C³), 122.0 (q, ¹J_{C-F} 278 Hz, CF₃), 116.1 (s, C²), 115.2 (s, C⁶), 87.8 (s, C⁴), 63.9 (q, ²J_{C-F} 38 Hz, C⁹), 55.4 (s, OMe), 51.0 (s, C⁸), 34.8 (s, C⁷); δ_{F} (CDCl₃) -74.2 (t, ³J_{F-H} 7.0 Hz); *m/z* (HRMS⁺) 423.9463 [M + H]⁺ (C₁₁H₁₂O₄F₃SI requires 423.9453), *R_f* = 0.16 (silica, Hex : DCM 3 : 1).

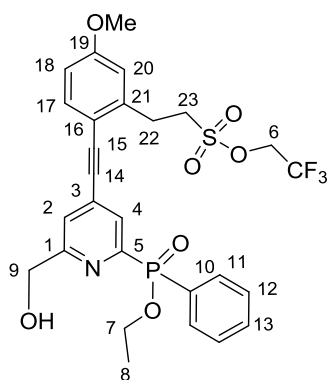
2,2,2-Trifluoroethyl 2-(5-methoxy-2-((trimethylsilyl)ethynyl)phenyl)ethanesulfonate, **88a**



2,2,2-Trifluoroethyl 2-(2-iodo-5-methoxyphenyl)ethanesulfonate, **88** (110 mg, 0.26 mmol), was dissolved in dry THF (1.5 mL) and the solution was degassed (freeze-thaw cycle) three times. Ethynyltrimethylsilane (55 μ L, 0.39 mmol) and NEt₃ (0.35 mL) were added and the solution degassed once more. [1,1'-bis(diphenylphosphino)ferrocene]palladium(II) chloride (30 mg, 0.03 mmol) and CuI (5 mg, 0.03 mmol) were added and the solution was degassed a further three times. The solution was stirred at 65 °C under argon for 16 h, solvent was removed under reduced pressure and the crude material purified by column chromatography (silica, DCM : Hex 1 : 4 to 1 : 2) to give a clear oil (76 mg, 75 %); δ_{H} (CDCl₃) 7.40 (1H, d, ³J_{H-H} 9 Hz, H⁵), 6.75 (2H, m, H²⁻⁶), 4.48 (2H, q, ³J_{H-F} 8 Hz, H⁹), 3.80 (3H, s, OMe), 3.52 (2H, m, H⁸), 3.27 (2H, m, H⁷), 0.25 (9H, s, SiMe₃); δ_{C} (CDCl₃) 160.0 (s, C¹), 140.6 (s, C³), 134.3 (s, C⁵), 122.2 (q, ¹J_{C-F} 278 Hz, CF₃), 115.1 (s, C²), 114.8 (s, C⁴), 112.8 (s, C⁶), 102.3 (s, C¹⁰), 98.2 (s, C¹¹), 63.6 (q, ²J_{C-F} 38 Hz, C⁹), 55.3 (s, OMe), 51.1 (s, C⁸), 29.2 (s, C⁷), -0.2 (s, SiMe₃); δ_{F} (CDCl₃) -74.3 (t, ³J_{F-H} 7.0 Hz); *m/z* (HRMS⁺) 417.0781 [M + H]⁺ (C₁₆H₂₁O₄F₃NaSSi requires 417.0774), *R_f* = 0.66 (silica, EtOAc : Hex 2 : 8).

2,2,2-Trifluoroethyl 2-(2-ethynyl-5-methoxyphenyl)ethanesulfonate, 89

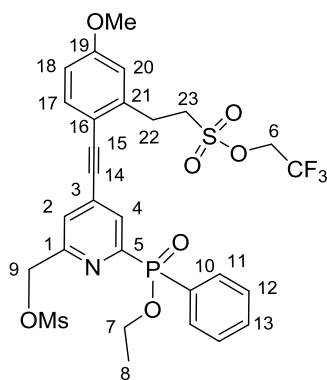
2,2,2-Trifluoroethyl 2-(5-methoxy-2-((trimethylsilyl)ethynyl)phenyl)ethanesulfonate, **88a** (45 mg, 0.11 mmol) was dissolved in anhydrous THF (0.8 mL) and triethylammonium dihydrofluoride (190 μ L, 1.1 mmol) was added. The mixture was stirred at 35 $^{\circ}$ C under argon for 48 h. The solvent was removed under reduced pressure to give a yellow oil which was subjected to column chromatography (silica, Hex : DCM 3 : 1 to 1 : 1) to give a clear oil (35 mg, 98 %); δ_{H} (CDCl_3) 7.42 (1H, d, $^3J_{\text{H-H}}$ 9 Hz, H⁵), 6.77 (2H, m, H²⁻⁶), 4.49 (2H, q, $^3J_{\text{H-F}}$ 8 Hz, H⁹), 3.80 (3H, s, OMe), 3.50 (2H, m, H⁸), 3.30 (2H, m, H⁷), 3.26 (1H, s, CH); δ_{C} (CDCl_3) 160.3 (s, C¹), 140.8 (s, C³), 134.7 (s, C⁵), 122.4 (q, $^1J_{\text{C-F}}$ 278 Hz, CF₃), 115.1 (s, C²), 113.7 (s, C⁴), 112.9 (s, C⁶), 81.0 (s, C¹¹), 80.8 (s, C¹⁰), 63.7 (q, $^2J_{\text{C-F}}$ 38.5 Hz, C⁹), 55.4 (s, OMe), 51.2 (s, C⁸), 29.2 (s, C⁷); δ_{F} (CDCl_3) -74.3 (t, $^3J_{\text{F-H}}$ 7.0 Hz); m/z (HRMS+) 323.0559 [M + H]⁺ (C₁₃H₁₄O₄F₃S requires 323.0565); R_f = 0.33 (silica, EtOAc : Hex 1 : 9).

2,2,2-Trifluoroethyl 2-(2-((2-(ethoxy(phenyl)phosphoryl)-6-(hydroxymethyl)pyridin-4-yl)ethynyl)-5-methoxyphenyl)ethanesulfonate, 90

Ethyl (4-bromo-6-hydroxymethylpyridin-2-yl)(phenyl)phosphinate, **31** (29 mg, 80 μ mol), was dissolved in anhydrous THF (1 mL) and the solution was degassed (freeze-thaw cycle) three times. 2,2,2-Trifluoroethyl 2-(2-ethynyl-5-methoxyphenyl)ethanesulfonate, **89** (40 mg, 120 μ mol) and NEt₃ (0.22 mL) were added and the solution degassed once more. [1,1'-

bis(diphenylphosphino)ferrocene]palladium(II) chloride (9 mg, 8 μmol) and CuI (1.5 mg, 8 μmol) were added and the solution was degassed a further three times. The solution was stirred at 65 $^{\circ}\text{C}$ under argon for 16 h, solvent was removed under reduced pressure and the crude material purified by column chromatography (silica, DCM : MeOH 0 to 2 %) to give a clear oil (25 mg, 52 %); δ_{H} (CDCl_3) 8.12 (1H, d $^3J_{\text{H-P}}$ 6 Hz, H^4), 7.95 (2H, m, H^{11}), 7.47 (5H, m, $\text{H}^{2-12-13-17}$), 6.84 (2H, m, H^{18-20}), 4.77 (2H, s, H^9), 4.57 (2H, q, $^3J_{\text{H-F}}$ 8 Hz, H^9), 4.15 (2H, m, H^7), 4.05 (1H, br, OH), 3.85 (3H, s, OMe), 3.56 (2H, m, H^{23}), 3.34 (2H, m, H^{22}), 1.39 (3H, d, $^3J_{\text{H-H}}$ 7 Hz, H^{10}); δ_{C} (CDCl_3) 161.7 (s, C^{19}), 160.1 (s, C^1), 154.5 (d, $^1J_{\text{C-P}}$ 153 Hz, C^5), 140.9 (s, C^{21}), 134.9 (s, C^{17}), 132.7 (s, C^3), 132.5 (s, C^{13}), 132.4 (s, C^{11}), 128.7 (s, C^4), 128.8 (s, C^{12}), 128.5 (s, C^2), 123.8 (s, C^{16}), 122.4 (q, $^1J_{\text{C-F}}$ 278 Hz, CF_3), 115.4 (s, C^{20}), 113.2 (s, C^{18}), 93.8 (s, C^{15}), 90.2 (s, C^{14}), 63.7 (s, C^9), 63.6 (q, $^2J_{\text{C-F}}$ 38.5 Hz, C^6), 62.1 (s, C^7), 55.5 (s, OMe), 51.7 (s, C^{23}), 29.1 (s, C^{22}), 16.6 (s, C^8); δ_{F} (CDCl_3) -74.2 (t, $^3J_{\text{F-H}}$ 7.0 Hz); δ_{P} (CDCl_3) +24.7; m/z (HRMS+) 598.1277 [$\text{M} + \text{H}$] $^+$ ($\text{C}_{27}\text{H}_{28}\text{NO}_7\text{F}_3\text{PS}$ requires 598.1276); R_f = 0.37 (silica; DCM : 3 % MeOH).

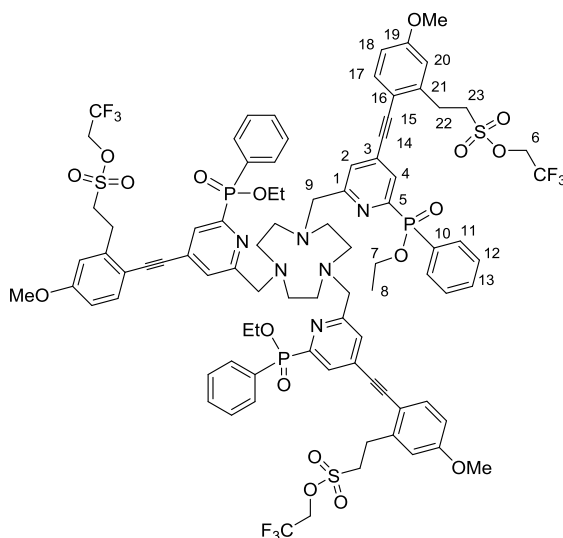
2,2,2-Trifluoroethyl 2-(2-((2-(ethoxy(phenyl)phosphoryl)-6-((methylsulfonyloxy)methyl)pyridin-4-yl)ethynyl)-5-methoxyphenyl)ethanesulfonate, **91**



2,2,2-Trifluoroethyl 2-(2-((2-(ethoxy(phenyl)phosphoryl)-6-(hydroxymethyl)pyridin-4-yl)ethynyl)-5-methoxyphenyl)ethanesulfonate, **90** (25 mg, 42 μmol) was dissolved in anhydrous THF (1 mL) and NEt_3 (17 μL , 0.12 mmol) was added. The mixture was stirred at 5 $^{\circ}\text{C}$ and methanesulfonyl chloride (5 μL , 65 μmol) was added. The reaction was monitored by TLC (silica; DCM : 5 % MeOH, R_f (product) = 0.44, R_f (reactant) = 0.33) and stopped after 15 min. The solvent was removed under reduced pressure and the residue dissolved in DCM (10 mL) and washed with NaCl solution (saturated, 10 mL). The aqueous layer was re-extracted with DCM (3 \times 10 mL) and the organic layers combined, dried over MgSO_4 and the solvent

removed under reduced pressure to leave a colourless oil (19 mg, 67 %); δ_{H} (CDCl_3) 8.15 (1H, dd, $^3J_{\text{H-P}}$ 6 Hz, $^4J_{\text{H-H}}$ 1.5 Hz, H^4), 7.96 (2H, ddd, $^3J_{\text{H-P}}$ 12.5 Hz, $^3J_{\text{H-H}}$ 8.5 Hz, $^4J_{\text{H-H}}$ 1.5 Hz, H^{11}), 8.15 (1H, s, H^2), 7.49 (4H, m, $\text{H}^{12-13-17}$), 6.85 (2H, m, H^{18-20}), 5.33 (2H, s, H^9), 4.59 (2H, q, $^3J_{\text{H-F}}$ 8 Hz, H^9), 4.15 (2H, m, H^7), 3.85 (3H, s, OMe), 3.56 (2H, m, H^{23}), 3.35 (2H, m, H^{22}), 3.03 (3H, s, Ms), 1.39 (3H, d, $^3J_{\text{H-H}}$ 7 Hz, H^{10}); δ_{F} (CDCl_3) -74.2 (t, $^3J_{\text{F-H}}$ 7.0 Hz); δ_{P} (CDCl_3) +24.7; m/z (HRMS+) 676.1036 [$\text{M} + \text{H}$] $^+$ ($\text{C}_{28}\text{H}_{30}\text{NO}_9\text{F}_3\text{PS}_2$ requires 676.1052); R_f = 0.44 (silica; DCM : 3 % MeOH).

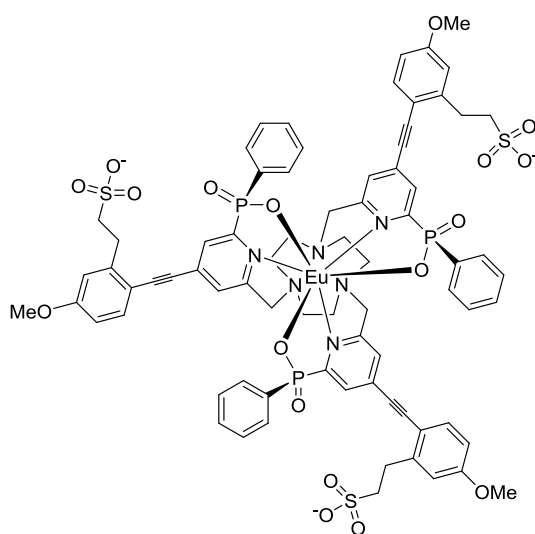
Tris(2,2,2-trifluoroethyl) 2,2',2''-(6,6',6''-(6,6',6''-(1,4,7-triazacyclononane-1,4,7-triyl)tris(methylene)tris(2-(ethoxy(phenyl)phosphoryl)pyridine-6,4-diyl))tris(ethyne-2,1-diyl))tris(3-methoxybenzene-6,1-diyl))triethanesulfonate, **92**



1,4,7-Triazacyclononane trihydrochloride (1.0 mg, 4.0 μmol) and (*S*)-2,2,2-trifluoroethyl 2-(2-((2-(ethoxy(phenyl)phosphoryl)-6-((methylsulfonyloxy)methyl)pyridin-4-yl)ethynyl)-5-methoxyphenyl)ethanesulfonate, **91** (8.8 mg, 13.0 μmol), were dissolved in anhydrous CH_3CN (1 mL) and K_2CO_3 (3.5 mg, 26.0 μmol) was added. KI (catalytical) was added to the reaction and the mixture was stirred under argon at 60 $^\circ\text{C}$ for 16 h. The reaction was cooled and the solution decanted from excess potassium salts. The solvent was removed under reduced pressure to give a yellow oil (4.0 mg, 57 %); δ_{H} (CDCl_3) 8.08 (3H, d, $^3J_{\text{H-P}}$ 6 Hz, H^4), 7.91 (6H, m, H^{11}), 7.42 (15H, m, $\text{H}^{2-12-13-17}$), 6.83 (6H, m, H^{18-20}), 4.57 (6H, q, $^3J_{\text{H-F}}$ 8 Hz, H^6), 4.15 (6H, m, H^7), 3.90 (6H, s, H^9), 3.85 (9H, s, OMe), 3.59 (6H, m, H^{23}), 3.37 (6H, m, H^{22}), 2.94 (12H, br, 9 N_3), 1.41 (9H, d, $^3J_{\text{H-H}}$ 7 Hz, H^{10}); δ_{C} (CDCl_3) 161.8 (s, C^{19}), 160.2 (s, C^1), 154.6 (d, $^1J_{\text{C-P}}$ 153 Hz, C^5), 140.9 (s, C^{21}), 134.9 (s, C^{17}), 132.7 (s, C^3), 132.3 (s, C^{13}), 132.4

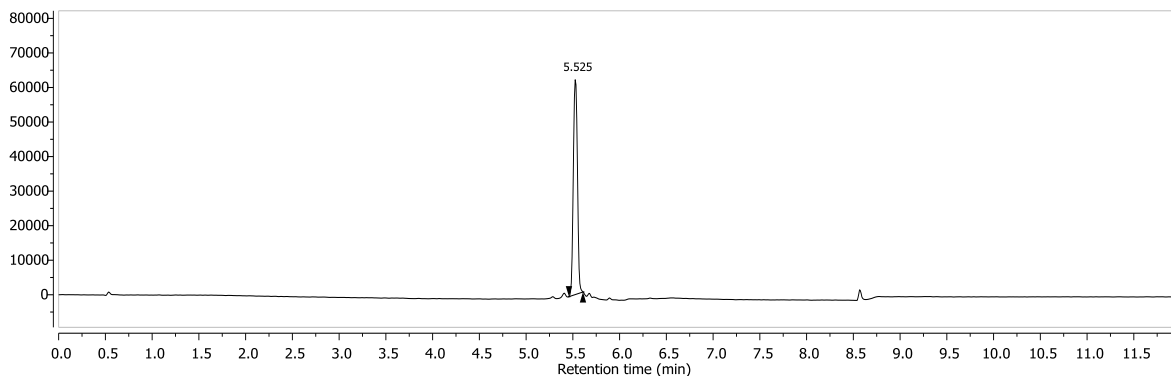
(s, C¹¹), 128.7 (s, C⁴), 128.9 (s, C¹²), 128.5 (s, C²), 123.8 (s, C¹⁶), 122.4 (q, ¹J_{C-F} 278 Hz, CF₃), 115.2 (s, C²⁰), 113.1 (s, C¹⁸), 93.8 (s, C¹⁵), 90.2 (s, C¹⁴), 63.9 (s, C⁹), 63.6 (q, ²J_{C-F} 38 Hz, C⁶), 62.1 (s, C⁷), 56.0 (br, ring C), 55.5 (s, OMe), 51.7 (s, C²³), 29.1 (s, C²²), 16.6 (s, C⁸); δ_F (CDCl₃) -74.2 (t, ³J_{F-H} 8 Hz); δ_P (CDCl₃) +25.2; *m/z* (HRMS⁺) 1867.453 [M + H]⁺ (C₈₇H₉₁N₆O₁₈F₉S₃P₃ requires 1867.462).

Eu(III) complex of 2,2',2''-(6,6',6''-(6,6',6''-(1,4,7-triazacyclononane-1,4,7-triyl)tris(methylene)tris(2-(hydroxy(phenyl)phosphoryl)pyridine-6,4-diyl))tris(ethyne-2,1-diyl)tris(3-methoxybenzene-6,1-diyl))triethanesulfonate, [EuL^{26a}]³⁻



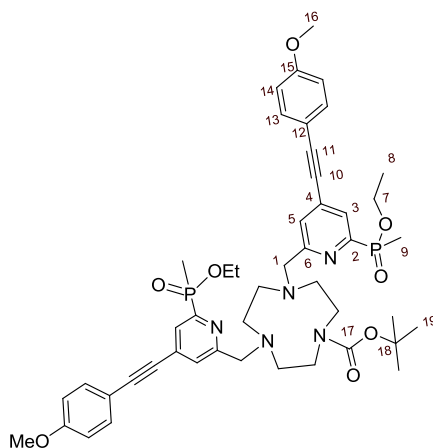
Tris(2,2,2-trifluoroethyl) 2,2',2''-(6,6',6''-(6,6',6''-(1,4,7-triazacyclononane-1,4,7-triyl)tris(methylene)tris(2-(ethoxy(phenyl)phosphoryl)pyridine-6,4-diyl))tris(ethyne-2,1-diyl)tris(3-methoxybenzene-6,1-diyl))triethanesulfonate, **92** (5.0 mg, 2.6 μmol) was dissolved in MeOH (1.5 mL) and a solution of KOH in H₂O was added (pH = 12). The mixture was heated to 60 °C under argon and monitored with ³¹P-NMR [δ_P(reactant) = +25.2, δ_P(product) = +14.6]. After 3 h the solution was cooled to RT and the pH was adjusted to 7 with HCl. Eu(AcO)₃H₂O (1.0 mg, 3.0 μmol) was added and the mixture heated to 65 °C overnight under argon to give the sulfonate protected complex (*m/z* (HRMS⁺) 1931.262 [M + H]⁺ (C₈₁H₇₆N₆O₁₈S₃P₃¹⁵¹EuF₉ requires 1931.265)). A solution of KOH in H₂O was added (pH = 14) and the mixture heated to 60 °C overnight. The solution was cooled to RT and the pH was adjusted to 7 with HCl. Further Eu(AcO)₃H₂O (1.0 mg, 3.0 μmol) was added and the mixture heated to 65 °C overnight. The solvent was removed under reduced pressure and the product purified by HPLC (*Method K*, *t_R* = 21.1 min) giving the triethylammonium salt as a white

solid (1.0 mg, 25 %); m/z (HRMS⁻) 841.1129 [MH]²⁻ (C₇₅H₇₂¹⁵¹EuN₆O₁₈P₃S₃ requires 841.1160); $\tau_{\text{H}_2\text{O}}$ = 1.15 ms; λ_{max} (H₂O) = 336 nm; ε = 58 mM⁻¹ cm⁻¹.



Method M, t_{R} = 5.5 min

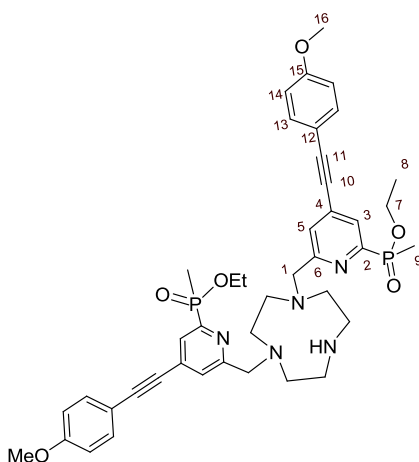
tert*-Butyl 4,7-bis((6-(ethoxy(methyl)phosphoryl)-4-((4-methoxyphenyl)ethynyl)pyridin-2-yl)methyl)-1,4,7-triazacyclononane-1-carboxylate, **94*



tert-Butyl-1,4,7-triazacyclononane-1-carboxylate, **93** (14 mg, 47 μmol) and ethyl(6-(ethylmethanesulfonate)-4-[2-(4-methoxyphenyl)ethynyl]pyridin-2-yl)(methyl)phosphinate, **19** (40 mg, 94 μmol) were dissolved in anhydrous CH₃CN (3 mL) and K₂CO₃ (13 mg, 94 μmol) was added. The mixture was stirred under argon at 60 °C overnight. The reaction was cooled and the solution decanted from excess potassium salts. The solvent was removed under reduced pressure to give a yellow oil (37 mg, 89 %): δ_{H} (CDCl₃) 7.96 (2H, m, H³), 7.65 (2H, bs, H⁵), 7.44 (4H, d, ³J_{H-H} 8.5 Hz, H¹³), 6.87 (4H, d, ³J_{H-H} 8.5 Hz, H¹⁴), 4.11 – 4.05 (2H, m, H⁷), 3.93, (2H, s, H¹), 3.92 (2H, s, H¹), 3.86 – 3.82 (2H, m, H⁷), 3.81 (6H, s, H¹⁶), 3.35 (4H, br m, ring Hs), 3.08 (4H, br m, ring Hs), 2.68 (4H, br m, ring Hs), 1.75 (3H, d, ²J_{H-P} 15 Hz, H⁹), 1.74 (3H, d, ²J_{H-P} 15 Hz, H⁹), 1.46 (9H, s, H¹⁹), 1.23 (3H, t, ³J_{H-H} 7 Hz, H⁸), 1.22 (3H, t, ³J_{H-H} 7 Hz,

H⁸); δ_C (CDCl₃) 161.6, 161.4 (d, ³J_{C-P} 20 Hz, C⁶), 160.5, 160.4 (s, C¹⁷), 155.6 (s, C¹⁵), 153.8, 153.6 (d, ¹J_{C-P} 165 Hz, C²), 133.6, 133.5 (s, C¹⁵), 132.5 (br m, C⁴), 127.6 (br m, C³), 126.4, 126.1 (d, ⁴J_{C-P} 3 Hz, C⁵), 114.2, 114.1 (s, C¹⁴), 113.9, 113.8 (s, C¹²), 95.6, 95.3 (s, C¹¹), 85.6, 85.4 (br m, C¹⁰), 79.4 (s, C¹⁸) 62.8, 62.5 (s, C¹), 60.9, 60.8 (d, ²J_{C-P} 3 Hz, C⁷), 55.3 (s, C¹⁶), 55.0 – 49.7 (br m, ring Cs), 28.6 (s, C¹⁹), 16.4 (d, ³J_{C-P} 6 Hz, C⁸), 13.3, 13.2 (d, ¹J_{C-P} 109 Hz, C⁹); δ_P (CDCl₃) +40.0, +39.9; *m/z* (HRMS⁺) 884.3937 [M + H]⁺ (C₄₇H₆₀O₈N₅P₂ requires 884.3917).

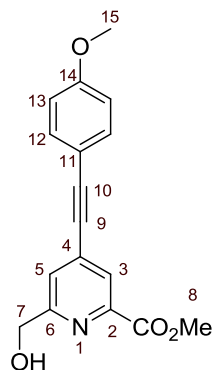
Diethyl-6,6'-(1,4,7-triazacyclononane-1,4-diyl)bis(methylene)bis(4-((4-methoxyphenyl)ethynyl)pyridine-6,2-diyl)bis(methylphosphate), 95



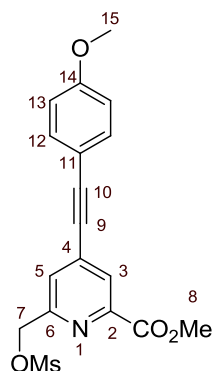
tert-Butyl 4,7-bis((6-(ethoxy(methyl)phosphoryl)-4-((4-methoxyphenyl)ethynyl)pyridin-2-yl)methyl)-1,4,7-triazacyclononane-1-carboxylate, **94** (37 mg, 60 μ mol) was dissolved in anhydrous DCM (3 mL) and TFA (0.7 mL) was added. The solution was stirred under argon at 23 °C for 45 min. The solvent was removed using a high vacuum line (without heating) and the residue re-dissolved in DCM (1 mL), which was again removed using the same method. This process was repeated 5 times to ensure complete removal of excess trifluoroacetic acid. The crude material was purified by HPLC (*Method A*, *t_R* = 11.8 min) to give a yellow oil (15 mg, 45 %); δ_H (CDCl₃) 7.95 (2H, d, ³J_{H-P} 6 Hz, H³), 7.46 (4H, d, ³J_{H-H} 9 Hz, H¹³), 7.41 (2H, bs, H⁵), 6.88 (4H, d, ³J_{H-H} 9 Hz, H¹⁴), 4.15 – 4.10 (2H, m, H⁷), 3.99 (4H, s, H¹), 3.92 – 3.87 (2H, m, H⁷), 3.81 (6H, s, H¹⁶), 3.19 (4H, br s, ring Hs), 3.07 (4H, br s, ring Hs), 2.69 (4H, br s, ring Hs), 1.76 (6H, d, ²J_{H-P} 15.0 Hz, H⁹), 1.27 (6H, t, ³J_{H-H} 7 Hz, H⁸); δ_C (CDCl₃) 160.7 (s, C¹⁵), 159.3 (d, ³J_{C-P} 20 Hz, C⁶), 154.4 (d, ¹J_{C-P} 157 Hz, C²), 133.7 (s, C¹³), 133.1 (d, ³J_{C-P} 11 Hz, C⁴), 127.7 (d, ²J_{C-P} 20 Hz, C³), 126.3 (d, ⁴J_{C-P} 3 Hz, C⁵), 114.2 (s, C¹⁴), 113.5 (s, C¹²), 96.4 (s, C¹¹), 85.0 (s, C¹⁰), 61.1 (d, ²J_{C-P} 6.3 Hz, C⁷), 60.1 (s, C¹), 55.3 (s, C¹⁶), 51.1 – 43.9 (br

m, ring Cs), 16.5 (d, $^3J_{C-P}$ 6 Hz, C⁸), 13.6 (d, $^1J_{C-P}$ 103 Hz, C⁹); δ_P (CDCl₃) +39.3; m/z (HRMS⁺) 784.3387 [M + H]⁺ (C₄₂H₅₂O₆N₅P₂ requires 784.3393).

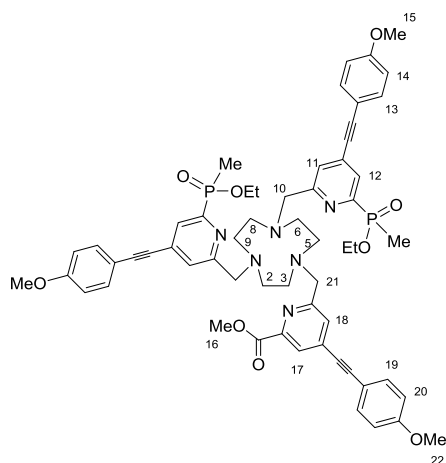
Methyl 6-(hydroxymethyl)-4-((4-methoxyphenyl)ethynyl)picolinate



6-(Hydroxymethyl)-4-iodopicolinate (100 mg, 0.34 mmol) was dissolved in dry THF (1.5 mL) and the solution was degassed (freeze-thaw cycle) three times. 4-Ethynylanisole (67 mg, 0.51 mmol) and NEt₃ (0.95 mL) were added and the solution degassed once more. [1,1'-bis(diphenylphosphino)ferrocene]palladium(II) chloride (40 mg, 0.034 mmol) and CuI (6 mg, 0.034 mmol) were added and the solution was degassed a further three times. The solution was stirred at 65 °C under argon for 12 h, solvent was removed under reduced pressure and the crude material purified by column chromatography (silica, DCM : MeOH 0 to 2 %) to give a dark yellow oil (98 mg, 95 %); δ_H (CDCl₃) 8.07 (1H, bs, H³), 7.59 (1H, bs, H⁵), 7.49 (2H, d, $^3J_{H-H}$ 9 Hz, H¹²), 6.90 (2H, d, $^3J_{H-H}$ 9 Hz, H¹³), 4.85 (2H, s, H⁷), 4.00 (3H, s, H⁸), 3.84 (3H, s, H¹⁵); δ_C (CDCl₃) 165.4 (s, CO), 160.7 (s, C⁶), 160.6 (s, C¹⁴), 147.3 (s, C²), 134.0 (s, C⁴), 133.8 (s, C¹²), 125.8 (s, C⁵), 125.4 (s, C³), 114.4 (s, C¹³), 113.8 (s, C¹¹), 96.0 (s, C¹⁰), 85.3 (s, C⁹), 64.7 (s, C⁷), 55.5 (s, C¹⁵), 53.1 (s, C⁸); (HRMS⁺) 298.1075 [M + H]⁺ (C₁₇H₁₆NO₄ requires 298.1079); R_f = 0.6 (silica, DCM: MeOH 9 : 1).

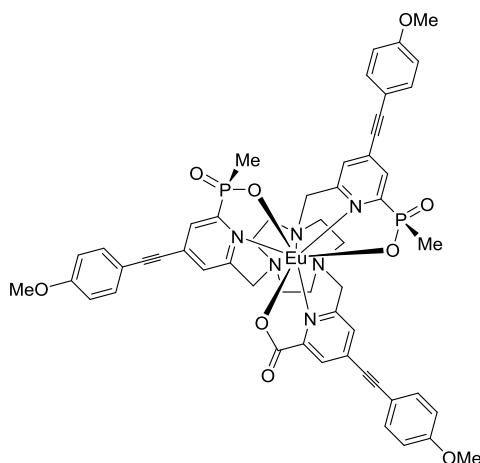
Methyl 4-((4-methoxyphenyl)ethynyl)-6-(((methylsulfonyl)oxy)methyl)picolinate, 96

Methyl 6-(hydroxymethyl)-4-((4-methoxyphenyl)ethynyl)picolinate (28 mg, 0.09 mmol) was dissolved in anhydrous THF (2 mL) and NEt_3 (40 μL , 0.27 mmol) was added. The mixture was stirred at 5 $^\circ\text{C}$ and methanesulfonyl chloride (11 μL , 0.13 mmol) was added. The reaction was monitored by TLC (silica, DCM : 5 % MeOH, $R_f(\text{product}) = 0.70$, $R_f(\text{reactant}) = 0.35$) and stopped after 15 min. The solvent was removed under reduced pressure and the residue dissolved in DCM (10 mL) and washed with NaCl solution (saturated, 8 mL). The aqueous layer was re-extracted with DCM (3×10 mL) and the organic layers combined, dried over MgSO_4 and the solvent removed under reduced pressure to leave a colourless oil (27 mg, 77 %); δ_{H} (CDCl_3) 8.14 (1H, bs, H^3), 7.70 (1H, bs, H^5), 7.50 (2H, d, $^3J_{\text{H-H}} 9$ Hz, H^{12}), 6.91 (2H, d, $^3J_{\text{H-H}} 9$ Hz, H^{13}), 5.40 (2H, s, H^7), 4.00 (3H, s, H^8), 3.84 (3H, s, H^{15}), 3.16 (3H, s, Ms); m/z (ESI) 376.1 $[\text{M} + \text{H}]^+$.

Methyl 6-((4,7-bis((6-(ethoxy(methyl)phosphoryl)-4-((4-methoxyphenyl)ethynyl)pyridin-2-yl)methyl)-1,4,7-triazacyclononan-1-yl)methyl)-4-((4-methoxyphenyl)ethynyl)picolinate, 97

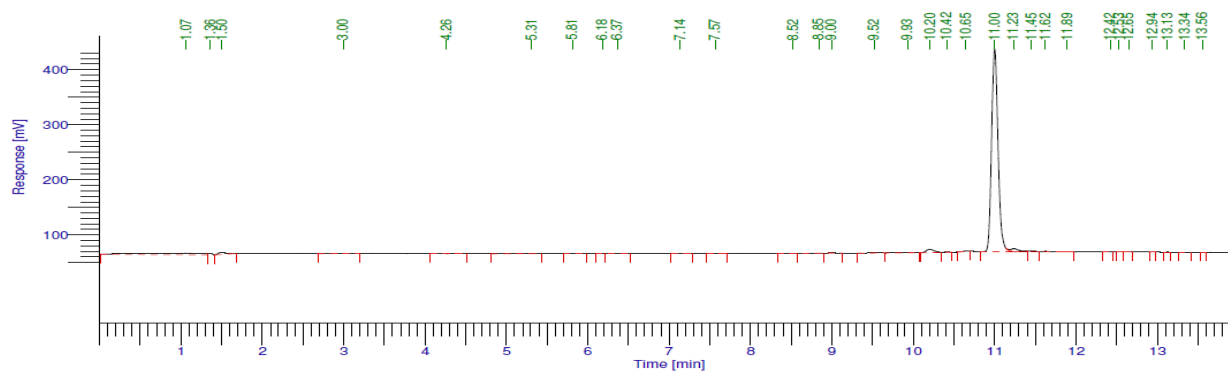
Methyl 4-((4-methoxyphenyl)ethynyl)-6-(((methylsulfonyl)oxy)methyl)picolinate, **96** (7.0 mg, 19 μmol) and diethyl 6,6'-(1,4,7-triazacyclononane-1,4-diyl)bis(methylene)bis(4-((4-methoxyphenyl)ethynyl)pyridine-6,2-diyl)bis(methylphosphinate), **95** (15.0 mg, 19 μmol) were dissolved in anhydrous CH_3CN (1.5 mL) and K_2CO_3 (6.0 mg, 40 μmol) was added. The mixture was stirred under argon at 60 $^\circ\text{C}$ for 24 h, after which time, the reaction was cooled and the solution decanted from excess potassium salts. The solvent was removed under reduced pressure to give an orange oil. The crude material was purified by HPLC (*Method A*, $t_{\text{R}} = 10.6$ min) to give a yellow oil (7.0 mg, 35 %); δ_{H} (CDCl_3) 8.06 (1H, s, H^{17}), 7.99 (2H, d, $^3J_{\text{H-P}}$ 6 Hz, H^{12}), 7.73 (1H, s, H^{16}), 7.67 (2H, d, H^{11}), 7.50 (2H, d, $^3J_{\text{H-H}}$ 8 Hz, H^{19}), 7.46 (4H, d, $^3J_{\text{H-H}}$ 8.0 Hz, H^{13}), 6.91 (2H, d, $^3J_{\text{H-H}}$ 8.0 Hz, H^{20}), 6.89 (4H, d, $^3J_{\text{H-H}}$ 8 Hz, H^{14}), 4.37 (2H, s, H^{21}), 4.23 (4H, s, H^{10}), 4.10 – 3.85 (4H, m, POCH_2), 3.97 (3H, s, H^{16}), 3.85 (3H, s, H^{22}), 3.83 (6H, s, H^{15}), 3.35 – 3.20 (12H, br, ring H), 1.73 (6H, d, $^2J_{\text{H-P}}$ 15 Hz, P-Me), 1.26 (6H, t, $^3J_{\text{H-H}}$ 7 Hz, CH_3 (Et)); δ_{P} (CDCl_3) +40.0; m/z (HRMS^+) 1063.429 [$\text{M} + \text{H}$] $^+$ ($\text{C}_{59}\text{H}_{65}\text{N}_6\text{O}_9\text{P}_2$ requires 1063.429).

Eu(III) complex of (*R,R*)-6-((4,7-bis((4-((4-methoxyphenyl)ethynyl)-6-(methoxydiphosphoryl)pyridin-2-yl)methyl)-1,4,7-triazacyclononan-1-yl)methyl)-4-((4-methoxyphenyl)ethynyl)picolinate, [EuL^8]



Methyl 6-((4,7-bis((6-(ethoxy(methyl)phosphoryl)-4-((4-methoxyphenyl)ethynyl)pyridin-2-yl)methyl)-1,4,7-triazacyclononan-1-yl)methyl)-4-((4-methoxyphenyl)ethynyl)picolinate, **97** (7.0 mg, 6.6 μmol) was dissolved in CD_3OD (1 mL) and a solution of NaOH in D_2O (0.1 M, 0.5 mL) was added. The mixture was heated to 60 $^\circ\text{C}$ under argon and monitored with ^{31}P -NMR [δ_{P} (reactant) = + 40.0, (δ_{P} (product) = + 25.6]. After 5 h the solution was cooled to RT

and the pH was adjusted to 7 with HCl. $\text{Eu}(\text{AcO})_3\text{H}_2\text{O}$ (2.4 mg, 6.6 μmol) was added and the mixture heated to 65 °C overnight under argon. The solvent was removed under reduced pressure giving a white solid (7.5 mg, quantitative yield); δ_{p} (CD_3OD) 50.2, 31.9; m/z (HRMS+) 1141.247 $[\text{M} + \text{H}]^+$ ($\text{C}_{54}\text{H}_{51}^{151}\text{EuN}_6\text{O}_9\text{P}_2$ requires 1141.247); $\tau_{\text{H}_2\text{O}} = 0.89$ ms; λ_{max} (H_2O) = 328 nm; $\varepsilon = 58 \text{ mM}^{-1} \text{ cm}^{-1}$.



Method C, $t_{\text{R}} = 11.0$ min

8 Appendix

Very bright europium complexes that stain cellular mitochondria

J.W. Walton, A. Bourdolle, S.J. Butler, M. Soulie, *M. Delbianco*, B.K. McMahon, R. Pal, H. Puschmann, J.M. Zwier, L. Lamarque, O. Maury, C. Andraudb, D. Parker
Chem. Commun., **2013**, 49, 1600

Complete stereocontrol in the synthesis of macrocyclic lanthanide complexes: direct formation of enantiopure systems for circularly polarised luminescence applications

N.H. Evans, R. Carr, *M. Delbianco*, R. Pal, D. S. Yufit, D. Parker
Dalton Trans., **2013**, 42, 15610

Utility of tris(4-bromopyridyl) europium complexes as versatile intermediates in the divergent synthesis of emissive chiral probes

S.J. Butler, *M. Delbianco*, N.H. Evans, A.T. Frawley, R. Pal, D. Parker, R.S. Puckrin, D.S. Yufit
Dalton Trans., **2014**, 43, 5721

Nouveaux agents complexants hydrosolubles et complexes de lanthanide correspondants,

L. Lamarque, *M. Delbianco*, S.J. Butler, D. Parker
World patent application, WO 2014/111661; PCT/FR20 14/0500085, published July 24, **2014**

Synthesis of *meta* and *para*-substituted aromatic sulfonate groups in polydentate phenylazaphosphinate ligands: enhancement of the water solubility of emissive europium (III) EuroTracker dyes

M. Delbianco, L. Lamarque, D. Parker
Org. Biomol. Chem., **2014**, 12, 8061

Bright, highly water soluble triazacyclononane europium complexes to detect ligand binding with time resolved-FRET microscopy

M. Delbianco, V. Sadovnikova, E. Bourrier, L. Lamarque, J.M. Zwier, D. Parker
Angew. Chem. Int. Ed., **2014**, 53, 10718

EuroTracker Dyes: design, synthesis, structure and photophysical properties of very bright europium complexes and their use in bioassays and cellular optical imaging

S.J. Butler, *M. Delbianco*, L. Lamarque, B.K. McMahon, E.R. Neil, R. Pal, D. Parker, J.W. Walton, J.M. Zwier
Dalton Trans. **2015**, (accepted for the DD15 issue as a Perspective article).

9 References

- ¹ A. Roda, M. Guardiglia, R. Ziessel, M. Mirasoli, E. Michelini, M. Musiani, *Microchem. J.*, **2007**, 85, 5
- ² P. Atkins, J. De Paula, *Physical Chemistry*, Oxford, **2006**, 8th Edition
- ³ N. Johnsson, K. Johnsson, *ACS Chem. Biol.*, **2007**, 2, 31
- ⁴ A. Waggoner, *Curr. Opin. Chem. Biol.*, **2006**, 10, 62
- ⁵ A. Von Bayer, *Chem. Ber.*, **1871**, 5, 255
- ⁶ E. Noelting, K. Dziewonsky, *Ber. Dtsch. Chem. Ges.*, **1905**, 38, 3516
- ⁷ J.E. Berlier, A. Rothe, G. Buller, J. Bradford, D.R. Gray, B.J. Filanoski, W.G. Telford, S. Yue, J. Liu, C.Y. Cheung, W. Chang, J.D. Hirsch, J.M. Beechem, R.P. Haugland, *J Histochem. Cytochem.*, **2003**, 51, 1699
- ⁸ R.B. Mujumdar, L.A. Ernst, S.R. Mujumdar, C.J. Lewis, A.S. Waggoner, *Bioconjugate Chem.*, **1993**, 4, 105
- ⁹ J. Karolin, L.B.A. Johansson, L. Strandberg, T. NyZ, *J. Am. Chem. Soc.*, **1994**, 116, 7801
- ¹⁰ R.Y. Tsien, *Ann. Rev. Neurosci.*, **1989**, 12, 227
- ¹¹ A. Mintaz, J. P.Y. Kao, R.Y. Tsien, *J. Biol. Chem.*, **1989**, 264, 14, 8171
- ¹² G.N. Phillips Jr, *Curr. Opin. Struct. Biol.*, **1997**, 7, 821
- ¹³ A. Cubitt, R. Heim, S. Adams, A. Goyd, L. Gross, R. Tsien, *Elsevier Science Ltd*, **1995**, 968
- ¹⁴ R. Bizzarri, M. Serresi, S. Luin, F. Beltram, *Anal. Bioanal. Chem.*, **2009**, 393, 11072
- ¹⁵ M. Ormo, A.B. Cubitt, K. Kallio, L.A. Gross, R.Y. Tsien, S.J. Remington, *Science*, **1996**, 273, 1392
- ¹⁶ N.C. Shaner, P.A. Steinbach, R.Y. Tsien, *Nature Methods*, **2005**, 2, 905
- ¹⁷ N.C. Shaner, R.E. Campbell, P.A. Steinbach, B.N.G. Giepmans, A.E. Palmer, R.Y. Tsien, *Nature Biotechnol.*, **2004**, 22, 1567
- ¹⁸ A.J. Sutherland, *Curr. Opin. Solid State Mater. Sci.*, **2002**, 6, 365
- ¹⁹ W. Chan, D. Maxwell, X. Gao, R.E. Bailey, M. Han, S. Nie, *Curr. Opin. Biotechnol.*, **2002**, 13, 40
- ²⁰ C. Wu, D.T. Chiu, *Angew. Chem. Int. Ed.*, **2013**, 52, 3086
- ²¹ V. Fernandez-Moreira, F.L. Thorp-Greenwood, M.P. Coogan, *Chem. Commun.*, **2010**, 46, 186
- ²² D. Parker, *Aust. J. Chem.* **2011**, 64, 239
- ²³ R.S. Davidson, *Chem. Soc. Rev.*, **1996**, 25, 241
- ²⁴ A. Beeby, S.W. Botchway, I.M. Clarkson, S. Faulkner, A.W. Parker, D. Parker, J.A.G. Williams, *J. Photochem. Photobiol.*, **2000**, 57, 83
- ²⁵ H. Ke, H. Wang, W.K. Wong, N.K. Mak, D.W.J. Kwong, K.L. Wong, H.L. Tamde, *Chem. Commun.*, **2010**, 46, 6678
- ²⁶ C.P. Montgomery, B.S. Murray, E.J. New, R. Pal, D. Parker, *Acc. Chem. Res.*, **2009**, 42, 925

- ²⁷ A. de Bettencourt-Dias, *The Rare Earth Elements*, Ed. By D.A. Atwood, **2012**, John Wiley & Sons
- ²⁸ D. Parker, *Coord. Chem. Rev.*, **2000**, 205, 109
- ²⁹ D. Parker, A. Beeby, J.A.G. Williams, *J. Chem Soc., Perkin Trans. 2*, **1996**, 1565
- ³⁰ D. Parker, *Chem. Soc. Rev.*, **2004**, 33, 156
- ³¹ A. Thibon, V.C. Pierre, *Anal. Bioanal. Chem.*, **2009**, 394, 107
- ³² A. D'Aleo, A. Picot, A. Beeby, J.A.G. Williams, B. Le Guennec, C. Andraud, O. Maury, *Inorg. Chem.*, **2008**, 47, 10258
- ³³ S.J. Butler, M. Delbianco, L. Lamarque, B.K. McMahon, E.R. Neil, R. Pal, D. Parker, J.W. Walton, J.M. Zwieter, *Dalton Trans.*, **2015**, DOI: 10.1039/C4DT02785J
- ³⁴ J. Andres, A.S. Chauvin, *Phys. Chem. Chem. Phys.*, **2013**, 15, 15981
- ³⁵ S.J. Butler, D. Parker, *Chem. Soc. Rev.*, **2013**, 42, 1652
- ³⁶ A. Beeby, I.M. Clarkson, R.S. Dickins, S. Faulkner, D. Parker, L. Royle, A.S. de Sousa, J.A. G. Williams, M. Woods, *J. Chem. Soc., Perkin Trans. 2*, **1999**, 493
- ³⁷ B. Alpha, J.M. Lehn, G. Mathis, *Angew. Chem. Int. Ed.*, **1987**, 26, 266
- ³⁸ A.P. de Silva, H.Q.M. Gunaratne, T.E. Rice, *Angew. Chem. Int. Ed.*, **1996**, 35, 2116
- ³⁹ E.G. Moore, A.P.S. Samuel, K.N. Raymond, *Acc. Chem. Res.*, **2009**, 42, 542
- ⁴⁰ E.G. Moore, C.J. Jocher, J. Xu, E.J. Werner, K.N. Raymond, *Inorg. Chem.* **2007**, 46, 5468
- ⁴¹ E.J. New, D. Parker, R.D. Peacock, *Dalton Trans.*, **2009**, 672
- ⁴² P. Atkinson, K.S. Findlay, F. Kielar, R. Pal, D. Parker, R.A. Poole, H. Puschmann, S.L. Richardson, P.A. Stenson, A.L. Thompson, J. Yu, *Org. Biomol. Chem.*, **2006**, 4, 1707
- ⁴³ H. Takalo, J. Kankare, E. Hänninen, *Acta Chem. Scand. B*, **1988**, 42, 373
- ⁴⁴ J.W. Walton, A. Bourdolle, S.J. Butler, M. Soulie, M. Delbianco, B.K. McMahon, R. Pal, H. Puschmann, J.M. Zwieter, L. Lamarque, O. Maury, C. Andraud, D. Parker, *Chem. Commun.*, **2013**, 49, 1600
- ⁴⁵ J.R. Lakowicz, *Principles of Fluorescence Spectroscopy*, **1999**, 2nd Edition
- ⁴⁶ P. Wu, L. Brand, *Anal. Biochem.*, **1994**, 218, 1
- ⁴⁷ S. Corbalan Garcia, J.C.A. Teruel, J.C. Gomez Fernandez, *Eur. J. Biochem.*, **1993**, 217, 737
- ⁴⁸ B. Schuler, W.A. Eaton, *Curr. Opin. Struct. Biol.*, **2008**, 18, 16
- ⁴⁹ L.E. Morrison, L.M. Stols, *Biochemistry*, **1993**, 32, 3095
- ⁵⁰ J.M. Zwieter, H. Bazin, L. Lamarque, G. Mathis, *Inorg. Chem.*, **2014**, 53, 1854
- ⁵¹ M. Gabourdes, V. Bourguine, G. Mathis, H. Bazin, B. Alpha-Bazin, *Anal. Biochem.*, **2004**, 105
- ⁵² F. Degorce, A. Card, S. Soh, E. Trinquet, G.P. Knapik, B. Xie, *Curr. Chem. Genomics*, **2009**, 3, 22.
- ⁵³ J. Xu, T.M. Corneillie, E.G. Moore, G.L. Law, N.G. Butlin, K.N. Raymond, *J. Am. Chem. Soc.*, **2011**, 133, 19900
- ⁵⁴ A. Emami-Nemini, T. Roux, M. Leblay, E. Bourrier, L. Lamarque, E. Trinquet, M.J. Lohse, *Nat Protoc.*, **2013**, 8, 1307

- ⁵⁵ G. Mathis, *Clin. Chem.*, **1995**, 41, 1391
- ⁵⁶ J. Zwier, T. Roux, M. Cottet, T. Durroux, S. Douzon, S. Bdioui, N. Gregor, E. Bourrier, N. Oueslati, L. Nicolas, N. Tinel, C. Boisseau, P. Yverneau, F. Charrier-Savourmin, M. Fink, E. Trinquet, *E. J. Biomol. Screening*, **2010**, 15, 1248
- ⁵⁷ <http://www.perkinelmer.co.uk/Catalog/Category/ID/LANCE%20Reagents>, accessed September 24th, **2014**
- ⁵⁸ G. Mathis, H. Bazin, *Lanthanide probes and materials*, Springer-Verlag Berlin Heidelberg, **2010**, 47
- ⁵⁹ L.J. Charbonniere, N. Hildebrandt, R. Ziessel, H.G. Lohmannsroben, *J. Am. Chem. Soc.*, **2006**, 128, 12800
- ⁶⁰ A.R. Clapp, I.L. Medintz, H. Mattoussi, *Chem. Phys. Chem.*, **2006**, 7, 47
- ⁶¹ A. Rodger, B. Norden, *Circular dichroism and linear dichroism*, Oxford, **1997**
- ⁶² S.M. Kelly, T.J. Jess, N.C. Price, *Biochim. Biophys. Acta*, **2005**, 1751, 119
- ⁶³ J.P. Riehl, F.S. Richardson, *Chem. Rev.*, **1986**, 86, 1
- ⁶⁴ K.E.S. Phillips, T.J. Katz, S. Jockusch, A.J. Lovinger, N.J. Turro, *J. Am. Chem. Soc.*, **2001**, 123, 11899
- ⁶⁵ J.E. Field, G. Muller, J.P. Riehl, D. Venkataraman, *J. Am. Chem. Soc.*, **2003**, 125, 11808
- ⁶⁶ K.D. Oyler, F.J. Coughlin, S. Bernhard, *J. Am. Chem. Soc.*, **2007**, 129, 210
- ⁶⁷ C. Schaffner-Hamann, A. von Zelewsky, A. Barbieri, F. Barigelletti, G. Muller, J.P. Riehl, A. Neels, *J. Am. Chem. Soc.*, **2004**, 126, 9339
- ⁶⁸ R. Carr, N.H. Evans, D. Parker, *Chem. Soc. Rev.*, **2012**, 41, 7673
- ⁶⁹ S.C.J. Meskers, C. Dennison, G.W. Canters, H.P.J.M. Dekkers, *J. Biol. Inorg. Chem.*, **1998**, 3, 663
- ⁷⁰ R. Carr, R. Puckrin, B.K. McMahon, R. Pal, D. Parker, L.O. Palsson, *Methods Appl. Fluoresc.*, **2014**, 2 24007
- ⁷¹ H. Donato, R.B. Martin, *J. Am. Chem. Soc.*, **1972**, 94, 4129
- ⁷² D.G. Smith, R. Pal, D. Parker, *Chem. Eur. J.*, **2012**, 18, 11604
- ⁷³ J. Schlesinger, J. Rajander, J.A. Ihalainen, D. Ramesh, P. Eklund, V. Fagerholm, P. Nuutila, O. Solin, *Inorg. Chem.*, **2011**, 50, 4260
- ⁷⁴ L. Lamarque, O. Maury, D. Parker, J. Zwier, J. W. Walton, A. Bourdolle, WO2013/011236 A1, **2013**
- ⁷⁵ M Soulié, F. Latzko, E. Bourrier, V. Placide, S.J. Butler, R. Pal, J.W. Walton, P.L. Baldeck, B. Le Guennic, C. Andraud, J.M. Zwier, L. Lamarque, D. Parker, O. Maury, *Chem. Eur. J.*, **2014**, 20, 8636
- ⁷⁶ C.F. Meares, T.G. Wensel, *Acc. Chem. Res.*, **1984**, 17, 20
- ⁷⁷ S. Dixit, J. Crain, W.C.K. Poon, J.L. Finney, A.K. Soper, *Nature*, **2002**, 416, 829
- ⁷⁸ L. Lamaque, D. Parker, S.J. Butler, M. Delbianco, WO 2014/111661, **2014**
- ⁷⁹ S.J. Butler, M. Delbianco, N.H. Evans, A.T. Frawley, R. Pal, D. Parker, R.S. Puckrin, D.S. Yufit, *Dalton Trans.*, **2014**, 43, 5721

- ⁸⁰ J.P.L. Cox, A.S. Craig, I.M. Helps, K.J. Jankowski, D. Parker, M.A.W. Eaton, A.W. Eaton, A.T. Millican, K. Millar, N.R.A. Beeley, B.A. Boyce, *J. Chem. Soc., Perkin Trans I*, **1990**, 2567
- ⁸¹ D. Parker, *Macrocyclic Synthesis*, Oxford, **1996**
- ⁸² T. Anker, G. Hilmersson, *Org. Lett.*, **2009**, 11, 503
- ⁸³ J.W. Walton, R. Carr, N.H. Evans, A.M. Funk, A.M. Kenwright, D. Parker, D.S. Yufit, M. Botta, S. De Pinto, K.L. Wong, *Inorg. Chem.*, **2012**, 51, 8042
- ⁸⁴ J.R. Morphy, D. Parker, R. Katakya, M.A.W. Eaton, A.T. Millican, R. Alexander, A. Harrison, C. Walker, *J. Chem. Soc. Perkin Trans 2*, **1990**, 573
- ⁸⁵ S. Rannan, N. Davis, *Org. Lett.*, **2000**, 2, 2117
- ⁸⁶ W.F. Schwindinger, T.G. Fawcett, R.A. Lalancette, J.A. Potenza, H.J. Schugar, *Inorg. Chem.*, **1980**, 19, 1379
- ⁸⁷ S.J. Butler, L. Lamarque, R. Pal, D. Parker, *Chem. Sci.*, **2014**, 5, 1750
- ⁸⁸ F. Kielar, C.P. Montgomery, E.J. New, D. Parker, R.A. Poole, S.L. Richardson, P.A. Stenson, *Org. Biomol. Chem.*, **2007**, 5, 2975
- ⁸⁹ C. Reichardt, *Chem. Rev.*, **1994**, 94, 2319
- ⁹⁰ A. Keppler, S. Gendreizig, T. Gronemeyer, H. Pick, H. Vogel, K. Johnsson, *Nature Biotech.*, **2003**, 21, 86
- ⁹¹ A.S. Kopin, E.W. McBride, C. Chen, R.M. Freidinger, D. Chen, C.M. Zhao, M. Beinborn, *PNAS*, **2003**, 100, 5525
- ⁹² A. Usiello, J.H. Baik, F. Rougé-Pont, R. Picetti, A. Dierich, M. LeMeur, P.V. Piazza, E. Borrelli, *Nature*, **2000**, 408, 199
- ⁹³ M. Delbianco, V. Sadovnikova, E. Bourrier, G. Mathis, L. Lamarque, J.M. Zwier, D. Parker, *Angew. Chem. Int. Ed.*, **2014**, 53, 10718
- ⁹⁴ J. M. Zwier, T. Roux, M. Cottet, T. Durroux, S. Douzon, S. Bdioui, N. Gregor, E. Bourrier, N. Oueslati, L. Nicolas, N. Tinel, C. Boisseau, P. Yverneau, F. Charrier-Savournin, M. Fink, E. Trinquet, *J. Biomol. Screening*, **2010**, 15, 1248
- ⁹⁵ F.J. Monsma, A.C. Barton, H.C. Kang, D.L. Brassard, R.P. Haugland, D.R. Sibley, *J. Neurochem.*, **1989**, 52, 1641
- ⁹⁶ H.E. Rajapakse, N. Gahlaut, S. Mohandessi, D. Yu, J.R. Turner, L.W. Miller, *Proc. Natl. Acad. Sci. USA*, **2010**, 107, 13582
- ⁹⁷ M. Rajendran, E. Yapici, L. W. Miller, *Inorg. Chem.*, **2014**, 53, 1839
- ⁹⁸ L. Li, J.Y. Han, B. Nguyen, K. Burgess, *J. Org. Chem.*, **2008**, 73, 1963
- ⁹⁹ S.L. Niu, G. Ulrich, R. Ziessel, A. Kiss, P.Y. Renard, A. Romieu, *Org. Lett.*, **2009**, 11, 2049
- ¹⁰⁰ J.C. Roberts, H. Gao, A. Gopalsamy, A. Kongsjahju, R.J. Patch, *Tetrahedron Lett.*, **1997**, 38, 355
- ¹⁰¹ S. Miller, *J. Org. Chem.*, **2010**, 75, 4632
- ¹⁰² A.M. Ali, B. Hill, S.D. Taylor, *J. Org. Chem.*, **2009**, 74, 3583
- ¹⁰³ S.M. Pauff, S.C. Miller, *J. Org. Chem.*, **2013**, 78, 711

- ¹⁰⁴ L. Rusha, S.C. Miller, *Chem. Commun.*, **2011**, 47, 2038
- ¹⁰⁵ e-EROS Encyclopedia of Reagents for Organic Synthesis, **2001**, John Wiley&Sons, CODEN:69KUHI
- ¹⁰⁶ J.N. Volle, D. Filippini, C. Midrier, M. Sobecki, M. Drag, D. Virieux, J.L. Pirat, *Synthesis*, **2011**, 15, 2490
- ¹⁰⁷ J.L. Montchamp, Y.R. Dumond, *J. Am. Chem. Soc.* **2001**, 123, 510
- ¹⁰⁸ K.B. Altamirano, Z. Huang, J.L. Montchamp, *Tetrahedron*, **2005**, 6315
- ¹⁰⁹ Y.R. Dumond, R.L. Baker, J.L. Montchamp, *Org. Lett.*, **2000**, 2, 3341
- ¹¹⁰ M. Delbianco, L. Lamarque, D. Parker, *Org. Biomol. Chem.*, **2014**, 12, 8061
- ¹¹¹ G. Blotny, *Tetrahedron Lett.*, **2003**, 44, 1499
- ¹¹² A.A. Padmapriya, G. Just., N.G. Lewis, *Synthetic Commun.*, **1985**, 15, 1057
- ¹¹³ P.G.M. Wuts, *J. Org. Chem.*, **1997**, 62, 430
- ¹¹⁴ N.G. Anderson, D.A. Lust, K.A. Colapret, J.H. Simpson, M.F. Malley, J.Z. Gougoutas, *J. Org. Chem.*, **1996**, 61, 7955
- ¹¹⁵ S. Caddick, J.D. Wilden, D.B. Judd, *J. Am. Chem. Soc.*, **2004**, 126, 1024
- ¹¹⁶ Z. Yang, B. Zhou, J. Xu, *Synthesis*, **2013**, 45, 1675
- ¹¹⁷ N. Sim, R. Pal, D. Parker, J. Engelmann, A. Mishra, S. Gottschalk, *Org. Biomol. Chem.*, **2014**, DOI:10.1039/c4ob01848f
- ¹¹⁸ P. Paoletti, C. Bellone, Q. Zhou, *Nat. Rev. Neurosci.*, **2013**, 14, 383
- ¹¹⁹ S. Cull-Candy, S. Brickley, M. Farranti, *Curr. Opin. Neurobiol.*, **2001**, 11, 327
- ¹²⁰ I.J. Reynolds, R. J. Miller, *Mol. Pharmacol.*, **1989**, 36, 758
- ¹²¹ C.F.G. Geraldès, M.P.M. Marques, A.D. Sherry, *Inorg. Chim. Acta*, **1987**, 139, 311
- ¹²² D. Parker, *Chem. Soc. Rev.*, **1990**, 19, 271
- ¹²³ C. Gateau, M. Mazzanti, J. Pecaut, F.A. Dunand, L. Helm, *Dalton Trans.*, **2003**, 2428
- ¹²⁴ E. Cole, R.C.B. Copley, J.A.K. Howard, D. Parker, G. Ferguson, J.F. Gallagher, B. Kaitner, A. Harrison, L. Royle, *J. Chem. Soc. Dalton Trans.*, **1994**, 1619
- ¹²⁵ N.H. Evans, R. Carr, M. Delbianco, R. Pal, D.S. Yufit, D. Parker, *Dalton Trans.*, **2013**, 42, 15610
- ¹²⁶ D. Parker, R. J. Taylor, *Tetrahedron*, **1987**, 43, 5451
- ¹²⁷ <http://www.htrf.com/usa/antibody-screening-cell-surface-targets>, accessed October 28th, **2014**
- ¹²⁸ S. Wang, P.S. Low, *J. Control. Release*, **1998**, 53, 39
- ¹²⁹ C. Naujokata, S. Lauferc, *J. Can. Res. Updates*, **2013**, 2, 36
- ¹³⁰ K.M. Stewart, K.L. Horton, S.O. Kelley, *Org. Biomol. Chem.*, **2008**, 6, 2242
- ¹³¹ R. Pal, A. Beeby, *Methods Appl. Fluoresc.*, **2014**, 2
- ¹³² S.J. Butler, B.K. McMahon, R. Pal, D. Parker, J.W. Walton, *Chem. Eur. J.*, **2013**, 19, 9511
- ¹³³ P.A. Gale, N. Busschaert, C.J. E. Haynes, L.E. Karagiannidis, I.L. Kirby, *Chem. Soc. Rev.*, **2014**, 43, 205
- ¹³⁴ Y.C. Cheng, W.H. Prusoff, *Biochem. Pharmacol.*, **1973**, 22, 3099

- ¹³⁵ N. Wang, R. Liu, Q. Xu, X. Liang, *Chem. Lett.*, **2006**, 35, 566
- ¹³⁶ A. Hamid, M. Hamida, *Synth. Commun.*, **2004**, 34, 377
- ¹³⁷ N. Newman, A. Modiano, Y. Shor, *J. Org. Chem.*, **1956**, 21, 671
- ¹³⁸ D. Peter, J. Tagat, C.A. Hergrueter, P. Helquist, *Tetrahedron Lett.*, **1977**, 52, 4573